

On the road towards targeted treatments
for T cell acute lymphoblastic leukemia:
a phosphoproteomic journey

Valentina Cordo'

Copyright 2023 © **V. Cordo'**

The Netherlands. All rights reserved. No parts of this thesis may be reproduced, stored in a retrieval system or transmitted in any form or by any means without permission of the author.

ISBN: 978-94-6458-972-6

Provided by thesis specialist Ridderprint, ridderprint.nl

Printing: Ridderprint

Cover Design: Valeria Sciacca

Layout and design: Eduard Boxem, persoonlijkproefschrift.nl

On the road towards targeted treatments for T cell acute lymphoblastic leukemia: a phosphoproteomic journey

**Op weg naar doelgerichte therapie voor T cel acute
lymfatische leukemie: een reis door het fosfoproteoom**

(met een samenvatting in het Nederlands)

Proefschrift

ter verkrijging van de graad van doctor aan de
Universiteit Utrecht
op gezag van de
rector magnificus, prof.dr. H.R.B.M. Kummeling,
ingevolge het besluit van het college voor promoties
in het openbaar te verdedigen op

donderdag 13 april 2023 des middags te 12.15 uur

door

Valentina Cordo'

Geboren op 23 april 1992
te Rho (MI), Italië

Promotoren:

Prof. dr. R. Pieters
Prof. dr. C.R. Jimenez

Copromotor:

Dr. J.P.P. Meijerink

Beoordelingscommissie:

Prof. dr. M.M. van den Heuvel (voorzitter)
Prof. dr. A.F.M. Altelaar
Prof. dr. R.P. Kuiper
Prof. dr. H. Verheul
Prof. dr. J. Cloos

CONTENTS

| | | |
|-------------------|---|-----|
| Chapter 1 | General introduction and layout of the thesis | 8 |
| Chapter 2 | Multi-omic approaches to improve outcome for T-cell acute lymphoblastic leukemia patients | 24 |
| Chapter 3 | Phosphoproteomic profiling of T cell acute lymphoblastic leukemia reveals targetable kinases and combination treatment strategies | 54 |
| Chapter 4 | T-cell acute lymphoblastic leukemia: a roadmap to targeted therapies | 98 |
| Chapter 5 | Integrative phosphoproteomic analysis of T cell acute lymphoblastic leukemia xenografts reveals active signaling pathways and potential therapeutical targets | 138 |
| Chapter 6 | A novel human cell line to investigate the pathophysiological IL7 signaling in T cell acute lymphoblastic leukemia | 178 |
| Chapter 7 | Summary, general discussion, and future perspectives | 210 |
| Appendices | Nederlandse samenvatting | 226 |
| | Riassunto in italiano | 230 |
| | List of publications | 234 |
| | Curriculum Vitae | 236 |
| | Acknowledgements | 237 |

CHAPTER 1



General introduction and layout of the thesis

INTRODUCTION

Cancer biology and precision oncology

Cancer, the *emperor of all maladies* [1], is still one of the major challenges of modern medicine. Cancer development is a multi-step, complex process in which cells acquire aberrant phenotypic capabilities that allow the evasion of all the control switches in the body [2, 3]. In the last twenty years, enormous progress has been made in the study of tumor biology. Recently, Douglas Hanahan described the updated *hallmarks of cancer* [4] as eight aberrant capabilities (sustained proliferation, evasion of growth suppression, enabled replicative immortality, activated invasion and metastasis, vascularization, resistance to cell death, evasion of immune destruction, and deregulated cellular metabolism) and two enabling characteristics (genome instability and tumor-promoted inflammation) at the basis of the neoplastic transformation. Interestingly, two additional emerging hallmarks, phenotypic plasticity and senescence, together with two novel enabling characteristics such as microbiome and epigenetic reprogramming, have been added as potential additional pieces to the intricate and still incomplete cancer picture [4].

The first step in the development of cancer is the progressive acquisition of mutations in the DNA of pre-neoplastic cells. Genomics had a pivotal role in the identification of DNA alterations in malignant cells. The booming sequencing technologies at the beginning of the twenty-first century, including next generation sequencing, allowed the mapping of the genetic defects that underlie the malignant transformation in several cancer types [5, 6] which ultimately resulted in the creation of the Cancer Genome Atlas [7], a pan-cancer investigational project that includes the genomic characterization of 33 different tumor types [5, 8-11] (<https://www.cancer.gov/tcga>). A targetable genetic aberration is a DNA defect that results in altered protein expression, protein activity, or unusual cellular phenotype that can be potentially exploited for the design of cancer therapies. Frequently, the DNA defects behind the aberrant phenotype affect the so-called *driver genes*. While some driver gene mutations are common to many cancer types, some tumors might have unique driver genes that characterize their phenotype [9]. Cancer cells are dependent on these aberrant genes, proteins, or phenotypes for their survival since the abnormality usually provides a selective proliferation and survival advantage. This *oncogenic addiction* [12] constitutes the strongest feature of the tumor and, at the same time, its own biggest vulnerability. In fact, oncogenic addictions can be potentially exploited as the *Achille's heel* of the cancer to switch off its malignant growth [13].

In the search for druggable targets in cancer, protein kinases emerged as one of the first molecules to study. Kinases are proteins that mediate all the cellular processes via a reversible post-translational modification called phosphorylation. Phosphorylation acts as the main switch in signal transduction, regulating the most important cellular functions such as control of the cell cycle, survival, motility, and differentiation [14]. The human genome encodes for about 560 kinases and kinase-coding genes are often altered in cancer [9]. Common aberrations detected in kinase-coding genes are not only mutations [15, 16] but also gene amplifications and gene fusions, such as *BCR-ABL1* in chronic myeloid leukemia (CML) [17] and *ALK* and *BRAF* fusions in several solid tumors [18]. A recent pan-cancer study estimated that gene fusions can drive the development of cancer in over 6% of the cases, with more than 1000 fusions involving a kinase-coding gene with a functional catalytic domain [10]. In particular, 19 kinase coding-genes were recurrently involved, including *FGFR*, *EGFR*, *BRAF*, and *ALK* [10]. Stransky and colleagues reported that 3% of tumors present an oncogenic kinase fusion [18]. Gene fusions frequently originate from chromosomal translocations and result in chimeric proteins with de-regulated expression and increased catalytic activity [19]. Furthermore, negative regulators of kinase activity such as phosphatases and tumor suppressor genes like *PTEN*, are also frequently inactivated in tumor cells [9], favoring an uncontrolled proliferation and promoting cell survival.

The year 2001 was a landmark moment in the history of oncology. The Food and Drug Administration (FDA) approved imatinib, the very first kinase inhibitor for the treatment of CML. Imatinib targets the tyrosine-kinase ABL1, and it was discovered as an inhibitor of the aberrant BCR-ABL1 fusion kinase, which is a chimeric protein with constitutive kinase activity that represents the main disease driver of CML [17]. Its approval was a breakthrough for modern medicine. For the first time, a selective drug, targeting only the aberrant feature of leukemic blasts while sparing normal cells, had been proven effective [20]. The approval of imatinib paved the way for the rise of *precision oncology* with the discovery of innovative, more selective agents targeting the aberrant molecular features of cancer [15]. Nowadays, for several tumor types such as *BRAF*-mutant melanoma, gastrointestinal stromal tumors, and advanced non-small cell lung cancer, the use of systematic chemotherapy is no longer the choice for first-line treatment but it is reserved as last option when all the other tailored treatments, including EGFR and ALK inhibitors, have failed [12].

As of May 2021, 71 small-molecule kinase inhibitors have been approved by the FDA and these agents target only 20% of the human kinome [21]. Therefore, there is still room



for kinase target discovery and drug development to extend the applicability of kinase inhibitors.

The presence of a mutated kinase-coding gene or the detection of a gene fusion can be used as a direct biomarker for therapy response. Such DNA alterations have been the main criteria for the assignment of patients to clinical trials investigating targeted drugs in the last twenty years (*genomic based-precision oncology*) [22]. Nevertheless, many clinical trials investigating molecularly-directed agents have often produced rather disappointing results. In fact, genomic-based precision oncology can result in minor clinical benefit either because the detected aberration cannot be targeted by currently approved or investigated agents (lack of an *actionable alteration*) [23-26], or because after an initial response, the insurgence of additional mutations during the treatment will provoke resistance to the monotherapy [27, 28] and favor the outgrowth of the resistant sub-population. Thus, in addition to the discovery of targets, predictive biomarkers of response and accurate diagnostic tests are also essential for the success of innovative treatments [29].

Resistance to a single drug can also be independent of the acquisition of novel mutations. Alternative feedback loops might compensate for the inhibition of a single kinase or pathway via different signaling routes [12, 30-32] or metabolic rewiring could favor resistance to the inhibition of a single signaling node [33-35]. Therefore, the design of effective combination treatments seems necessary to overcome tumor heterogeneity, adaptation, and disease progression [36].

Functional precision medicine to address the cancer complexity

Genomics has been pivotal for the development of precision oncology. Nevertheless, there is an underestimation of the role of non-genetic mechanisms that drive cancer phenotypes and therapy resistance [37]. It is well established now that a single treatment will not provide a long-lasting effect, and to prevent the occurrence of therapy resistance and disease relapses, effective combination treatments are needed [38]. However, several important questions arise: *how do we identify a non-genetic cancer vulnerability? Is it possible to unravel the cancer complexity? How do we effectively combine targeted agents?*

Sengupta and colleagues reported that in a cohort of over 6500 tumors, only 3% of the cases presented an actionable lesion that could be targeted with an FDA-approved agent. Nevertheless, when adding to the identification of targetable mutations also transcriptome, protein expression, and protein phosphorylation analyses as well as drug repurposing,

the potential druggability of tumors could be raised up to 16% [39]. This study highlights the added value of more integrated, multi-omic approaches compared to genomic only-driven strategies [23]. Therefore, the molecular tumor profiling should address the cancer complexity, including post-translational events [40].

Recently, the concept of *functional precision medicine* has taken the spotlight. In fact, while DNA aberrations are static features of the tumor [37], the cancer phenotype can rapidly change. Thus, there is a need for dynamic and functional analyses that can capture and follow cancer development and adaptation before and after treatment [37]. The recent results from the EXALT prospective clinical trial [41] revealed the feasibility of *ex vivo* drug screening of over 100 targeted agents as a functional precision medicine approach to assign patients with hematological malignancies to the most appropriate tailored treatment. In fact, direct testing of the patient's tumor cells sensitivity to a panel of drugs can give, in a relatively short turnaround time, strong evidence of the tumor phenotype. Furthermore, Malani and colleagues reported the successful establishment of a *functional precision medicine tumor board* that includes not only the *ex vivo* drug testing of more than 500 compounds, but also the integration of multi-omic analyses (such as whole-exome sequencing, RNA sequencing, pathway enrichment analyses, and phospho-flow measurements) for the identification of biological insights and response biomarkers in acute myeloid leukemia (AML) [42]. Precision medicine programs have been initiated for the molecular investigation of relapsed/refractory pediatric cancers as well, like the MOSCATO-01 trial [43], ESMART (NCT02813135), INFORM [26], and the iTHER (individualized THERapy) trial which includes not only the identification of DNA and RNA aberrations but also the generation of organoids from tumor biopsies which are used for the *ex vivo* drug screenings of 170 compounds [44]. Similarly, for refractory/relapsed pediatric acute lymphoblastic leukemia or lymphoblastic lymphoma cases, the upcoming HEM-iSMART trial will investigate the assignment of patients to targeted treatments based on the tumor molecular profile which includes DNA and RNA sequencing but also *ex vivo* drug response profiling [45].

Thus, while genomics allowed the rise of precision medicine, it seems to be necessary to go beyond genomics to further uncover the potential of precision oncology.



Mass spectrometry-based phosphoproteomics: a functional read-out for target identification and treatment selection

Innovative therapeutic agents such as small-molecule inhibitors and immunotherapies do not target DNA aberrations but proteins, the effectors of signal transduction and the main determinants of the cancer phenotypes. Therefore, protein expression patterns, active signaling pathways, and aberrant kinase activities can provide useful information for drug prioritization and the design of effective combination treatments in the context of personalized medicine.

Mass spectrometry (MS)-based phosphoproteomics has been pivotal in the study of cancer signaling networks [46-48] since it allows the simultaneous investigation of multiple proteins and signaling routes without the need for any *a priori* knowledge or pathway selection. Global analyses of protein phosphorylation at the single amino acid resolution have allowed the mapping of signal transduction pathways and the identification of kinases and their substrates as targetable cancer vulnerabilities, regardless of their mutational status ([49, 50], this thesis). Phosphoproteomic-guided identification of hyper-active kinases and kinase activity rankings have been proven important tools for the appropriate selection of therapeutical targets, for the design of personalized treatment combinations in case of monotherapy resistance, and for the elucidation of predictive response biomarkers ([50-55], this thesis). Additionally, phosphoproteome profiling has facilitated the identification of new disease subtypes [50, 56]. Phosphoproteomic analyses have been successfully integrated with DNA sequencing, RNA, and protein expression data to create a *proteogenomic* profile for several cancer types [56-60]. The Clinical Proteomic Tumor Analysis Consortium (CPTAC) [61] established in 2011, is driving the proteogenomic characterization of cancer to enhance precision oncology and to promote the direct translation of discovered biological insights into clinical practice (<https://proteomics.cancer.gov/programs/cptac>).

The large-scale application of chemical proteomics and kinome profiling allowed the elucidation of kinase-drug interactions [62] and highlighted unknown targets of several kinase inhibitors [62, 63]. The *target landscape of clinical kinase drugs* [62] provides valuable information that supports drugs repurposing beyond their primary application thanks to the identification of additional targets, and uncovered mechanism of unwanted side effects upon treatment.

MS-based proteomics and phosphoproteomics have revealed unexpected biological insights and provided essential tools to favor the translation of preclinical research findings

from *bench-to bedside*, adding a fundamental, functional value to genomic-driven precision oncology [64-66].

Pediatric T cell acute lymphoblastic leukemia

Cancer development is generally considered a disease associated with aging, but unfortunately, the incidence of pediatric cancer, particularly childhood leukemia, has been notably increasing [67, 68]. T cell acute lymphoblastic leukemia (T-ALL) is a rare hematological malignancy. In fact, while ALL is the most common form of cancer in children, T-ALL accounts for about only 15% of the pediatric ALL cases [69] and it is characterized by the aberrant proliferation of immature T cell progenitors. Intensive, risk-adapted, multi-agent chemotherapy-based regimens [70, 71] have raised the overall survival (OS) of T-ALL patients above 80%. Nevertheless, in the last two decades, no improvements in the 5- and 10-year OS have been achieved for T-ALL [68]. Despite the rather favorable OS, one out of five pediatric T-ALL patients will ultimately die as a result of relapse and/or therapy-refractory disease. Upon disease relapse, most T-ALL cases are resistant to further treatment due to acquired therapy resistance. Furthermore, survivors have a higher risk to suffer from organ failure and development of secondary malignancies caused by the intensive treatment.

At this moment, the current treatment regimens have been optimized and reached the upper limit of the balance between cure rate and acute toxicities, indicating that further intensification of the chemotherapeutic regimen for high-risk and relapsed patients is not feasible [72, 73] and that additional, more selective therapeutical options are of utmost importance to improve survival and limit treatment-induced severe side effects.

The capability of cancer cells to evade terminal differentiation or to prevent the differentiation commitment has been recently recognized as additional hallmark of cancer [4]. Thanks to the aberrant expression of developmental transcription factors, which are normally active during the early stages of embryonic development, leukemic cells maintain a progenitor-like state that assures a differentiation arrest and favors an aberrant proliferation. In fact, extensive transcriptome and genome sequencing studies uncovered that the disease drivers of T-ALL are developmental transcription factors ectopically expressed due to genomic rearrangements [74-76]. While kinase aberrations are not the main disease drivers, secondary mutations in receptors (e.g., *NOTCH1*, *IL7R*) [77, 78], kinase-coding genes (e.g., *JAK1*, *JAK3*, *FLT3*, *AKT*, *PIK3*, *NRAS*) [76, 78, 79] and their regulators (e.g., *PTEN*) [76, 80, 81] can support the leukemogenesis and favor the proliferation and survival of leukemic

blasts. Additionally, fusions involving kinase-coding genes are rare in T-ALL [82, 83] and often present only in minor leukemic subclones, like for the *NUP214-ABL1* fusion in various T-ALL patients [84], thus limiting the possibilities for a genomic-driven precision medicine approach.

LAYOUT OF THIS THESIS

Hematological malignancies are underrepresented in the current pan-cancer international studies where usually AML is taken as a reference for blood cancers. However, given the diverse genetic aberrations that characterize each blood cancer and the consequent different treatment protocols designed, AML cannot be used as a model for other hematological malignancies such as ALL. T-ALL is not included in the current TCGA dataset (<https://www.cancer.gov/about-nci/organization/ccg/research/structural-genomics/tcga/studied-cancers>) nor in the CPTAC initiative (<https://pdc.cancer.gov/pdc/>) at the moment, indicating a lack of systematic analysis of this cancer type, especially at the (phospho) proteome and proteogenomic level. Furthermore, unlike any other type of leukemia, no targeted therapy has been approved for the treatment of T-ALL patients yet, and the lack of accurate predictive biomarkers hampers the correct assignment of patients to tailored treatments. Therefore, we aimed to go beyond the genomics of T-ALL and search for non-genomic dependencies that could be exploited as leukemic vulnerabilities.

Chapter 2 offers an overview of the current state of knowledge on the genetics of T-ALL. Moreover, we highlight how functional studies investigating signaling pathways at the RNA and protein level can offer valuable opportunities to unravel mechanisms of therapy resistance and uncover novel putative therapeutical targets. We suggest an integrative, multi-omic approach to study T-ALL under every aspect to capture the disease complexity and to find the *Achille's heel* of the disease.

In **chapter 3**, we showcase the application of global phosphoproteomic profiling and kinase activity inference for the identification of targetable kinases in T-ALL and for the design of personalized combination therapies. By using a panel of T-ALL cell lines and four patient-derived xenograft (PDX) models, we provide an overview of kinase activation in T-ALL and we uncover a role for INSR/IGF-1R signaling in sustaining resistance to the kinase inhibitor dasatinib in T-ALL cases with an elevated LCK and SRC kinase activity.

Multiple precision medicines are currently under clinical investigation for the treatment of T-ALL. In **chapter 4**, we provide an extensive literature review on targetable genomic lesions and active signaling pathways in T-ALL. Furthermore, we give a comprehensive overview of all the targeted agents in current clinical trials as well as relevant compounds that showed promising results in preclinical T-ALL models. These agents include different classes of small-molecule inhibitors and immunotherapies.

Despite the elucidation of recurrent signaling mutations in T-ALL, the use of such aberrations as prognostic or response biomarkers is still controversial [85]. In **chapter 5**, we describe an *ex vivo* drug screening on a panel of 47 T-ALL PDXs. Furthermore, we report targetable mutations, and we integrate the genomic information with microarray-based transcriptomic, proteomic, and phosphoproteomic analyses to highlight relevant signaling pathways and determinants of drug sensitivity. By using 11 matched diagnostic-relapse PDXs, we show that selected signaling patterns (e.g., protein expression, pathway activation, and kinase activities) are retained at relapse.

PDXs have become fundamental tools in preclinical research. In **chapter 6**, we report the establishment of a novel PDX-derived T-ALL cell line that can be cultured *in vitro* in the presence of human IL7. Given the predominant role of exogenous IL7 in sustaining blast proliferation and favoring resistance to glucocorticoid therapy [86], the cornerstone of T-ALL treatment, we leverage this new cell line to study IL7-induced kinase signaling and to possibly identify effective combination therapies.

Chapter 7 summarizes the main findings and arguments of this thesis, with a broader look at future T-ALL preclinical and translational investigations. The **Appendices** include a layman's summary of the work described in this thesis in Dutch and Italian.



REFERENCES

1. Mukherjee, S., *The Emperor of All Maladies: A Biography of Cancer*. 2010: Scribner.
2. Hanahan, D. and R.A. Weinberg, *The hallmarks of cancer*. Cell, 2000. **100**(1): p. 57-70.
3. Hanahan, D. and R.A. Weinberg, *Hallmarks of cancer: the next generation*. Cell, 2011. **144**(5): p. 646-74.
4. Hanahan, D., *Hallmarks of Cancer: New Dimensions*. Cancer Discov, 2022. **12**(1): p. 31-46.
5. Kandoth, C., et al., *Mutational landscape and significance across 12 major cancer types*. Nature, 2013. **502**(7471): p. 333-339.
6. Tamborero, D., et al., *Comprehensive identification of mutational cancer driver genes across 12 tumor types*. Sci Rep, 2013. **3**: p. 2650.
7. Cancer Genome Atlas Research, N., et al., *The Cancer Genome Atlas Pan-Cancer analysis project*. Nat Genet, 2013. **45**(10): p. 1113-20.
8. Sanchez-Vega, F., et al., *Oncogenic Signaling Pathways in The Cancer Genome Atlas*. Cell, 2018. **173**(2): p. 321-337 e10.
9. Bailey, M.H., et al., *Comprehensive Characterization of Cancer Driver Genes and Mutations*. Cell, 2018. **174**(4): p. 1034-1035.
10. Gao, Q., et al., *Driver Fusions and Their Implications in the Development and Treatment of Human Cancers*. Cell Rep, 2018. **23**(1): p. 227-238 e3.
11. Schaub, F.X., et al., *Pan-cancer Alterations of the MYC Oncogene and Its Proximal Network across the Cancer Genome Atlas*. Cell Syst, 2018. **6**(3): p. 282-300 e2.
12. Cohen, P., D. Cross, and P.A. Janne, *Kinase drug discovery 20 years after imatinib: progress and future directions*. Nat Rev Drug Discov, 2021. **20**(7): p. 551-569.
13. Weinstein, I.B. and A. Joe, *Oncogene addiction*. Cancer Res, 2008. **68**(9): p. 3077-80; discussion 3080.
14. Cohen, P., *The origins of protein phosphorylation*. Nat Cell Biol, 2002. **4**(5): p. E127-30.
15. Lynch, T.J., et al., *Activating mutations in the epidermal growth factor receptor underlying responsiveness of non-small-cell lung cancer to gefitinib*. N Engl J Med, 2004. **350**(21): p. 2129-39.
16. Davies, H., et al., *Mutations of the BRAF gene in human cancer*. Nature, 2002. **417**(6892): p. 949-54.
17. Druker, B.J., et al., *Effects of a selective inhibitor of the Abl tyrosine kinase on the growth of Bcr-Abl positive cells*. Nat Med, 1996. **2**(5): p. 561-6.
18. Stransky, N., et al., *The landscape of kinase fusions in cancer*. Nat Commun, 2014. **5**: p. 4846.
19. Rabbitts, T.H., *Chromosomal translocations in human cancer*. Nature, 1994. **372**(6502): p. 143-9.
20. Druker, B.J., et al., *Five-year follow-up of patients receiving imatinib for chronic myeloid leukemia*. N Engl J Med, 2006. **355**(23): p. 2408-17.
21. Attwood, M.M., et al., *Trends in kinase drug discovery: targets, indications and inhibitor design*. Nat Rev Drug Discov, 2021. **20**(11): p. 839-861.
22. Letai, A., *Functional Precision Medicine: Putting Drugs on Patient Cancer Cells and Seeing What Happens*. Cancer Discov, 2022. **12**(2): p. 290-292.

23. van der Zwet, J.C.G., et al., *Multi-omic approaches to improve outcome for T-cell acute lymphoblastic leukemia patients*. *Adv Biol Regul*, 2019. **74**: p. 100647.
24. Massard, C., et al., *High-Throughput Genomics and Clinical Outcome in Hard-to-Treat Advanced Cancers: Results of the MOSCATO 01 Trial*. *Cancer Discov*, 2017. **7**(6): p. 586-595.
25. Marquart, J., E.Y. Chen, and V. Prasad, *Estimation of the Percentage of US Patients With Cancer Who Benefit From Genome-Driven Oncology*. *JAMA Oncol*, 2018. **4**(8): p. 1093-1098.
26. van Tilburg, C.M., et al., *The Pediatric Precision Oncology INFORM Registry: Clinical Outcome and Benefit for Patients with Very High-Evidence Targets*. *Cancer Discov*, 2021. **11**(11): p. 2764-2779.
27. Quintas-Cardama, A., H.M. Kantarjian, and J.E. Cortes, *Mechanisms of primary and secondary resistance to imatinib in chronic myeloid leukemia*. *Cancer Control*, 2009. **16**(2): p. 122-31.
28. Flaherty, K.T., et al., *Molecular Landscape and Actionable Alterations in a Genomically Guided Cancer Clinical Trial: National Cancer Institute Molecular Analysis for Therapy Choice (NCI-MATCH)*. *J Clin Oncol*, 2020. **38**(33): p. 3883-3894.
29. Fridlyand, J., et al., *Considerations for the successful co-development of targeted cancer therapies and companion diagnostics*. *Nat Rev Drug Discov*, 2013. **12**(10): p. 743-55.
30. Fritsche-Guenther, R., et al., *Strong negative feedback from Erk to Raf confers robustness to MAPK signalling*. *Mol Syst Biol*, 2011. **7**: p. 489.
31. Klempner, S.J., A.P. Myers, and L.C. Cantley, *What a tangled web we weave: emerging resistance mechanisms to inhibition of the phosphoinositide 3-kinase pathway*. *Cancer Discov*, 2013. **3**(12): p. 1345-54.
32. Prahallad, A., et al., *PTPN11 Is a Central Node in Intrinsic and Acquired Resistance to Targeted Cancer Drugs*. *Cell Rep*, 2015. **12**(12): p. 1978-85.
33. Bergers, G. and S.M. Fendt, *The metabolism of cancer cells during metastasis*. *Nat Rev Cancer*, 2021. **21**(3): p. 162-180.
34. Apfel, V., et al., *Therapeutic Assessment of Targeting ASNS Combined with L-Asparaginase Treatment in Solid Tumors and Investigation of Resistance Mechanisms*. *ACS Pharmacol Transl Sci*, 2021. **4**(1): p. 327-337.
35. Herranz, D., et al., *Metabolic reprogramming induces resistance to anti-NOTCH1 therapies in T cell acute lymphoblastic leukemia*. *Nat Med*, 2015. **21**(10): p. 1182-9.
36. Plana, D., A.C. Palmer, and P.K. Sorger, *Independent Drug Action in Combination Therapy: Implications for Precision Oncology*. *Cancer Discov*, 2022. **12**(3): p. 606-624.
37. Letai, A., P. Bholra, and A.L. Welm, *Functional precision oncology: Testing tumors with drugs to identify vulnerabilities and novel combinations*. *Cancer Cell*, 2022. **40**(1): p. 26-35.
38. Al-Lazikani, B., U. Banerji, and P. Workman, *Combinatorial drug therapy for cancer in the post-genomic era*. *Nat Biotechnol*, 2012. **30**(7): p. 679-92.
39. Sengupta, S., et al., *Integrative omics analyses broaden treatment targets in human cancer*. *Genome Med*, 2018. **10**(1): p. 60.
40. Berlanga, P., et al., *The European MAPPYACTS Trial: Precision Medicine Program in Pediatric and Adolescent Patients with Recurrent Malignancies*. *Cancer Discov*, 2022. **12**(5): p. 1266-1281.
41. Kornauth, C., et al., *Functional Precision Medicine Provides Clinical Benefit in Advanced Aggressive Hematologic Cancers and Identifies Exceptional Responders*. *Cancer Discov*, 2022. **12**(2): p. 372-387.



42. Malani, D., et al., *Implementing a Functional Precision Medicine Tumor Board for Acute Myeloid Leukemia*. *Cancer Discov*, 2022. **12**(2): p. 388-401.
43. Harttrampf, A.C., et al., *Molecular Screening for Cancer Treatment Optimization (MOSCATO-01) in Pediatric Patients: A Single-Institutional Prospective Molecular Stratification Trial*. *Clin Cancer Res*, 2017. **23**(20): p. 6101-6112.
44. Langenberg, K., E. Dolman, and J. Molenaar, *Abstract A40: Integration of high-throughput drug screening on patient-derived organoids into pediatric precision medicine programs: The future is now!* *Cancer Research*, 2020. **80**(14_Supplement): p. A40-A40.
45. Brivio, E., et al., *Targeted inhibitors and antibody immunotherapies: Novel therapies for paediatric leukaemia and lymphoma*. *Eur J Cancer*, 2022. **164**: p. 1-17.
46. Hijazi, M., et al., *Reconstructing kinase network topologies from phosphoproteomics data reveals cancer-associated rewiring*. *Nat Biotechnol*, 2020. **38**(4): p. 493-502.
47. Drake, J.M., et al., *Phosphoproteome Integration Reveals Patient-Specific Networks in Prostate Cancer*. *Cell*, 2016. **166**(4): p. 1041-1054.
48. Cutillas, P.R., *Role of phosphoproteomics in the development of personalized cancer therapies*. *Proteomics Clin Appl*, 2015. **9**(3-4): p. 383-95.
49. Archer, T.C., et al., *Proteomics, Post-translational Modifications, and Integrative Analyses Reveal Molecular Heterogeneity within Medulloblastoma Subgroups*. *Cancer Cell*, 2018. **34**(3): p. 396-410 e8.
50. Rikova, K., et al., *Global survey of phosphotyrosine signaling identifies oncogenic kinases in lung cancer*. *Cell*, 2007. **131**(6): p. 1190-203.
51. Beekhof, R., et al., *INKA, an integrative data analysis pipeline for phosphoproteomic inference of active kinases*. *Mol Syst Biol*, 2019. **15**(4): p. e8250.
52. van Alphen, C., et al., *Phosphotyrosine-based Phosphoproteomics for Target Identification and Drug Response Prediction in AML Cell Lines*. *Mol Cell Proteomics*, 2020. **19**(5): p. 884-899.
53. Frejno, M., et al., *Proteome activity landscapes of tumor cell lines determine drug responses*. *Nat Commun*, 2020. **11**(1): p. 3639.
54. Franciosa, G., et al., *Proteomics of resistance to Notch1 inhibition in acute lymphoblastic leukemia reveals targetable kinase signatures*. *Nat Commun*, 2021. **12**(1): p. 2507.
55. Casado, P., et al., *Kinase-substrate enrichment analysis provides insights into the heterogeneity of signaling pathway activation in leukemia cells*. *Sci Signal*, 2013. **6**(268): p. rs6.
56. Gillette, M.A., et al., *Proteogenomic Characterization Reveals Therapeutic Vulnerabilities in Lung Adenocarcinoma*. *Cell*, 2020. **182**(1): p. 200-225 e35.
57. Mun, D.G., et al., *Proteogenomic Characterization of Human Early-Onset Gastric Cancer*. *Cancer Cell*, 2019. **35**(1): p. 111-124 e10.
58. Mani, D.R., et al., *Cancer proteogenomics: current impact and future prospects*. *Nat Rev Cancer*, 2022. **22**(5): p. 298-313.
59. Krug, K., et al., *Proteogenomic Landscape of Breast Cancer Tumorigenesis and Targeted Therapy*. *Cell*, 2020. **183**(5): p. 1436-1456 e31.
60. Casado, P., et al., *Proteomic and genomic integration identifies kinase and differentiation determinants of kinase inhibitor sensitivity in leukemia cells*. *Leukemia*, 2018. **32**(8): p. 1818-1822.
61. Ellis, M.J., et al., *Connecting genomic alterations to cancer biology with proteomics: the NCI Clinical Proteomic Tumor Analysis Consortium*. *Cancer Discov*, 2013. **3**(10): p. 1108-12.
62. Klaeger, S., et al., *The target landscape of clinical kinase drugs*. *Science*, 2017. **358**(6367).

63. Wiechmann, S., et al., *Chemical Phosphoproteomics Sheds New Light on the Targets and Modes of Action of AKT Inhibitors*. ACS Chem Biol, 2021. **16**(4): p. 631-641.
64. Macklin, A., S. Khan, and T. Kislinger, *Recent advances in mass spectrometry based clinical proteomics: applications to cancer research*. Clin Proteomics, 2020. **17**: p. 17.
65. Casado, P., et al., *Impact of phosphoproteomics in the translation of kinase-targeted therapies*. Proteomics, 2017. **17**(6).
66. Casado, P., et al., *Implementation of Clinical Phosphoproteomics and Proteomics for Personalized Medicine*. Methods Mol Biol, 2022. **2420**: p. 87-106.
67. Steliarova-Foucher, E., et al., *International incidence of childhood cancer, 2001-10: a population-based registry study*. Lancet Oncol, 2017. **18**(6): p. 719-731.
68. Reedijk, A.M.J., et al., *Progress against childhood and adolescent acute lymphoblastic leukaemia in the Netherlands, 1990-2015*. Leukemia, 2021. **35**(4): p. 1001-1011.
69. Patel, A.A., et al., *Biology and Treatment Paradigms in T Cell Acute Lymphoblastic Leukemia in Older Adolescents and Adults*. Curr Treat Options Oncol, 2020. **21**(7): p. 57.
70. Pieters, R., et al., *Successful Therapy Reduction and Intensification for Childhood Acute Lymphoblastic Leukemia Based on Minimal Residual Disease Monitoring: Study ALL10 From the Dutch Childhood Oncology Group*. J Clin Oncol, 2016. **34**(22): p. 2591-601.
71. Jeha, S., et al., *Improved CNS Control of Childhood Acute Lymphoblastic Leukemia Without Cranial Irradiation: St Jude Total Therapy Study 16*. J Clin Oncol, 2019. **37**(35): p. 3377-3391.
72. van Binsbergen, A.L., et al., *Efficacy and toxicity of high-risk therapy of the Dutch Childhood Oncology Group in childhood acute lymphoblastic leukemia*. Pediatr Blood Cancer, 2022. **69**(2): p. e29387.
73. Inaba, H. and C.H. Pui, *Advances in the Diagnosis and Treatment of Pediatric Acute Lymphoblastic Leukemia*. J Clin Med, 2021. **10**(9).
74. Ferrando, A.A., et al., *Gene expression signatures define novel oncogenic pathways in T cell acute lymphoblastic leukemia*. Cancer Cell, 2002. **1**(1): p. 75-87.
75. Homminga, I., et al., *Integrated transcript and genome analyses reveal NKX2-1 and MEF2C as potential oncogenes in T cell acute lymphoblastic leukemia*. Cancer Cell, 2011. **19**(4): p. 484-97.
76. Liu, Y., et al., *The genomic landscape of pediatric and young adult T-lineage acute lymphoblastic leukemia*. Nat Genet, 2017. **49**(8): p. 1211-1218.
77. Weng, A.P., et al., *Activating mutations of NOTCH1 in human T cell acute lymphoblastic leukemia*. Science, 2004. **306**(5694): p. 269-71.
78. Li, Y., et al., *IL-7 Receptor Mutations and Steroid Resistance in Pediatric T cell Acute Lymphoblastic Leukemia: A Genome Sequencing Study*. PLoS Med, 2016. **13**(12): p. e1002200.
79. Zhang, J., et al., *The genetic basis of early T-cell precursor acute lymphoblastic leukaemia*. Nature, 2012. **481**(7380): p. 157-63.
80. Gutierrez, A., et al., *High frequency of PTEN, PI3K, and AKT abnormalities in T-cell acute lymphoblastic leukemia*. Blood, 2009. **114**(3): p. 647-50.
81. Zuurbier, L., et al., *The significance of PTEN and AKT aberrations in pediatric T-cell acute lymphoblastic leukemia*. Haematologica, 2012. **97**(9): p. 1405-13.
82. Graux, C., et al., *Fusion of NUP214 to ABL1 on amplified episomes in T-cell acute lymphoblastic leukemia*. Nat Genet, 2004. **36**(10): p. 1084-9.
83. Steimle, T., et al., *Clinico-biological features of T-cell acute lymphoblastic leukemia with fusion proteins*. Blood Cancer J, 2022. **12**(1): p. 14.



Chapter 1

84. Graux, C., et al., *Heterogeneous patterns of amplification of the NUP214-ABL1 fusion gene in T-cell acute lymphoblastic leukemia*. *Leukemia*, 2009. **23**(1): p. 125-33.
85. Burns, M.A., et al., *Identification of prognostic factors in childhood T-cell acute lymphoblastic leukemia: Results from DFCI ALL Consortium Protocols 05-001 and 11-001*. *Pediatr Blood Cancer*, 2021. **68**(1): p. e28719.
86. Delgado-Martin, C., et al., *JAK/STAT pathway inhibition overcomes IL7-induced glucocorticoid resistance in a subset of human T-cell acute lymphoblastic leukemias*. *Leukemia*, 2017. **31**(12): p. 2568-2576.



CHAPTER 2



Multi-omic approaches to improve outcome for T-cell acute lymphoblastic leukemia patients

Jordy C.G. van der Zwet¹, Valentina Cordo¹, Kirsten Canté-Barrett¹ and Jules P.P. Meijerink¹

¹ Princess Máxima Center for Pediatric Oncology, Utrecht, The Netherlands

Published in *Advances in Biological Regulation* (2019)

DOI: [10.1016/j.jbior.2019.100647](https://doi.org/10.1016/j.jbior.2019.100647)

PMID: 31523030

ABSTRACT

In the last decade, tremendous progress in curative treatment has been made for T-ALL patients using high-intensive, risk-adapted multi-agent chemotherapy. Further treatment intensification to improve the cure rate is not feasible as it will increase the number of toxic deaths. Hence, about 20% of pediatric patients relapse and often die due to acquired therapy resistance. Personalized medicine is of utmost importance to further increase cure rates and is achieved by targeting specific initiation, maintenance or resistance mechanisms of the disease. Genomic sequencing has revealed mutations that characterize genetic subtypes of many cancers including T-ALL. However, leukemia may have various activated pathways that are not accompanied by the presence of mutations. Therefore, screening for mutations alone is not sufficient to identify all molecular targets and leukemic dependencies for therapeutic inhibition. We review the extent of the driving type A and the secondary type B genomic mutations in pediatric T-ALL that may be targeted by specific inhibitors. Additionally, we review the need for additional screening methods on the transcriptional and protein levels. An integrated 'multi-omic' screening will identify potential targets and biomarkers to establish significant progress in future individualized treatment of T-ALL patients.

T-ALL subtypes and driving oncogenes

T-cell acute lymphoblastic leukemia (T-ALL) is the malignant expansion of immature, arrested T-cells at various stages of thymocyte development. The European Group for the Immunological Characterization of Leukemias (EGIL) distinguished three T-ALL subtypes by virtue of their expression of Cluster of Differentiation markers (CD-markers). These subtypes were denoted as early, cortical and mature T-ALL (1). The outcome of cortical T-ALL was found superior over the outcome of both other subtypes (2, 3).

The first T-ALL oncogenes were identified by resolving the translocations from T-cell receptor (TCR) gene enhancers or promoters to other chromosomes as a consequence of errors in VDJ recombination events. This led to the discovery of the *TAL1* oncogene for patients harboring the t(1;14)(p34;q11) translocation (4, 5), *LYL1* in a patient with a t(7;19)(q34;p13) translocation (6) and *TLX1/HOX11* in patients bearing t(10;14)(q24;q11) translocations (7-11). For *TAL1*, small deletions were identified in approximately 12-25% of pediatric patients that result in repositioning of the *TAL1* coding region behind the *STIL* gene promoter (12-14). Whereas *TAL1* abnormalities are predominantly associated with late cortical development (15), *TLX1*-rearranged patients mostly resemble early cortical thymocytes (16). Since these initial discoveries, extensive molecular and cytogenetic analyses have resolved many additional oncogenic rearrangements in nearly 80 percent of the T-ALL patients (**Table 1**) (17-24).

The first genome-wide gene expression analysis that distinguished the T-ALL subtype from other leukemic types was performed by the group of Eric Lander (25). Shortly after, the gene signatures of immature, early and late cortical T-cell developmental stages in T-ALL patient samples could be distinguished that were characterized by ectopic expression levels of oncogenic transcription factors including *LYL1*, *TLX1/HOX11* or *TAL1*, respectively (26). Whereas expression of *TLX1* and *TAL1* are driven by chromosomal rearrangements, *LYL1*-positive T-ALL patients are devoid of *LYL1* rearrangements. Some early cortical T-ALL patients express the *TLX1*-related gene *TLX3/HOX11L2* due to a cryptic (5;14)(q35;q32) chromosomal translocation in approximately 25 percent of pediatric T-ALL patients (26, 27). Later gene expression microarray studies distinguished at least four T-ALL groups, *i.e.* the immature, TLX, proliferative and TALLMO subtypes (28-30). Identification of additional oncogenes extended previous observations that each subtype was characterized by specific oncogenic rearrangements that facilitate specific blocks in T-cell development and drive T-ALL. Each genetic subtype is discussed below.

Table 1. Oncogene rearrangements in T-ALL.

| Oncogene activation | Enhancer/promoters | Incidence (%) | Associated subtype | Ref |
|---------------------------|---|---------------|--------------------|----------------------------|
| <i>TAL1, TAL2, LYL1</i> | <i>TCRB (enh), TCRAD (enh), STIL (promoter), TCF7**</i> , Myb-Enh mut. | 27, <1, <1 | TALLMO | (4-6, 12, 13, 75, 156-158) |
| <i>LMO1, LMO2, LMO3</i> | <i>TCRB (enh), TCRAD (enh), MBNL1, STAG2</i> , Myb-Enh mut., 11q13 deletion | 5, 12, <1 | TALLMO | (72, 73, 156, 159, 160) |
| <i>TLX1</i> | <i>TCRB (enh), TCRAD (V-gene promoter), DDX30**</i> | 5 | Proliferative | (7-11) |
| <i>NKX2-1, NKX2-2</i> | <i>TCRAD (enh), TCRB (enh)</i> | 5 | Proliferative | (29) |
| <i>TLX3</i> | <i>BCL11B (enh), TCRB (enh), TCRAD (V-gene promoter), CAPSL</i> | 21 | TLX | (26, 27, 43, 161, 162) |
| <i>HOXA9/A10</i> | <i>TCRB (enh)</i> | <2 | TLX/ ETP-ALL | (28, 163-165) |
| <i>MEF2C</i> | <i>PITX2</i> | <2 | ETP-ALL | (29) |
| <i>SP1</i> | <i>BCL11B (enh)</i> | <1 | ETP-ALL | (29) |
| <i>LMO2**</i> | <i>BCL11B (enh)</i> | <1 | ETP-ALL | |
| <i>NKX2.5</i> | <i>BCL11B(enh), TCRAD (enh)</i> | <1 | ETP-ALL | (29, 166, 167) |
| <i>LCK</i> | <i>TCRB (enh)</i> | <1 | unknown | |
| <i>MYB</i> | <i>TCRB (enh), duplications</i> | <2 | unknown | (168-170) |
| <i>CCND2</i> | <i>TCRB (enh)</i> | <1 | unknown | (171) |
| Oncogenic fusions | Partner gene | Incidence | Associated subtype | Ref |
| <i>PICALM (HOXA act.)</i> | <i>MLLT10</i> | 3 | TLX/ ETP-ALL | (29, 172) |
| <i>KTM2A (HOXA act.)</i> | <i>MLLT1, ENL, MLLT10, MLLT4, MLLT6, CT45A4</i> | <2 | TLX/ ETP-ALL | (38, 173) |
| <i>SET (HOXA act.)</i> | <i>NUP214</i> | 2 | TLX/ ETP-ALL | (29, 30, 174) |
| <i>SP11</i> | <i>STMN1, TCF7</i> | <1 | ETP-ALL (post-ETP) | (40) |
| <i>RUNX1</i> | <i>AFF3, EVX</i> | <1 | ETP-ALL | (29, 37) |
| <i>ABL1</i> | <i>BCR, EML1, ZMIZ1, NUP214 (episomal), SLC9A3R1, ETV6, MBNL1, ZBTB16*</i> | <1 | ETP-ALL/*TALLMO | (29, 38, 39, 175-185) |
| <i>ETV6</i> | <i>JAK2, NCOA2, INO80D, ABL1, CTNNB1</i> | <1 | ETP-ALL | (37, 38) |
| <i>MLLT10 (HOXA act.)</i> | <i>PICALM, XPO1, NAP1L1, DDX3X, KTM2A, FAM17A1, CAPS2, HNRNP11</i> | | TLX/ ETP-ALL | (29, 37-39, 186) |
| <i>NUP214</i> | <i>ABL1 (episomal), SET, SQSTM1</i> | 6 | ETP-ALL | (37) |
| <i>NUP98</i> | <i>RAP1GDS1, CCDC28A, LNP1, PSIP1, DDX10, VRK1</i> | <2 | ETP-ALL | (38, 39) |

**ABL1-ZBTB16* rearrangements found in 2 TALLMO patients; **unpublished unique rearrangement

Immature subtype (ETP-ALL)

Immature T-ALL patients are characterized by high expression levels of *BCL2*, *LYL1*, *LMO2*, *HHEX* and *MEF2C*, reflecting activation of self-renewal genes that are also expressed in hematopoietic stem cells (29, 31). This profile matched with the immature T-ALL entity that was identified based on its resemblance to normal early thymocyte progenitor cells (ETP) (32-34). This subtype was accordingly denoted ETP-ALL. In-depth molecular-cytogenetic analysis of immature/ETP-ALL patient samples revealed unique rearrangements of the *MEF2C* transcription factor in some patients while others contained *ETV6*-coupled fusions of the *MEF2C* co-factor *NCOA2/TIFF* (29, 35, 36). Rearrangements that affect other *MEF2C* transcriptional regulators—including *SPI1*, *NKX2.5* and a *RUNX1-AFF3* fusion product—have also been reported in ETP-ALL (**Table 1**) (29).

Since the introduction of next-generation sequencing, various additional fusions have been identified in ETP-ALL patients affecting *ETV6*, *KTM2A*, *RUNX1*, *ABL*, *MLLT10*, *NUP214* and *NUP98* (**Table 1**) (37-39). A Japanese study on 121 pediatric T-ALL cases identified recurrent *SPI1* (encoding PU.1) fusions including *STMN1-SPI1* and *TCF7-SPI1* fusions in ETP-ALL patients that highly expressed *MEF2C*, *HHEX*, *FLT3* and *ckIT* (40). In contrast to most other ETP-ALL patients (37), ETP-ALL cases bearing *SPI1* fusion products were characterized by recurrent activating *NOTCH1* mutations (40). Some ETP-ALL patients bear rearrangements that result in the activation of various members of the *HOXA* gene cluster (**Table 1**, *HOXA* act). Such *HOXA*-positive ETP-ALL patients were related to high intrinsic chemo-resistance and very poor outcome in the French GRAALL-2003 and -2005 studies (41, 42).

TLX subtype

Most patients that cluster in the TLX subtype are characterized by *TLX3* rearrangements (29). Whereas some patients express the $\gamma\delta$ TCR, other TLX patients have a more immature phenotype that lack TCR surface expression suggesting that this disease entity is associated with early $\gamma\delta$ lineage of development (43, 44). The TLX cluster also comprises patients with *HOXA*-activating events including *SET-NUP214*, *PICALM-MLLT10* or *MLL* fusion products (29, 38).

TLX3 rearrangements mostly reposition the *TLX3* oncogene from 5q35 in close proximity to the *BCL11B* enhancer at 14q32, thereby inactivating one functional allele of the *BCL11B* haplo-insufficient tumor suppressor gene (27, 45). *BCL11B* is a critical transcription factor that commits early developing thymocytes to the $\alpha\beta$ lineage of T-cell development (46-48). *TLX3-BCL11B* rearrangements may therefore impair $\alpha\beta$ differentiation potential and

consequently drive differentiation towards the $\gamma\delta$ lineage. Some TLX patients also inactivate the second, non-rearranged *BCL11B* allele that may further block $\alpha\beta$ lineage commitment potential (49-51). TLX3 itself may also switch off the TCR $\alpha\beta$ lineage program. As a strong repressor (52), TLX3 represses the *TRCA* enhancer in an ETS-dependent fashion thereby limiting *TCRA* recombination events (53). As a significant number of *TLX3*-rearranged cases express cytoplasmic TCRB (44), it cannot be ruled out that *TLX3-BCL11B* rearrangements may initially have occurred in $\alpha\beta$ lineage cortical thymocytes that subsequently diverged towards the $\gamma\delta$ lineage as a consequence of BCL11B insufficiency and/or TLX3 expression (54). Some early studies reported an association of *TLX3* rearrangements with poor outcome (16, 26, 55-58), but no such association has been reported for patients treated on contemporary treatment protocols.

Proliferative subtype

T-ALL patients that express a proliferative gene signature are frequently characterized by *TLX1* or *NKX2-1* translocations (29). Historically, *TLX1* translocated patients have been associated with superior outcome compared to patients from other T-ALL subtypes (16, 59-61). *TLX1* translocation breakpoints mostly occur downstream of *TLX1*, coupling the *TCRB* enhancer downstream of *TLX1* in *TCRB*-translocated patients. However, in *TCRAD* translocated patients the *TLX1* genomic breaks are positioned upstream and positions *TLX1* behind promoters of *TCRAD* V-gene segments, possibly because the *TCRAD* enhancer is repressed by TLX1 similar to the repressor function of TLX3 (53). Various patients of the proliferative cluster contain translocations or inversions involving the *NKX2-1* or the homologous *NKX2-2* homeobox genes (29). In these patients, ectopic *NKX2-1/2-2* oncogene expression levels are driven as consequence of their close proximities to *TCRB* or *TCRAD* enhancers (29). The presence of recurrent *NKX2-1* aberrations in T-ALL has been confirmed in other studies (39, 62). Remarkably, most *TLX1*-rearranged patients also express low levels of *NKX2-1* in the absence of *NKX2-1* rearrangements implying direct regulation of *NKX2-1* by TLX1 (29).

TALLMO subtype

Patients with a TALLMO gene expression profile represent nearly half of all pediatric T-ALL patients (26, 28, 29, 38). Just as in normal hematopoietic erythroid precursors, TAL1 and TAL2 proteins form transcription complexes with E2A/HEB, RUNX1, GATA3, and MYB co-factors that are bridged by LMO1 or LMO2 in these T-ALL cells (63, 64). In addition to recurrent *TAL1* translocations or *SIL-TAL1* deletions that drive ectopic TAL1 expression, other TALLMO patients bear alternative *TCRB* or *TCRAD* rearrangements that ectopically drive

TAL2, *LYL1*, *LMO1*, *LMO2* or *LMO3* oncogenes (6, 26, 28, 29, 65-71). Almost a quarter of all TALLMO patients harbor a combination of 2 different aberrations that affect both members of *TAL1* and *LMO2* gene families. In addition, small insertion/deletion (INDEL) mutations have recently been identified that create strong MYB binding sites in or upstream of *TAL1*, *LMO1* or *LMO2* loci in nearly 6 percent of pediatric/young adult T-ALL patients (38). Recruitment of MYB at these sites results in the assembly of a TAL1 super-enhancer complex that strongly drives oncogene expression (72-75).

Non-driver mutations in T-ALL

In addition to the driving oncogenes or oncogene fusion products that characterize the four predominant T-ALL subtypes and that are denoted type A aberrations (76), various other recurrent aberrations including point- or INDEL mutations, chromosomal gains and losses have been described for T-ALL (19, 20, 23, 24). These aberrations are not necessarily disease-initiating events as they mostly appear in leukemia subclones (76). These mutations were accordingly denoted as type B mutations. These mutations provide advantages for oncogenesis, disease progression, relapse, or induce therapy resistance. Historic research and recent next-generation sequencing studies have now revealed over 100 genes that are recurrently mutated, amplified or deleted in T-ALL (**Table 2**) (37-39, 77-80). The majority of these genetic alterations impact on cell cycle by inactivating cell cycle inhibitors or by loss of *Rb* (38), or ectopically activate signaling pathways that are important for T-cell development including NOTCH1 (81-85), cytokine signaling cascades (86-90) or their downstream pathways (91-95). Other mutations frequently involve (in)activation of transcriptional regulators, epigenetic reprogramming enzymes, components of ribosomes that affect protein translation, protein-modifying enzymes, or genes that are involved in the chromatin architecture and DNA looping, DNA repair or DNA synthesis. An overview of all mutations is listed in **Table 2**, along with the cellular processes they affect and notable associations.

Table 2. Mutations in cellular pathways or processes in T-ALL.

| Process/ Pathway | Genes | Associations | Therapeutic compounds | Ref |
|---------------------------------|--|--------------------------------|--------------------------------------|--|
| Cell cycle | CDKN2A/B, CDKN1B, CDKN1C, CCND3, RB | Low in ETP-ALL | CDK4/6 inhibitors | (28, 38-40, 78, 80, 92, 171) |
| NOTCH signaling | NOTCH1, FBXW7 | GPR, favorable | NOTCH inhibitors | (38-40, 78, 80-85, 186-190) |
| IL7R-JAK-STAT | IL7Ra, JAK1, JAK3, PTPN2, STAT5B | Steroid resistance | JAK, MEK or PIM1 inhibitors | (37-40, 78, 80, 88, 89, 113-119, 150, 189, 191-194) |
| RAS-MEK-ERK | N/K-RAS, NF1, PTPN11, BRAF | Steroid resistance | MEK-inhibitors | (37-40, 78, 80, 93, 113, 114, 120) |
| PI3K-AKT | PIK3R1, PIK3CA, PIK3CD, AKT | Poor | AKT or mTOR inhibitor | (38, 40, 78, 92, 113) |
| PTEN | PTEN | Poor, therapy failure, relapse | PI3K, AKT or mTOR inhibitors | (38-40, 91, 92, 95, 108, 109, 111, 112, 114, 191, 195-197) |
| Receptors and kinases | ABL1, ALK, cKIT, FLT3, FAT1, ECTZL, SH2B3 | x | ABL-class tyrosine kinase inhibitors | (37, 38, 40, 77, 78, 80, 86, 87, 97, 198, 199) |
| Transcription factors | RUNX1, ETV6, BCL11B, WT1, PHF6, TCF7, LEF1, CTNNB1, GATA3, IKZF1, MYC, MYB, CREBBP, MLLT10 | x | BET inhibitors | (29, 37-40, 49, 50, 52, 78, 80, 168, 169, 200-203) |
| Transcription co-factors | EP300, MED12, SMARCA4, ATRX, CNOT1, CNOT3, CNOT6 | x | x | (38-40, 78, 80, 204) |
| Polycomb complex | EED, SUZ12, EZH2, ASXL1 | x | x | (37, 39, 40, 80, 200, 205) |
| Epigenetic enzymes | KDM6A, SETD2, KMT2A, KMT2D, KMT2C, DNMT3A, IDH1, IDH2 | x | HDAC or methyltransferase inhibitors | (37-40, 77, 78, 103, 198, 200) |
| Ribosomes | RPL5, RPL0, RPL22, del6q | x | ABT-199 | (38-40, 78, 204, 206-209) |
| Protein stability | USP7, USP9X | x | Bortezomib | (38-40, 80, 200) |
| Chromatine remodeling | CTCF | x | x | (38-40, 80) |
| DNA repair | P53, P53BP1, ATM, MSH2, MSH6, PMS2 | x | x | (38-40, 78, 80, 93) |
| Adhesion | DNM2 | x | x | (37-40, 78, 80, 198, 210, 211) |
| Steroid receptor | NR3C1 | x | x | (78, 98) |
| Therapy resistance | NT5C2 | Only observed in relapse | x | (40, 80, 212) |
| Apoptosis | BCL2 protein expression* | ETP-ALL | ABT-199, ABT-737 | (78, 213-216) |

* No mutations for BCL2 have been reported

While type B mutations occur in all T-ALL subtypes, ETP-ALL patients typically harbor the highest mutational load compared to the other subtypes (37, 78) and have been associated with an inferior steroid response (96). ETP-ALL is distinguished from other subtypes in the genetic landscape by the relative enrichment of specific type B events, which includes activating mutations in the tyrosine kinase receptor gene *FLT3*, mutations in the IL-7R (interleukin-7 receptor) signaling pathway (i.e. in *IL7R*, *JAK1* and/or *JAK3*) or recurrent 5q-deletions that affect the *NR3C1* gene locus (37, 97, 98). In contrast, ETP-ALL patients have a lower frequency of deletions affecting cell cycle regulators including *CDKN2A/B*, *CDKN1B* or *CDKN1C* and have lower incidences of NOTCH1-activating mutations (38, 40, 78). Although ETP-ALL was initially associated with extremely poor outcome (32, 90, 99-104), treatment intensification in contemporary risk-adapted treatment protocols has improved outcome for ETP-ALL patients and is now comparable to the outcome of other T-ALL patients (33, 105-107). The only exception is the *HOXA*-activated ETP-ALL group that still has a very poor outcome (41, 42). Other type B events that cluster with specific T-ALL subtypes include strong NOTCH1-activating mutations in *TLX3*-rearranged ALL, and activating *PIK3R1* or *PIK3CG* events, *PTEN*-inactivating mutations and inactivating *USP7* mutations in TALLMO subtype patients (**Table 2**). In contrast to NOTCH1-activating mutations, *PTEN*-inactivating events have been associated with poor outcome in various studies (78, 92, 95, 108-111) but not in the MRC UKALL2003 cohort (112).

Mutations in genes encoding various IL-7R signaling molecules (i.e. *IL7R*, *JAK1/3*, *STAT5B*, *N/KRAS* or *AKT*) have been found in nearly 35% of pediatric T-ALL patients and are associated with inferior event free survival (37-40, 78, 80, 88, 89, 93, 113-121). These pathway mutations are predominantly found in ETP-ALL and TLX subtypes and occur in a near mutually exclusive manner (78, 113). Moreover, JAK-STAT and RAS/PTEN alterations are often identified in chemorefractory patients, and identified in higher frequencies at disease relapse. Similar to mutations affecting *IL7R*, these mutations predict for very poor outcome of relapsed T-ALL (80, 122). One of the explanations for this is that aberrant IL-7R signaling results in increased cellular resistance towards steroid treatment (78).

Combined omic-based targeted therapies: opportunities in T-ALL

Contemporary multi-agent and risk-adapted protocols have boosted survival rates to approximately 80 percent, with the number of toxic deaths now almost equaling the number of patients that relapse (123). This proves that further treatment intensification is not feasible and there is an urgent need for targeted compounds in individualized treatment protocols for high-risk T-ALL patients. Given our profound understanding of pathogenic drivers and

mutations in T-ALL, various targeted compounds could be implemented in the near future to improve outcome for refractory/relapsed T-ALL and may allow implementation in first-line treatment for high-risk T-ALL patients in the future.

Roughly 50% of all pediatric cancer patients present with a potentially druggable genetic event, with aberrations in NOTCH-, mitogen-activated protein kinase (MAPK)-, or receptor tyrosine kinase (RTK)-signaling and cell cycle control as potential targets for future T-ALL treatment regimens (124). The question remains whether introduction of single targeted compounds in current chemotherapy backbones will improve treatment outcome. In adult metastasized carcinoma patients genomics-directed treatment strategies only yielded minimal prognostic benefits (125-127). The effect of single targeted compound treatment might be disappointing in T-ALL since many of the targetable processes are the result of type B mutations that are frequently found at subclonal levels (128). Targeted inhibition should therefore not be expected to eradicate the complete leukemic burden. However, some subclonal mutations give rise to therapy resistance and could therefore still serve as essential targets for therapy. In the case of IL-7R pathway mutations, MEK and AKT are attractive targets for selective inhibitors that synergize with steroid treatment (78). Moreover, mutated subclones may actually reflect pathway dependency and/or drug sensitivity of the entire leukemic population. Therefore, the effect of combined treatment could extend beyond the elimination of mutated cells. For example, this has been implemented in the phase1/2 SeluDex trial in which dexamethasone treatment is given in combination with the MEK-inhibitor Selumetinib for relapse or refractory RAS-mutant BCP-ALL (129) and is now open for relapsed/refractory T-ALL patients as well.

The observed benefit of combining targeted treatment with standard chemotherapeutics may extend beyond the treatment of patients that harbor specific (subclonal) mutations. Loh *et al.* demonstrated that in two out of three high risk-ALL cases no somatic mutations could be identified in tyrosine kinase-coding genes, despite their gene expression profiles that point to active kinase signaling (130). This indicates that patients with activated kinase signaling benefit from targeted therapy, especially those who lack druggable genetic targets. To decipher the full pathogenic program and to pinpoint novel biomarkers for both therapy and prognosis, an integrated approach that combines data on the genomic, transcriptomic and proteomic level may be required to identify additional druggable targets (131). This so-called 'multi-omic' approach could reveal other tumor targets, and therefore provides an opportunity to increase the detail and complexity of basket-trials for small numbers of patients or for individualized patient treatment programs (132)

(**Figure 1**). Refinement of treatment strategies, as a direct consequence of this advanced screening approach, could consequently improve outcome. Since for most hematological malignancies sufficient patient material can be obtained at diagnosis, testing on these three levels indeed seems feasible for T-ALL. In the next two paragraphs, we will highlight the current progress and application of transcriptome sequencing and proteomics in ALL.

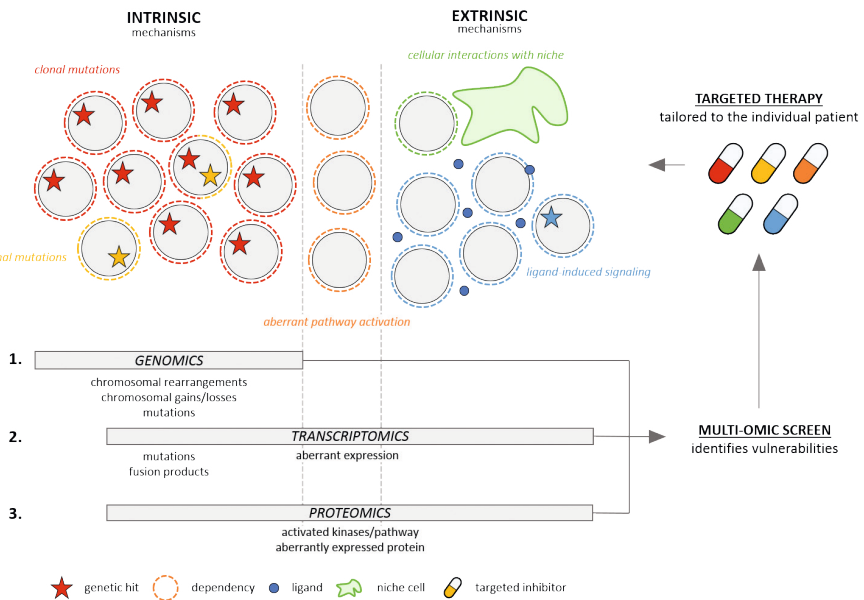


Figure 1. Intrinsic mechanisms (e.g. by genetic hits (stars)), extrinsic mechanisms (e.g. by interaction with niche (green) or ligand-induced (blue)) and aberrant pathway activation with unknown cause (orange) involved in disease initiation, maintenance or drug resistance that may be observed in leukemic blasts. Integration of genomics, transcriptomics and proteomics identifies the vulnerabilities caused by these pathogenic events. As a result, it allows for the precise use of targeted compounds that (in combination with standard chemotherapeutics) can enhance treatment effectiveness and ultimately may improve survival.

Integration of transcriptome sequencing

In the last few years, great technological advances in sequencing have been applied not only to DNA analysis but to RNA as well. RNA-sequencing of the leukemia transcriptome has a prominent role in the identification of novel splice variants and fusion transcripts that drive or sustain tumorigenesis. As mentioned before, RNA-sequencing studies have led to the discovery of various novel and cryptic fusion transcripts in T-ALL (39, 122, 133) and T-lymphoblastic lymphoma patients (134) that had not been identified earlier by genome sequencing or molecular-cytogenetic tests. The Total XVII protocol (NTC03117751) for the treatment of ALL at the St. Jude children's hospital integrates information from RNA

sequencing with RT-PCR or FISH to detect potential druggable fusions at diagnosis that are then used for therapy stratification. While the pipeline for fusion detection from RNA-seq data will give results already at day 15 of the induction therapy, additional whole-genome sequencing information is available only at later stages of the treatment (135).

Cancer cells rely on altered mechanisms of signal transduction that boost cell cycle progression and proliferation (136). When pathological pathway activation is not predicted by genomic aberrations, different approaches like transcriptome sequencing will be required to identify the *Achilles' heel* of the disease. Quantitative measurement of pathway activity inferred from target gene mRNA levels have been developed for various signaling pathways, e.g. the Oncosignal platform by Philips Healthcare, and provides a molecular phenotype of the tumor (137-140). It generates an automated and reliable quantitative readout of specific pathways that are highly activated in malignant cells that can support the choice of relevant small-molecule inhibitors. Furthermore, it can potentially predict therapy resistance due to the activation of compensatory/escape mechanisms.

Integration of proteomics

An additional way to discover novel oncogenic dependencies or identify new biomarkers is to analyze the cancer proteome. Mass spectrometry-based global proteomic analyses have been pivotal in the identification of changes in protein expression as well as in post-translational modifications, in particular phosphorylation (141, 142). These changes at the phospho-protein level reflect altered signal transduction that cannot be detected at the DNA or RNA level. Protein kinases are one of the major effectors of signal transduction. Nevertheless, direct quantification of activity levels of kinases has been challenging and requires *a priori* knowledge of the enzyme of interest. In the past decade, an increasing interest in post-translational modifications and their role in cancer led to development of workflows for the identification of alterations in protein phosphorylation levels as functional readout for enzyme hyper-activity. High-throughput phospho-proteome data can therefore provide direct information on pathway signaling.

In 2013, Casado *et al.* demonstrated that kinase activity inferred from analysis of global phospho-proteome data of different hematological cancer cell lines correlates with differential drug responses (143). Phospho-proteomic analyses have also been applied to the identification of putative therapy response biomarkers in ALL (reviewed in (144, 145)). In T-ALL, the phospho-proteomic studies investigating signal transduction have been limited to either a kinome microarray system—identifying differentially phosphorylated peptides

for pediatric B-ALL versus T-ALL samples (146)—or by using Reverse-Phase Protein Array (RPPA) that identified hyper-activation of the mTOR/STAT3 and LCK/calceurin axes in pediatric ETP-ALL (147). Based on the latter study, the authors suggested LCK hyper-activity as possible resistance factor for steroid treatment in T-ALL (148). Both kinome array and RPPA are valuable tools but can only detect changes in a subset of pre-defined proteins and therefore do not allow for screening of the entire (phospho)proteome. Unbiased mass spectrometry-based phospho-proteomic studies dedicated to T-ALL are necessary to unravel specific pathological signaling pathways and escape mechanisms. The identification and the degree of pathway activation with subsequent downstream effects will provide a rationale for therapy stratification and will lead to the identification of novel disease specific- or individualized biomarkers (149).

Functional screening into practice: IL-7R-signaling and steroid resistance

IL-7R pathway activation by interleukin-7 (IL-7) even in the absence of IL-7R pathway mutations has also been shown to confer steroid resistance in T-ALL patients (96, 150). This indicates that pathway activation (and subsequent drug responsiveness) can depend on the availability of growth factors, and may provide an underlying mechanism for increased therapy resistance for local, niche embedded leukemia cells. For patients that present with this so called 'IL-7 dependent steroid resistance' (150), pathway inhibition by combined MEK or AKT inhibition with steroid treatment to restore steroid sensitivity may be equally effective as for patients that harbor IL-7R pathway mutations. Increase in the phosphorylation of STAT5 or the activation of downstream STAT5 target genes following IL-7 stimulation are important biomarkers to identify these patients for whom integration of phospho-proteomics and transcriptomics at diagnosis is needed.

Both proteomic and transcriptomic analyses have identified novel treatment targets or biomarkers that represent pathway activation downstream of the IL-7R before. For example, phospho-proteomic profiling of JAK3 mutated leukemia cells—that signal downstream of the IL-7R but do not impair steroid sensitivity in contrast to JAK1 mutations (78)—identified non-JAK-STAT druggable targets that were affected by mutant JAK3 signaling (151). Combined pathway inhibition of these targets with Ruxolitinib or Tofacitinib (JAK-inhibitors) worked synergistically *in vitro* and *in vivo* (151), indicating that proteomic profiling serves as a powerful tool to improve personalized medicine. Additionally, transcriptional and epigenetic research identified that the STAT5B^{N642H} mutation—which leads to strong STAT5B pathway activation—increases its binding at regions that are also bound by epigenetic regulators such as EZH2 and SUZ12 (118, 119, 152). STAT5B^{N642H} expressing T-cells showed a higher

expression level and activity of the EZH2 target gene Aurora kinase B (*Aurkb*), yielding sensitivity for treatment with a specific Aurora Kinase B inhibitor (AT9283) (152). High *PIM1* expression downstream of STAT5 signaling has also been identified by transcriptional analysis, and PIM1 inhibition was demonstrated effective in (IL-7 mediated) JAK-STAT activated leukemias (153-155).

The observations for JAK3 and STAT5 illustrate that pathway activation and dependency, as measured by proteomic and transcriptomic approaches, predict sensitivity to selective inhibitors and may improve outcome by optimization of personalized medicine. Additionally, screening at multiple levels provides additional biomarkers that can be used for targeted therapy regardless of signaling mutations. For example, RNA sequencing could reveal significant *PIM1* overexpression (in the absence of *JAK* or *STAT5B* mutations as determined by genomic screening) and could therefore provide a rationale for treatment with a selective PIM1-inhibitor for individual patients. As another example, phospho-proteomic results that point to activation of the AKT pathway in a T-ALL patient vouches for combination treatment with an AKT-inhibitor. Thus, 'multi-omics' screening approaches will excel the choice of targets to inhibit in personalized medicine. It will help clinicians to individualize treatment and optimize basket-trials in refractory/relapsed T-ALL patients. Moreover, a multi-omics functional screening with subsequent therapeutic consequences at the start of treatment might prevent (early) relapse, therefore significantly increasing the survival rate of T-ALL patients.

Concluding remarks

Given our profound understanding of genomic aberrations in T-ALL, we can now successfully identify oncogenic driving lesions in nearly 80% of T-ALL patients (**Table 1**). Additionally, patients frequently present with non-driver mutations at the subclonal level for which some relate to inferior outcome or therapy resistance (**Table 2**). At present, the majority of small-molecule inhibitors that could be applied in clinical trials target these subclonal mutations and may offer therapeutic effect if the mutation in the subclone is indicative for a vulnerability of the total leukemic population. Genomic screening in T-ALL should therefore not only focus on driving events, but also on identifying genetic aberrations for which a selective inhibitor combined with standard chemotherapeutics drugs can lead to a maximal treatment response. Integration of genomic sequencing, RNA sequencing and phospho-proteomics in a 'multi-omics' functional screening will uncover the complete *Achilles' heel* of the leukemia, allowing great improvement of personalized medicine and eventually patient outcome as a result of the precise use of targeted compounds (**Figure 1**).

DECLARATION OF INTERESTS

None.

FUNDING

This study received funding by Stichting Kinderen Kankervrij (KiKa219 and KiKa295) and KWF Kankerbestrijding (KWF2016_10355).



REFERENCES

1. Bene MC, Castoldi G, Knapp W, Ludwig WD, Matutes E, Orfao A, et al. Proposals for the immunological classification of acute leukemias. European Group for the Immunological Characterization of Leukemias (EGIL). *Leukemia*. 1995;9(10):1783-6.
2. Pui CH, Behm FG, Crist WM. Clinical and biologic relevance of immunologic marker studies in childhood acute lymphoblastic leukemia. *Blood*. 1993;82(2):343-62.
3. Nihues T, Kapaun P, Harms DO, Burdach S, Kramm C, Korholz D, et al. A classification based on T cell selection-related phenotypes identifies a subgroup of childhood T-ALL with favorable outcome in the COALL studies. *Leukemia*. 1999;13(4):614-7.
4. Begley CG, Aplan PD, Davey MP, Nakahara K, Tchorz K, Kurtzberg J, et al. Chromosomal translocation in a human leukemic stem-cell line disrupts the T-cell antigen receptor delta-chain diversity region and results in a previously unreported fusion transcript. *Proc Natl Acad Sci U S A*. 1989;86(6):2031-5.
5. Finger LR, Kagan J, Christopher G, Kurtzberg J, Hershfield MS, Nowell PC, et al. Involvement of the TCL5 gene on human chromosome 1 in T-cell leukemia and melanoma. *Proc Natl Acad Sci U S A*. 1989;86(13):5039-43.
6. Mellentin JD, Smith SD, Cleary ML. *lyl-1*, a novel gene altered by chromosomal translocation in T cell leukemia, codes for a protein with a helix-loop-helix DNA binding motif. *Cell*. 1989;58(1):77-83.
7. Dube ID, Kamel-Reid S, Yuan CC, Lu M, Wu X, Corpus G, et al. A novel human homeobox gene lies at the chromosome 10 breakpoint in lymphoid neoplasias with chromosomal translocation t(10;14). *Blood*. 1991;78(11):2996-3003.
8. Hatano M, Roberts CW, Minden M, Crist WM, Korsmeyer SJ. Deregulation of a homeobox gene, HOX11, by the t(10;14) in T cell leukemia. *Science*. 1991;253(5015):79-82.
9. Kennedy MA, Gonzalez-Sarmiento R, Kees UR, Lampert F, Dear N, Boehm T, et al. HOX11, a homeobox-containing T-cell oncogene on human chromosome 10q24. *Proc Natl Acad Sci U S A*. 1991;88(20):8900-4.
10. Lu M, Gong ZY, Shen WF, Ho AD. The *tcl-3* proto-oncogene altered by chromosomal translocation in T-cell leukemia codes for a homeobox protein. *EMBO J*. 1991;10(10):2905-10.
11. Dube ID, Raimondi SC, Pi D, Kalousek DK. A new translocation, t(10;14)(q24;q11), in T cell neoplasia. *Blood*. 1986;67(4):1181-4.
12. Brown L, Cheng JT, Chen Q, Siciliano MJ, Crist W, Buchanan G, et al. Site-specific recombination of the *tal-1* gene is a common occurrence in human T cell leukemia. *EMBO J*. 1990;9(10):3343-51.
13. Bernard O, Lecointe N, Jonveaux P, Souyri M, Mauchauffe M, Berger R, et al. Two site-specific deletions and t(1;14) translocation restricted to human T-cell acute leukemias disrupt the 5' part of the *tal-1* gene. *Oncogene*. 1991;6(8):1477-88.
14. Aplan PD, Lombardi DP, Ginsberg AM, Cossman J, Bertness VL, Kirsch IR. Disruption of the human SCL locus by "illegitimate" V-(D)-J recombinase activity. *Science*. 1990;250(4986):1426-9.
15. Macintyre EA, Smit L, Ritz J, Kirsch IR, Strominger JL. Disruption of the SCL locus in T-lymphoid malignancies correlates with commitment to the T-cell receptor alpha beta lineage. *Blood*. 1992;80(6):1511-20.

16. Cave H, Suci S, Preudhomme C, Poppe B, Robert A, Uyttebroeck A, et al. Clinical significance of HOX11L2 expression linked to t(5;14)(q35;q32), of HOX11 expression, and of SIL-TAL fusion in childhood T-cell malignancies: results of EORTC studies 58881 and 58951. *Blood*. 2004;103(2):442-50.
17. Armstrong SA, Look AT. Molecular genetics of acute lymphoblastic leukemia. *J Clin Oncol*. 2005;23(26):6306-15.
18. Look AT. Oncogenic transcription factors in the human acute leukemias. *Science*. 1997;278(5340):1059-64.
19. Meijerink JP, den Boer ML, Pieters R. New genetic abnormalities and treatment response in acute lymphoblastic leukemia. *Semin Hematol*. 2009;46(1):16-23.
20. Belder L, Ferrando A. The genetics and mechanisms of T cell acute lymphoblastic leukaemia. *Nat Rev Cancer*. 2016;16(8):494-507.
21. Raimondi SC, Privitera E, Williams DL, Look AT, Behm F, Rivera GK, et al. New recurring chromosomal translocations in childhood acute lymphoblastic leukemia. *Blood*. 1991;77(9):2016-22.
22. Rubnitz JE, Look AT. Molecular genetics of childhood leukemias. *J Pediatr Hematol Oncol*. 1998;20(1):1-11.
23. Iacobucci I, Mullighan CG. Genetic Basis of Acute Lymphoblastic Leukemia. *J Clin Oncol*. 2017;35(9):975-83.
24. Van Vlierberghe P, Ferrando A. The molecular basis of T cell acute lymphoblastic leukemia. *J Clin Invest*. 2012;122(10):3398-406.
25. Golub TR, Slonim DK, Tamayo P, Huard C, Gaasenbeek M, Mesirov JP, et al. Molecular classification of cancer: class discovery and class prediction by gene expression monitoring. *Science*. 1999;286(5439):531-7.
26. Ferrando AA, Neuberg DS, Staunton J, Loh ML, Huard C, Raimondi SC, et al. Gene expression signatures define novel oncogenic pathways in T cell acute lymphoblastic leukemia. *Cancer Cell*. 2002;1(1):75-87.
27. Bernard OA, Busson-LeConiat M, Ballerini P, Mauchauffe M, Della Valle V, Monni R, et al. A new recurrent and specific cryptic translocation, t(5;14)(q35;q32), is associated with expression of the Hox11L2 gene in T acute lymphoblastic leukemia. *Leukemia*. 2001;15(10):1495-504.
28. Soulier J, Clappier E, Cayuela JM, Regnault A, Garcia-Peydro M, Dombret H, et al. HOXA genes are included in genetic and biologic networks defining human acute T-cell leukemia (T-ALL). *Blood*. 2005;106(1):274-86.
29. Homminga I, Pieters R, Langerak AW, de Rooi JJ, Stubbs A, Verstegen M, et al. Integrated transcript and genome analyses reveal NKX2-1 and MEF2C as potential oncogenes in T cell acute lymphoblastic leukemia. *Cancer Cell*. 2011;19(4):484-97.
30. Van Vlierberghe P, van Grotel M, Tchinda J, Lee C, Beverloo HB, van der Spek PJ, et al. The recurrent SET-NUP214 fusion as a new HOXA activation mechanism in pediatric T-cell acute lymphoblastic leukemia. *Blood*. 2008;111(9):4668-80.
31. McCormack MP, Young LF, Vasudevan S, de Graaf CA, Codrington R, Rabbitts TH, et al. The Lmo2 oncogene initiates leukemia in mice by inducing thymocyte self-renewal. *Science*. 2010;327(5967):879-83.
32. Coustan-Smith E, Mullighan CG, Onciu M, Behm FG, Raimondi SC, Pei D, et al. Early T-cell precursor leukaemia: a subtype of very high-risk acute lymphoblastic leukaemia. *Lancet Oncol*. 2009;10(2):147-56.

33. Zuurbier L, Gutierrez A, Mullighan CG, Cante-Barrett K, Gevaert AO, de Rooij J, et al. Immature MEF2C-dysregulated T-cell leukemia patients have an early T-cell precursor acute lymphoblastic leukemia gene signature and typically have non-rearranged T-cell receptors. *Haematologica*. 2014;99(1):94-102.
34. Bernt KM, Hunger SP, Neff T. The Functional Role of PRC2 in Early T-cell Precursor Acute Lymphoblastic Leukemia (ETP-ALL) - Mechanisms and Opportunities. *Front Pediatr*. 2016;4:49.
35. Nagel S, Meyer C, Quentmeier H, Kaufmann M, Drexler HG, MacLeod RA. MEF2C is activated by multiple mechanisms in a subset of T-acute lymphoblastic leukemia cell lines. *Leukemia*. 2008;22(3):600-7.
36. Strehl S, Nebral K, Konig M, Harbott J, Strobl H, Ratei R, et al. ETV6-NCOA2: a novel fusion gene in acute leukemia associated with coexpression of T-lymphoid and myeloid markers and frequent NOTCH1 mutations. *Clin Cancer Res*. 2008;14(4):977-83.
37. Zhang J, Ding L, Holmfeldt L, Wu G, Heatley SL, Payne-Turner D, et al. The genetic basis of early T-cell precursor acute lymphoblastic leukaemia. *Nature*. 2012;481(7380):157-63.
38. Liu Y, Easton J, Shao Y, Maciaszek J, Wang Z, Wilkinson MR, et al. The genomic landscape of pediatric and young adult T-lineage acute lymphoblastic leukemia. *Nat Genet*. 2017;49(8):1211-8.
39. Chen B, Jiang L, Zhong ML, Li JF, Li BS, Peng LJ, et al. Identification of fusion genes and characterization of transcriptome features in T-cell acute lymphoblastic leukemia. *Proc Natl Acad Sci U S A*. 2018;115(2):373-8.
40. Seki M, Kimura S, Isobe T, Yoshida K, Ueno H, Nakajima-Takagi Y, et al. Recurrent SPI1 (PU.1) fusions in high-risk pediatric T cell acute lymphoblastic leukemia. *Nat Genet*. 2017;49(8):1274-81.
41. Bond J, Machand T, Touzart A, Cieslak A, Trinquand A, Sutton L, et al. An early thymic progenitor phenotype predicts outcome exclusively in HOXA-overexpressing adult T-cell acute lymphoblastic leukemia: a group for research in adult acute lymphoblastic leukemia study. *Haematologica*. 2016;this issue.
42. Ben Abdelali R, Asnafi V, Petit A, Micol JB, Callens C, Villarese P, et al. The prognosis of CALM-AF10-positive adult T-cell acute lymphoblastic leukemias depends on the stage of maturation arrest. *Haematologica*. 2013;98(11):1711-7.
43. Berger R, Dastugue N, Busson M, Van Den Akker J, Perot C, Ballerini P, et al. t(5;14)/HOX11L2-positive T-cell acute lymphoblastic leukemia. A collaborative study of the Groupe Francais de Cytogenetique Hematologique (GFCH). *Leukemia*. 2003;17(9):1851-7.
44. van Grotel M, Meijerink JP, van Wering ER, Langerak AW, Beverloo HB, Buijs-Gladdines JG, et al. Prognostic significance of molecular-cytogenetic abnormalities in pediatric T-ALL is not explained by immunophenotypic differences. *Leukemia*. 2008;22(1):124-31.
45. Li L, Zhang JA, Dose M, Kueh HY, Mosadeghi R, Gounari F, et al. A far downstream enhancer for murine Bcl11b controls its T-cell specific expression. *Blood*. 2013;122(6):902-11.
46. Li L, Leid M, Rothenberg EV. An early T cell lineage commitment checkpoint dependent on the transcription factor Bcl11b. *Science*. 2010;329(5987):89-93.
47. Li P, Burke S, Wang J, Chen X, Ortiz M, Lee SC, et al. Reprogramming of T cells to natural killer-like cells upon Bcl11b deletion. *Science*. 2010;329(5987):85-9.
48. Yui MA, Feng N, Rothenberg EV. Fine-scale staging of T cell lineage commitment in adult mouse thymus. *J Immunol*. 2010;185(1):284-93.
49. De Keersmaecker K, Real PJ, Gatta GD, Palomero T, Sulis ML, Tosello V, et al. The TLX1 oncogene drives aneuploidy in T cell transformation. *Nat Med*. 2010;16(11):1321-7.

50. Gutierrez A, Kentsis A, Sanda T, Holmfeldt L, Chen SC, Zhang J, et al. The BCL11B tumor suppressor is mutated across the major molecular subtypes of T-cell acute lymphoblastic leukemia. *Blood*. 2011;118(15):4169-73.
51. Wakabayashi Y, Watanabe H, Inoue J, Takeda N, Sakata J, Mishima Y, et al. Bcl11b is required for differentiation and survival of alphabeta T lymphocytes. *Nat Immunol*. 2003;4(6):533-9.
52. Della Gatta G, Palomero T, Perez-Garcia A, Ambesi-Impiombato A, Bansal M, Carpenter ZW, et al. Reverse engineering of TLX oncogenic transcriptional networks identifies RUNX1 as tumor suppressor in T-ALL. *Nat Med*. 2012;18(3):436-40.
53. Dadi S, Le Noir S, Payet-Bornet D, Lhermitte L, Zacarias-Cabeza J, Bergeron J, et al. TLX homeodomain oncogenes mediate T cell maturation arrest in T-ALL via interaction with ETS1 and suppression of TCRalpha gene expression. *Cancer Cell*. 2012;21(4):563-76.
54. Asnafi V, Beldjord K, Libura M, Villarese P, Millien C, Ballerini P, et al. Age-related phenotypic and oncogenic differences in T-cell acute lymphoblastic leukemias may reflect thymic atrophy. *Blood*. 2004;104(13):4173-80.
55. Ballerini P, Blaise A, Busson-Le Coniat M, Su XY, Zucman-Rossi J, Adam M, et al. HOX11L2 expression defines a clinical subtype of pediatric T-ALL associated with poor prognosis. *Blood*. 2002;100(3):991-7.
56. Gottardo NG, Jacoby PA, Sather HN, Reaman GH, Baker DL, Kees UR. Significance of HOX11L2/TLX3 expression in children with T-cell acute lymphoblastic leukemia treated on Children's Cancer Group protocols. *Leukemia*. 2005;19(9):1705-8.
57. Mauvieux L, Leymarie V, Helias C, Perrusson N, Falkenrodt A, Lioure B, et al. High incidence of Hox11L2 expression in children with T-ALL. *Leukemia*. 2002;16(12):2417-22.
58. van Grotel M, Meijerink JP, Beverloo HB, Langerak AW, Buys-Gladdines JG, Schneider P, et al. The outcome of molecular-cytogenetic subgroups in pediatric T-cell acute lymphoblastic leukemia: a retrospective study of patients treated according to DCOG or COALL protocols. *Haematologica*. 2006;91(9):1212-21.
59. Ferrando AA, Neuberg DS, Dodge RK, Paietta E, Larson RA, Wiernik PH, et al. Prognostic importance of TLX1 (HOX11) oncogene expression in adults with T-cell acute lymphoblastic leukaemia. *Lancet*. 2004;363(9408):535-6.
60. Kees UR, Heerema NA, Kumar R, Watt PM, Baker DL, La MK, et al. Expression of HOX11 in childhood T-lineage acute lymphoblastic leukaemia can occur in the absence of cytogenetic aberration at 10q24: a study from the Children's Cancer Group (CCG). *Leukemia*. 2003;17(5):887-93.
61. Schneider NR, Carroll AJ, Shuster JJ, Pullen DJ, Link MP, Borowitz MJ, et al. New recurring cytogenetic abnormalities and association of blast cell karyotypes with prognosis in childhood T-cell acute lymphoblastic leukemia: a pediatric oncology group report of 343 cases. *Blood*. 2000;96(7):2543-9.
62. La Starza R, Lettieri A, Pierini V, Nofrini V, Gorello P, Songia S, et al. Linking genomic lesions with minimal residual disease improves prognostic stratification in children with T-cell acute lymphoblastic leukaemia. *Leuk Res*. 2013;37(8):928-35.
63. Hsu HL, Wadman I, Baer R. Formation of in vivo complexes between the TAL1 and E2A polypeptides of leukemic T cells. *Proc Natl Acad Sci U S A*. 1994;91(8):3181-5.
64. Porcher C, Chagraoui H, Kristiansen MS. SCL/TAL1: a multifaceted regulator from blood development to disease. *Blood*. 2017;129(15):2051-60.
65. Van Vlierberghe P, van Grotel M, Beverloo HB, Lee C, Helgason T, Buijs-Gladdines J, et al. The cryptic chromosomal deletion del(11)(p12p13) as a new activation mechanism of LMO2 in pediatric T-cell acute lymphoblastic leukemia. *Blood*. 2006;108(10):3520-9.



66. Homminga I, Vuerhard MJ, Langerak AW, Buijs-Gladdines J, Pieters R, Meijerink JP. Characterization of a pediatric T-cell acute lymphoblastic leukemia patient with simultaneous LYL1 and LMO2 rearrangements. *Haematologica*. 2012;97(2):258-61.
67. Simonis M, Klous P, Homminga I, Galjaard RJ, Rijkers EJ, Grosveld F, et al. High-resolution identification of balanced and complex chromosomal rearrangements by 4C technology. *Nat Methods*. 2009;6(11):837-42.
68. Hammond SM, Crable SC, Anderson KP. Negative regulatory elements are present in the human LMO2 oncogene and may contribute to its expression in leukemia. *Leuk Res*. 2005;29(1):89-97.
69. McGuire EA, Hockett RD, Pollock KM, Bartholdi MF, O'Brien SJ, Korsmeyer SJ. The t(11;14)(p15;q11) in a T-cell acute lymphoblastic leukemia cell line activates multiple transcripts, including Ttg-1, a gene encoding a potential zinc finger protein. *Mol Cell Biol*. 1989;9(5):2124-32.
70. Nam CH, Rabbitts TH. The role of LMO2 in development and in T cell leukemia after chromosomal translocation or retroviral insertion. *Mol Ther*. 2006;13(1):15-25.
71. Royer-Pokora B, Loos U, Ludwig WD. TTG-2, a new gene encoding a cysteine-rich protein with the LIM motif, is overexpressed in acute T-cell leukaemia with the t(11;14)(p13;q11). *Oncogene*. 1991;6(10):1887-93.
72. Li Z, Abraham BJ, Berezovskaya A, Farah N, Liu Y, Leon T, et al. APOBEC signature mutation generates an oncogenic enhancer that drives LMO1 expression in T-ALL. *Leukemia*. 2017.
73. Rahman S, Magnussen M, Leon TE, Farah N, Li Z, Abraham BJ, et al. Activation of the LMO2 oncogene through a somatically acquired neomorphic promoter in T-cell acute lymphoblastic leukemia. *Blood*. 2017.
74. Sengupta S, George RE. Super-Enhancer-Driven Transcriptional Dependencies in Cancer. *Trends Cancer*. 2017;3(4):269-81.
75. Mansour MR, Abraham BJ, Anders L, Berezovskaya A, Gutierrez A, Durbin AD, et al. Oncogene regulation. An oncogenic super-enhancer formed through somatic mutation of a noncoding intergenic element. *Science*. 2014;346(6215):1373-7.
76. Van Vlierberghe P, Pieters R, Beverloo HB, Meijerink JP. Molecular-genetic insights in paediatric T-cell acute lymphoblastic leukaemia. *Br J Haematol*. 2008;143(2):153-68.
77. Van Vlierberghe P, Ambesi-Impiombato A, Perez-Garcia A, Haydu JE, Rigo I, Hadler M, et al. ETV6 mutations in early immature human T cell leukemias. *J Exp Med*. 2011;208(13):2571-9.
78. Li Y, Buijs-Gladdines JG, Cante-Barrett K, Stubbs AP, Vroegindeweij EM, Smits WK, et al. IL-7 Receptor Mutations and Steroid Resistance in Pediatric T cell Acute Lymphoblastic Leukemia: A Genome Sequencing Study. *PLoS Med*. 2016;13(12):e1002200.
79. Kunz JB, Rausch T, Bandapalli OR, Eilers J, Pechanska P, Schuessele S, et al. Pediatric T-cell lymphoblastic leukemia evolves into relapse by clonal selection, acquisition of mutations and promoter hypomethylation. *Haematologica*. 2015;100(11):1442-50.
80. Richter-Pechanska P, Kunz JB, Hof J, Zimmermann M, Rausch T, Bandapalli OR, et al. Identification of a genetically defined ultra-high-risk group in relapsed pediatric T-lymphoblastic leukemia. *Blood Cancer J*. 2017;7(2):e523.
81. Weng AP, Ferrando AA, Lee W, Morris JPt, Silverman LB, Sanchez-Irizarry C, et al. Activating mutations of NOTCH1 in human T cell acute lymphoblastic leukemia. *Science*. 2004;306(5694):269-71.
82. Akhondji S, Sun D, von der Lehr N, Apostolidou S, Klotz K, Maljukova A, et al. FBXW7/hCDC4 is a general tumor suppressor in human cancer. *Cancer Res*. 2007;67(19):9006-12.

83. Malyukova A, Dohda T, von der Lehr N, Akhoondi S, Corcoran M, Heyman M, et al. The tumor suppressor gene hCDC4 is frequently mutated in human T-cell acute lymphoblastic leukemia with functional consequences for Notch signaling. *Cancer Res.* 2007;67(12):5611-6.
84. O'Neil J, Grim J, Strack P, Rao S, Tibbitts D, Winter C, et al. FBW7 mutations in leukemic cells mediate NOTCH pathway activation and resistance to gamma-secretase inhibitors. *J Exp Med.* 2007;204(8):1813-24.
85. Thompson BJ, Buonamici S, Sulis ML, Palomero T, Vilimas T, Basso G, et al. The SCFFBW7 ubiquitin ligase complex as a tumor suppressor in T cell leukemia. *J Exp Med.* 2007;204(8):1825-35.
86. Paietta E, Ferrando AA, Neuberger D, Bennett JM, Racevskis J, Lazarus H, et al. Activating FLT3 mutations in CD117/KIT(+) T-cell acute lymphoblastic leukemias. *Blood.* 2004;104(2):558-60.
87. Van Vlierberghe P, Meijerink JP, Stam RW, van der Smissen W, van Wering ER, Beverloo HB, et al. Activating FLT3 mutations in CD4+/CD8- pediatric T-cell acute lymphoblastic leukemias. *Blood.* 2005;106(13):4414-5.
88. Shochat C, Tal N, Bandapalli OR, Palmi C, Ganmore I, te Kronnie G, et al. Gain-of-function mutations in interleukin-7 receptor-alpha (IL7R) in childhood acute lymphoblastic leukemias. *J Exp Med.* 2011;208(5):901-8.
89. Zenatti PP, Ribeiro D, Li W, Zuurbier L, Silva MC, Paganin M, et al. Oncogenic IL7R gain-of-function mutations in childhood T-cell acute lymphoblastic leukemia. *Nat Genet.* 2011;43(10):932-9.
90. Neumann M, Heesch S, Gokbuget N, Schwartz S, Schlee C, Benlasfer O, et al. Clinical and molecular characterization of early T-cell precursor leukemia: a high-risk subgroup in adult T-ALL with a high frequency of FLT3 mutations. *Blood Cancer J.* 2012;2(1):e55.
91. Palomero T, Sulis ML, Cortina M, Real PJ, Barnes K, Ciofani M, et al. Mutational loss of PTEN induces resistance to NOTCH1 inhibition in T-cell leukemia. *Nat Med.* 2007;13(10):1203-10.
92. Gutierrez A, Sanda T, Grebliunaite R, Carracedo A, Salmena L, Ahn Y, et al. High frequency of PTEN, PI3K, and AKT abnormalities in T-cell acute lymphoblastic leukemia. *Blood.* 2009;114(3):647-50.
93. Kawamura M, Ohnishi H, Guo SX, Sheng XM, Minegishi M, Hanada R, et al. Alterations of the p53, p21, p16, p15 and RAS genes in childhood T-cell acute lymphoblastic leukemia. *Leuk Res.* 1999;23(2):115-26.
94. Yamamoto T, Isomura M, Xu Y, Liang J, Yagasaki H, Kamachi Y, et al. PTPN11, RAS and FLT3 mutations in childhood acute lymphoblastic leukemia. *Leuk Res.* 2006;30(9):1085-9.
95. Mendes RD, Sarmento LM, Cante-Barrett K, Zuurbier L, Buijs-Gladdines JG, Povoia V, et al. PTEN microdeletions in T-cell acute lymphoblastic leukemia are caused by illegitimate RAG-mediated recombination events. *Blood.* 2014;124(4):567-78.
96. Maude SL, Dolai S, Delgado-Martin C, Vincent T, Robbins A, Selvanathan A, et al. Efficacy of JAK/STAT pathway inhibition in murine xenograft models of early T-cell precursor (ETP) acute lymphoblastic leukemia. *Blood.* 2015;125(11):1759-67.
97. Neumann M, Coskun E, Fransecky L, Mochmann LH, Bartram I, Sartangi NF, et al. FLT3 mutations in early T-cell precursor ALL characterize a stem cell like leukemia and imply the clinical use of tyrosine kinase inhibitors. *PLoS One.* 2013;8(1):e53190.
98. La Starza R, Barba G, Demeyer S, Pierini V, Di Giacomo D, Gianfelici V, et al. Deletions of the long arm of chromosome 5 define subgroups of T-cell acute lymphoblastic leukemia. *Haematologica.* 2016;101(8):951-8.

99. Gutierrez A, Dahlberg SE, Neuberger DS, Zhang J, Grebliunaite R, Sanda T, et al. Absence of Biallelic TCR[gamma] Deletion Predicts Early Treatment Failure in Pediatric T-Cell Acute Lymphoblastic Leukemia. *J Clin Oncol*. 2010;28(24):3816-23.
100. Inukai T, Kiyokawa N, Campana D, Coustan-Smith E, Kikuchi A, Kobayashi M, et al. Clinical significance of early T-cell precursor acute lymphoblastic leukaemia: results of the Tokyo Children's Cancer Study Group Study L99-15. *Br J Haematol*. 2012;156(3):358-65.
101. Ma M, Wang X, Tang J, Xue H, Chen J, Pan C, et al. Early T-cell precursor leukemia: a subtype of high risk childhood acute lymphoblastic leukemia. *Front Med*. 2012;6(4):416-20.
102. Allen A, Sireci A, Colovai A, Pinkney K, Sulis M, Bhagat G, et al. Early T-cell precursor leukemia/lymphoma in adults and children. *Leuk Res*. 2013;37(9):1027-34.
103. Van Vlierberghe P, Ambesi-Impiombato A, De Keersmaecker K, Hadler M, Paietta E, Tallman MS, et al. Prognostic relevance of integrated genetic profiling in adult T-cell acute lymphoblastic leukemia. *Blood*. 2013;122(1):74-82.
104. Yang YL, Hsiao CC, Chen HY, Lin KH, Jou ST, Chen JS, et al. Absence of biallelic TCRgamma deletion predicts induction failure and poorer outcomes in childhood T-cell acute lymphoblastic leukemia. *Pediatr Blood Cancer*. 2012;58(6):846-51.
105. Farah N, Kirkwood AA, Rahman S, Leon T, Jenkinson S, Gale RE, et al. Prognostic impact of the absence of biallelic deletion at the TRG locus for pediatric patients with T-cell acute lymphoblastic leukemia treated on the Medical Research Council UK Acute Lymphoblastic Leukemia 2003 trial. *Haematologica*. 2018;103(7):e288-e92.
106. Wood BL, Winter SS, Dunsmore KP, Devidas M, Chen S, Asselin BL, et al. T-lymphoblastic leukemia (T-ALL) shows excellent outcome, lack of significance of the early thymic precursor (ETP) immunophenotype, and validation of the prognostic value of end-induction minimal residual disease (MRD) in Children's Oncology Group (COG) study AALL0434. *Blood*. 2014;124(21):1.
107. Patrick K, Wade R, Goulden N, Mitchell C, Moorman AV, Rowntree C, et al. Outcome for children and young people with Early T-cell precursor acute lymphoblastic leukaemia treated on a contemporary protocol, UKALL 2003. *Br J Haematol*. 2014;166(3):421-4.
108. Zuurbier L, Petricoin EF, 3rd, Vuerhard MJ, Calvert V, Kooi C, Buijs-Gladdines JG, et al. The significance of PTEN and AKT aberrations in pediatric T-cell acute lymphoblastic leukemia. *Haematologica*. 2012;97(9):1405-13.
109. Trinquand A, Tanguy-Schmidt A, Ben Abdelali R, Lambert J, Beldjord K, Lengline E, et al. Toward a NOTCH1/FBXW7/RAS/PTEN-based oncogenetic risk classification of adult T-cell acute lymphoblastic leukemia: a Group for Research in Adult Acute Lymphoblastic Leukemia study. *J Clin Oncol*. 2013;31(34):4333-42.
110. Paganin M, Grillo MF, Silvestri D, Scapinello G, Buldini B, Cazzaniga G, et al. The presence of mutated and deleted PTEN is associated with an increased risk of relapse in childhood T cell acute lymphoblastic leukaemia treated with AIEOP-BFM ALL protocols. *Br J Haematol*. 2018;182(5):705-11.
111. Jotta PY, Ganazza MA, Silva A, Viana MB, da Silva MJ, Zambaldi LJ, et al. Negative prognostic impact of PTEN mutation in pediatric T-cell acute lymphoblastic leukemia. *Leukemia*. 2010;24(1):239-42.
112. Jenkinson S, Kirkwood AA, Goulden N, Vora A, Linch DC, Gale RE. Impact of PTEN abnormalities on outcome in pediatric patients with T-cell acute lymphoblastic leukemia treated on the MRC UKALL2003 trial. *Leukemia*. 2016;30(1):39-47.
113. Cante-Barrett K, Spijkers-Hagelstein JA, Buijs-Gladdines JG, Uitdehaag JC, Smits WK, van der Zwet J, et al. MEK and PI3K-AKT inhibitors synergistically block activated IL7 receptor signaling in T-cell acute lymphoblastic leukemia. *Leukemia*. 2016;30(9):1832-43.

114. Flex E, Petrangeli V, Stella L, Chiaretti S, Hornakova T, Knoops L, et al. Somatically acquired JAK1 mutations in adult acute lymphoblastic leukemia. *J Exp Med*. 2008;205(4):751-8.
115. Jeong EG, Kim MS, Nam HK, Min CK, Lee S, Chung YJ, et al. Somatic mutations of JAK1 and JAK3 in acute leukemias and solid cancers. *Clin Cancer Res*. 2008;14(12):3716-21.
116. Asnafi V, Le Noir S, Lhermitte L, Gardin C, Legrand F, Vallantin X, et al. JAK1 mutations are not frequent events in adult T-ALL: a GRAALL study. *Br J Haematol*. 2010;148(1):178-9.
117. Bains T, Heinrich MC, Loriaux MM, Beadling C, Nelson D, Warrick A, et al. Newly described activating JAK3 mutations in T-cell acute lymphoblastic leukemia. *Leukemia*. 2012;26(9):2144-6.
118. Kontro M, Kuusanmaki H, Eldfors S, Burmeister T, Andersson EI, Bruserud O, et al. Novel activating STAT5B mutations as putative drivers of T-cell acute lymphoblastic leukemia. *Leukemia*. 2014;28(8):1738-42.
119. Bandapalli OR, Schuessle S, Kunz JB, Rausch T, Stutz AM, Tal N, et al. The activating STAT5B N642H mutation is a common abnormality in pediatric T-cell acute lymphoblastic leukemia and confers a higher risk of relapse. *Haematologica*. 2014;99(10):e188-92.
120. Balgobind BV, Van Vlierberghe P, van den Ouweland AM, Beverloo HB, Terlouw-Kromosoeto JN, van Wering ER, et al. Leukemia-associated NF1 inactivation in patients with pediatric T-ALL and AML lacking evidence for neurofibromatosis. *Blood*. 2008;111(8):4322-8.
121. Oliveira ML, Akkapeddi P, Ribeiro D, Melao A, Barata JT. IL-7R-mediated signaling in T-cell acute lymphoblastic leukemia: An update. *Adv Biol Regul*. 2019;71:88-96.
122. Gianfelici V, Chiaretti S, Demeyer S, Di Giacomo F, Messina M, La Starza R, et al. RNA sequencing unravels the genetics of refractory/relapsed T-cell acute lymphoblastic leukemia. Prognostic and therapeutic implications. *Haematologica*. 2016;101(8):941-50.
123. Pieters R, de Groot-Kruseman H, Van der Velden V, Fiocco M, van den Berg H, de Bont E, et al. Successful Therapy Reduction and Intensification for Childhood Acute Lymphoblastic Leukemia Based on Minimal Residual Disease Monitoring: Study ALL10 From the Dutch Childhood Oncology Group. *J Clin Oncol*. 2016;34(22):2591-601.
124. Grobner SN, Worst BC, Weischenfeldt J, Buchhalter I, Kleinheinz K, Rudneva VA, et al. The landscape of genomic alterations across childhood cancers. *Nature*. 2018;555(7696):321-7.
125. Massard C, Michiels S, Ferte C, Le Deley MC, Lacroix L, Hollebecque A, et al. High-Throughput Genomics and Clinical Outcome in Hard-to-Treat Advanced Cancers: Results of the MOSCATO 01 Trial. *Cancer Discov*. 2017;7(6):586-95.
126. Marquart J, Chen EY, Prasad V. Estimation of the Percentage of US Patients With Cancer Who Benefit From Genome-Driven Oncology. *JAMA Oncol*. 2018;4(8):1093-8.
127. Le Tourneau C, Delord JP, Goncalves A, Gavoille C, Dubot C, Isambert N, et al. Molecularly targeted therapy based on tumour molecular profiling versus conventional therapy for advanced cancer (SHIVA): a multicentre, open-label, proof-of-concept, randomised, controlled phase 2 trial. *Lancet Oncol*. 2015;16(13):1324-34.
128. Ma X, Liu Y, Liu Y, Alexandrov LB, Edmonson MN, Gawad C, et al. Pan-cancer genome and transcriptome analyses of 1,699 paediatric leukaemias and solid tumours. *Nature*. 2018;555(7696):371-6.
129. Matheson EC, Thomas H, Case M, Blair H, Jackson RK, Masic D, et al. Glucocorticoids and selumetinib are highly synergistic in RAS pathway mutated childhood acute lymphoblastic leukemia through upregulation of BIM. *Haematologica*. 2019.
130. Loh ML, Zhang J, Harvey RC, Roberts K, Payne-Turner D, Kang H, et al. Tyrosine kinome sequencing of pediatric acute lymphoblastic leukemia: a report from the Children's Oncology Group TARGET Project. *Blood*. 2013;121(3):485-8.

131. Doll S, Gnad F, Mann M. The Case for Proteomics and Phospho-Proteomics in Personalized Cancer Medicine. *Proteomics Clin Appl.* 2019;13(2):e1800113.
132. Worst BC, van Tilburg CM, Balasubramanian GP, Fiesel P, Witt R, Freitag A, et al. Next-generation personalised medicine for high-risk paediatric cancer patients - The INFORM pilot study. *Eur J Cancer.* 2016;65:91-101.
133. Atak ZK, Gianfelici V, Hulselmans G, De Keersmaecker K, Devasia AG, Geerdens E, et al. Comprehensive analysis of transcriptome variation uncovers known and novel driver events in T-cell acute lymphoblastic leukemia. *PLoS Genet.* 2013;9(12):e1003997.
134. Lopez-Nieva P, Fernandez-Navarro P, Grana-Castro O, Andres-Leon E, Santos J, Villa-Morales M, et al. Detection of novel fusion-transcripts by RNA-Seq in T-cell lymphoblastic lymphoma. *Sci Rep.* 2019;9(1):5179.
135. Inaba H, Azzato EM, Mullighan CG. Integration of Next-Generation Sequencing to Treat Acute Lymphoblastic Leukemia with Targetable Lesions: The St. Jude Children's Research Hospital Approach. *Front Pediatr.* 2017;5:258.
136. Hanahan D, Weinberg RA. Hallmarks of cancer: the next generation. *Cell.* 2011;144(5):646-74.
137. van Ooijen H, Hornsveld M, Dam-de Veen C, Velter R, Dou M, Verhaegh W, et al. Assessment of Functional Phosphatidylinositol 3-Kinase Pathway Activity in Cancer Tissue Using Forkhead Box-O Target Gene Expression in a Knowledge-Based Computational Model. *Am J Pathol.* 2018;188(9):1956-72.
138. Stolpe AV, Holtzer L, van Ooijen H, de Inda MA, Verhaegh W. Enabling precision medicine by unravelling disease pathophysiology: quantifying signal transduction pathway activity across cell and tissue types. *Sci Rep.* 2019;9(1):1603.
139. van de Stolpe A. Quantitative Measurement of Functional Activity of the PI3K Signaling Pathway in Cancer. *Cancers (Basel).* 2019;11(3).
140. Verhaegh W, van Ooijen H, Inda MA, Hatzis P, Versteeg R, Smid M, et al. Selection of personalized patient therapy through the use of knowledge-based computational models that identify tumor-driving signal transduction pathways. *Cancer Res.* 2014;74(11):2936-45.
141. Jimenez CR, Verheul HM. Mass spectrometry-based proteomics: from cancer biology to protein biomarkers, drug targets, and clinical applications. *Am Soc Clin Oncol Educ Book.* 2014:e504-10.
142. Cutillas PR. Role of phosphoproteomics in the development of personalized cancer therapies. *Proteomics Clin Appl.* 2015;9(3-4):383-95.
143. Casado P, Alcolea MP, Iorio F, Rodriguez-Prados JC, Vanhaesebroeck B, Saez-Rodriguez J, et al. Phosphoproteomics data classify hematological cancer cell lines according to tumor type and sensitivity to kinase inhibitors. *Genome Biol.* 2013;14(4):R37.
144. Lopez Villar E, Wu D, Cho WC, Madero L, Wang X. Proteomics-based discovery of biomarkers for paediatric acute lymphoblastic leukaemia: challenges and opportunities. *J Cell Mol Med.* 2014;18(7):1239-46.
145. Lopez Villar E, Wang X, Madero L, Cho WC. Application of oncoproteomics to aberrant signalling networks in changing the treatment paradigm in acute lymphoblastic leukaemia. *J Cell Mol Med.* 2015;19(1):46-52.
146. van der Sligte NE, Scherpen FJ, Meeuwssen-de Boer TG, Lourens HJ, Ter Elst A, Diks SH, et al. Kinase activity profiling reveals active signal transduction pathways in pediatric acute lymphoblastic leukemia: a new approach for target discovery. *Proteomics.* 2015;15(7):1245-54.
147. Serafin V, Lissandron V, Buldini B, Bresolin S, Paganin M, Grillo F, et al. Phosphoproteomic analysis reveals hyperactivation of mTOR/STAT3 and LCK/Calcineurin axes in pediatric early T-cell precursor ALL. *Leukemia.* 2017;31(4):1007-11.

148. Serafin V, Capuzzo G, Milani G, Minuzzo SA, Pinazza M, Bortolozzi R, et al. Glucocorticoid resistance is reverted by LCK inhibition in pediatric T-cell acute lymphoblastic leukemia. *Blood*. 2017;130(25):2750-61.
149. Beekhof R, van Alphen C, Henneman AA, Knol JC, Pham TV, Rolfs F, et al. INKA, an integrative data analysis pipeline for phosphoproteomic inference of active kinases. *Mol Syst Biol*. 2019;15(4):e8250.
150. Delgado-Martin C, Meyer LK, Huang BJ, Shimano KA, Zinter MS, Nguyen JV, et al. JAK/STAT pathway inhibition overcomes IL7-induced glucocorticoid resistance in a subset of human T-cell acute lymphoblastic leukemias. *Leukemia*. 2017;31(12):2568-76.
151. Degryse S, de Bock CE, Demeyer S, Govaerts I, Bornschein S, Verbeke D, et al. Mutant JAK3 phosphoproteomic profiling predicts synergism between JAK3 inhibitors and MEK/BCL2 inhibitors for the treatment of T-cell acute lymphoblastic leukemia. *Leukemia*. 2018;32(3):788-800.
152. Pham HTT, Maurer B, Prchal-Murphy M, Grausenburger R, Grundschober E, Javaheri T, et al. STAT5BN642H is a driver mutation for T cell neoplasia. *J Clin Invest*. 2018;128(1):387-401.
153. De Smedt R, Peirs S, Morscio J, Matthijssens F, Roels J, Reunes L, et al. Pre-clinical evaluation of second generation PIM inhibitors for the treatment of T-cell acute lymphoblastic leukemia and lymphoma. *Haematologica*. 2019;104(1):e17-e20.
154. de Bock CE, Demeyer S, Degryse S, Verbeke D, Sweron B, Gielen O, et al. HOXA9 Cooperates with Activated JAK/STAT Signaling to Drive Leukemia Development. *Cancer Discov*. 2018;8(5):616-31.
155. Ribeiro D, Melao A, van Boxtel R, Santos CI, Silva A, Silva MC, et al. STAT5 is essential for IL-7-mediated viability, growth, and proliferation of T-cell acute lymphoblastic leukemia cells. *Blood Adv*. 2018;2(17):2199-213.
156. Meijerink JP. Genetic rearrangements in relation to immunophenotype and outcome in T-cell acute lymphoblastic leukaemia. *Best Pract Res Clin Haematol*. 2010;23(3):307-18.
157. Aplan PD, Lombardi DP, Reaman GH, Sather HN, Hammond GD, Kirsch IR. Involvement of the putative hematopoietic transcription factor SCL in T-cell acute lymphoblastic leukemia. *Blood*. 1992;79(5):1327-33.
158. Wang J, Jani-Sait SN, Escalon EA, Carroll AJ, de Jong PJ, Kirsch IR, et al. The t(14;21)(q11.2;q22) chromosomal translocation associated with T-cell acute lymphoblastic leukemia activates the BHLHB1 gene. *Proc Natl Acad Sci U S A*. 2000;97(7):3497-502.
159. Hu S, Qian M, Zhang H, Guo Y, Yang J, Zhao X, et al. Whole-genome noncoding sequence analysis in T-cell acute lymphoblastic leukemia identifies oncogene enhancer mutations. *Blood*. 2017;129(12):3264-8.
160. Chen S, Nagel S, Schneider B, Kaufmann M, Meyer C, Zaborski M, et al. Novel non-TCR chromosome translocations t(3;11)(q25;p13) and t(X;11)(q25;p13) activating LMO2 by juxtaposition with MBNL1 and STAG2. *Leukemia*. 2011;25(10):1632-5.
161. Hansen-Hagge TE, Schafer M, Kiyoi H, Morris SW, Whitlock JA, Koch P, et al. Disruption of the RanBP17/Hox11L2 region by recombination with the TCRdelta locus in acute lymphoblastic leukemias with t(5;14)(q34;q11). *Leukemia*. 2002;16(11):2205-12.
162. Su XY, Busson M, Della Valle V, Ballerini P, Dastugue N, Talmant P, et al. Various types of rearrangements target TLX3 locus in T-cell acute lymphoblastic leukemia. *Genes Chromosomes Cancer*. 2004;41(3):243-9.
163. Bergeron J, Clappier E, Cauwelier B, Dastugue N, Millien C, Delabesse E, et al. HOXA cluster deregulation in T-ALL associated with both a TCRD-HOXA and a CALM-AF10 chromosomal translocation. *Leukemia*. 2006;20(6):1184-7.

164. Cauwelier B, Cave H, Gervais C, Lessard M, Barin C, Perot C, et al. Clinical, cytogenetic and molecular characteristics of 14 T-ALL patients carrying the TCRbeta-HOXA rearrangement: a study of the Groupe Francophone de Cytogenetique Hematologique. *Leukemia*. 2007;21(1):121-8.
165. Speleman F, Cauwelier B, Dastugue N, Cools J, Verhasselt B, Poppe B, et al. A new recurrent inversion, inv(7)(p15q34), leads to transcriptional activation of HOXA10 and HOXA11 in a subset of T-cell acute lymphoblastic leukemias. *Leukemia*. 2005;19(3):358-66.
166. Nagel S, Kaufmann M, Drexler HG, MacLeod RA. The cardiac homeobox gene NKX2-5 is deregulated by juxtaposition with BCL11B in pediatric T-ALL cell lines via a novel t(5;14)(q35.1;q32.2). *Cancer Res*. 2003;63(17):5329-34.
167. Przybylski GK, Dik WA, Grabarczyk P, Wanzeck J, Chudobska P, Jankowski K, et al. The effect of a novel recombination between the homeobox gene NKX2-5 and the TRD locus in T-cell acute lymphoblastic leukemia on activation of the NKX2-5 gene. *Haematologica*. 2006;91(3):317-21.
168. Clappier E, Cuccuini W, Kalota A, Crinquette A, Cayuela JM, Dik WA, et al. The C-MYB locus is involved in chromosomal translocation and genomic duplications in human T-cell acute leukemia (T-ALL) - the translocation defining a new T-ALL subtype in very young children. *Blood*. 2007;110(4):1251-61.
169. Lahortiga I, De Keersmaecker K, Van Vlierberghe P, Graux C, Cauwelier B, Lambert F, et al. Duplication of the MYB oncogene in T cell acute lymphoblastic leukemia. *Nat Genet*. 2007;39(5):593-5.
170. O'Neil J, Tchinda J, Gutierrez A, Moreau L, Maser RS, Wong KK, et al. Alu elements mediate MYB gene tandem duplication in human T-ALL. *J Exp Med*. 2007;204(13):3059-66.
171. Clappier E, Cuccuini W, Cayuela JM, Vecchione D, Baruchel A, Dombret H, et al. Cyclin D2 dysregulation by chromosomal translocations to TCR loci in T-cell acute lymphoblastic leukemias. *Leukemia*. 2006;20(1):82-6.
172. Dik WA, Brahim W, Braun C, Asnafi V, Dastugue N, Bernard OA, et al. CALM-AF10+ T-ALL expression profiles are characterized by overexpression of HOXA and BMI1 oncogenes. *Leukemia*. 2005;19(11):1948-57.
173. Ferrando AA, Armstrong SA, Neuberg DS, Sallan SE, Silverman LB, Korsmeyer SJ, et al. Gene expression signatures in MLL-rearranged T-lineage and B-precursor acute leukemias: dominance of HOX dysregulation. *Blood*. 2003;102(1):262-8.
174. Quentmeier H, Schneider B, Rohrs S, Romani J, Zaborski M, Macleod RA, et al. SET-NUP214 fusion in acute myeloid leukemia- and T-cell acute lymphoblastic leukemia-derived cell lines. *J Hematol Oncol*. 2009;2:3.
175. Barber KE, Martineau M, Harewood L, Stewart M, Cameron E, Strefford JC, et al. Amplification of the ABL gene in T-cell acute lymphoblastic leukemia. *Leukemia*. 2004;18(6):1153-6.
176. Bernasconi P, Calatroni S, Giardini I, Inzoli A, Castagnola C, Cavigliano PM, et al. ABL1 amplification in T-cell acute lymphoblastic leukemia. *Cancer Genet Cytogenet*. 2005;162(2):146-50.
177. Graux C, Cools J, Melotte C, Quentmeier H, Ferrando A, Levine R, et al. Fusion of NUP214 to ABL1 on amplified episomes in T-cell acute lymphoblastic leukemia. *Nat Genet*. 2004;36(10):1084-9.
178. Graux C, Stevens-Kroef M, Lafage M, Dastugue N, Harrison CJ, Mugneret F, et al. Heterogeneous patterns of amplification of the NUP214-ABL1 fusion gene in T-cell acute lymphoblastic leukemia. *Leukemia*. 2009;23(1):125-33.
179. Stergianou K, Fox C, Russell NH. Fusion of NUP214 to ABL1 on amplified episomes in T-ALL-- implications for treatment. *Leukemia*. 2005;19(9):1680-1.

180. De Keersmaecker K, Graux C, Odero MD, Mentens N, Somers R, Maertens J, et al. Fusion of EML1 to ABL1 in T-cell acute lymphoblastic leukemia with cryptic t(9;14)(q34;q32). *Blood*. 2005;105(12):4849-52.
181. Van Limbergen H, Beverloo HB, van Drunen E, Janssens A, Hahlen K, Poppe B, et al. Molecular cytogenetic and clinical findings in ETV6/ABL1-positive leukemia. *Genes Chromosomes Cancer*. 2001;30(3):274-82.
182. Fabbiano F, Santoro A, Felice R, Catania P, Cannella S, Majolino I. bcr-abl rearrangement in adult T-lineage acute lymphoblastic leukemia. *Haematologica*. 1998;83(9):856-7.
183. Quentmeier H, Cools J, Macleod RA, Marynen P, Uphoff CC, Drexler HG. e6-a2 BCR-ABL1 fusion in T-cell acute lymphoblastic leukemia. *Leukemia*. 2005;19(2):295-6.
184. Colleoni GW, Yamamoto M, Kerbaux J, Serafim RC, Lindsey CJ, Costa FF, et al. BCR-ABL rearrangement in adult T-cell acute lymphoblastic leukemia. *Am J Hematol*. 1996;53(4):277-8.
185. De Braekeleer E, Douet-Guilbert N, Rowe D, Bown N, Morel F, Berthou C, et al. ABL1 fusion genes in hematological malignancies: a review. *Eur J Haematol*. 2011;86(5):361-71.
186. Bond J, Bergon A, Durand A, Tigaud I, Thomas X, Asnafi V, et al. Cryptic XPO1-MLLT10 translocation is associated with HOXA locus deregulation in T-ALL. *Blood*. 2014;124(19):3023-5.
187. Kox C, Zimmermann M, Stanulla M, Leible S, Schrappe M, Ludwig WD, et al. The favorable effect of activating NOTCH1 receptor mutations on long-term outcome in T-ALL patients treated on the ALL-BFM 2000 protocol can be separated from FBXW7 loss of function. *Leukemia*. 2010;24(12):2005-13.
188. Zuurbier L, Homminga I, Calvert V, te Winkel ML, Buijs-Gladdines JG, Kooi C, et al. NOTCH1 and/or FBXW7 mutations predict for initial good prednisone response but not for improved outcome in pediatric T-cell acute lymphoblastic leukemia patients treated on DCOG or COALL protocols. *Leukemia*. 2010;24(12):2014-22.
189. Asnafi V, Buzyn A, Le Noir S, Baleyrier F, Simon A, Beldjord K, et al. NOTCH1/FBXW7 mutation identifies a large subgroup with favorable outcome in adult T-cell acute lymphoblastic leukemia (T-ALL): a Group for Research on Adult Acute Lymphoblastic Leukemia (GRAALL) study. *Blood*. 2009;113(17):3918-24.
190. Breit S, Stanulla M, Flohr T, Schrappe M, Ludwig WD, Tolle G, et al. Activating NOTCH1 mutations predict favorable early treatment response and long-term outcome in childhood precursor T-cell lymphoblastic leukemia. *Blood*. 2006;108(4):1151-7.
191. Bandapalli OR, Zimmermann M, Kox C, Stanulla M, Schrappe M, Ludwig WD, et al. NOTCH1 activation clinically antagonizes the unfavorable effect of PTEN inactivation in BFM-treated children with precursor T-cell acute lymphoblastic leukemia. *Haematologica*. 2013;98(6):928-36.
192. Kleppe M, Lahortiga I, El Chaar T, De Keersmaecker K, Mentens N, Graux C, et al. Deletion of the protein tyrosine phosphatase gene PTPN2 in T-cell acute lymphoblastic leukemia. *Nat Genet*. 2010;42(6):530-5.
193. Kleppe M, Soulier J, Asnafi V, Mentens N, Hornakova T, Knoops L, et al. PTPN2 negatively regulates oncogenic JAK1 in T-cell acute lymphoblastic leukemia. *Blood*. 2011;117(26):7090-8.
194. Melao A, Spit M, Cardoso BA, Barata JT. Optimal interleukin-7 receptor-mediated signaling, cell cycle progression and viability of T-cell acute lymphoblastic leukemia cells rely on casein kinase 2 activity. *Haematologica*. 2016;101(11):1368-79.
195. Szarzynska-Zawadzka B, Kunz JB, Sedek L, Kosmalka M, Zdon K, Biecek P, et al. PTEN abnormalities predict poor outcome in children with T-cell acute lymphoblastic leukemia treated according to ALL IC-BFM protocols. *Am J Hematol*. 2019;94(4):E93-E6.

196. Maser RS, Choudhury B, Campbell PJ, Feng B, Wong KK, Protopopov A, et al. Chromosomally unstable mouse tumours have genomic alterations similar to diverse human cancers. *Nature*. 2007;447(7147):966-71.
197. Silva A, Yunes JA, Cardoso BA, Martins LR, Jotta PY, Abecasis M, et al. PTEN posttranslational inactivation and hyperactivation of the PI3K/Akt pathway sustain primary T cell leukemia viability. *J Clin Invest*. 2008;118(11):3762-74.
198. Neumann M, Heesch S, Schlee C, Schwartz S, Gokbuget N, Hoelzer D, et al. Whole-exome sequencing in adult ETP-ALL reveals a high rate of DNMT3A mutations. *Blood*. 2013;121(23):4749-52.
199. Perez-Garcia A, Ambesi-Impiombato A, Hadler M, Rigo I, LeDuc CA, Kelly K, et al. Genetic loss of SH2B3 in acute lymphoblastic leukemia. *Blood*. 2013;122(14):2425-32.
200. Huether R, Dong L, Chen X, Wu G, Parker M, Wei L, et al. The landscape of somatic mutations in epigenetic regulators across 1,000 paediatric cancer genomes. *Nat Commun*. 2014;5:3630.
201. Van Vlierberghe P, Palomero T, Khiabani H, Van der Meulen J, Castillo M, Van Roy N, et al. PHF6 mutations in T-cell acute lymphoblastic leukemia. *Nat Genet*. 2010;42(4):338-42.
202. Tosello V, Mansour MR, Barnes K, Paganin M, Sulis ML, Jenkinson S, et al. WT1 mutations in T-ALL. *Blood*. 2009;114(5):1038-45.
203. Gutierrez A, Sanda T, Ma W, Zhang J, Grebliunaite R, Dahlberg S, et al. Inactivation of LEF1 in T-cell acute lymphoblastic leukemia. *Blood*. 2010;115(14):2845-51.
204. De Keersmaecker K, Atak ZK, Li N, Vicente C, Patchett S, Girardi T, et al. Exome sequencing identifies mutation in CNOT3 and ribosomal genes RPL5 and RPL10 in T-cell acute lymphoblastic leukemia. *Nat Genet*. 2013;45(2):186-90.
205. Ntziachristos P, Tsirigos A, Van Vlierberghe P, Nedjic J, Trimarchi T, Flaherty MS, et al. Genetic inactivation of the polycomb repressive complex 2 in T cell acute lymphoblastic leukemia. *Nat Med*. 2012;18(2):298-301.
206. Girardi T, Vereecke S, Sulima SO, Khan Y, Fancello L, Briggs JW, et al. The T-cell leukemia-associated ribosomal RPL10 R98S mutation enhances JAK-STAT signaling. *Leukemia*. 2018;32(3):809-19.
207. Rao S, Lee SY, Gutierrez A, Perrigoue J, Thapa RJ, Tu Z, et al. Inactivation of ribosomal protein L22 promotes transformation by induction of the stemness factor, Lin28B. *Blood*. 2012;120(18):3764-73.
208. Gachet S, El-Chaar T, Avran D, Genesca E, Catez F, Quentin S, et al. Deletion 6q Drives T-cell Leukemia Progression by Ribosome Modulation. *Cancer Discov*. 2018;8(12):1614-31.
209. Kampen KR, Sulima SO, Verbelen B, Girardi T, Vereecke S, Fancello L, et al. Correction: The ribosomal RPL10 R98S mutation drives IRES-dependent BCL-2 translation in T-ALL. *Leukemia*. 2019;33(4):1055-62.
210. Ge Z, Li M, Zhao G, Xiao L, Gu Y, Zhou X, et al. Novel dynamin 2 mutations in adult T-cell acute lymphoblastic leukemia. *Oncol Lett*. 2016;12(4):2746-51.
211. Tremblay CS, Brown FC, Collett M, Saw J, Chiu SK, Sonderegger SE, et al. Loss-of-function mutations of Dynamin 2 promote T-ALL by enhancing IL-7 signalling. *Leukemia*. 2016;30(10):1993-2001.
212. Tzoneva G, Perez-Garcia A, Carpenter Z, Khiabani H, Tosello V, Allegretta M, et al. Activating mutations in the NT5C2 nucleotidase gene drive chemotherapy resistance in relapsed ALL. *Nat Med*. 2013;19(3):368-71.

213. Chonghaile TN, Roderick JE, Glenfield C, Ryan J, Sallan SE, Silverman LB, et al. Maturation stage of T-cell acute lymphoblastic leukemia determines BCL-2 versus BCL-XL dependence and sensitivity to ABT-199. *Cancer Discov.* 2014;4(9):1074-87.
214. Kawashima-Goto S, Imamura T, Tomoyasu C, Yano M, Yoshida H, Fujiki A, et al. BCL2 Inhibitor (ABT-737): A Restorer of Prednisolone Sensitivity in Early T-Cell Precursor-Acute Lymphoblastic Leukemia with High MEF2C Expression? *PLoS One.* 2015;10(7):e0132926.
215. Peirs S, Matthijssens F, Goossens S, Van de Walle I, Ruggiero K, de Bock CE, et al. ABT-199 mediated inhibition of BCL-2 as a novel therapeutic strategy in T-cell acute lymphoblastic leukemia. *Blood.* 2014;124(25):3738-47.
216. Suryani S, Carol H, Chonghaile TN, Frismantas V, Sarmah C, High L, et al. Cell and molecular determinants of in vivo efficacy of the BH3 mimetic ABT-263 against pediatric acute lymphoblastic leukemia xenografts. *Clin Cancer Res.* 2014;20(17):4520-31.



CHAPTER 3



Phosphoproteomic profiling of T cell acute lymphoblastic leukemia reveals targetable kinases and combination treatment strategies

Valentina Cordo¹, Mariska T. Meijer¹, Rico Hagelaar¹, Richard R. de Goeij-de Haas^{2,3}, Vera M. Poort¹, Alex A. Henneman^{2,3}, Sander R. Piersma^{2,3}, Thang V. Pham^{2,3}, Koichi Oshima⁴, Adolfo A. Ferrando⁴, Guido J.R. Zaman⁵, Connie R. Jimenez^{2,3,6}, and Jules P.P. Meijerink^{1,6}

¹ Princess Máxima Center for Pediatric Oncology, Utrecht, the Netherlands

² OncoProteomics Laboratory, Cancer Center Amsterdam, Amsterdam University Medical Centers, VU University, Amsterdam, the Netherlands

³ Department of Medical Oncology, Cancer Center Amsterdam, Amsterdam University Medical Centers, VU University, Amsterdam, the Netherlands

⁴ Institute for Cancer Genetics, Columbia University Medical Center, New York, NY, USA

⁵ Oncolines B.V., Oss, the Netherlands.

⁶ These authors jointly supervised this work: Connie R. Jimenez and Jules P.P. Meijerink

Published in *Nature Communications* (2022)

DOI: 10.1038/s41467-022-28682-1

PMID: 35217681

ABSTRACT

Protein kinase inhibitors are amongst the most successful cancer treatments, but targetable kinases activated by genomic abnormalities are rare in T cell acute lymphoblastic leukemia. Nevertheless, kinases can be activated in the absence of genetic defects. Thus, phosphoproteomics can provide information on pathway activation and signaling networks that offer opportunities for targeted therapy. Here, we describe a mass spectrometry-based global phosphoproteomic profiling of 11 T cell acute lymphoblastic leukemia cell lines to identify targetable kinases. We report a comprehensive dataset consisting of 21,000 phosphosites on 4,896 phosphoproteins, including 217 kinases. We identify active Src-family kinases signaling as well as active cyclin-dependent kinases. We validate putative targets for therapy *ex vivo* and identify potential combination treatments, such as the inhibition of the INSR/IGF-1R axis to increase the sensitivity to dasatinib treatment. *Ex vivo* validation of selected drug combinations using patient-derived xenografts provides a *proof-of-concept* for phosphoproteomics-guided design of personalized treatments.

INTRODUCTION

T cell acute lymphoblastic leukemia (T-ALL) is an aggressive malignancy arising from aberrant proliferation of immature T cell progenitors and accounts for about 15% of pediatric ALL cases ¹. The current risk-adapted, multi-agent chemotherapeutic regimen has led to an overall survival rate exceeding 80%. Nevertheless, one out of five children with T-ALL will relapse within four years after the start of therapy. Further intensification of the current high-risk treatment protocols seems not feasible due to serious and even fatal detrimental side effects, such as toxicities and infections ². Relapsed T-ALL patients have a poor prognosis and are refractory towards further treatment. Therefore, the identification of novel therapeutic options for refractory/relapsed patients remains an urgent need. Thanks to extensive genome sequencing studies, the genetic drivers of T-ALL have been identified as developmental transcription factors that are ectopically expressed due to chromosomal rearrangements (reviewed in Belver et al.³ and van der Zwet et al.⁴). Unlike other leukemias, genomic rearrangements involving kinase-coding genes are scarce in T-ALL. The most common aberration involving a kinase-coding gene is the *NUP214-ABL1* episomal amplification, which is found in less than 6% of T-ALL patients at diagnosis and is often detected only in minor leukemic sub-clones ⁵. Recurrent activating mutations detected in kinase-coding genes or kinase regulators involve the PI3K-AKT axis (*AKT1*, *PIK3CD*, *PIK3R1*), the *JAK-STAT* (*IL7R*, *JAK1*, and *JAK3* which is mutated in about 16% of T-ALL cases ⁶), or the Ras signaling pathways (*PTPN11*, *NF1*, *N-RAS*, *K-RAS*), while in some early T cell precursor (ETP)-ALL cases, Fms-like tyrosine kinase (*FLT3*) mutations and/or overexpression are found ⁷. Additionally, other potentially druggable kinases reported for T-ALL include the JAK-family member tyrosine kinase 2 (TYK2) which can be activated either by rare *gain-of-function* mutations or IL-10 signaling ^{8,9}, the cell cycle regulators Polo-like kinases (PLKs) and Aurora kinases (AURKs) ^{10,11}, and the PIM1 kinase which can be upregulated by active IL-7 signaling, upon glucocorticoid-induced *IL7RA* expression, or in the presence of IL-7R pathway mutations ^{12,13}.

Nevertheless, genomic-guided targeted therapies can show disappointing results due to the sub-clonal nature of these mutations (*i.e.*, leukemia heterogeneity) ^{5,14}. The treatment pressure can drive the selection of minor resistant clones ¹⁵, induce the acquisition of novel mutations ¹⁶ or activate alternative feedback loops that drive therapy resistance. Leukemic cells rely on an enhanced kinase signaling that promotes aberrant proliferation and survival. Protein kinases can be activated in the absence of gene fusions or mutations in their coding sequences. In fact, except for mutations in *JAK1/2* and *FLT3*, no other somatic mutation in

tyrosine kinase-coding genes were found in 45 high-risk B-ALL cases, although the gene expression profiles indicated an active kinase signaling¹⁷. Therefore, proteome analyses can provide additional insights into active signaling pathways and kinases that could be exploited for targeted therapy. Mass spectrometry (MS)-based phosphoproteomics importantly contributed to the identification of signaling pathways and protein networks that can be targeted for cancer therapy¹⁸⁻²⁰. Recently, Frejno and colleagues performed a large-scale proteome and phosphoproteome profiling of 125 cancer cell lines to create a proteomic activity landscape that can predict drug sensitivity *in vitro*²¹. Moreover, additional phosphoproteomic studies identified determinants of sensitivity to clinical kinase inhibitors in acute myeloid leukemia (AML) cell lines²² and primary cells²³. In the context of T-ALL, reverse phase protein array (RPPA)-based proteomic studies identified highly active signaling pathways in ETP-ALL such as the mTOR/STAT3 and LCK/calcineurin²⁴. Additionally, Degryse and colleagues applied phosphoproteomics to investigate the signaling pathways downstream of mutant *JAK3* in T-ALL²⁵. Recently, Franciosa and colleagues used proteomic analyses to unravel the mechanisms of resistance to NOTCH1 inhibition in T-ALL²⁶. Nevertheless, to our knowledge, no unbiased, MS-based phosphoproteomic study to predict drug sensitivity has hitherto been performed in T-ALL. Here, we present an exploratory MS-based, unbiased, global profiling of tyrosine, serine, and threonine phosphorylation in a panel of T-ALL cell lines and patient-derived xenografts (PDXs) to identify relevant kinase signaling and to predict novel dependencies. We validate highly active kinases as potential targets for therapy *in vitro* using both cell lines and PDX models. Furthermore, we demonstrate how the application of phosphoproteomics can guide the *ex vivo* identification of synergistic combination treatments and the selection of the most appropriate therapeutical strategy for personalized medicine.

RESULTS

Unbiased analysis of the global phosphoproteome in T-ALL cell lines

to explore the phosphoproteome of human T-ALL, we performed global, unbiased mass spectrometry-based phosphoproteomic profiling of protein extracts from 11 T-ALL cell lines (**Supplementary Table 1**) as illustrated in **Fig. 1a**. Following phospho-tyrosine (pY) peptide immunoprecipitation, we identified about 3,800 phosphosites while the titanium dioxide (TiO₂)-based enrichment yielded over 17,000 phosphosites. The identification of phospho-tyrosine peptides was notably higher for HSB-2 cells compared to the other cell lines (**Supplementary Fig. 1a**). This higher recovery correlates with an enhanced overall

phospho-tyrosine signal in the unsupervised phosphopeptides cluster analysis which was also confirmed by western blotting (**Supplementary Fig. 1b** and **c**).

To identify (hyper) active protein kinases that may be targeted by small-molecule inhibitors, the Integrative iNferred Kinase Activity (INKA) pipeline²⁷ was used to infer highly active kinases from phosphoproteomic data. This analysis pipeline provides a numerical single score as proxy for kinases activity detected in a sample. The kinase ranking from the pY dataset revealed the broad activation of the Src-family kinases (SFKs) LCK, SRC, and FYN in all the cell lines analyzed, while other Src-family members such as ABL1, LYN, and FGR were detected only in specific lines, including PEER (ABL1), ALL-SIL (ABL1), MOLT-16 (LYN), LOUCY (LYN), and HPB-ALL (FGR) (**Fig. 1b**, **Supplementary Fig. 1d**, and **Supplementary Fig. 2a-f**). Three cell lines present a known genetic aberration that involves a kinase-coding gene, including the *TCR β -LCK* translocation in the HSB-2 line and the *NUP214-ABL1* fusions in the cell lines ALL-SIL and PEER. Correspondingly, we identified LCK and ABL1 as highest-ranking kinases in these three lines, respectively (**Fig. 1b**). Nevertheless, LCK shows high activation even in the absence of known genetic alterations in the remaining lines. Other active kinases identified include the cyclin-dependent kinases CDK1 and CDK2, the housekeeping kinases GSK3 α/β , the insulin receptor (INSR) and the insulin-like growth factor receptor (IGF-1R) as illustrated in **Fig. 1b**.

The INKA ranking obtained from the TiO₂ dataset confirmed high activation of the cell cycle regulators CDK1 and CDK2 as a general hallmark for all lines. Additionally, INKA uncovered other potentially relevant kinases such as the dual-specificity kinase CLK1, the p21-activated kinases PAK1 and PAK2, and AKT1 (**Fig. 1c** and **Supplementary Fig. 3**). Interestingly, some cell lines showed a modest mTOR activity, while Jurkat cells had high MAPK/ERK activity, with MAPK1 and MAPK3 ranking 5 and 12 respectively in the TiO₂-INKA plot (**Fig. 1c**). To assess the reproducibility of our pipeline, two biological replicates for LOUCY and CCRF-CEM were included for both phospho-enrichment procedures. As illustrated in **Fig. 1d**, the biological duplicates showed high correlation ($R^2 \geq 0.76$) among INKA scores for the pY and the TiO₂ datasets. Similarly, a high correlation ($R^2 \geq 0.89$) was found between technical duplicates for the TiO₂ enrichment in eight other lines (**Supplementary Fig. 4**). We then compared the T-ALL INKA scores with the INKA scores of a published AML phosphoproteomic dataset²². We identified differential (FDR < 0.1) kinase activities that characterize the myeloid and lymphoid lineages, further highlighting the relevance of the acquired phosphoproteome data. Both types of leukemia have high activation of SFKs. However, while T-ALL shows high activity of LCK, SRC, ABL1, YES1, and

FYN, AML cells show activation of LYN and HCK only (**Fig. 1e**). Interestingly, the ETP-ALL-like cell line LOUCY and the *LMO2*-rearranged MOLT-16 cells show activation of LYN and HCK as well (**Fig. 1b** and **1e**), indicating that subsets of T-ALL cells can present myeloid-like signaling features, along with the expression of known immature markers such as CD34. Furthermore, we could identify other subtype-specific kinases such as the Bruton Tyrosine Kinase BTK and FLT3 for AML, while ITK and ZAP70 were identified for T-ALL (**Fig. 1e**). These activities reflect active signaling pathways and can arise independently from known activating mutations in kinase-coding genes in these lines. Therefore, our data give a comprehensive overview of kinase activation in T-ALL cell line models and points to several potentially targetable activities that could represent novel leukemia vulnerabilities.

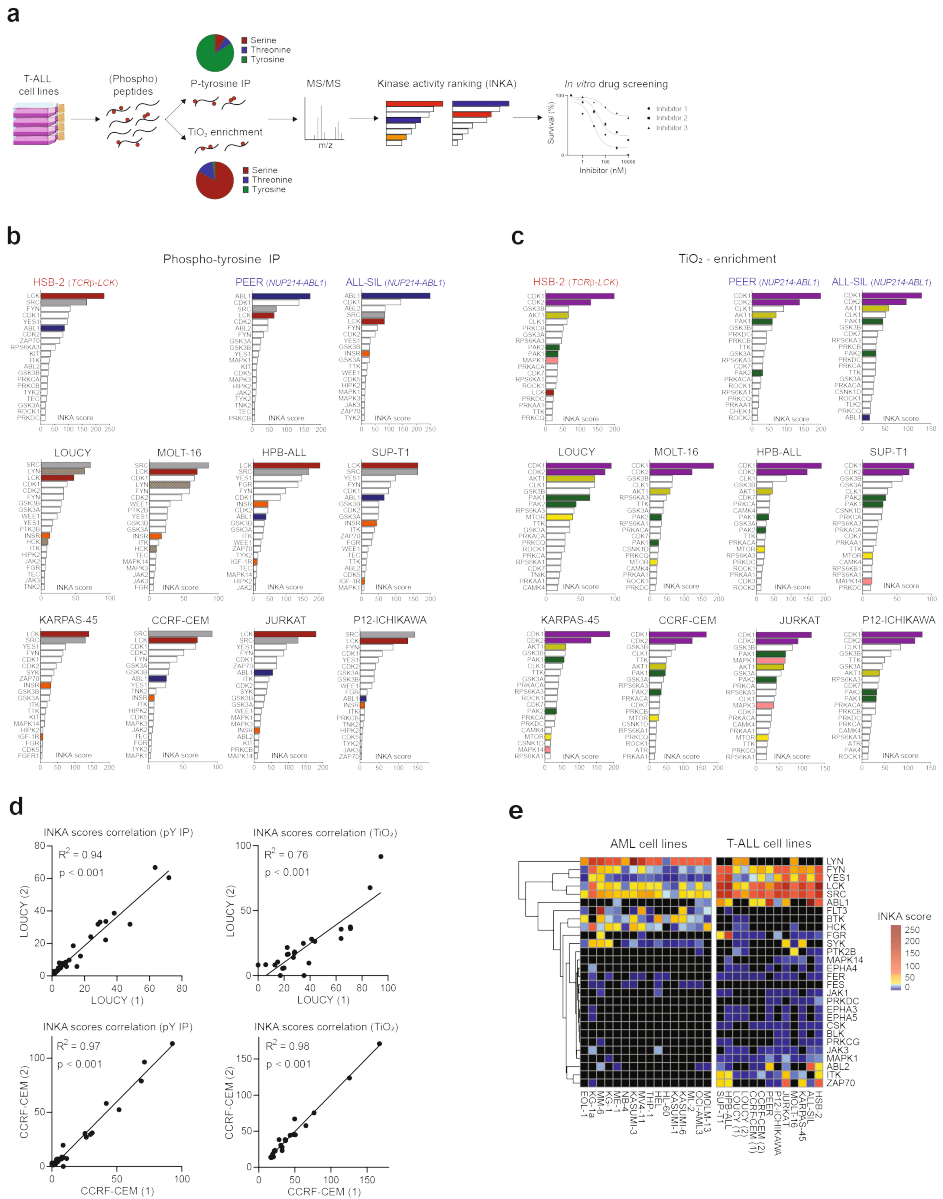


Figure 1. Phosphoproteomic profiling and INKA analysis identify active kinases in T-ALL. **a** Experimental overview. Protein extracts from 11 T-ALL cell lines were enriched for phosphopeptides by anti-phosphotyrosine immunoprecipitation (IP) and titanium dioxide (TiO₂)-enrichment. Phosphorylated proteins were identified by liquid chromatography-tandem mass spectrometry (LC-MS/MS). Kinase activities were inferred and ranked using the INKA pipeline²⁷ and selected kinase inhibitors were tested *in vitro*. **b** Top20 INKA kinases inferred from the phospho-tyrosine (pY) dataset. Each bar plot illustrates the highest 20 active kinases in each cell line ranked on their INKA score. Red, LCK; blue, ABL1; grey, SRC; orange, INSR/IGF-1R; striped pattern, myeloid-lineage kinases (LYN and HCK). **c** Top20 INKA kinases inferred from the TiO₂ dataset. Each bar plot illustrates the highest 20 active kinases in each cell line ranked on their INKA score (each graph is representative of a technical duplicate). Purple, CDK1/2; dark green, PAK1/2; light green, AKT; yellow, mTOR; pink, MAPK; red, LCK, Blue: ABL1. **d** INKA scores correlation plots for biological duplicates in pY and TiO₂ datasets. Each

plot shows the correlation of the INKA scores between biological duplicates for LOUCY and CCRF-CEM cell lines in both the pY and TiO₂ datasets (Pearson's correlation, two-sided Student's t-test, $p < 0.001$). **e** Heatmap illustrating significantly different (FDR < 0.1) kinases based on INKA scores in T-ALL (pY dataset) and AML (pY dataset; ²²) cell lines.

The CDK1/2 inhibitor milciclib effectively induces G1-cell cycle arrest in T-ALL cell lines *in vitro*

Based on the kinases identified in our phosphoproteome profiling study, we tested the sensitivity of the cell lines to multiple kinase inhibitors *in vitro* (**Supplementary Table 2**) to uncover signaling dependencies that can be exploited for targeted therapy. Despite the high ranking of CLK1 (Top7 TiO₂-INKA ranking in every cell line, **Fig.1c**), the CLK1 inhibitor TG-003 had only limited cytotoxic efficacy in these lines (**Supplementary Fig. 5a**). In addition, the PAK1/2 inhibitor FRAX597 showed some effects in ALL-SIL and HSB-2 cells, with IC₅₀ values around 400nM, but was less effective in the other cell lines (IC₅₀ values above 1 μ M; **Supplementary Fig. 5b**). Therefore, CLK1 or PAK1/2 inhibition alone do not suffice to effectively impair T-ALL cell survival. Similar results were obtained with the AKT inhibitor ipatasertib (**Supplementary Fig. 5c**). Despite the low ranking of mTOR activity, the mTOR inhibitor sirolimus significantly reduced cell viability at nanomolar concentrations in five cell lines (**Supplementary Fig. 5d**). Of note, no effect was seen upon mTOR inhibition in healthy human thymocytes (Supplementary Fig. 5e). Jurkat cells showed high ERK activity (MAKP1 and MAPK3), but cells were insensitive to the MEK inhibitor selumetinib, indicating that Jurkat cells do not essentially depend on ERK signaling for survival (**Supplementary Fig. 5f**). In the TiO₂-INKA dataset, CDK1 and CDK2 were the top2 ranking kinases in all cell lines analyzed (**Fig.1c**). Interestingly, the CDK1/2 inhibitor milciclib induced an effective reduction of cell survival in all lines tested, with IC₅₀ values between 50nM and 1 μ M (**Fig. 2a**). To investigate the mechanism of action, we performed cell cycle analysis that highlighted an induction of G1-arrest upon milciclib treatment (**Fig. 2b**). Annexin V/PI staining revealed that induction of apoptosis only occurs at higher drug concentrations (1 μ M) with a drastic effect in HSB-2 cells and a less pronounced effect in the remaining lines, indicating that milciclib mainly acts as a cytostatic drug (**Fig. 2c**). To investigate potential cytotoxic mechanisms in HSB-2 cells, we looked for possible off-target effects of milciclib. Thus, we browsed the publicly available chemical proteomic database ProteomicsDB ^{28,29} (<https://www.proteomicsdb.org/>) and found that milciclib can also inhibit LCK (EC₅₀ 1.4 μ M). We validated the reduced phosphorylation of SFKs, including LCK, upon milciclib treatment by western blot (**Fig. 2d**). Since HSB-2 cells present a driver *TCR β -LCK* translocation that induces ectopic LCK expression, cells highly depend on LCK signaling for their survival. Therefore, milciclib efficacy in T-ALL could be higher in LCK-dependent cells. Eventually, we confirmed milciclib treatment efficacy in 4 T-ALL patient-derived xenografts treated *ex vivo* (**Supplementary Fig. 5g and h**).

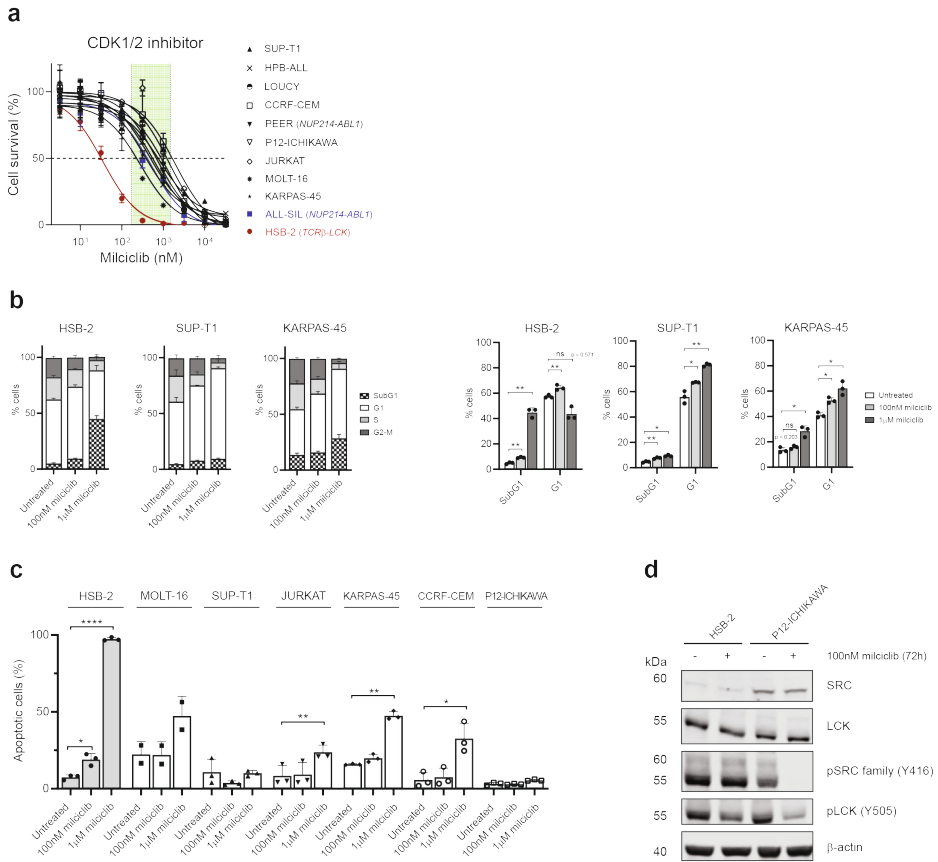


Figure 2. The CDK1/2 inhibitor miliciclib induces G1 arrest in T-ALL cell lines. **a** Dose-response curves of miliciclib treatment in 11 T-ALL cell lines. Cells were treated with increasing concentrations of miliciclib (3.2nM-32μM range) in triplicate and cell viability was assessed after 72 hours using the colorimetric MTT assay. Cell survival was calculated in comparison to the untreated control. Each point represents the mean and standard deviation of the triplicate. The green box shows the corresponding clinical concentration range of miliciclib used in patients enrolled in clinical trials⁵¹. **b** Cell cycle analysis upon miliciclib treatment. Cells were treated with either 100nM or 1μM miliciclib for 72 hours and cell cycle analysis was performed via Hoechst-DNA staining and FACS analysis. The graphs show the average and standard deviation of three independent experiments. Significance was determined using a paired, two-tailed Student's t-test and annotated as "ns" (not significant, $p \geq 0.05$), * ($p < 0.05$), ** ($p < 0.01$). **c** Detection of apoptotic cells upon miliciclib treatment. Cells were treated with either 100nM or 1μM miliciclib for 72 hours and Annexin V/ Propidium Iodide (PI) staining was used to detect apoptosis. Apoptotic cells were identified as the sum of the Annexin V+ cells and Annexin V+/PI+ cells. The percentage of apoptotic cells is calculated compared to untreated control cells. The graphs show the average and standard deviation of three independent experiments. Significance was determined using a paired, two-tailed Student's t-test and annotated as * ($p < 0.05$), ** ($p < 0.01$), **** ($p < 0.0001$). If not annotated, the results were not significant ($p \geq 0.05$). **d** Western blot analysis upon miliciclib treatment. HSB-2 cells and P12-ICHIKAWA cells were treated with 100nM miliciclib for 72 hours and 20μg of protein was used for each condition. The image is representative of three independent experiments.



T-ALL cell lines show limited sensitivity to SRC-family kinases inhibition *in vitro*

To further investigate the potential of LCK as therapeutic target, we analyzed the pY dataset. A predominant role of Src-family members emerged among the detected tyrosine kinases, in particular LCK and SRC (**Fig. 1b**). Despite the ranking of SRC and LCK as Top2 pY-kinases in most lines (**Fig. 1b** and Supplementary **Fig. 2a** and **b**), only HSB-2 and ALL-SIL cells were highly sensitive to ATP-competitive SRC/ABL inhibitors (dasatinib, ponatinib, bosutinib, nilotinib, and imatinib) with IC_{50} values below 100nM. These lines are characterized by a *TCR β -LCK* translocation or a *NUP214-ABL1* fusion, respectively (**Fig. 3a**). The PEER cell line, also described as a *NUP214-ABL1* fusion-positive line, had a low sensitivity to SKFs inhibition (IC_{50} for SRC/ABL inhibitors above 1 μ M except for ponatinib, 834nM. Fig. 3a). The remaining cell lines responded to increasing doses of SRC/ABL inhibitors, but at concentrations beyond the clinically relevant concentrations that are achieved in patient's plasma (**Supplementary Fig. 6a-e**). Similar results were obtained with the LCK inhibitor A-420983 (**Fig. 3a**). Given the broad activation of SKFs detected, we then investigated the effects of dasatinib treatment. Western blotting confirmed high expression of both SRC and LCK in the cell line panel (**Fig. 3b**) and the lines with the highest LCK and SRC expression were used to investigate the effect of dasatinib *in vitro*. Dasatinib treatment (100nM) for three days induced an effective decrease of phospho-LCK and phospho-SRC in all these lines as well as an apparent downregulation of total LCK expression (**Fig. 3c**), without affecting the cell viability (**Fig. 3a** and **Supplementary Fig. 6f**) while HSB-2 cells show induction of apoptosis already after 16 hours of dasatinib treatment (**Supplementary Fig. 6g**). Thus, our data suggest that LCK and SRC are highly active in T-ALL, but the pharmacological inhibition of these activities is only effective in HSB-2 and ALL-SIL that harbor rearrangements in *LCK* or *NUP214-ABL1*, respectively. Remarkably, dasatinib-resistant T-ALL cell lines also downregulate LCK upon dasatinib treatment, indicating their limited dependency on LCK activity for their survival. Therefore, the inhibition of LCK alone seems not a universal effective treatment for every T-ALL, possibly due to the activation of alternative signaling routes.

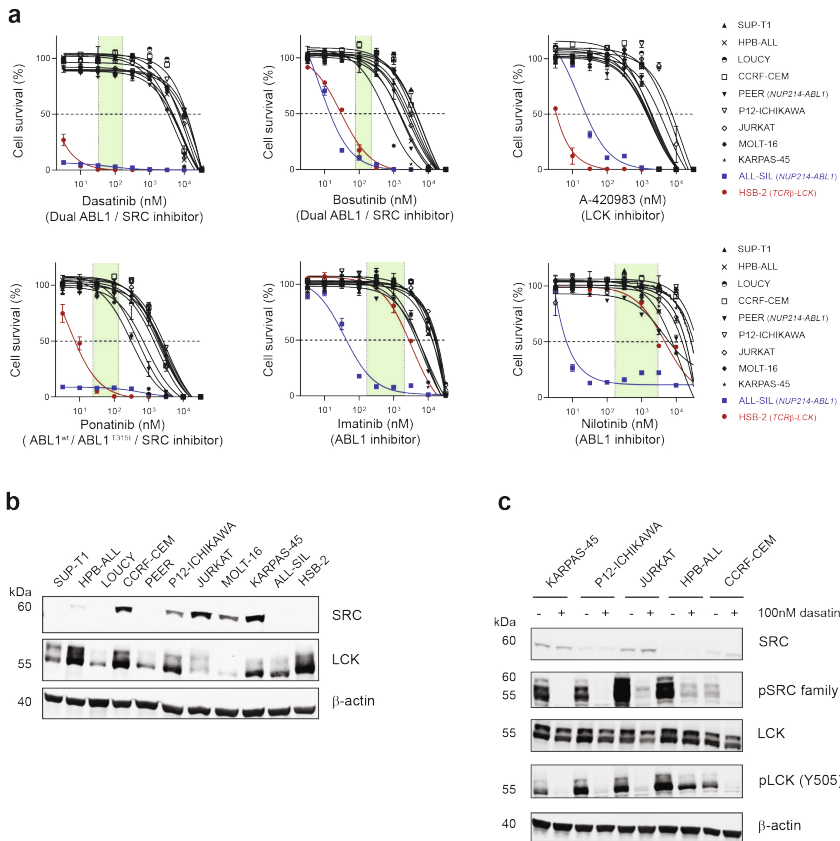


Figure 3. T-ALL cell lines show limited sensitivity to SFKs inhibition *in vitro*. **a** Dose-response curves of SFKs inhibitors treatment in 11 T-ALL cell lines. Cells were treated with increasing concentrations of different SFKs inhibitors: dasatinib, bosutinib, A-420983, ponatinib, imatinib and nilotinib (3.2nM–32 μ M range) in duplo and cell viability was assessed after 72 hours using the ATPLite assay (PerkinElmer). Cell survival was calculated in comparison to the untreated control. Each point represents the mean and standard deviation of the duplicate. The green box shows the range of clinical concentrations either derived from pharmacodynamics studies or based on drug dosages used in current clinical trials⁵²⁻⁵⁵. **b** Western blot analysis showing LCK and SRC expression in untreated T-ALL cell lines. 30 μ g of protein input was used for each sample. The image is representative of two independent experiments. **c** Western blot analysis upon dasatinib treatment. Cell lines expressing high levels of LCK and/or SRC were treated with 100nM dasatinib for 72 hours and 30 μ g of protein was used per sample. The image is representative of two independent experiments.



Inhibition of the INSR/IGF-1R axis sensitizes T-ALL cells to dasatinib treatment *in vitro*

To further investigate the role and the possible targeting of Src-family kinases in T-ALL, we looked for possible upstream kinases or receptors that can explain the activation of LCK and the other SFKs. Interestingly, INSR and IGF-1R were amongst the top20-activated kinases in the pY-INKA profiles for nine out of 11 lines (**Fig.1b** and **Fig. 4a**). Therefore, we tested the sensitivity of these lines to the INSR/IGF-1R inhibitor BMS-754807. ALL-SIL, HPB-ALL, and MOLT-16 demonstrated sensitivity to single BMS-754807 treatment with IC_{50} values below 300nM while most of the other cell lines had IC_{50} values around 1 μ M (**Fig. 4b**). SUP-T1 and Jurkat cells were resistant to BMS-754807 treatment (IC_{50} approximately 10 μ M) despite the predicted INSR/IGF-1R activity (**Fig. 4b**) possibly due to alternative survival signaling pathways. Since SRC can act as signal transducer downstream of several membrane-receptors, we questioned whether lines with active SRC, LCK, and INSR/IGF-1R signaling could benefit from combined SFKs and INSR/IGF-1R signaling inhibition. Therefore, we evaluated the effect of the addition of a low BMS-754807 dose (IC_{20}) to the dasatinib treatment *in vitro*. The lowest dose of dasatinib tested (3.2nM) in combination with low concentrations of BMS-754807 (30-300nM) showed a synergistic and superior effect compared to the single treatments (**Fig. 4c** and **d**). For SUP-T1 cells, the addition of 30nM BMS-754807 to the dasatinib treatment strongly enhanced the cytotoxic effects ($CI < 0.1$; **Fig. 4d**). As validation of the combined treatment strategy, two other INSR/IGF-1R inhibitors were tested in SUP-T1 cells, linsitinib (OSI-906) and GSK-4529A, respectively. Like the BMS-754807 single treatment, SUP-T1 cells showed low sensitivity to both INSR/IGF-1R inhibitors as monotherapy (**Supplementary Fig. 7a** and **b**). However, the combination of a low dose (IC_{20}) of linsitinib or GSK-4529A to the dasatinib treatment *in vitro* confirmed the synergism of simultaneous SRC/LCK and INSR/IGF-1R inhibition (**Fig. 4e**).

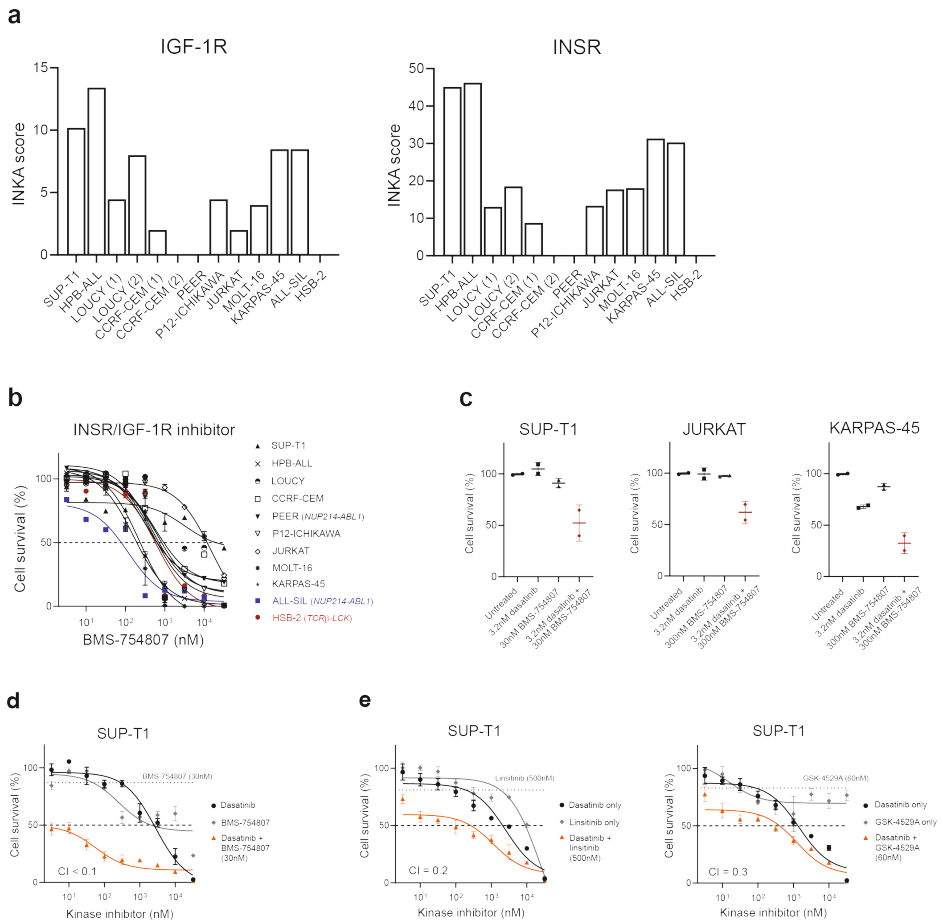


Figure 4. IGF-1R inhibition can sensitize cells to dasatinib treatment. **a** Bar plots of the INKA scores inferred from the pY dataset for IGF-1R and INSR in each cell line. **b** Dose-response curves of BMS-754807 treatment in 11 T-ALL cell lines. Cells were treated with increasing concentrations of the INSR/IGF-1R inhibitor BMS-754807 (3.2nM–32μM range) in duplicates. Cell survival after 72 hours was calculated in comparison to the untreated control. Each point represents the mean and the standard deviation of the duplicates. **c** Sensitivity to dasatinib, BMS-754807 and the combination of 3.2nM dasatinib with the IC₂₀ concentration of BMS-754807 (30–300nM) for SUP-T1, Jurkat and KARPAS-45 cells. Data is shown as mean and standard deviation of two independent experiments performed in triplicate. **d** Dose-response curves of dasatinib, BMS-754807 and combination of dasatinib and a fixed concentration of BMS-754807 treatment in SUP-T1 cells. Cells were treated for 72 hours with increasing concentrations of either dasatinib or BMS-754807 alone or with a combination of dasatinib (3.2nM–32μM range) with a fixed concentration of BMS-754807 (30nM, corresponding to the IC₂₀ of the single treatment for SUP-T1 cells indicated by the dotted line), in triplicate. Cell survival was calculated in comparison to the untreated control. The graph is representative of three independent experiments. CI: combination Index. **e** Dose-response curves of dasatinib, linsitinib, GSK-4524A and combination of dasatinib and a fixed concentration of either linsitinib or GSK-4529A treatment in SUP-T1 cells. Cells were treated for 72 hours with increasing concentrations of dasatinib or linsitinib/GSK-4529A alone or with a combination of dasatinib (3.2nM–32μM range) with a fixed concentration of linsitinib (500nM, corresponding to the IC₂₀ of the single treatment for SUP-T1 cells indicated by the dotted line) or GSK-4529A (60nM, corresponding to the IC₂₀ of the single treatment for SUP-T1 cells indicated by the dotted line), in triplicate. Cell survival was calculated in comparison to the untreated control. The graph is representative of three independent experiments. CI: Combination Index.



To investigate the mechanisms for the synergistic efficacy of this drug combination, we performed western blotting using SUP-T1 cells after treatment with dasatinib, BMS-754807, or their combination. Single 3.2nM dasatinib treatment reduced the phosphorylation of SFKs and ERK1/2 while single 30nM BMS-754807 treatment reduced the phosphorylation of IGF-1R β as well as AKT (S473) (**Fig. 5a**). No effect was detected on phospho-mTOR or phospho-p70 S6 kinase upon BMS-754807 treatment (Fig. 5a), indicating that the IGF-1R signaling converges mainly on AKT. Interestingly, upon IGF-1R inhibition, a slight increase in phosphorylation of SFKs was noticed (phospho-SRC family Y416), further pointing to a potential cross-talk between IGF-1R and SFKs. In fact, the combination of 3.2nM dasatinib and 30nM BMS-754807 showed a further decrease in the activation of IGF-1R (phospho-IGF-1R β Y1135), phospho-AKT (S473) and phospho-SFKs (**Fig. 5a**). To further validate a role for AKT in IGF-1R and SFKs signaling, we tested the cytotoxic effects of the ATP-competitive AKT inhibitor ipatasertib and its combination with dasatinib treatment. Addition of 100nM ipatasertib to the dasatinib treatment enhanced the cytotoxic effects (CI<0.3; **Fig. 5b**). Thus, our data show that co-targeting of activated IGF-1R/AKT and SFKs (summarized in **Fig. 5c**) can extend the potential usage of dasatinib in T-ALL.

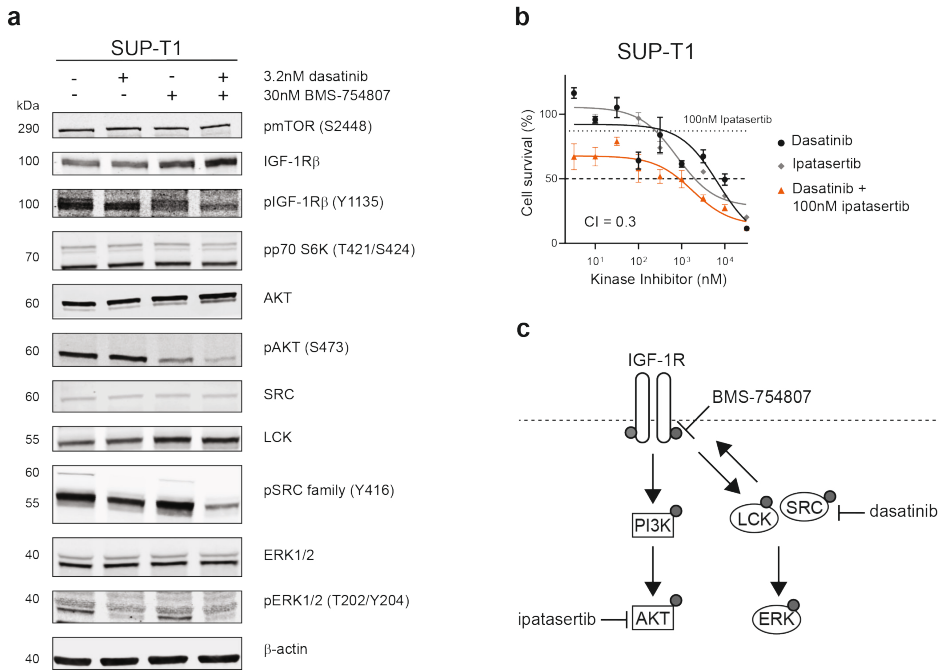


Figure 5. Concomitant inhibition of SFKs and IGF-1R inhibits AKT. **a** Western blot of SUP-T1 cells treated with dasatinib, BMS-754807 or combination treatment. Cells were incubated for 72 hours with 3.2nM dasatinib, 30nM BMS-754807 or combined 3.2nM dasatinib and 30nM BMS-754807. 50 μ g of protein input was used for each sample. The image is representative of two independent experiments. **b** Dose-response curves of dasatinib, ipatasertib and combination of dasatinib and a fixed concentration of ipatasertib treatment in SUP-T1 cells. Cells were treated for 72 hours with increasing concentrations of either dasatinib or ipatasertib alone or with a combination of dasatinib (3.2nM–32 μ M range) with a fixed concentration of ipatasertib (100nM, corresponding to the IC₂₀ of the single treatment for SUP-T1 cells indicated by the dotted line), in triplicate. The data is presented as mean and standard deviation of the mean. The graph is representative of three independent experiments. CI: Combination Index. **c** Graphical summary of the potential targeting of the INSR/IGF-1R axis and the SFKs signaling.

INKA-guided *ex vivo* drug screenings identify synergistic combinations in T-ALL patient-derived xenografts

To validate our approach, we performed phosphotyrosine proteome profiling followed by INKA prediction of active kinases using human T-ALL blasts that were obtained from four different murine patient-derived xenografts (**Fig. 6a**). INKA prediction of active tyrosine kinases highlighted SFKs activation (LCK, SRC, FYN, and YES1) in all the PDXs analyzed, as well as activation of the INSR/IGF-1R axis in two PDXs (PDX-01 and PDX-02) and to a lesser extent in PDX-04 that presented only INSR activity with a low ranking (**Fig. 6b**). All PDXs showed sensitivity to dasatinib treatment *ex vivo* with IC₅₀ values lower than 100nM while PDX-01 showed also high sensitivity to the BMS-754807 single treatment with an IC₅₀

of 234nM (**Fig. 6c**). To further validate the SFKs and INSR/IGF-1R combined inhibition as a putative treatment strategy, blasts obtained from the four different T-ALL PDXs were treated with either dasatinib, BMS-754807 or the combination of both drugs *ex vivo* using a 10-by-10 drug combination matrix as illustrated in Fig. 6a. Zero-Interaction Potency (ZIP) analysis³⁰ of the drug matrix identified synergy between dasatinib and BMS-754807 treatment in one out of four PDXs (PDX-02) already at nanomolar concentrations, as illustrated in Fig. 6d. PDX-01 showed already high sensitivity to both single treatments (**Fig. 6c**) with the drug combination treatment yielding only an additive effect (ZIP synergy scores lower than 10). However, PDX-02 which had lower sensitivity to BMS-754807 single treatment (IC_{50} 675nM), showed high synergy upon combined dasatinib and BMS-754807 treatment, indicating that an active INSR/IGF-1R axis is a targetable vulnerability. Importantly, none of the PDXs carried any somatic mutation in the *INSR* or *IGF1R* gene (**Supplementary Data 1**), highlighting the power of phosphoproteomics in uncovering non-genomic targets for therapy. Consistent with a lack of INSR/IGF-1R activity (**Fig. 6b**), PDX-03 did not benefit from the combination treatment (**Fig. 6d**). For PDX-04, INKA analysis predicted only INSR activity with a low ranking (16/20; **Fig. 6b**) indicating that INSR is not one of the dominant activities and thus explaining the lack of synergy upon combination treatment. Nevertheless, PDX-04 presented high Janus kinases (JAKs) activity which was absent in the other PDXs (**Fig. 6b**). Interestingly, the high JAK3 activity correlated with the presence of an activating *JAK3*^{M511} mutation (**Supplementary Data 1**). Therefore, we tested whether the combination of the JAK inhibitor ruxolitinib with dasatinib could be an effective treatment option for this specific T-ALL case. As shown in Fig. 6e, PDX-04 was the only sample sensitive to ruxolitinib *ex vivo* (IC_{50} < 100nM) while the other PDXs remained completely insensitive to the treatment (IC_{50} > 10 μ M). Moreover, ZIP analysis of the drug combination matrix identified synergy between ruxolitinib and dasatinib only when high JAK activity was predicted (PDX-04, **Fig. 6f**). Thus, the prediction of highly active kinases from phosphoproteomic data can guide the *ex vivo* evaluation of effective drug combination treatments which can differ from patient to patient.

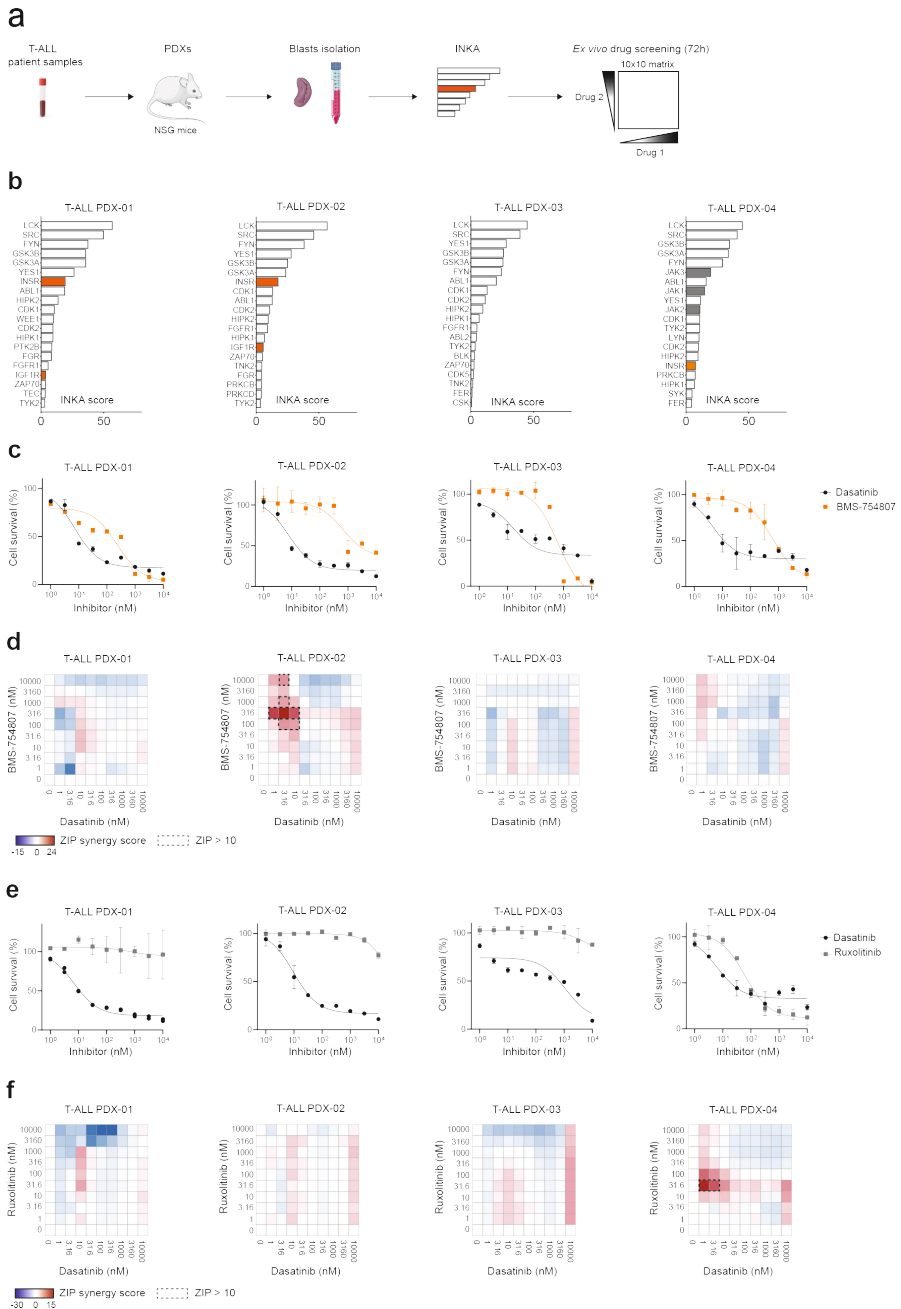


Figure 6. INKA prediction of active kinases identifies synergistic combinations in patient-derived xenografts. **a** PDXs were obtained from T-ALL primary cells expanded in NSG mice. Purified human blasts were used for phosphoproteomics, INKA analyses, and *ex vivo* drug screening using a 10-by-10 drug concentrations matrix. **b** Top20 INKA kinases from the phosphotyrosine (pY) dataset. Each bar plot illustrates the highest 20 active kinases in four PDXs ranked on their INKA score. Orange, INSR/IGF-1R; grey, JAKs; **c** Dose-response curves of dasatinib and BMS-754807 in T-ALL PDX cells (T-ALL

PDX-01 to 04). Cells were treated for 72 hours with increasing concentrations of either dasatinib or BMS-754807 (1nM–10 μ M range) and viability was calculated in relation to untreated control cells (DMSO only). Each point represents the mean and standard deviation of the duplicate. **d** Zero-Interaction Potency (ZIP) synergy scores for the combination of dasatinib and BMS-754807 in a 1nM–10 μ M concentration range. Cells were treated with either one of the single drugs or a drug combination for 72 hours in duplicate. Cell survival was calculated in comparison to untreated cells (DMSO only). ZIP values lower than 0 indicate an antagonistic effect of the drug combination (blue), values between 0 and 10 indicate an additive effect (white to light red) while values above 10 (corresponding to a deviation from the reference model above 10%) indicate synergy (dark red and outside black dashed line). Each drug screening was performed in duplicate. **e** Dose-response curves of dasatinib and ruxolitinib in T-ALL PDX cells. Cells were treated for 72 hours with increasing concentrations of either dasatinib or ruxolitinib (1nM–10 μ M range) and viability was calculated in relation to untreated control cells (DMSO only). Each point represents the mean and standard deviation of the duplicate. **f** ZIP synergy scores for the combination of dasatinib and ruxolitinib in a 1nM - 10 μ M concentration range. Cells were treated with either one of the single drugs or a drug combination for 72 hours in duplicate. Relative viability was calculated in comparison to untreated cells (DMSO only). Each drug screening was performed in duplicate. Source data are provided as a Source Data file.

DISCUSSION

The identification of new targeted drugs is urgently needed to prevent relapses, overcome therapy resistance, and avoid excessive toxicities for T-ALL patients. Genomic-guided therapy has thus far not led to the wide implementation of targeted agents in T-ALL^{31,32}. However, protein analyses can provide useful insights for the identification of cellular dependencies that translates into targetable leukemia vulnerabilities⁴. In this study, we performed an exploratory, global, unbiased phosphoproteome profiling to identify targetable kinases in T-ALL and to establish a proteome platform that can complement genomic analyses for the investigation of leukemia dependencies. In our initial analysis of 11 T-ALL cell lines, we identified highly active tyrosine kinases (LCK, SRC, FYN, YES1, LYN, INSR, and IGF-1R) as well as serine/threonine kinases (CDK1/2, AKT, and PAK1/2). Moreover, the comparison of the phosphoproteomes of T-ALL and AML revealed active kinases that reflect differences in their hematopoietic lineages of origin, independently of the presence of known signaling mutations, highlighting the additional value of MS-based phosphoproteome profiling. Next, we screened several clinical kinase inhibitors *in vitro* and found that the CDK1/CDK2 inhibitor milciclib has a cytostatic effect in T-ALL cells. Milciclib is under clinical investigation for the treatment of thymoma and hepatocellular carcinoma³³. Currently, clinical studies are investigating other CDKs inhibitors (ribociclib and palbociclib) for the treatment of relapsed T-ALL¹² and milciclib may be an additional treatment option.

Cells with *ABL1* or *LCK* driving oncogenic aberrations showed high sensitivity to SRC/ABL inhibitors, including dasatinib, while the remaining cell lines had a limited response, despite the prediction of highly active Src-family members. Therefore, elevated LCK activity seems not to translate into cellular dependency in all T-ALL specimens. In 2017,

Frismantas and colleagues showed that up to 30% of T-ALLs were sensitive to dasatinib *ex vivo* in the absence of *ABL1* abnormalities. This dasatinib-responsiveness correlated with higher levels of phosphorylated SRC in sensitive cells³⁴. In line with this previous study, our PDX models showed high sensitivity to dasatinib *ex vivo* in the absence of *LCK* or *SRC* mutations (**Supplementary Data 1**), underscoring the potential use of this drug for T-ALL treatment. Recently, a pharmacogenomic study on pediatric T-ALL identified *LCK*, but not *SRC*, as driver of dasatinib sensitivity in up to 40% of pediatric T-ALL cases. The observed *LCK* activity correlated with pre-TCR signaling and relatively more mature developmental stages (TAL/LMO)³⁵, while immature ETP-ALL cells were less sensitive to dasatinib. In our study, the immature T-ALL cell line LOUCY indeed showed lower *LCK* activity but increased activation of myeloid kinases such as *LYN* and *HCK*. Given the lower response to dasatinib for most of the cell lines in our panel, possibly due to the presence of alternative escape signaling routes, we found that the co-inhibition of the *INSR/IGF-1R* axis and SFKs was strongly synergistic. We provided evidence that the *INSR/IGF-1R* axis is active in most T-ALL cell lines and that the pharmacological inhibition of *IGF-1R* sensitizes T-ALL cells to dasatinib treatment, indicating important cross-talks between *INSR/IGF-1R* and SFKs. These results are in line with previous studies that identified *INSR/IGF-1R* activation as a bypass mechanism in solid tumors with intrinsic resistance to tyrosine kinase inhibitors³⁶⁻³⁸. Moreover, preclinical investigations showed that a subset of T-ALL cells is sensitive to *INSR/IGF-1R* inhibition without presenting any activating mutations in these receptor kinase-coding genes^{39,40}. We validated the targeting of active *INSR/IGF-1R* signaling either as single treatment or in combination with dasatinib in two PDX models. In line with previous observations, both PDXs did not carry any somatic mutation in *INSR* or *IGF1R*. The lack of mutations that could explain the active *INSR/IGF-1R* signaling underscores the role of phosphoproteomics in highlighting relevant signaling nodes which would have not been uncovered via genomic analyses. Interestingly, Gocho and colleagues showed modulation of *INSR* activity upon dasatinib treatment in dasatinib-sensitive T-ALL patient-derived murine xenografts³⁵, further strengthening the observation that the *INSR/IGF-1R* and SFKs signaling can be interconnected and can mutually affect each other, as summarized in Fig. 5c, and illustrated in kinase-substrate relation networks in Supplementary Fig. 8. Two studies highlighted the role of dendritic cells and tumor-associated myeloid cells in supporting T-ALL growth in stromal niches via *IGF-1R* activation^{41,42}, emphasizing the relevance of this signaling pathway in the pathobiology of T-ALL. The tumor niche can provide a protective microenvironment, and therefore the simultaneous blocking of *IGF-1R* and SFKs signaling should be further investigated for T-ALL patients. Furthermore, since several studies highlighted a role for *LCK* in supporting resistance to

glucocorticoids in T-ALL^{43,44}, targeting LCK activation could provide additional benefits to other combination therapies. Multiple clinical trials are investigating the JAK inhibitor ruxolitinib for the treatment of T-ALL in the presence of *JAK* mutations¹². Here, we show that ruxolitinib treatment is effective *ex vivo* in T-ALL cells with elevated JAK kinase activity. Interestingly, the elevated JAK3 activity correlated with the presence of an activating *JAK3* mutation, highlighting that driving oncogenic aberrations can also be detected at the signaling level. Moreover, ruxolitinib can synergize with dasatinib treatment in JAK- and SFKs-activated cells, indicating another putative combinatorial strategy for selected T-ALL cases. Therefore, our phosphoproteomic profiling provides a platform for the investigation of combinatorial treatments and for the identification of non-genomic leukemia dependencies. Such dependencies can be further exploited as leukemia vulnerabilities for personalized treatment.

INKA-based selection of (combination) treatments has been already validated in the context of solid tumors²⁷ and acute myeloid leukemia^{22,45}, underscoring the functional value of the pipeline. Future T-ALL studies should include an *in vitro* screening platform that can allow blasts proliferation *ex vivo* to study drugs affecting the cell cycle, as well as an extended PDXs cohort comprising all the different T-ALL subtypes. *Further in vivo* investigations of selected drug combinations should address not only the efficacy and tolerability of these treatments (*i.e.*, toxicities) but also the role of the microenvironmental niches that can support blasts growth and survival. Such investigations could allow the direct translation of the preclinical findings to the clinical settings. In conclusion, we provide evidence that phosphoproteomics can guide the selection of targets for *ex vivo* drug screening to evaluate the most effective treatment strategy.

METHODS

Cell culture

Cell lines (Supplementary Table 1) were purchased from DSMZ (Germany) or ATCC (USA) and maintained in RPMI1640 + GlutaMax[®] (Gibco) supplemented with 10% fetal bovine serum (Gibco) and antibiotics at a density of $0.2\text{-}2 \times 10^6$ cells/ml in a humidified incubator with 5% CO₂ at 37°C. Cells were periodically tested for the absence of mycoplasma contamination using the MycoAlert Mycoplasma Detection Kit (Lonza cat# LT07-118). Cell lines authentication was performed via short tandem repeat (STR) profiling.

Western Blotting

Membranes were incubated with the following primary antibodies (1:1,000 dilution, if not stated otherwise): anti-P-Tyr-1000 (Cell Signaling Technology cat# 8954), anti-Lck (Cell Signaling Technology cat# 2752), anti-Src L4A1 (Cell Signaling Technology cat# 2110), anti-phospho Lck (Tyr505) (Cell Signaling Technology cat# 2751), anti-phospho Src Family (Tyr416) (Cell Signaling Technology cat# 2101), anti-IGF1R β (Cell Signaling Technology cat# 3027), anti-phospho IGF1R β (Tyr1135) (Cell Signaling Technology cat# 3918), anti-phospho mTOR (Ser2448) (Cell Signaling Technology cat# 2971), anti-phospho p70 S6K (Thr421/Ser424) (Cell Signaling Technology cat# 9204), anti-AKT (Cell Signaling Technology cat# 9272), anti-phospho AKT (Ser473) (Cell Signaling Technology cat# 9271), anti-p44-42 MAPK (ERK1/2) (137F5) (Cell Signaling Technology cat# 4695), anti-phospho p44-42 MAPK (Thr202/Tyr204) (D13.14.4E) (Cell Signaling Technology cat# 4370), anti-cleaved caspase-3 (Asp175) (Cell Signaling Technology cat# 9661), and anti- β actin (Abcam, cat# ab6276, 1:10,000).

For protein bands staining, SDS-PAGE gels were stained using the Colloidal Blue Staining kit (Invitrogen cat# LC6025) according to the manufacturer protocol. Uncropped and unprocessed blots are provided in the Source Data file.

Flow cytometry

Experiments were performed using the ZE5 flow cytometer (BioRAD). For cell cycle analysis, 200,000 cells per condition were stained with Hoechst (7.5 μ g/ml) for 1 hour at 37 $^{\circ}$ C and then incubated for 15 minutes on ice before FACS analysis. For Annexin V/propidium iodide (PI) staining of apoptotic cells, 200,000 cells were stained with Annexin V-APC antibody (Biolegend cat# 640920) diluted 1:20 in Annexin V-binding buffer (Invitrogen cat# V13246) for 15 minutes at room temperature (RT) in the dark. PI (Miltenyi) was added at a final concentration of 0.5 μ g/ml just before the FACS measurement. Data analysis was performed using FlowJo v10.7.1 (FlowJo). Examples of the sequential gatings used for the FACS data analyses are shown in Supplementary Fig. 9.

Generation of patient-derived xenografts

Blasts obtained from pediatric patients diagnosed with T-ALL were provided by the Dutch Childhood Oncology Group (DCOG) upon signed informed consent and in accordance with the declaration of Helsinki. Animal experiments were approved by the Animal Welfare Committee of the Princess Máxima Center for pediatric oncology (Utrecht, the Netherlands) and were carried out at the animal facility of the Hubrecht Institute (Utrecht,

the Netherlands) under specific pathogen-free conditions and in accordance with animal welfare, FELASA (Federation of European Laboratory Animal Science Associations), ethical, and institutional guidelines. Mice were hosted in individually ventilated cages in groups of 2-3 mice per cage. Briefly, viably frozen human blasts were intravenously injected into immunocompromised NOD/scid/Gamma (NSG) female mice of 8-10 weeks of age (Charles River, France). Mice were constantly monitored for leukemia development and disease burden was assessed by detection of human CD45+ cells in the murine blood by tail vein cut and FACS analysis. Mice were sacrificed when presenting symptoms of leukemia (lack of grooming and activity, hunched back position, visible loss of weight) or when the circulating human CD45+ cells reached 50%. Human blasts were isolated from the murine spleen using the Lymphoprep density gradient separation (STEMCELL technologies, Canada). Purified blasts were either immediately harvested for phosphoproteomic analyses or viably frozen until further usage. The mutational status of primary cells and their related PDXs was previously investigated by whole-exome sequencing ⁴⁶. The full list of somatic mutations of the T-ALL xenografts used in this study is reported in Supplementary Data 1.

Phosphorylated peptide enrichment and mass spectrometry analysis

Cell lines were harvested in their exponential growth phase to preserve physiological signaling while human CD45+ blast obtained from the murine spleen were immediately harvested after the Lymphoprep density gradient separation. Briefly, cells were spun down at 250 x g for 5 minutes, washed in cold PBS, spun down again, and harvested in 9M urea/20mM HEPES (pH 8) lysis buffer containing 1mM sodium orthovanadate, 2.5mM sodium pyrophosphate, and 1mM β -glycerophosphate. Cell lysates were thoroughly vortexed at maximum speed for 30 seconds, snap-frozen in liquid nitrogen and stored at -80°C until further usage. Before the enrichment step, lysates were thawed, sonicated three times at 18-micron amplitude (30 seconds on/60 seconds off) using the MSE Soniprep 150 sonicator (MSE) on ice. Cleared lysates were diluted to a concentration of 2mg/ml and 5mg of protein input was used for each sample. Proteins were reduced with 2mM DTT for 30 minutes at 55°C, alkylated using 5mM iodoacetamide for 15 minutes at RT in the dark and eventually digested overnight with Sequencing Grade Modified Trypsin (Promega cat# V5111) at RT. Digested peptides were purified using OASIS HLB Cartridges (6 cc, 500 mg Sorbent, 60 μ m particle size. Waters cat# 186000115) and lyophilized. Phospho-tyrosine peptides were enriched via immunoprecipitation (IP) using the PTMScan® Phospho-Tyrosine Rabbit mAb (P-Tyr-1000) Kit (Cell Signaling Technology cat# 8803) according to the manufacturer protocol, using 4 μ l of bead slurry for each mg of protein input. Phospho-tyrosine peptides were eluted in 0.15% trifluoroacetic acid (TFA) and the unbound peptide fraction was used

for complementary phospho-serine and phospho-threonine peptides capturing using custom-made TiO₂ C8-fitted tips. Eventually, eluted phosphorylated peptides were desalted using 20 µl SDB-XC StageTips (Prepared from Empore™ SPE Disks with SDB-XC, Sigma cat# 66884-U) prior to LC-MS analysis. For global protein expression analysis, 1 µg of total lysate was subjected to liquid chromatography-mass spectrometry (LC-MS). LC-MS analyses were performed as previously described²⁷. Briefly, phosphopeptides were dried in a vacuum centrifuge and dissolved in 20 µl 0.5% trifluoroacetic acid (TFA)/4% acetonitrile (ACN) prior to injection; 18 µl was injected using partial loop injection. Peptides were separated by an Ultimate 3000 nanoLC-MS/MS system (Thermo Fisher) equipped with a 50 cm × 75 µm ID Acclaim Pepmap (C18, 1.9 µm) column. After injection, peptides were trapped at 3 µl/min on a 10 mm × 75 µm ID Acclaim Pepmap trap at 2% buffer B (buffer A: 0.1% formic acid (FA); buffer B: 80% ACN, 0.1% FA) and separated at 300 nl/min in a 10–40% buffer B gradient in 90 min (125 min inject-to-inject) at 35°C. Eluting peptides were ionized at a potential of +2 kV into a Q Exactive HF mass spectrometer (Thermo Fisher). Intact masses were measured from m/z 350–1400 at resolution 120,000 (at m/z 200) in the Orbitrap using an AGC target value of 3E6 charges and a maxIT of 100 ms. The top 15 for peptide signals (charge-states 2+ and higher) were submitted to MS/MS in the HCD (higher-energy collision) cell (1.4 amu isolation width, 26% normalized collision energy). MS/MS spectra were acquired at resolution 15,000 (at m/z 200) in the Orbitrap using an AGC target value of 1E6 charges, a maxIT of 64 ms and an underfill ratio of 0.1%. This results in an intensity threshold for MS/MS of 1.3E5. Dynamic exclusion was applied with a repeat count of 1 and an exclusion time of 30 s. For peptide and protein identification, MS/MS spectra were searched against theoretical spectra from the UniProt complete human proteome FASTA file (release January 2018, 42,258 entries) using the MaxQuant 1.6.0.16 software⁴⁷ with the following settings: enzyme specificity= trypsin, missed cleavages allowed= 2, fixed modification= cysteine carboxamidomethylation; variable modification= serine, threonine and tyrosine phosphorylation, methionine oxidation, and N-terminal acetylation; MS tolerance= 4.5 ppm and MS/MS tolerance= 20 ppm. For both peptide and protein identifications, the false discovery rate was set at 1% for filtering using a decoy database strategy. The minimal peptide length was set at 7 amino acids, the minimum Andromeda score for modified peptides at 40, and the corresponding minimum delta score at 6. Moreover, the “match between runs” option was used to propagate the peptides identification across samples.

Isolation of human thymocytes and *ex vivo* drug treatment

Normal pediatric thymic tissues were obtained according to the study protocol TCbio-18-181 approved by the ethical committee and the biobank of the Utrecht university medical center

(the Netherlands). Informed written consent for research purposes was provided by all the legal guardians of the participants. Briefly, after surgical removal, thymic tissue biopsies were mechanically disrupted in RPMI-1640 medium (Gibco) supplemented with fetal bovine serum (Gibco) and antibiotics to obtain a single-cell suspension. Isolated thymocytes were washed in PBS and contaminating red blood cells were removed via osmotic shock using the RBC lysis buffer (BioLegend, cat #420301) according to the manufacturer protocol. Cells were diluted to a concentration of 2.5×10^6 cells/ml and dispensed into a 384 multi well plate (Corning) using the semi-automated Multidrop dispenser (Thermo Fisher) in duplicates. Drugs were diluted in DMSO at a concentration of 10mM and dispensed using a TECAN D300e digital dispenser in a range of 1nM – 10 μ M. Cell viability was evaluated at the time of seeding (t=0) and after 72 hours incubation using the CellTiter-Glo luminescence assay (Promega) according to the manufacturer protocol.

INKA analyses

Inference of highly active kinases from phosphoproteomic data was performed as previously described ²⁷. Integrative iNferred Kinase Activity (INKA) scores are calculated based on 4 parameters: the sum of all phosphorylated peptides belonging to a kinase; the detection of the phosphorylated kinase activation domain (kinase-centric parameters), 3) the detection of known phosphorylated substrates and the presence of predicted phosphorylated substrates (substrate-centric parameters) ^{22,27}. The latest version of the INKA pipeline is available online at <https://inkascore.org/>.

Drug screenings

Cytotoxicity assays were performed as previously described ⁴⁸. Alternatively, cells were seeded in triplicate in 96-multiwell plates and incubated with kinase inhibitors (Supplementary Table 2) in a concentration range from 3.2nM to 32 μ M for 72 hours. For combination treatment assays in cell lines, a fixed concentration of BMS-754807, linsitinib, GSK-4529A, or ipatasertib was added to the dasatinib range. Cell viability was calculated in relation to untreated control cells using the colorimetric Thiazolyl Blue Tetrazolium Bromide (MTT) assay (Sigma-Aldrich cat# 475989). Graphs were obtained using the GraphPad Prism 9.0.1 software (GraphPad Prism, nonlinear regression, inhibitor vs response; three parameters). Synergy upon treatment combination was calculated using the Chou-Talalay method ⁴⁹, according to the following formula: combination index (CI) = $D1/Dx1 + D2/Dx2$ where $Dx1$ and $Dx2$ are the IC_{50} of the single drugs while $D1$ and $D2$ are the drug concentrations achieving 50% reduction in cell viability in the combined treatment.

For synergy testing in PDXs, viably frozen T-ALL blasts purified from the murine spleen were thawed and cultured in RPMI1640 + GlutaMax® (Gibco) supplemented with 20% fetal calf serum (Gibco) and antibiotics in the absence of cytokines and feeder layer. Cells were dispensed into a 384 multi well plate (Corning) using the semi-automated Multidrop dispenser (Thermo Fisher) in duplicates. Drugs were diluted in DMSO at a concentration of 10mM and dispensed using a TECAN D300e digital dispenser in a range of 1nM – 10µM. Cell viability was evaluated at the time of seeding (t=0) and after 72 hours incubation using the CellTiter-Glo luminescence assay (Promega) according to the manufacturer protocol. Synergy was evaluated using the SynergyFinder R package (version 2.4.16)⁵⁰ applying the Zero-Interaction Potency (ZIP) method³⁰. In case of negative inhibition values, a partial correction was applied to avoid an overestimation of the synergistic effect with a combined treatment³⁰. Drug combinations with a ZIP synergy score higher than 10 (corresponding to a deviation from the reference model above 10%) were considered synergistic.

Data availability

The mass spectrometry proteomics data have been deposited to the ProteomeXchange Consortium via the PRIDE partner repository with the dataset identifier PXD024807 (<http://proteomecentral.proteomexchange.org/cgi/GetDataset?ID=PX024807>). The human Swiss-Prot database used for raw data search was downloaded from the UniProt database (<https://www.uniprot.org/>). The AML phosphoproteomic data²² used in Fig. 1e was downloaded from the ProteomeXchange Consortium using the accession code PXD007237 (<http://proteomecentral.proteomexchange.org/cgi/GetDataset?ID=PX007237>). The targets of milciclib were identified browsing the ProteomicsDB database^{28,29} (<https://www.proteomicsdb.org/>).

Code availability

The latest version of the INKA code used in this manuscript is available online at <https://inkascore.org/>.

Statistical analyses

Statistical analyses were performed via a paired, two-sided Student's t-test using the GraphPad Prism 9.0.1 software (GraphPad Prism). The number of biological replicates and the exact p-values are indicated in the figure legends.

ACKNOWLEDGMENTS

This study was supported by the Dutch Cancer Society (KWF Kankerbestrijding, grant KWF2016_10355 to V.C.) and the foundation Kinderen Kankervrij (grant Kika-295 to M.T.M. and KiKa-335 to V.M.P.). Furthermore, Cancer Center Amsterdam and the Netherlands Organization for Scientific Research (NWO Middelgroot, #91116017) are acknowledged for the support of the mass spectrometry infrastructure. The authors would like to thank dr. Bram van Wijk for providing the thymic tissue and Chris Meulenbroeks for the thymocytes isolation.

AUTHOR CONTRIBUTIONS

V.C. designed and performed experiments, analyzed data, performed bioinformatic analyses, and wrote the manuscript. M.T.M., R.R.d.G.-d.H., and V.M.P performed experiments. R.H., A.A.H., and T.V.P. performed bioinformatic analyses. S.R.P. performed the mass spectrometry measurements and analyzed data. K.O. and A.A.F. provided samples. G.J.R.Z. provided the LCK inhibitor and expertise in drug screening. C.R.J. and J.P.P.M. designed and supervised the study and revised the manuscript.

COMPETING INTERESTS

G.J.R.Z. is founder, shareholder, and managing director of Oncolines B.V. All the other authors declare no conflict of interest.

REFERENCES

- 1 Winter, S. S. *et al.* Improved Survival for Children and Young Adults With T-Lineage Acute Lymphoblastic Leukemia: Results From the Children's Oncology Group AALL0434 Methotrexate Randomization. *J Clin Oncol* **36**, 2926-2934, doi:10.1200/JCO.2018.77.7250 (2018).
- 2 Jeha, S. *et al.* Improved CNS Control of Childhood Acute Lymphoblastic Leukemia Without Cranial Irradiation: St Jude Total Therapy Study 16. *J Clin Oncol* **37**, 3377-3391, doi:10.1200/JCO.19.01692 (2019).
- 3 Belver, L. & Ferrando, A. The genetics and mechanisms of T cell acute lymphoblastic leukaemia. *Nat Rev Cancer* **16**, 494-507, doi:10.1038/nrc.2016.63 (2016).
- 4 van der Zwet, J. C. G., Cordo, V., Cante-Barrett, K. & Meijerink, J. P. P. Multi-omic approaches to improve outcome for T-cell acute lymphoblastic leukemia patients. *Adv Biol Regul* **74**, 100647, doi:10.1016/j.jbior.2019.100647 (2019).
- 5 Graux, C. *et al.* Heterogeneous patterns of amplification of the NUP214-ABL1 fusion gene in T-cell acute lymphoblastic leukemia. *Leukemia* **23**, 125-133, doi:10.1038/leu.2008.278 (2009).
- 6 Vicente, C. *et al.* Targeted sequencing identifies associations between IL7R-JAK mutations and epigenetic modulators in T-cell acute lymphoblastic leukemia. *Haematologica* **100**, 1301-1310, doi:10.3324/haematol.2015.130179 (2015).
- 7 Liu, Y. *et al.* The genomic landscape of pediatric and young adult T-lineage acute lymphoblastic leukemia. *Nat Genet* **49**, 1211-1218, doi:10.1038/ng.3909 (2017).
- 8 Sanda, T. *et al.* TYK2-STAT1-BCL2 pathway dependence in T-cell acute lymphoblastic leukemia. *Cancer Discov* **3**, 564-577, doi:10.1158/2159-8290.CD-12-0504 (2013).
- 9 Akahane, K. *et al.* Anti-leukaemic activity of the TYK2 selective inhibitor NDI-031301 in T-cell acute lymphoblastic leukaemia. *Br J Haematol* **177**, 271-282, doi:10.1111/bjh.14563 (2017).
- 10 Sparta, A. M. *et al.* Therapeutic targeting of Polo-like kinase-1 and Aurora kinases in T-cell acute lymphoblastic leukemia. *Cell Cycle* **13**, 2237-2247, doi:10.4161/cc.29267 (2014).
- 11 Jiang, J. *et al.* Direct Phosphorylation and Stabilization of MYC by Aurora B Kinase Promote T-cell Leukemogenesis. *Cancer Cell* **37**, 200-215 e205, doi:10.1016/j.ccell.2020.01.001 (2020).
- 12 Cordo, V., van der Zwet, J. C. G., Cante-Barrett, K., Pieters, R. & Meijerink, J. P. P. T-cell Acute Lymphoblastic Leukemia: A Roadmap to Targeted Therapies. *Blood Cancer Discov* **2**, 19-31, doi:10.1158/2643-3230.BCD-20-0093 (2021).
- 13 De Smedt, R. *et al.* Targeting cytokine- and therapy-induced PIM1 activation in preclinical models of T-cell acute lymphoblastic leukemia and lymphoma. *Blood* **135**, 1685-1695, doi:10.1182/blood.2019003880 (2020).
- 14 Furness, C. L. *et al.* The subclonal complexity of STIL-TAL1+ T-cell acute lymphoblastic leukaemia. *Leukemia* **32**, 1984-1993, doi:10.1038/s41375-018-0046-8 (2018).
- 15 Tzoneva, G. *et al.* Clonal evolution mechanisms in NT5C2 mutant-relapsed acute lymphoblastic leukaemia. *Nature* **553**, 511-514, doi:10.1038/nature25186 (2018).
- 16 Shah, N. P. *et al.* Sequential ABL kinase inhibitor therapy selects for compound drug-resistant BCR-ABL mutations with altered oncogenic potency. *J Clin Invest* **117**, 2562-2569, doi:10.1172/JCI30890 (2007).
- 17 Loh, M. L. *et al.* Tyrosine kinome sequencing of pediatric acute lymphoblastic leukemia: a report from the Children's Oncology Group TARGET Project. *Blood* **121**, 485-488, doi:10.1182/blood-2012-04-422691 (2013).

- 18 Hijazi, M., Smith, R., Rajeeve, V., Bessant, C. & Cutillas, P. R. Reconstructing kinase network topologies from phosphoproteomics data reveals cancer-associated rewiring. *Nat Biotechnol* **38**, 493-502, doi:10.1038/s41587-019-0391-9 (2020).
- 19 Cutillas, P. R. Role of phosphoproteomics in the development of personalized cancer therapies. *Proteomics Clin Appl* **9**, 383-395, doi:10.1002/prca.201400104 (2015).
- 20 Doll, S., Gnad, F. & Mann, M. The Case for Proteomics and Phospho-Proteomics in Personalized Cancer Medicine. *Proteomics Clin Appl* **13**, e1800113, doi:10.1002/prca.201800113 (2019).
- 21 Frejno, M. *et al.* Proteome activity landscapes of tumor cell lines determine drug responses. *Nat Commun* **11**, 3639, doi:10.1038/s41467-020-17336-9 (2020).
- 22 van Alphen, C. *et al.* Phosphotyrosine-based Phosphoproteomics for Target Identification and Drug Response Prediction in AML Cell Lines. *Mol Cell Proteomics* **19**, 884-899, doi:10.1074/mcp.RA119.001504 (2020).
- 23 Casado, P. *et al.* Proteomic and genomic integration identifies kinase and differentiation determinants of kinase inhibitor sensitivity in leukemia cells. *Leukemia* **32**, 1818-1822, doi:10.1038/s41375-018-0032-1 (2018).
- 24 Serafin, V. *et al.* Phosphoproteomic analysis reveals hyperactivation of mTOR/STAT3 and LCK/ Calcineurin axes in pediatric early T-cell precursor ALL. *Leukemia* **31**, 1007-1011, doi:10.1038/leu.2017.13 (2017).
- 25 Degryse, S. *et al.* Mutant JAK3 phosphoproteomic profiling predicts synergism between JAK3 inhibitors and MEK/BCL2 inhibitors for the treatment of T-cell acute lymphoblastic leukemia. *Leukemia* **32**, 788-800, doi:10.1038/leu.2017.276 (2018).
- 26 Franciosa, G. *et al.* Proteomics of resistance to Notch1 inhibition in acute lymphoblastic leukemia reveals targetable kinase signatures. *Nat Commun* **12**, 2507, doi:10.1038/s41467-021-22787-9 (2021).
- 27 Beekhof, R. *et al.* INKA, an integrative data analysis pipeline for phosphoproteomic inference of active kinases. *Mol Syst Biol* **15**, e8250, doi:10.15252/msb.20188250 (2019).
- 28 Samaras, P. *et al.* ProteomicsDB: a multi-omics and multi-organism resource for life science research. *Nucleic Acids Res* **48**, D1153-D1163, doi:10.1093/nar/gkz974 (2020).
- 29 Klaeger, S. *et al.* The target landscape of clinical kinase drugs. *Science* **358**, doi:10.1126/science.aan4368 (2017).
- 30 Yadav, B., Wennerberg, K., Aittokallio, T. & Tang, J. Searching for Drug Synergy in Complex Dose-Response Landscapes Using an Interaction Potency Model. *Comput Struct Biotechnol J* **13**, 504-513, doi:10.1016/j.csbj.2015.09.001 (2015).
- 31 Massard, C. *et al.* High-Throughput Genomics and Clinical Outcome in Hard-to-Treat Advanced Cancers: Results of the MOSCATO 01 Trial. *Cancer Discov* **7**, 586-595, doi:10.1158/2159-8290.CD-16-1396 (2017).
- 32 Marquart, J., Chen, E. Y. & Prasad, V. Estimation of the Percentage of US Patients With Cancer Who Benefit From Genome-Driven Oncology. *JAMA Oncol* **4**, 1093-1098, doi:10.1001/jamaoncol.2018.1660 (2018).
- 33 Villa, E. *et al.* Phase IIa safety and efficacy of milciclib, a pan-cyclin dependent kinase inhibitor, in unresectable, sorafenib-refractory or -intolerant hepatocellular carcinoma patients. *Journal of Clinical Oncology* **38**, e16711-e16711, doi:10.1200/JCO.2020.38.15_suppl.e16711 (2020).
- 34 Frismantas, V. *et al.* Ex vivo drug response profiling detects recurrent sensitivity patterns in drug-resistant acute lymphoblastic leukemia. *Blood* **129**, e26-e37, doi:10.1182/blood-2016-09-738070 (2017).

- 35 Gocho, Y. *et al.* Network-based systems pharmacology reveals heterogeneity in LCK and BCL2 signaling and therapeutic sensitivity of T-cell acute lymphoblastic leukemia. *Nat Cancer* **2**, 284-299, doi:10.1038/s43018-020-00167-4 (2021).
- 36 Vyse, S. *et al.* Quantitative phosphoproteomic analysis of acquired cancer drug resistance to pazopanib and dasatinib. *J Proteomics* **170**, 130-140, doi:10.1016/j.jprot.2017.08.015 (2018).
- 37 Zanella, E. R. *et al.* IGF2 is an actionable target that identifies a distinct subpopulation of colorectal cancer patients with marginal response to anti-EGFR therapies. *Sci Transl Med* **7**, 272ra212, doi:10.1126/scitranslmed.3010445 (2015).
- 38 Wan, X., Yeung, C., Heske, C., Mendoza, A. & Helman, L. J. IGF-1R Inhibition Activates a YES/SFK Bypass Resistance Pathway: Rational Basis for Co-Targeting IGF-1R and Yes/SFK Kinase in Rhabdomyosarcoma. *Neoplasia* **17**, 358-366, doi:10.1016/j.neo.2015.03.001 (2015).
- 39 Gusscott, S. *et al.* IGF1R Derived PI3K/AKT Signaling Maintains Growth in a Subset of Human T-Cell Acute Lymphoblastic Leukemias. *PLoS One* **11**, e0161158, doi:10.1371/journal.pone.0161158 (2016).
- 40 Rodrigues Alves, A. P. N. *et al.* IGF1R/IRS1 targeting has cytotoxic activity and inhibits PI3K/AKT/mTOR and MAPK signaling in acute lymphoblastic leukemia cells. *Cancer Lett* **456**, 59-68, doi:10.1016/j.canlet.2019.04.030 (2019).
- 41 Triplett, T. A. *et al.* Endogenous dendritic cells from the tumor microenvironment support T-ALL growth via IGF1R activation. *Proc Natl Acad Sci U S A* **113**, E1016-1025, doi:10.1073/pnas.1520245113 (2016).
- 42 Lyu, A. *et al.* Tumor-associated myeloid cells provide critical support for T-ALL. *Blood* **136**, 1837-1850, doi:10.1182/blood.2020007145 (2020).
- 43 Serafin, V. *et al.* Glucocorticoid resistance is reverted by LCK inhibition in pediatric T-cell acute lymphoblastic leukemia. *Blood* **130**, 2750-2761, doi:10.1182/blood-2017-05-784603 (2017).
- 44 Shi, Y. *et al.* Phase II-like murine trial identifies synergy between dexamethasone and dasatinib in T-cell acute lymphoblastic leukemia. *Haematologica* **106**, 1056-1066, doi:10.3324/haematol.2019.241026 (2021).
- 45 Cucchi, D. G. J. *et al.* Phosphoproteomic Characterization of Primary AML Samples and Relevance for Response Toward FLT3-inhibitors. *Hemasphere* **5**, e606, doi:10.1097/HS9.0000000000000606 (2021).
- 46 Oshima, K. *et al.* Mutational and functional genetics mapping of chemotherapy resistance mechanisms in relapsed acute lymphoblastic leukemia. *Nature Cancer* **1**, 1113-1127, doi:10.1038/s43018-020-00124-1 (2020).
- 47 Tyanova, S., Temu, T. & Cox, J. The MaxQuant computational platform for mass spectrometry-based shotgun proteomics. *Nat Protoc* **11**, 2301-2319, doi:10.1038/nprot.2016.136 (2016).
- 48 Li, Y. *et al.* IL-7 Receptor Mutations and Steroid Resistance in Pediatric T cell Acute Lymphoblastic Leukemia: A Genome Sequencing Study. *PLoS Med* **13**, e1002200, doi:10.1371/journal.pmed.1002200 (2016).
- 49 Chou, T. C. & Talalay, P. Quantitative analysis of dose-effect relationships: the combined effects of multiple drugs or enzyme inhibitors. *Adv Enzyme Regul* **22**, 27-55, doi:10.1016/0065-2571(84)90007-4 (1984).
- 50 Zheng, S. *et al.* SynergyFinder Plus: towards a better interpretation and annotation of drug combination screening datasets. *bioRxiv*, 2021.2006.2001.446564, doi:10.1101/2021.06.01.446564 (2021).

Chapter 3

- 51 Weiss, G. J. *et al.* Phase I study of the safety, tolerability and pharmacokinetics of PHA-848125AC, a dual tropomyosin receptor kinase A and cyclin-dependent kinase inhibitor, in patients with advanced solid malignancies. *Invest New Drugs* **30**, 2334-2343, doi:10.1007/s10637-011-9774-6 (2012).
- 52 Cortes, J. E. *et al.* Ponatinib in refractory Philadelphia chromosome-positive leukemias. *N Engl J Med* **367**, 2075-2088, doi:10.1056/NEJMoa1205127 (2012).
- 53 Abbas, R. & Hsyu, P. H. Clinical Pharmacokinetics and Pharmacodynamics of Bosutinib. *Clin Pharmacokinet* **55**, 1191-1204, doi:10.1007/s40262-016-0391-6 (2016).
- 54 Hijiya, N. *et al.* Pharmacokinetics of Nilotinib in Pediatric Patients with Philadelphia Chromosome-Positive Chronic Myeloid Leukemia or Acute Lymphoblastic Leukemia. *Clin Cancer Res* **26**, 812-820, doi:10.1158/1078-0432.CCR-19-0090 (2020).
- 55 Zwaan, C. M. *et al.* Dasatinib in children and adolescents with relapsed or refractory leukemia: results of the CA180-018 phase I dose-escalation study of the Innovative Therapies for Children with Cancer Consortium. *J Clin Oncol* **31**, 2460-2468, doi:10.1200/JCO.2012.46.8280 (2013).

SUPPLEMENTARY INFORMATION

Supplementary Data 1 is available online at:

<https://www.nature.com/articles/s41467-022-28682-1>



SUPPLEMENTARY DATA

Supplementary Table 1. Characteristics of the T-ALL cell lines used in this study.

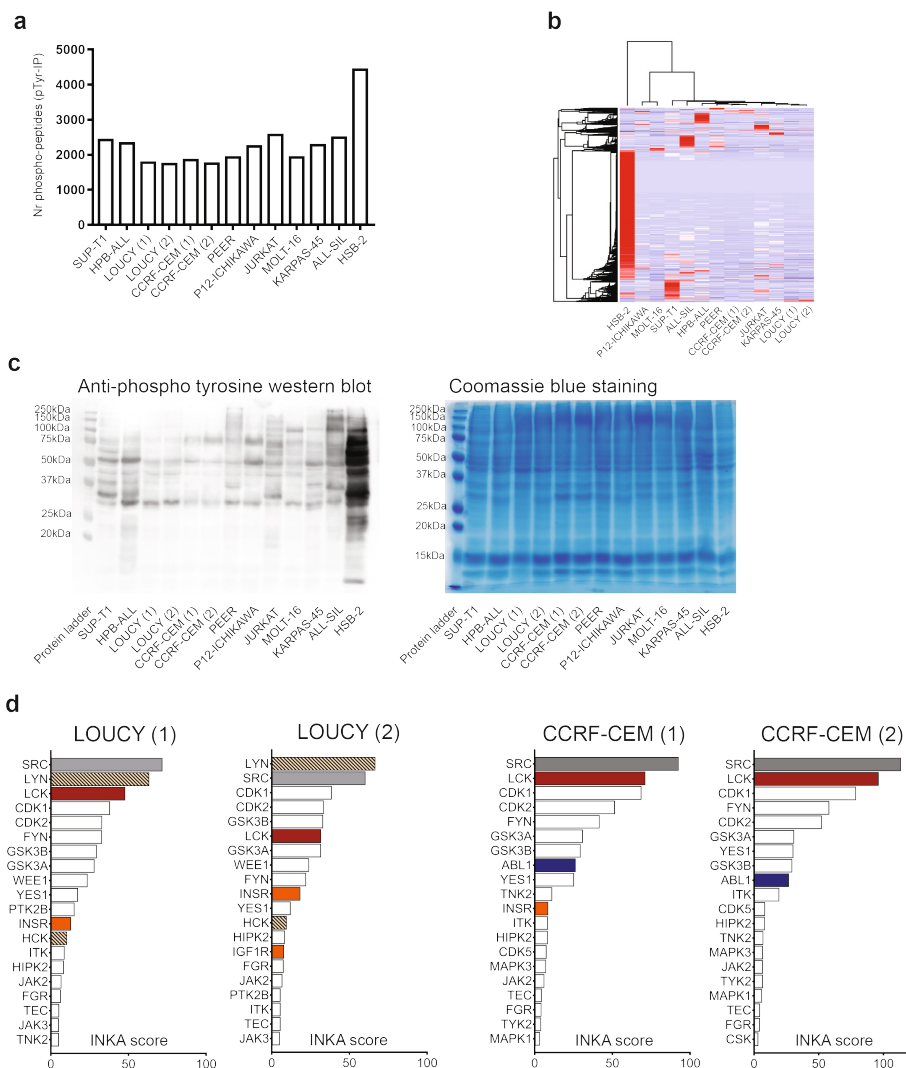
| Cell line | ATCC id | DSMZ id | ECACC id | Origin | Immuno-phenotype | Translocations / Fusions | Mutated oncogenes | Subgroup (rearranged oncogene (t)) |
|------------------|-----------|---------|----------|------------|---|----------------------------------|--|------------------------------------|
| JURKAT | TIB-152 | ACC-282 | - | PB (Rel) | CD2+, CD3+, CD5+, CD6+, CD7+, TCRαβ+, TCRγδ- | | FBXW7, NOTCH1, TP53 | TAL/LMO |
| HPB-ALL | - | ACC-483 | - | PB (Dx) | CD2+, CD3+, CD4+, CD5+, CD6+, CD7+, CD8+, TCRαβ+, TCRγδ- | BCL11B-TLX3 | FBXW7, PTEN, TP53, WT1, HRAS | TLX (TLX3r) |
| LOUCY | CRL-2629 | ACC-394 | - | PB | CD2-, CD3+, CD4-, CD5+, CD +, CD7+, CD8-, TCRαβ-, TCRγδ- | SET-NUP214 | TP53 | ETP-ALL/immature |
| HSB-2 | CCL-120.1 | ACC-435 | - | PB | CD2-, cyCD3 +, smCD3-, CD4-, CD5+, CD6+, CD7+, CD8+, TCRαβ- | TCRB-LCK SIL-TAL1 | NOTCH1, NRAS | TAL/LMO (TAL1r) |
| PEER | - | ACC-6 | - | PB (Rel) | CD2-, CD3+, CD4+, CD5+, CD6+, CD7+, TCRγδ+ | NUP214-ABL1 NKX2.5- BCL11B | NOTCH1, TP53 | ETP-ALL (NKX2.5r) |
| ALL-SIL | - | ACC-511 | - | PB (Rel) | cyCD3+, CD3-, CD4+, CD5+, CD6+, CD7+, CD8+, TCRαβ-, TCRγδ- | NUP214-ABL1 | NOTCH1 | TLX1/NKX2.1 (TLX1r) |
| CCRF-CEM | CCL-119 | ACC-240 | - | PB (Rel) | CD2-, CD3+, CD4+, CD5+, CD6+, CD7 +, CD8 - | | FBXW7, NOTCH1, KRAS, PIK3CA, FLT3 | TAL/LMO (TAL1r) |
| KARPAS45 | - | - | 6072602 | BM (Dx) | | MLL-AFX | FBXW7, NOTCH1, TP53, WT1, JAK3, CDKN2A | HOXA (MLLr) |
| P12- ICHIKAWA | - | ACC-34 | - | PB | cyCD3+, CD4+, CD5+, CD6+, CD7+, CD8-, TCRαβ-, TCRγδ- | | FBXW7, NOTCH1, NRAS, PTEN, TP53 | TAL/LMO (LMO2r) |
| SUP-T1 | CRL-1942 | ACC-140 | - | PE (T-LBL) | CD2+, cyCD3+, CD4+, CD5+, CD6+, CD7+, CD8+, TCRαβ-, TCRγδ- | | PHF6, PIK3CA, LCK, PTEN, RB1, TP53, JAK3 | T-LBL |
| MOLT16 | - | ACC-29 | - | PB (Rel) | CD2+, CD3+, CD4-, CD5+, CD6+, CD7+, CD8 -, CD13 -, CD19 -, CD34 -, TCRαβ+, TCRγδ- | | PIK3CA, TP53, WT1 | TAL/LMO (LMO2r) |

Source: DSMZ, ATCC, cansAR, COSMIC, Kalender-Atak *et al*.¹, Quentmeier *et al*.²

Abbreviations: r, rearranged; PB, peripheral blood; BM, bone marrow; PE, pleural effusion; T-LBL, T-cell lymphoblastic lymphoma; Dx, diagnosis; Rel, relapse.

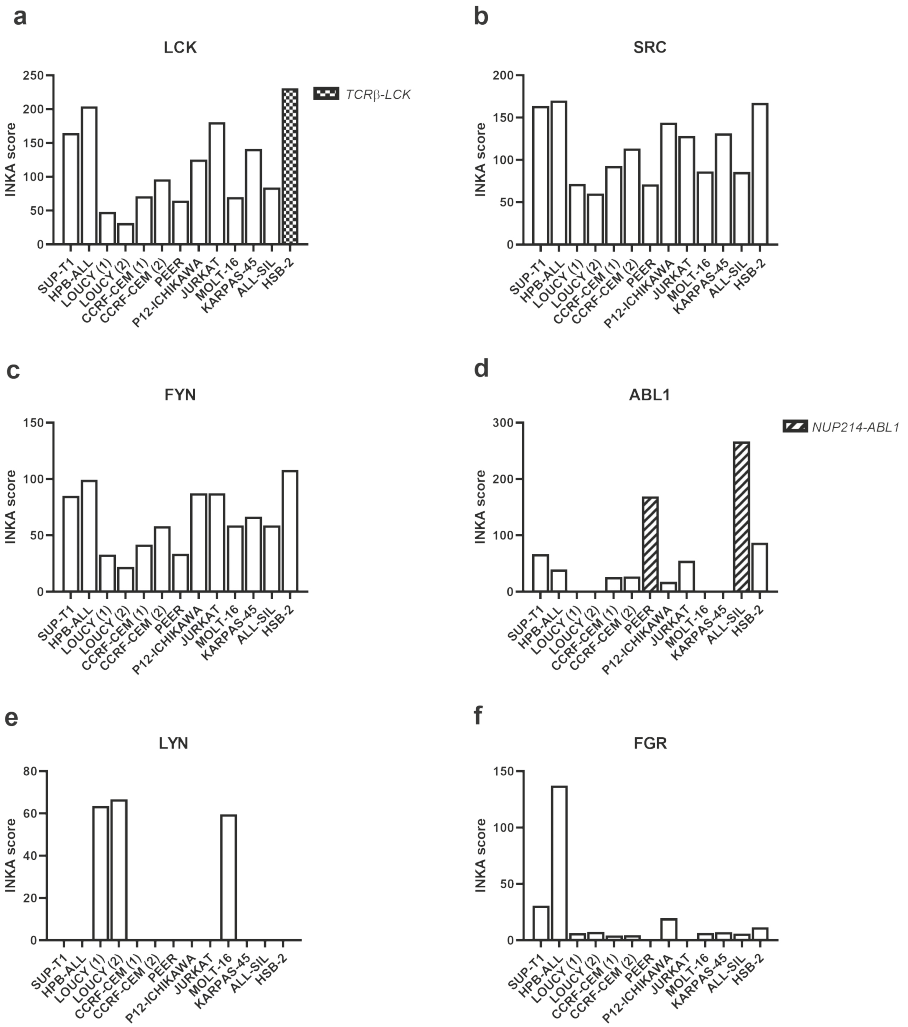
Supplementary Table 2. Kinase inhibitors used in this study.

| Kinase inhibitor | Target | Supplier | Catalog number | CAS number |
|-------------------------|---------------|----------------------------|-----------------------|-------------------|
| Milciclib | CDK1/2 | MedChemExpress | HY-10424 | 802539-81-7 |
| Dasatinib | ABL1/SFK | Sigma-Aldrich | CDS023389 | 302962-49-8 |
| Imatinib mesylate | BCR-ABL1 | Sigma-Aldrich | SML1027 | 220127-57-1 |
| Ponatinib | ABL1/SFK | MedChemExpress | HY-12047 | 943319-70-8 |
| Bosutinib | ABL1/SFK | MedChemExpress | HY-10158 | 380843-75-4 |
| Nilotinib | BCR-ABL1 | MedChemExpress | HY-10159 | 641571-10-0 |
| A-420983 | LCK | Provided by Oncolines B.V. | | 330789-03-2 |
| BMS-754807 | INSR/IGF-1R | MedChemExpress | HY-10200 | 1001350-96-4 |
| Linsitinib (OSI-906) | INSR/IGF-1R | MedChemExpress | HY-10191 | 867160-71-2 |
| GSK1904529A | INSR/IGF-1R | MedChemExpress | HY-10524 | 1089283-49-7 |
| TG003 | CLK1 | MedChemExpress | HY-15338 | 719277-26-6 |
| FRAX597 | PAK | MedChemExpress | HY-15542A | 1286739-19-2 |
| Ipatasertib | AKT | MedChemExpress | HY-15186 | 1001264-89-6 |
| Selumetinib | MEK1/2 | Selleckchem | S1008 | 606143-52-6 |
| Sirolimus | mTOR | MedChemExpress | HY-10219 | 53123-88-9 |
| Ruxolitinib | JAK | Selleckchem | S1378 | 941678-49-5 |



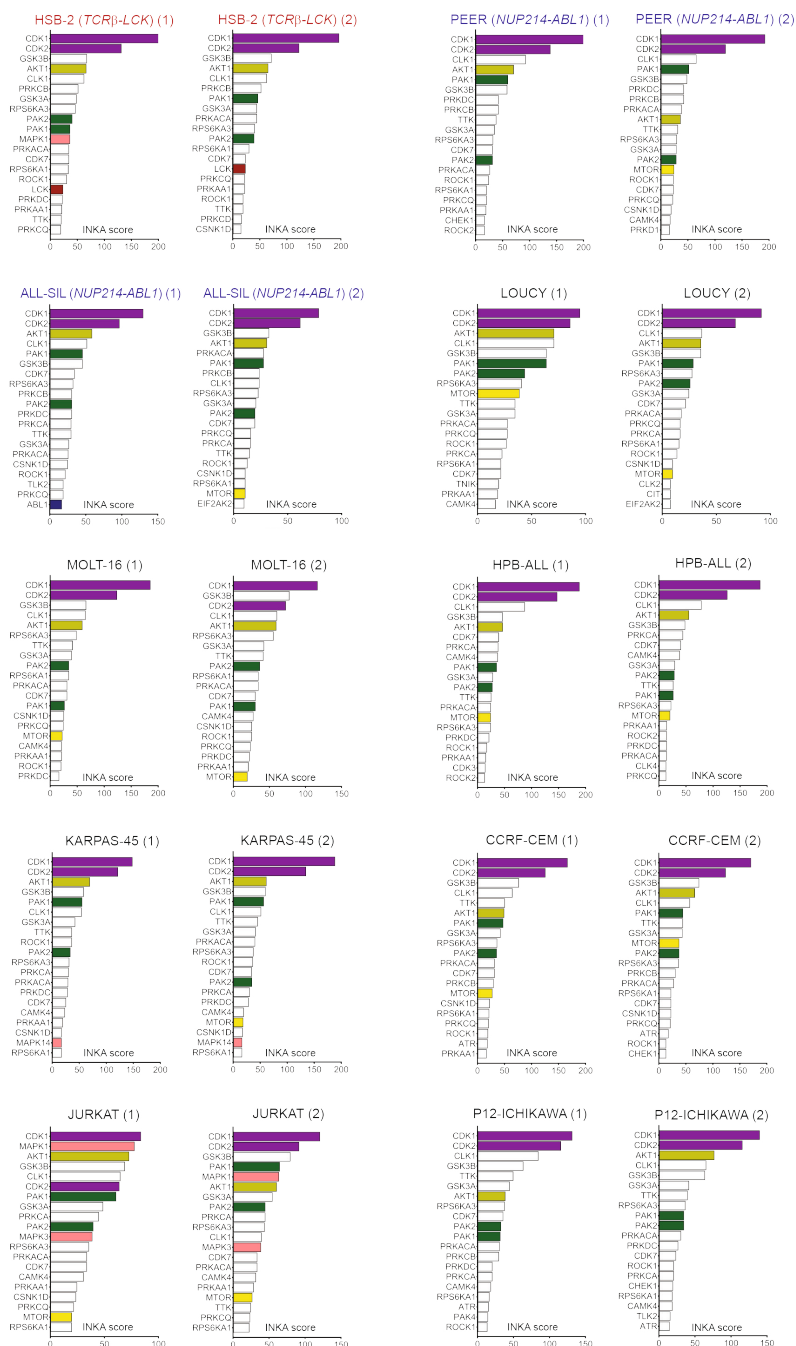
Supplementary Figure 1. Phospho-peptides recovery and differences among T-ALL cell lines. a

Number of phospho-peptides recovered and identified in each sample following an anti-phosphorylated tyrosine immunoprecipitation. For LOUCY and CCRF-CEM, two biological replicates were used as internal reproducibility control. **b** Unsupervised clustering of phosphorylated peptides identified in each sample following an anti-phosphorylated tyrosine immunoprecipitation. **c** Anti phospho-tyrosine western blotting was performed on total lysates (30 μ g for each cell line) prior to phospho-peptides enrichment to evaluate the total tyrosine phosphorylation in each sample. Coomassie blue gel staining was used as a parallel loading control to assure equal protein loading. Figures are representative of two independent experiments. **d** Top20 INKA kinases inferred from the phospho-tyrosine (pY) dataset. Each bar plot illustrates the highest 20 active kinases in each cell line (biological duplicates for LOUCY and CCRF-CEM) ranked on their INKA score. Red, LCK; blue, ABL1; grey, SRC; orange, INSR/IGF-1R; striped pattern, myeloid-lineage kinases (LYN and HCK).

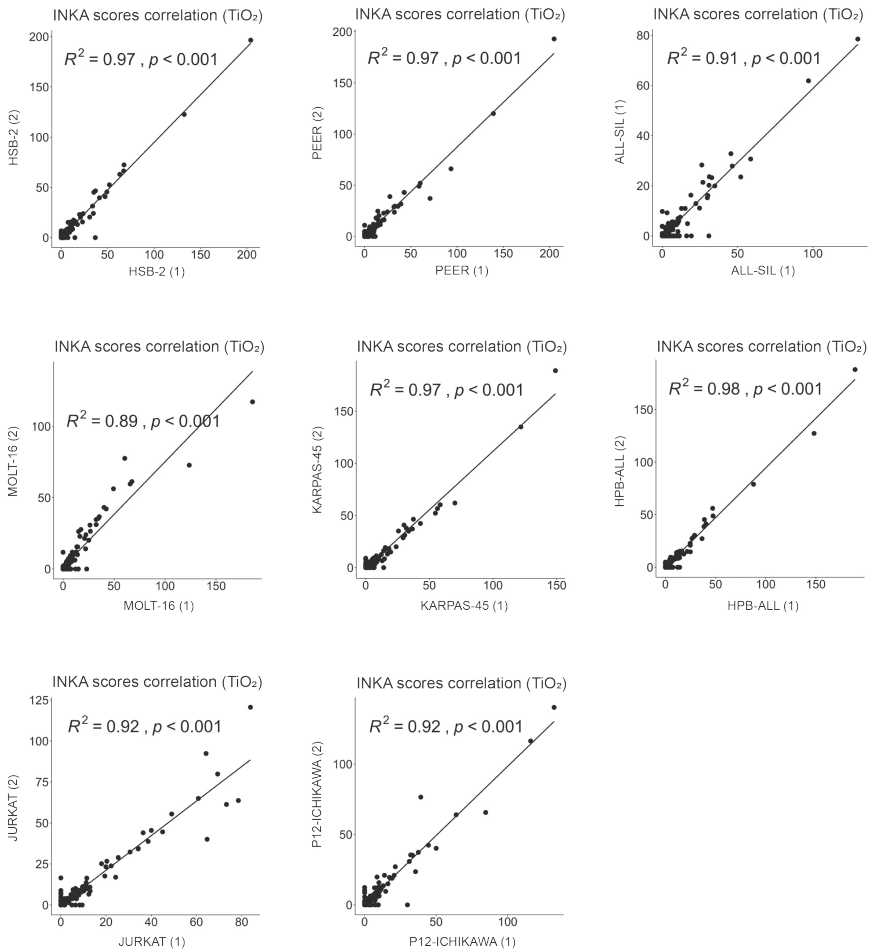


Supplementary Figure 2. INKA scores for several Src-family kinases (SFKs). Each bar plot illustrates the INKA scores for different SFK members in each cell line (pY dataset). **a** LCK. The dotted pattern indicates the presence of a *TCRβ-LCK* translocation (HSB-2 cell line). **b** SRC. **c** FYN. **d** ABL1. The striped pattern indicates the presence of a *NUP214-ABL1* fusion (PEER and ALL-SIL lines). **e** LYN. **f** FGR.



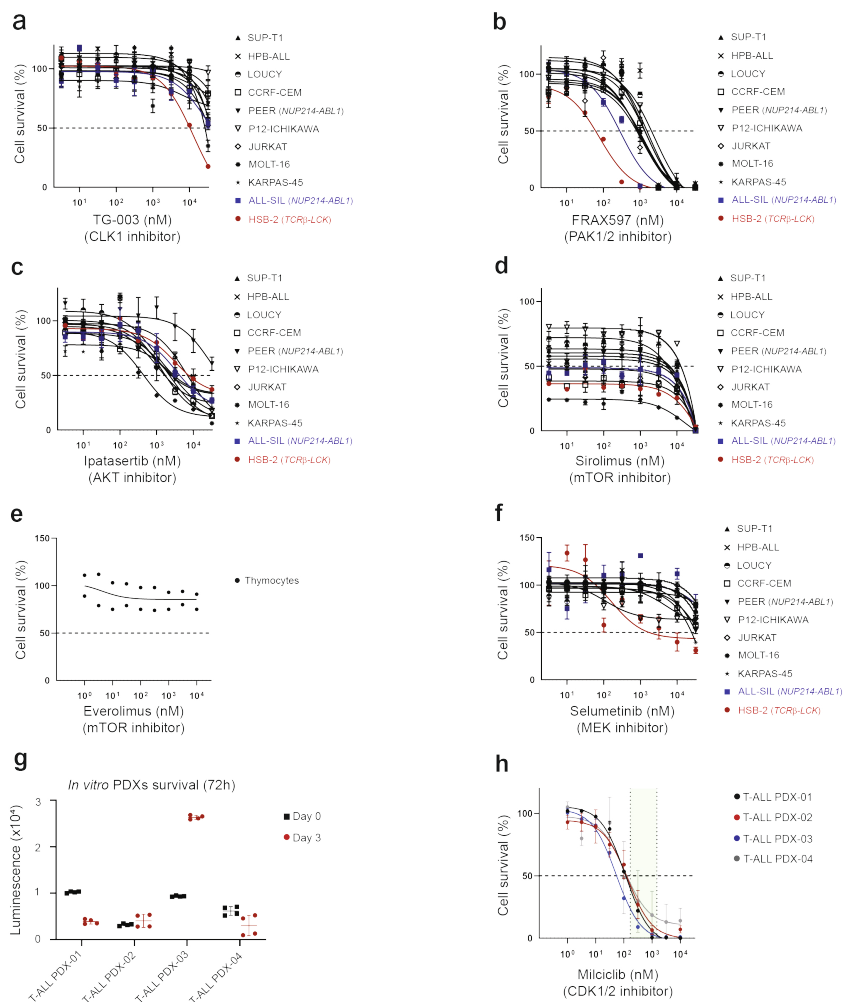


Supplementary Figure 3. Top20 INKA kinases inferred from the TiO2 dataset. Each bar plot illustrates the highest 20 active kinases in each cell line ranked on their INKA score (technical duplicates for 10 cell lines are shown). Purple, CDK1/2; dark green, PAK1/2; light green, AKT; yellow, mTOR; pink, MAPK; red, LCK, Blue: ABL1.



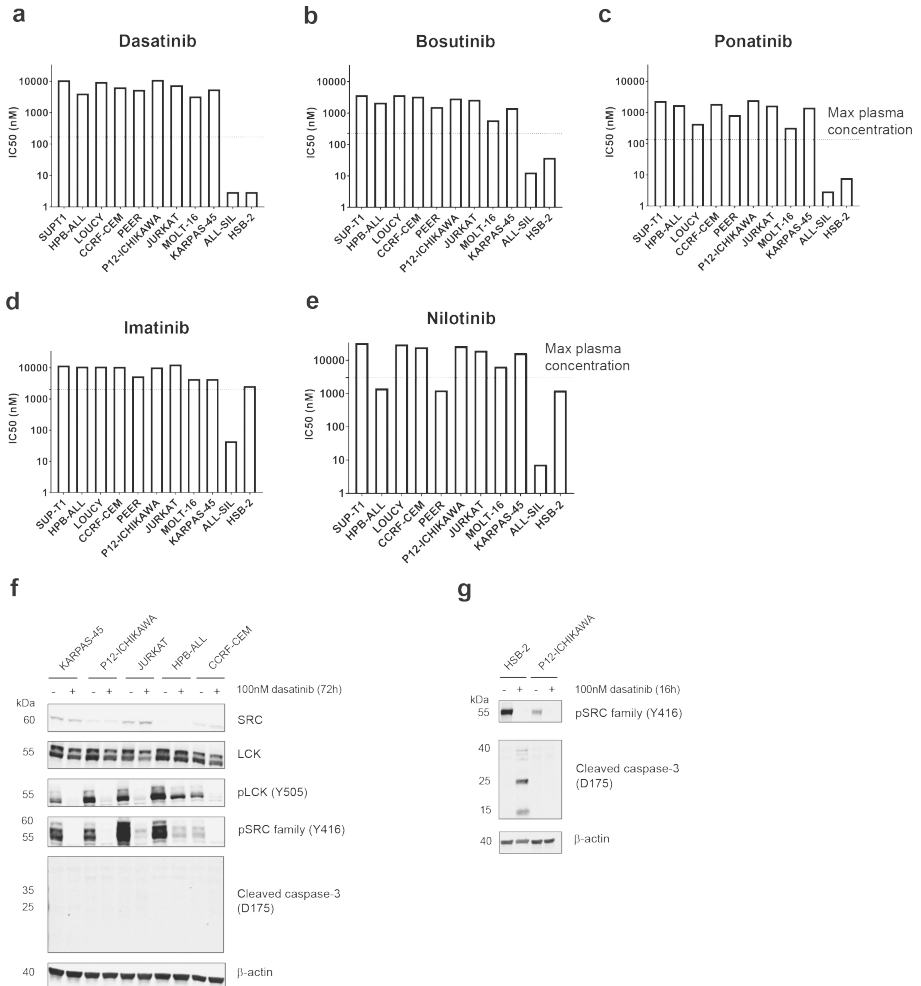
Supplementary Figure 4. Correlation plots TiO_2 dataset. Each plot shows the correlation of the INKA scores between technical duplicates in the TiO_2 dataset for 8 cell lines (Pearson's correlation, two-sided t-test, $p < 0.001$).





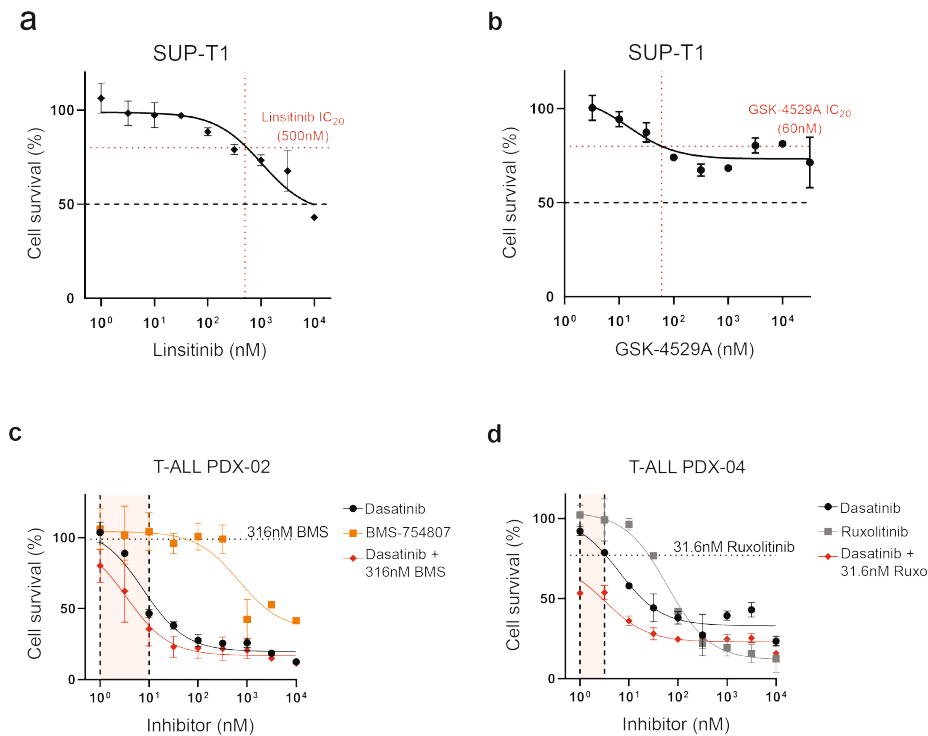
Supplementary Figure 5. Dose-response curves of kinase inhibitors (CLK1i, PAKi, AKTi, mTORi, MEKi, CDKi). Dose-response curves of kinase inhibitors treatment. Cell lines were treated with increasing concentrations of the CLK1 inhibitor TG-003 (**a**), PAK inhibitor FRAX597 (**b**), AKT inhibitor ipatasertib (**c**), mTOR inhibitor sirolimus (**d**) in a 3.2nM–32 μ M range in triplicate and cell viability was assessed after 72 hours using the colorimetric MTT assay. Cell survival was calculated in comparison to the untreated control. Each point represents the mean and standard deviation of the triplicate. **e** Dose-response curves of everolimus treatment *ex vivo* in healthy thymocytes isolated from a pediatric thymic biopsy. Cells were treated with increasing concentrations (1nM–10 μ M) of everolimus in duplicates. Cell survival was calculated in comparison to the untreated control (DMSO only). **f** Dose-response curves of selumetinib treatment in T-ALL cell lines. Each point represents the mean and standard deviation of the triplicate. **g** *In vitro* survival of blasts obtained from four T-ALL patient-derived murine xenografts (PDXs). Luminescence signal recorded at day 0 (time of seeding) and day 3 (72h culture). Symbols indicate replicates per conditions (N = 4), the horizontal line the mean, and the error bars indicate the average of the mean. **h** Dose-response curves of milciclib treatment *ex vivo* in 4 PDXs. Cells were treated with increasing concentrations of milciclib (1nM–10 μ M) for 72 hours and the survival was calculated in comparison to the untreated control (DMSO only). The green box indicates the clinical concentration range of milciclib. Each point represents the mean and standard

deviation of the duplicate.

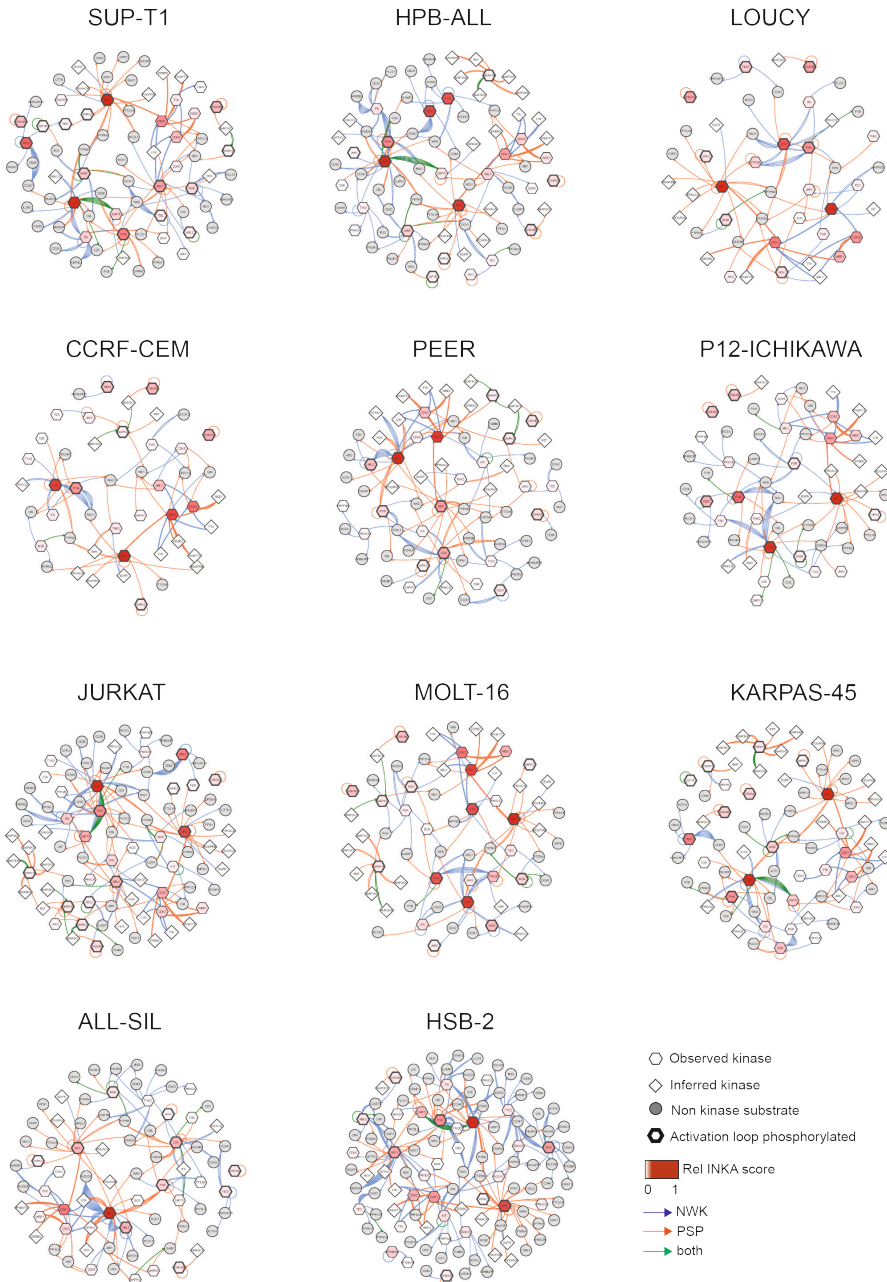


Supplementary Figure 6. IC₅₀ values for different kinase inhibitors tested in T-ALL cell lines and *in vitro* SFKs inhibition. Each bar plot shows the IC₅₀ values for each cell line for the SFKs/ABL inhibitors tested. The dotted line indicates the highest plasma concentration achieved in patients. **a** dasatinib, **b** bosutinib, **c** ponatinib, **d** imatinib, **e** nilotinib. **f** Western blot analysis upon dasatinib treatment *in vitro*. Cell lines expressing high levels of LCK and/or SRC were treated with 100nM dasatinib for 72 hours. The image is representative of two independent experiments. **g** Western blot analysis upon dasatinib treatment *in vitro*. A dasatinib-sensitive cell line (HSB-2) and a dasatinib-resistant cell line (P12-ICHIKAWA) were treated with 100nM dasatinib for 16 hours. The image is representative of two independent experiments.





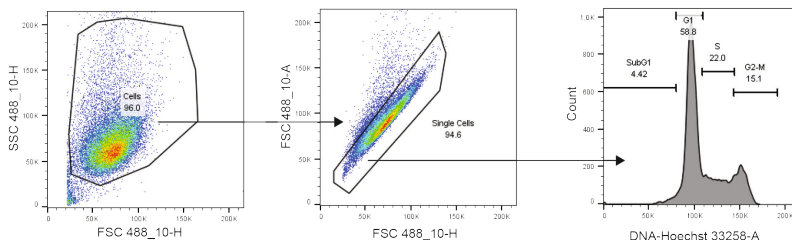
Supplementary Figure 7. Dose-response curves of the INSR/IGF-1R inhibitors linsitinib and GSK-4529A in SUP-T1 cells and combination treatment *ex vivo* in PDXs. Dose-response curves of linsitinib (**a**) and GSK-4529A (**b**) in SUP-T1 cells. Cells were treated for 72 hours with increasing concentrations of linsitinib (1nM–10 μ M range) or GSK-4529A (3.2nM–32 μ M range) as single treatment. Cell survival was calculated in comparison to the untreated control. Each point represents the mean and standard deviation of the triplicate. **c** Dose-response curves of dasatinib, BMS-754807 and combination treatment *ex vivo* in PDX-02. Cells were treated for 72 hours and viability was calculated in relation to untreated control cells (DMSO only). Each point represents the mean and standard deviation of the duplicate. The red box indicates the area of synergy of the drug matrix. **d** Dose-response curves of dasatinib, ruxolitinib and combination treatment *ex vivo* in PDX-04. Cells were treated for 72 hours and viability was calculated in relation to untreated control cells (DMSO only). Each point represents the mean and standard deviation of the duplicate. The red box indicates the area of synergy of the drug matrix.



Supplementary Figure 8. Kinase substrate-networks. Each graph represents the main kinase-substrate relation networks inferred from the phosphoproteomic data (pY dataset) by INKA analysis for each T-ALL cell line.

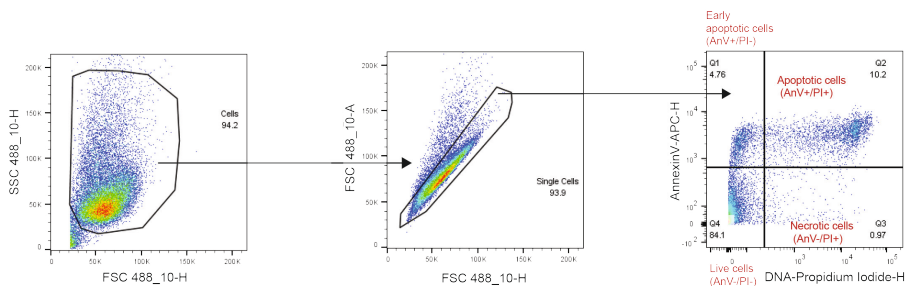
a

Gating used for Figure 2b
Cell cycle analysis



b

Gating used for Figure 2c
Annexin V / PI staining of apoptotic cells



Supplementary Figure 9. Gating strategy for FACS analysis of cell cycle and apoptosis (Figures 2b and 2c). **a** The first gating is made to remove debris based on size, then the selected cellular population is gated again to remove duplets, and eventually the phases of the cell cycle are defined based on the peaks in the distribution of the Hoechst (UV) signal intensity (histogram). Processed data are shown in Figure 2b. **b** The first gating is made to remove debris based on size, then the selected cellular population is gated to remove duplets, and eventually gated cells are defined as live (Annexin V-/PI-), necrotic (Annexin V-/PI+), early apoptotic (Annexin V+/PI-), and apoptotic (Annexin V+/PI+). Processed data are shown in Figure 2c where apoptotic cells are defined as the sum of early apoptotic (Annexin V+/PI-) and apoptotic (Annexin V+/PI+) cells.

SUPPLEMENTARY REFERENCES

- 1 Kalender Atak, Z. *et al.* High accuracy mutation detection in leukemia on a selected panel of cancer genes. *PLoS One* **7**, e38463, doi:10.1371/journal.pone.0038463 (2012).
- 2 Quentmeier, H. *et al.* The LL-100 panel: 100 cell lines for blood cancer studies. *Sci Rep* **9**, 8218, doi:10.1038/s41598-019-44491-x (2019).



CHAPTER 4



T-cell acute lymphoblastic leukemia: a roadmap to targeted therapies

Valentina Cordo¹, Jordy C.G. van der Zwet¹, Kirsten Canté-Barrett¹, Rob Pieters¹ and Jules P.P. Meijerink¹

¹ Princess Máxima Center for Pediatric Oncology, Utrecht, the Netherlands

Published in *Blood Cancer Discovery* (2021)

DOI: 10.1158/2643-3230.BCD-20-0093

PMID: 34661151

ABSTRACT

T-cell acute lymphoblastic leukemia (T-ALL) is an aggressive hematological malignancy characterized by aberrant proliferation of immature thymocytes. Despite an overall survival of 80% in the pediatric setting, 20% of T-ALL patients ultimately die from relapsed or refractory disease. Therefore, there is an urgent need for novel therapies. Molecular-genetic analyses and sequencing studies have led to the identification of recurrent T-ALL genetic drivers. This review summarizes the main genetic drivers and targetable lesions of T-ALL and gives a comprehensive overview of the novel treatments for T-ALL patients that are currently under clinical investigation or that are emerging from preclinical research.

SIGNIFICANCE

T-ALL is driven by oncogenic transcription factors that act along with secondary acquired mutations. These lesions, together with active signaling pathways, may be targeted by therapeutic agents. Bridging research and clinical practice can accelerate the testing of novel treatments in clinical trials, offering an opportunity for patients with poor outcome.

INTRODUCTION

T-cell acute lymphoblastic leukemia (T-ALL) arises from the accumulation of genetic lesions during T-cell development in the thymus, resulting in differentiation arrest and aberrant proliferation of immature progenitors. T-ALL accounts for only 10-15% of pediatric and up to 25% of adult ALL cases (1), with an overall survival (OS) of 80% in the pediatric setting that has been achieved using a risk-based stratification towards intensive, multi-agent combination chemotherapeutic protocols (2). OS rates for adult T-ALL patients are lower than 50% due to higher treatment-related toxicities (1). Patients are assigned to standard-, medium- or high-risk group based on initial steroid response and minimal residual disease (MRD) after the first two courses of chemotherapy (3,4). The risk-based therapeutic regimen consists of steroids, microtubules-destabilizing agents (vincristine), alkylating agents (cyclophosphamide), anthracyclines (doxorubicin, daunorubicin), anti-metabolites (methotrexate, MTX), nucleoside analogues (6-mercaptopurine, thioguanine, cytarabine), hydrolyzing enzymes (*L*-asparaginase) and in some cases it is followed by stem cell transplantation. Some of these conventional chemotherapeutics have a lymphoid lineage-specific effect in ALL. In fact, lymphoblasts have low asparagine synthetase activity and thus they are very sensitive to exogenous asparagine depletion by *L*-asparaginase. Moreover, ALL blasts are susceptible to methotrexate treatment due to a higher accumulation of MTX-polyglutamate metabolites that increases MTX intracellular retention and its anti-leukemic effect in these cells (5). Risk-based intensification of the therapeutic regimen has greatly improved the survival rate for pediatric (6) and young adult patients treated on pediatric-based protocols (1). Nevertheless, still one out of five pediatric T-ALL patients dies within five years after first diagnosis from relapsed disease and therapy resistance (refractory disease) or from treatment-related mortalities, including toxicity and infections. Therefore, further intensification of the treatment protocol does not seem feasible for high-risk patients (6) and there is an urgent need for implementation of targeted therapies. Furthermore, molecular biomarkers, in addition to MRD detection, could improve the upfront identification of high-risk patients and therefore guide the treatment of these patients with an intensified chemotherapeutic regimen or, whenever available, targeted agents. Unfortunately, such genetic biomarkers are not included in the risk stratification of newly diagnosed T-ALL patients yet.

The clinical testing of targeted agents in the oncology field has dramatically increased over the last years. Nevertheless, targeted treatment options for T-ALL patients remain limited. In fact, unlike other leukemias such as CML and Philadelphia-positive ALL (Ph⁺-

ALL), which are kinase-driven malignancies, the initiating events in T-ALL cause the ectopic expression of transcription factors (type A aberrations) that drive leukemogenesis. However, the additional genetic lesions that are required for full transformation into malignancy (the so-called type B mutations) potentially serve as druggable vulnerabilities. Therefore, the thorough investigation of T-ALL oncogenic molecular pathways and their intricate RNA and protein signaling networks that sustain proliferation and survival can offer opportunities for the implementation of personalized targeted therapies (7). Potential limitations to the use of targeted drugs in pediatric T-ALL include clonal heterogeneity of the disease, resulting in only partial elimination of leukemia cells upon therapy. Therefore, resistant clones may be selected and survive under the selective pressure of treatment (8,9). Similar resistance mechanisms have already been demonstrated for conventional chemotherapeutics such as the glucocorticoids-selected *NR3C1* mutations (10-12) and the 6-mercaptopurine (6MP)-selected *NT5C2* mutations in chemo-resistant relapsed ALL (11,13). Already in 2017, the Innovative Therapies for Children with Cancer (ITCC) consortium advised a change in the setup of early phase pediatric clinical trials in order to accelerate the access of interesting drugs to randomized trials (14). ITCC has proposed to extrapolate data from adult clinical trials as starting point for *first-in-child* trial designs. Additionally, ITCC suggested the addition of homogeneous expansion cohorts to assess pharmacodynamic and pharmacokinetic parameters for the therapeutic agents tested and to detect early signs of antitumor activities. Furthermore, it has become evident that molecular tumor profiling is needed to study cancer heterogeneity, to understand therapy-induced mutations and the insurgence of relapse (14). **Table S1** offers an overview of current clinical trials that investigate targeted agents for T-ALL. In the following paragraphs, we summarize the main recurrent T-ALL oncogenic drivers and targetable genetic lesions and highlight the most important preclinical and clinical evidence to implement promising drugs in clinical trials for T-ALL patients. In particular, we discuss agents that target activated pathways by specific genomic lesions in T-ALL and drugs already approved for cancer treatment that are under clinical investigation for T-ALL patients. Moreover, we briefly discuss novel therapeutic options for which promising pre-clinical results were obtained in T-ALL models and that should be taken into consideration for future research. The agents discussed here include modifiers of apoptosis, inhibitors of transcriptional regulators, signal transduction, cell cycle and immunotherapies. **Figure 1** offers a visual summary of the relevant targets and therapeutic agents described throughout this review.

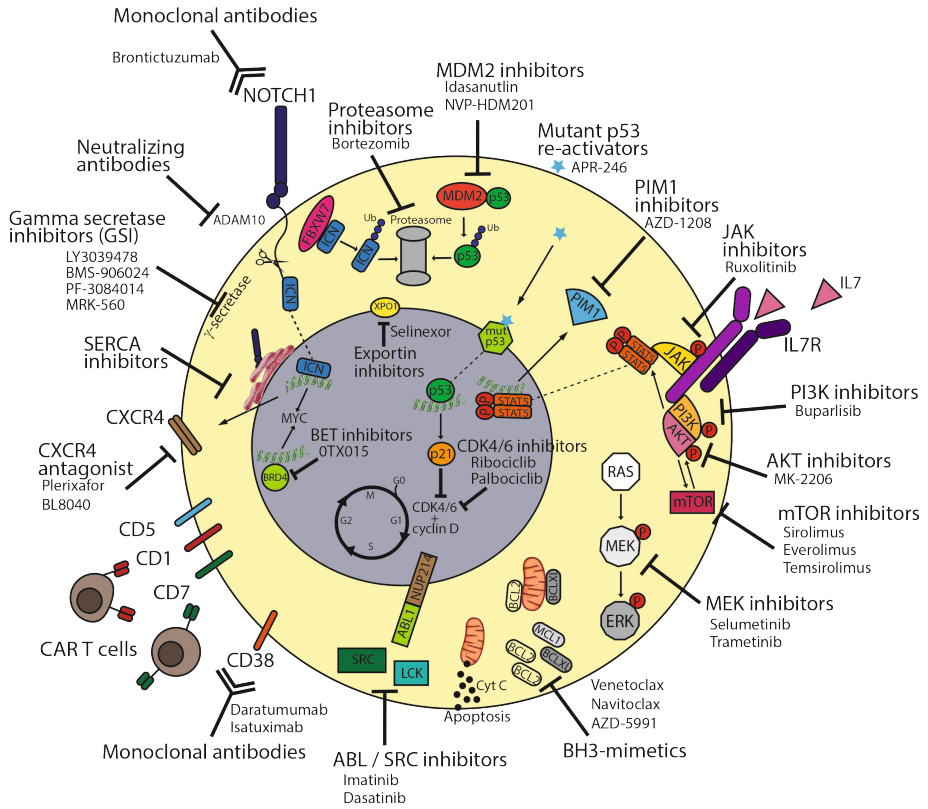


Figure 1. Targeted therapies to tackle T-ALL vulnerabilities. Oncogenic NOTCH1 signaling can be inhibited via different strategies such as monoclonal antibodies blocking the NOTCH1 receptor itself (brontictuzumab), monoclonal antibodies blocking the ADAM10 metalloprotease that releases extracellular NOTCH1, gamma secretase inhibitors (GSI) preventing the release of intracellular ICN1, SERCA inhibitors that block the maturation of NOTCH1 and its localization on the cell surface. Since NOTCH1-mutated T-ALL cases can present higher CXCR4 surface expression, CXCR4 antagonists (plerixafor, BL8040) can be used to tackle NOTCH1-driven T-ALL as well. Immunotherapy approaches for T-ALL include monoclonal antibodies against surface CD38 (daratumumab, isatuximab) as well as CAR T-cells directed towards surface CD1, CD5, CD7 and CD38. The increased expression of anti-apoptotic BH3 proteins such as BCL2 and BCLXL can be counteracted by the use of BH3 mimetics (venetoclax, navitoclax and AZD5991). The oncogenic signaling of ABL1-fusion proteins as well as aberrant activity of Src-family kinases can be inhibited by the tyrosine kinase inhibitors imatinib and dasatinib. The aberrant IL7R signaling cascade can be tackled using multiple targeted agents including JAK inhibitors (ruxolitinib), PIM1 inhibitors (AZD-1208), PI3K inhibitors (buparlisib), AKT inhibitors (MK-2206), mTOR inhibitors (sirolimus, everolimus, temsirolimus) and MEK inhibitors (selumetinib, trametinib). APR-246 can bind mutant p53 and restore its wild-type, tumor suppressor function while MDM2 inhibitors (idasanutlin, NVP-HDM201) can prevent wild-type p53 ubiquitination and consequent degradation via the proteasome. Alternatively, tumor suppressor proteins degradation can be prevented by proteasome inhibitors (bortezomib). Increased activity of cell cycle regulators CDK4/6 can be blocked by CDK inhibitors (ribociclib, palbociclib) while aberrant transcription induced by BRD4 can be targeted by BET inhibitors (OTX015). Nuclear trafficking of oncogenic mRNA and proteins can be targeted via XPO1 inhibitors (selinexor).



ONCOGENIC DRIVERS AND T-ALL SUBTYPES

Historically, three main T-ALL differentiation stages were identified based on the expression of cluster of differentiation (CD) markers on the cell surface and were denoted as early/precortical, cortical and mature in analogy with the thymocytes developmental stages (15). With the rapid development of (cyto)genetic technologies and NGS in the last two decades, it was possible to identify genetic drivers that, in case of T-ALL, are transcription factors that are ectopically activated due to chromosomal rearrangements or deletions (reviewed in ref. (7)). Initially using gene expression profiling (16,17) which has been replaced by the identification of recurrent genomic abnormalities via genome sequencing (18,19), T-ALL patients can be clustered in 4 main subtypes with characteristic oncogenic aberrations, namely early thymocyte progenitor (ETP)/immature-ALL, TLX, TLX1/NKX2.1 (originally denoted as proliferative subgroup) and TAL/LMO. **Figure 2** illustrates the main features of each subtype.

The ETP-ALL group includes the most immature T-ALL cases (approximately 10% of the total T-ALL cases) that present a gene expression profile similar to hematopoietic stem cells and myeloid progenitors, with a high expression of self-renewal genes including *LMO2*, *LYL1* and *HHEX* and the anti-apoptotic *BCL2* (20). The mechanisms for high *BCL2* expression in ETP-ALL are still poorly understood: the expression of this anti-apoptotic protein could reflect a stem cell-like feature of immature cells, or it could be due to *STAT5* activation downstream of recurrent *IL7* signaling pathway mutations within this subgroup (21,22). ETP-ALL cases show increased expression of the transcription factor *MEF2C* or genetic aberrations of *MEF2C*-associated transcription regulators such as *SPI1*, *RUNX1*, *ETV6-NCOA2* and *NKX2.5* (16). Interestingly, ETP-ALL blasts have higher mutational loads compared to blasts of other T-ALL subtypes (21,22). In particular, while *NOTCH1* activating mutations and cell cycle regulators' *CDKN2A/2B* inactivating mutations are relatively rare in ETP-ALL, recurrent activating aberrations involve kinase encoding genes, such as *FLT3*, *NRAS*, *IL7R*, *JAK1* and *JAK3* (21,22). Additionally, recurrent 5q deletions result in deletion of the *NR3C1* locus, encoding for the glucocorticoid receptor (GCR) (22,23). Interestingly, recent evidence demonstrated that reduced GCR expression can induce steroid resistance in T-ALL (12). Some ETP-ALL cases present genomic aberrations that activate genes of the *HOXA* locus. Such activating events have been correlated to chemo-resistance and inferior outcome in adult ETP-ALL (24).

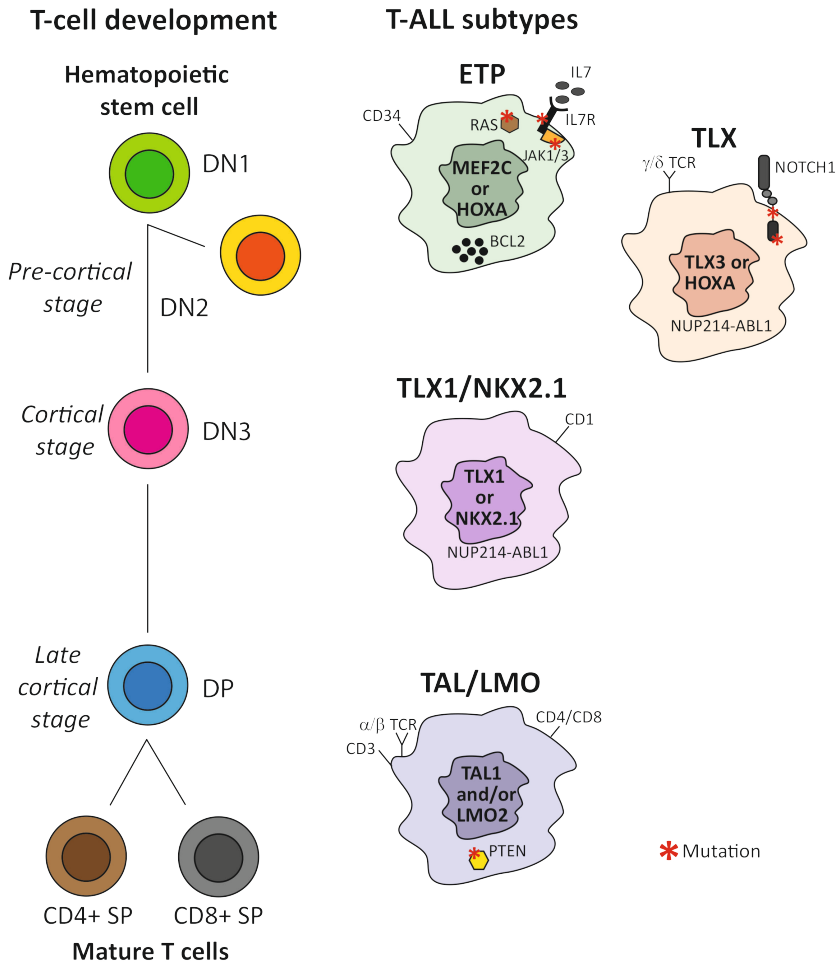


Figure 2. Thymocytes developmental stages and T-ALL subtypes. Early thymocyte progenitor (ETP)-ALL subtype is driven by aberrant *MEF2C* or *HOXA* gene expression, present frequent mutations in the IL7 signaling cascade and shows higher *BCL2* protein expression. Similar to hematopoietic progenitors, ETP-ALL blasts express stem cell markers such as CD34. The TLX subgroup, driven by either *TLX3* or *HOXA* activating events, often present *NOTCH1* mutations and, in some cases, expression of the $\gamma\delta$ T-cell receptor (TCR), in analogy to the pre-cortical $\gamma\delta$ T-cell progenitors (DN2 stage). The TLX1/NKX2.1 subgroup is driven by either *NKX2.1* or *TLX1* aberrations. TLX-rearranged cases can present the oncogenic *NUP214-ABL1* fusion. The TAL/LMO subgroup, driven by the expression of the oncogenes *TAL1* and *LMO2*, includes the most mature T-ALL cases. As for late cortical (SP) T-cell progenitors, TAL/LMO blasts express mature T-cell surface markers such as CD4, CD8, CD3 and $\alpha\beta$ TCR and often present *PTEN* mutations.

The TLX group includes immature cases that either lack a functional T-cell receptor (TCR) or present a $\gamma\delta$ TCR, in line with early or $\gamma\delta$ T-cell lineage development (DN2 stage). A recent study suggests that patients with $\gamma\delta$ T-ALL have higher MRD levels after induction chemotherapy compared to other T-ALL cases (25). Common genetic lesions within the



TLX group include rearrangements of the transcription factor *TLX3* (16,17), mostly as consequence of recurrent *TLX3-BCL11B* translocations (26). These aberrations result in haplo-insufficiency of the tumor suppressor *BCL11B* (27), which is a crucial regulator of the α/β lineage commitment during differentiation. Moreover, *TLX3*-rearranged T-ALL often have *NOTCH1*-activating mutations (28) and aberrations in epigenetic regulators such as PHF6 and CTCF (18). Similar to various ETP-ALL cases, some TLX patients harbor alternative *HOXA* driving events instead of *TLX3*-activating lesions (16).

The common features of the TLX1/NKX2.1 T-ALL group are genomic rearrangements involving either *TLX1* or *NKX2.1*, CD1 expression and differentiation arrest at the cortical (DN3-DP) stage of T-cell development. These cases present higher expression of genes involved in cell cycle regulation and progression, DNA duplication and spindle assembly (16,17). T-ALL cases with TLX1 or NKX2.1 aberrations have been associated with excellent treatment outcomes (reviewed in (7)).

The TAL/LMO T-ALL subgroup comprises nearly half of all pediatric T-ALL patients and it is characterized by ectopic expression of *TAL1* (either via translocation or *SIL-TAL1* deletion), *TAL2*, *LYL1*, *LMO1*, *LMO2* or *LMO3* (driven by *TCRB* or *TCRAD* rearrangements) (16,17). Immuno-phenotypes of TAL/LMO patients mostly resemble late cortical (CD4+ SP or CD8+ SP) T-cell development stages. *PTEN* mutations are most common in this subgroup and have been associated with poor outcome (29). In addition, *PIK3R1* or *PIK3CG* activating lesions are frequent within this cluster (30,31). Moreover, *TAL1*-rearranged cases often have mutations in the ubiquitin-specific protease USP7 that regulates MDM2 and TP53 stability (18).

CURRENT AND NOVEL POSSIBILITIES FOR TARGETED THERAPY

In the following paragraphs, we will discuss various classes of drugs and biological agents that provide novel strategies for targeted treatment. These are classified as modifiers of apoptosis, inhibitors of transcription regulation, signal transduction, cell cycle and immunotherapies.

Modifiers of apoptosis

BH3 mimetics

Encouraged by significant responses of the BCL2 inhibitor venetoclax (ABT-199) in chronic lymphatic leukemia (CLL) (32), BH3 mimetics became of great interest for the treatment of various hematological malignancies. The sensitivity towards BH3 mimetics can be determined by BH3 profiling, a functional screening method that determines the 'priming of death' state in cells by measuring specific BCL2 family member (e.g. BCL2, BCLXL and/or MCL1) dependencies (33). BH3 profiling of T-ALL cell lines and patient blasts identified a dependency on BCL2 in ETP-ALL and BCLXL in the remaining subtypes of T-ALL (34). Consequently, immature/ETP-ALL cells are most responsive to venetoclax while other T-ALL subtypes are more sensitive to navitoclax (ABT-263) treatment, respectively (34,35). The BCL2/BCLW/BCLXL inhibitor navitoclax induces significant cell death in both T-ALL and BCP-ALL PDX models (36), but it can induce severe thrombocytopenia *in vivo*. First reports on pediatric and adult relapsed/refractory T-ALL patients treated with venetoclax alone or combined with navitoclax showed promising results (37,38). However, various resistance mechanisms towards venetoclax treatment have been reported in several hematological malignancies including T-ALL, such as acquired *BCL2* mutations, altered mitochondrial fitness or MCL1 upregulation (36,39-41). Combination treatment of venetoclax with other BH3 mimetics or PI3K/AKT/mTOR inhibitors significantly increases cell toxicity and overcomes venetoclax-induced resistance (39,40). The MCL1 inhibitor S63845 also induces efficient cell death in various T-ALL cell lines as single treatment (39), therefore serving as an interesting alternative to venetoclax, especially given the limited dependency on BCL2 in most T-ALL patients (34). Measuring BCL2 family dependencies can enable guided application of different BH3 mimetics for individualized medicine. In addition, the mitochondrial priming for apoptosis correlates with clinical responses in ALL and predicts for chemo-sensitivity, empowering the use of BH3 profiling as a functional screen in pediatric leukemia (42).

Transcriptional regulator inhibitors

NOTCH1 inhibitors

Over 70% of T-ALL cases present *NOTCH1*-activating mutations (*gain-of-function*) and up to 25% of patients harbor mutations in the *FBXW7* gene (18), which mediates the proteasomal degradation of NOTCH1. Gamma-secretase inhibitors (GSI) have been extensively studied as potential treatment for NOTCH1-activated tumors. Despite promising pre-clinical results,

GSI failed during clinical trials due to insufficient efficacy (even in presence of *NOTCH1* mutations) and excessive gastro-intestinal toxicity caused by the concomitant inhibition of NOTCH2 in the gut epithelium (reviewed in (43)). Preclinical data showed that simultaneous administration of corticosteroid can relieve gastro-intestinal toxicity and enhance the GSI anti-tumor activity (44). Current clinical trials are investigating whether combined GSI and dexamethasone administration could be an effective therapeutic approach (NCT02518113, NCT01363817). As an alternative strategy, Habets and co-workers showed a safe, selective GSI-targeting of NOTCH1 signaling in T-ALL using a PSEN1 inhibitor (MRK-560) (45). While intestinal epithelial cells express both PSEN1 and PSEN2 subunits of the γ -secretase proteolytic complex, T-ALL cells only express PSEN1. *In vivo* preclinical data showed that γ -secretase inhibition by MRK-560 has anti-leukemic activity without causing intestinal toxicity in T-ALL patient-derived mouse xenografts, offering a promising alternative therapeutic approach for NOTCH1-activated T-ALL cases (45). It is fair to question whether, despite high prevalence of *NOTCH1* mutations in T-ALL, GSI is a valid strategy to efficiently and safely target this mutant protein and the consequent altered transcriptional program.

Additional strategies to block aberrant NOTCH1 signaling include monoclonal antibodies (46) or SERCA (sarco-endoplasmic reticulum Ca^{2+} -ATPase) inhibitors that blocks NOTCH1 protein maturation by preventing its localization on the cell membrane (47). Other approaches to tackle oncogenic NOTCH1 involve the targeting of molecules that are activated upon NOTCH1-induced signaling. For example, it has been reported that GSI-resistant T-ALL cells express lower levels of the anti-apoptotic protein MCL1. Since MCL1 can counteract the inhibition of BCL2 and BCLXL, cells with lower MCL1 expression are vulnerable to navitoclax treatment (48). At last, another emerging druggable player within NOTCH1 oncogenic signaling is CXCR4 (CD184), the chemokine receptor for CXCL12 that is released by stromal cells in the thymus. CXCR4 is upregulated in NOTCH1-driven T-ALL and promotes survival and proliferation in the bone marrow niche (reviewed in (49)). Therefore, CXCR4 antagonists, which are already largely used in the clinic to promote stem cells mobilization into the bloodstream, could be repurposed as therapeutic option for leukemic patients. In fact, the novel CXCR4 inhibitor BL8040 is now in phase II clinical trial for relapsed T-ALL/LBL patients (**Table S1**). Together these studies show that there is potential for targeting mutant NOTCH1 or its downstream signaling.

BET inhibitors

Bromodomain (BRD)-containing proteins affect gene transcription via binding to acetylated histones. Their functions include remodeling of the chromatin, modifying histones and

modulating transcription itself (50). The bromodomain and extraterminal (BET) family of BRD-containing proteins consists of four members: BRD2, BRD3, BRD4 and the testis-specific BRDT. One of the first small molecules developed to selectively inhibit BET proteins was JQ1 (50). In leukemia, BRD4-activity can drive aberrant MYC expression. Since *MYC* is an important and direct NOTCH1-target gene (51), *NOTCH1*-mutated T-ALL cases have increased MYC expression. In preclinical T-ALL models, JQ1 competes with BRD4, resulting in reduced MYC expression, decreased cell proliferation and impaired tumor growth (52). Moreover, JQ1 treatment can synergize with vincristine (53) and also with the BCL2 inhibitor venetoclax (54). Interestingly, T-ALL cells that acquire resistance to γ -secretase inhibitors remain responsive to BRD4 inhibition by JQ1 (55), indicating that *NOTCH1*-mutated patients could benefit from BET inhibitor treatment. In addition to *MYC*, JQ1 also lowers the transcription of another important NOTCH1 target gene, the IL7 receptor (*IL7R*) (56). Moreover, another BRD4-dependent transcription factor, ETS1 can cooperate with NOTCH1 during leukemogenesis. Since Ets1 deletion sensitizes T-ALL cells to GSI (57), targeting NOTCH1 transcriptional cofactors could offer an alternative strategy to treat NOTCH1-driven T-ALL cases.

Cancer cells often use super-enhancer structures to restore and sustain oncogene expression. Guo and colleagues (58) showed that JQ1-resistant leukemic cells can restore MYC expression via enhancer remodeling. However, combined BET and CDK7 (transcriptional regulator) inhibition in JQ1-resistant cells effectively abrogates MYC expression. Pharmacological targeting of CDK7 results in decreased enhancer activity in T-ALL and epigenetic reprogramming, in particular for NOTCH1-related enhancers that are not affected by GSI treatment (59). CDK7 inhibition also effectively disrupts the TAL1 super-enhancer (60), highlighting that disruption of oncogenic transcription complexes may be an effective approach for T-ALL treatment when direct targeting of mutant genes, proteins or pathways is not possible. Therefore, the investigation of the epigenetic state of leukemia cells can provide additional insights to guide the use of targeted treatments. Despite promising results in preclinical models, JQ1 has a very short half-life that limits its applicability as therapeutic agent *in vivo*. Nevertheless, several novel BET inhibitors have been developed by multiple companies and they are currently under investigation in oncology trials, highlighting the great interest in these epigenetic drugs and their potential application (61). Among these novel agents, OTX015 was proven effective in preclinical leukemia models (62).

Signal transduction inhibitors

ABL1 / Src-family kinases inhibitors

Differently from B-ALL cases, T-ALL patients with *ABL1* fusions are rare (18,63). The most common *ABL1* aberration in T-ALL is the *NUP214-ABL1* fusion due to an episomal amplification of the 9q34 region, which was one of the few discovered T-ALL lesions that can be directly targeted by a kinase inhibitor (63). Usually, *NUP214-ABL1* rearrangements are particularly present at the sub-clonal level (64). Novel *ZBTB16-ABL1* and *ZMIZ1-ABL1* fusions have been identified in rare T-ALL cases ((65) and unpublished observations), resulting in sensitivity towards imatinib and dasatinib treatment in preclinical models (65). Interestingly, in 2017, Bourquin and colleagues identified a subgroup of T-ALL patients that are highly sensitive to dasatinib treatment *in vitro* despite the absence of *ABL1* aberrations, suggesting a role for SRC kinase as putative novel target for therapy (66). Other studies proposed the lymphocytic specific kinase LCK, which is often highly expressed in T-ALL, as prime dasatinib target in T-ALL (67,68). Based on these pre-clinical data, patients presenting high SRC phosphorylation and/or increased LCK expression could potentially benefit from dasatinib treatment. Therefore, in addition to genomic analyses, further investigation of the phospho-proteome could highlight aberrantly activated proteins (7) that could serve as biomarkers for dasatinib responsiveness when *ABL1* abnormalities are not present.

JAK inhibitors

JAK-STAT pathway activation in T-ALL is mainly observed in the context of IL7-induced signaling or caused by activating mutations in the *IL7R* gene or in genes encoding downstream effectors (e.g. *JAK1*, *JAK3* or *STAT5*) that are recurrently found at diagnosis (18,21,69). Active JAK-STAT signaling leads to the upregulation of various anti-apoptotic and pro-survival proteins including BCL2 and PIM1 and contributes to steroid resistance (21,70,71). Ruxolitinib, an FDA-approved JAK1/2-inhibitor for the treatment of myeloproliferative neoplasms (MPNs) and graft-versus-host disease (GvHD) blocks JAK-STAT signaling regardless of the presence of mutations (72). In T-ALL, ruxolitinib shows efficacy in IL7-responsive T-ALL and ETP-ALL (69). Ruxolitinib treatment can synergize with dexamethasone treatment to overcome IL7-induced steroid resistance in both T-ALL and ETP-ALL patients. Multiple trials are under way to test the efficacy of ruxolitinib for JAK-mutated T-ALL (**Table S1**) or Philadelphia-like BCP-ALL with CRLF2-rearrangements and/or JAK mutations (NCT2723994, NCT03117751 and NCT02420717), despite the fact that the clinical responses to ruxolitinib in MPNs seem rather limited (73). This indicates that

the role of JAK inhibitors should be carefully considered in future treatment regimens of T-ALL.

PIM1 inhibitors

When exploring alternative treatment options for aberrant JAK-STAT signaling, *PIM1* was identified as a direct STAT5 transcriptional target gene that is also upregulated by physiological IL7-induced signaling (71,74,75). Expression of the pro-survival PIM1 kinase is mainly observed in pre-cortical T-ALL, with the highest expression in the TLX and ETP-ALL subtypes (71,74,76,77). This is in agreement with the higher occurrence of activating mutations in the IL7R signaling pathway in these T-ALL subtypes, including *JAK1/3* and *STAT5B* mutations (18,21,22,78). PIM1 inhibition has proven efficacy in T-ALL using *in vitro* and *in vivo* models, with an increased effect observed for ETP-ALL blasts (74,77). Both phospho-STAT5 and PIM1 expression levels can be used as a predictive biomarker for response to JAK inhibitors (74). PIM1 inhibition paradoxically results in enhanced MAPK-ERK signaling and may explain the observed synergy of combined PIM1 and MEK inhibitors treatment (74,79). Additionally, synergistic effects of PIM1 inhibitors in combination with venetoclax or dexamethasone have been observed (77,80) indicating that PIM1 could be a valuable therapeutic target to counteract unfavorable hallmarks of immature /ETP-ALL cases such as high BCL2 expression and steroid resistance.

PI3K-AKT-mTOR inhibitors

High PI3K-AKT-mTOR signaling is frequently observed in T-ALL and can be caused by a variety of cellular events, including activating mutations in *PI3K* or *AKT*, inactivating lesions in the tumor suppressor gene *PTEN* or by post-translational modification of these molecules (21,30,31,81). *PTEN* inactivating events are predominantly observed in T-ALL patients that belong to the TAL/LMO subtype. PTEN loss is associated with poor prognosis in T-ALL, resulting in higher risk of disease relapse (29,30,81,82). Additionally, IL7R-signaling mutations that frequently occur in ETP-ALL and TLX subtypes also activate the downstream PI3K-AKT pathway and correlate with steroid resistance and inferior event-free survival (21,78). Pan-PI3K inhibitors have shown higher efficacy in inhibiting cell growth and survival of T-ALL cell lines compared to inhibitors that target only specific catalytic subunit(s) of PI3K (83). Preclinical *in vitro* studies demonstrate synergy between PI3K-inhibitors and several chemotherapeutic agents including doxorubicin, nelarabine and glucocorticoids (21,84,85). Moreover, dual PI3K/mTOR inhibitors seem to be even more effective and also synergize with a wide range of chemotherapeutics (85-88).

The effects of first generation allosteric mTOR inhibitors rapamycin (sirolimus) and rapalogues RAD001 (everolimus) and CCI-779 (temsirolimus) have been largely investigated in T-ALL (86,89,90). These inhibitors only target mTORC1 and can paradoxically activate AKT via PI3K-mTORC2 in some cell types (reviewed in (91)). Second generation ATP-competitive dual mTORC1/mTORC2 inhibitors are more efficient in inducing apoptosis in T-ALL blasts since they also interfere with more downstream PI3K-AKT-mTOR signaling effectors, including a strong inhibition of 4EBP1 phosphorylation (92). The stronger cytotoxic effects and broad PI3K-AKT pathway regulation of dual-inhibitors (e.g. PI3K/mTOR and mTORC1/mTORC2 inhibitors) compared to PI3K- or mTORC1-only inhibitors provides evidence that dual inhibitors are more suitable for future clinical trials (91,93).

Alternatively, the oncogenic signaling of the PI3K-AKT-mTOR axis can also be targeted by direct AKT inhibition. The allosteric AKT inhibitor MK-2206 inhibits AKT and impairs downstream activation of mTORC1, mTORC2, GSK3 and FOXO in various T-ALL cell lines (94). Additionally, MK-2206 synergizes with steroids in primary T-ALL patient samples (21,94). ATP-competitive AKT inhibitors like AZD5363 also demonstrate cytotoxic effect against T-ALL cells *in vitro* (95).

MEK inhibitors

The presence of mutations in *N-* and *K-RAS* genes at diagnosis, which strongly activate the MAPK-ERK signaling, predicts for inferior outcome in both BCP- and T-ALL patients (82,96-98). Additionally, a high prevalence of these mutations in ALL patients is found at relapse (10). Although not significantly enriched in relapsed T-ALL, the presence of *RAS* mutations in relapsed pediatric T-ALL patients predicts for extremely poor outcome (99). *MAPK-ERK* activating mutations, which may be selected under the pressure of treatment, can contribute to steroid resistance (21,78,100). MEK inhibitors induce cell death in *RAS*-mutant cells and synergize with glucocorticoids in primary T-ALL patient cells and *in vivo* BCP-ALL models (21,97,101,102). These findings led to the ongoing SeluDex trial that combines the MEK inhibitor selumetinib with dexamethasone for the treatment of relapsed adult and pediatric BCP- and T-ALL patients (NCT03705507; **Table S1**). As IL7R and JAK1 signaling mutations strongly activate downstream MEK-ERK signaling, in addition to the JAK-STAT and PI3K-AKT pathways, and strongly provoke steroid resistance in T-ALL (21), patients having such IL7R signaling mutations should also become eligible for selumetinib treatment.

Cell cycle inhibitors

CDK inhibitors

More than 70% of T-ALL cases downregulate CDKN2A/B (18), negative regulators of cyclin-dependent kinases (CDK) 4/6, either via recurrent gene deletions, sporadic mutations or promoter hypermethylation (103). Therefore, the CDK4/6 inhibitors palbociclib and ribociclib could be potential therapeutic options for T-ALL patients. Palbociclib induces cell cycle arrest in T-ALL cells and can suppress leukemia progression in animal models (104). Moreover, another preclinical study proved that the CDK4/6 inhibitor ribociclib can act synergistically with glucocorticoids and mTOR inhibitors in both T-ALL cell lines and murine models (90). Current phase I clinical trials for relapsed/refractory pediatric ALL (**Table S1**) are investigating the tolerability of the combination of ribociclib with everolimus and dexamethasone (NCT03740334) or the addition of palbociclib to the standard re-induction chemotherapeutic regimen (NCT03792256). Other aberrations involving cell cycle regulators include overexpression of the NOTCH1 target Cyclin D3, and CDK6 (18,19,21,65,99). Moreover, deletions of CDKN1B (p27^{KIP1}), which is a negative regulator of Cyclin E-CDK2 complex, have been reported in about 13% of T-ALL patients (18). Therefore, inhibitors targeting CDK2 might be of interest for the treatment of T-ALL as well. In 2017, Moharram and colleagues reported the efficacy of the CDK1/2/5/9 inhibitor dinaciclib in preclinical T-ALL models (105). Despite the promising results, a clinical trial had already showed only transient effect of dinaciclib treatment for adult leukemia patients (106).

Nelarabine

Active cell cycle may increase the sensitivity to nucleoside analogues treatment. Nelarabine is a purine nucleoside analogue that inhibits DNA synthesis and showed higher efficacy in T-ALL compared to other malignancies. Whether this is an exclusive T-ALL effect still remains debatable. Nevertheless, T-lymphoblasts show higher accumulation of nelarabine active metabolite ara-G with consequent increased cytotoxicity compared to other hematopoietic cells (107), making T-ALL cells more susceptible to this treatment. At the moment, it is the only novel drug approved for the treatment of relapsed T-ALL/LBL cases. As single agent for relapsed or refractory T-ALL in children and young adults, nelarabine had a response rate of over 50% (108). In adults these response rates were somewhat lower (36% achieved complete remission), but they still provided encouraging results for relapsed cases by inducing clinical remissions that facilitated access to stem cell transplantation (109). However, nelarabine treatment can have significant neurologic side effects depending on other central nervous system-directed therapy, in particular in

children older than 10 years of age (110). The results of nelarabine safety and efficacy trials in T-cell acute lymphoblastic leukemia/lymphoma patients highlight considerable single agent activity in the relapse setting that facilitates disease control. Moreover, nelarabine can be combined with other drugs with non-overlapping toxicities. The Children's Oncology Group recently published the results of a randomized phase III trial investigating the addition of nelarabine to the chemotherapeutic treatment for newly diagnosed pediatric and young adult T-ALL patients. The increased disease free-survival rate as well as the decreased CNS relapse incidence without excessive toxicity, supports the inclusion of nelarabine into frontline therapy for pediatric T-ALL, especially for high-risk cases (111).

Drugs targeting mutant p53

Mutations that inactivate p53 are rare in T-ALL patients at diagnosis (1-6%) but show an increased incidence at relapse and correlate with poor prognosis (18,99). A recent study showed that p53-mutant sub-clones that were detected at first relapse can give rise to clonal p53 mutations detectable in post-stem cell transplantation relapses. Furthermore, in these patients, p53 mutations correlated with an extremely short time-to-relapse (112). Various re-activators of mutant p53 that induce restoration of the wild-type conformation are in preclinical investigation (113). Interestingly, leukemic blasts from a T-ALL patient who relapsed after stem cell transplantation, showed sensitivity *ex vivo* to the p53 re-activator APR-246 (112). APR-246 already showed promising results for p53-mutant patients affected by other hematological malignancies (NCT00900614) and could be a suitable option for T-ALL patients that relapse after stem cell transplantation and present with p53 mutations.

Drugs targeting wild-type p53

P53 signaling pathway can be impaired despite the presence of wild-type p53 by overexpression of physiological p53 inhibitors such as MDM2 or MDM4. In fact, p53 activity can be restored by targeting the E3 ubiquitin-ligase MDM2. The MDM2 antagonist idasanutlin disrupts the MDM2-p53 interaction and prevents p53 degradation. Currently, idasanutlin has reached phase I/II clinical trial investigation for pediatric ALL (NCT04029688). Furthermore, another MDM2 inhibitor, NVP-HDM201, is currently investigated in a phase I/II clinical trial for wild-type p53 tumors, including relapsed ALL (NCT02143635). Lastly, the MDM2/MDM4 stapled peptide ALRN-6924 has reached clinical investigation in pediatric patients with relapsed ALL (NCT03654716).

Immunotherapies

Antibody-based therapy

Monoclonal antibodies can be applied in immunotherapies and have entered various trials for T-cell lymphoma (reviewed and summarized in (114)). Surprisingly, only a few have been considered in the treatment of ALL such as anti-CD38 antibodies. CD38 is a transmembrane receptor that is expressed on subsets of myeloid, lymphoid and some non-hematological cells. The anti-CD38 monoclonal antibody daratumumab was initially developed for multiple myeloma and was approved by the FDA in 2015 and the EMA in 2016 as a single agent for relapsed/refractory multiple myeloma patients. CD38 is also a promising target for T-ALL as it is robustly and consistently expressed on T-ALL and ETP-ALL blasts at diagnosis, during chemotherapy treatment, and at relapse (115). Moreover, daratumumab displayed great efficacy in 14 out of 15 patient-derived xenograft models in NOD/Scid/IL2R-gamma null (NSG) mice (115). Of note, the cytotoxic efficacy of daratumumab in NSG mice—that do not have B, T, NK cells, and complement factors—seems therefore independent of T-cell mediated or complement-dependent cytotoxicity. CD38 expression on regulatory B and T-cells as well as on myeloid suppressor cells results in their depletion by daratumumab, which could boost anti-tumor responses (116). Clinical trials will reveal whether daratumumab has an even higher efficacy than that observed in NSG mice, as both T-cell mediated toxicity and repression of regulatory cells will be active in T-ALL patients. Recently, daratumumab has been successfully administered for compassionate use to three CD38-positive ALL patients who experienced multiple relapses, with one patient that relapsed after an allogeneic stem cell transplantation (117). Two patients had T-ALL while the third had a CD19/CD22-negative pre B-ALL and all three achieved an MRD-negative remission after daratumumab treatment. Trials combining daratumumab treatment with standard chemotherapy for pediatric and young adult ALL patients are in phase II (NCT03384654; EudraCT 2017-003377-34). Another anti-CD38 monoclonal antibody that is under clinical investigation is isatuximab. An isatuximab trial for adult T-ALL patients in the USA was closed prematurely due to lack of response, while the NCT03860844 trial for pediatric patients with refractory/relapsed acute leukemia is still ongoing.

Pre-clinical evidences suggest that TCR-expressing T-ALL blasts can be targeted by anti-CD3 antibodies. In fact, the activation of persistent TCR signaling induced by antibodies engaging CD3, leads to cell death *in vitro* and *in vivo* (118), suggesting a novel targeted therapeutic option for T-ALL cases that present TCR expression.

Cellular therapy

Genetically engineered autologous chimeric antigen receptor T-cells (CAR T) have been used successfully as therapy for various malignancies including relapsed ALL. An extensive review recently addressed the challenges and potential solutions for the use of CAR T-cells in T-cell malignancies and lists all currently ongoing trials (119). Initially, the challenge to harvest sufficient mature T-cells from patients with T-cell malignancies without any lymphoblast contamination hampered the development of CAR T-cells against T-ALL/LBL. Most of the CAR T therapies developed so far are dependent on harvesting sufficient autologous and healthy T-cells from a single patient. The production of allogenic CAR T-cells would eliminate this challenge by using genetically modified T-cells from a healthy donor (reviewed in (120)). Additionally, the fratricide effect – the paradigm that CAR T-cells share the same surface markers with their malignant T-cell targets – would rapidly self-extinguish the CAR T-cells. After the first approval of the anti-CD19 CAR T for the treatment of pediatric relapsed B-ALL patients, many different surface proteins have been investigated for the development of novel CAR T therapies directed towards T-cell malignancies, including CD5, CD7, CD1 and CD38. One of the advantages of anti-CD5 CAR T-cells is the rapid internalization of CD5 from their cell surface, resulting in a limited and transient fratricide effect (121). Nevertheless, the internalization of CD5 can happen on blasts as well, offering an escape mechanism for leukemia cells that needs to be taken into account. Currently, a phase I anti-CD5 CAR T-cell trial is ongoing for patients with CD5-positive T-ALL or T-cell lymphoma (NCT03081910). As CD5 is expressed on most T-ALL subtypes while it is absent or expressed at low levels on ETP-ALL cells, there is need for additional CAR T-cells that can target ETP-ALL as well. CD7 is a promising target on T-lymphoblasts but is also highly expressed on effector T-cells. To minimize the fratricide effect, the CRISPR-Cas9 gene editing technology has been used to remove the endogenous *CD7* gene from these CAR T cells (122). A clinical trial using these modified anti-CD7 CAR T-cells for treating CD7-positive T-ALL/LBL has been designed (NCT03690011). However, since CD7 is expressed on all thymocytes and T-cells, patients receiving CD7 CAR T-cell treatment risk a lifelong T-cell depletion and immunodeficiency that might impair a broad use in the clinic. In order to avoid such side effects and to regulate the activity of these cellular therapies, some CARs have been designed to express an inducible suicide gene (e.g. caspase 9) that can be selectively activated upon administration of a small molecule (reviewed in (123)). As an alternative strategy to target CD7, a second generation, fratricide-resistant anti-CD7 CAR T-cells have been developed using T cells from healthy donors (UCART7) (124). These CAR T-cells have been genetically altered to be not only *CD7* deficient, but also to lack the *TCRAD* gene to eliminate the risk for an allogenic CAR T-cell mediated graft-versus-

host disease (GvHD). Of note, such an allogeneic product can be immediately available for treatment of multiple patients as an “off-the-shelf” product. Promising results on the use of another allogeneic anti-CD7 CAR T cells have been recently presented at the American Association for Cancer Research virtual meeting in April 2020. Dr X. Wang reported the preliminary exciting data on the efficacy of a single infusion of TruUCAR™ GC027 (Gracell Biotechnologies) after 6 days of lympho-depleting chemotherapy in 5 adult refractory/relapsed T-ALL patients enrolled in a phase I clinical trial in China (ChiCTR1900025311). Four patients achieved complete response at day 28 with manageable cytokine release syndrome and absence of neurotoxicities and GvHD, while one patient that had received the lowest CAR T dose relapsed. Three out of four patients remained in complete remission at day 161 of follow-up. Future evaluations will investigate the duration of the remissions induced by this treatment (125).

CD1a is another promising target for refractory or relapsed cortical T-ALL (126). Moreover, CD1a is only expressed during the proliferative phase of thymocyte development and not on immature progenitor cells or mature T-cells, limiting the risk of complete immunodeficiency after treatment. Recently, the development of fratricide-resistant anti-CD1a CAR T-cells for the treatment of CD1a-positive T-ALL has been reported (126). However, since CD1-positive cortical T-ALL patients have been associated with excellent outcomes, it is not known what percentage of relapsed T-ALL patients will express CD1 and thus benefit from such a CAR T therapy.

As discussed in the previous session, CD38 is widely expressed on T-lymphoblasts, thus the development of anti-CD38 CAR T has also been pursued (127). Recently, the treatment of a relapsed adult B-ALL patient was reported with the occurrence of serious side effects including cytokine release syndrome and damage to lung and liver tissues that also express the CD38 antigen (128). Therefore, caution and accurate target choices are warranted to extend the repertoire of safe and effective CAR T-cell treatments.

OTHER PROMISING TARGETED TREATMENTS IN DEVELOPMENT

Oncology drug development is constantly growing, and several potential novel candidates have been recently put into the spotlight. New potentially promising compounds that should be kept in consideration for upcoming studies will be discussed below.

OBI-3424 is a *first-in-class* targeted treatment for liquid and solid tumors that overexpress the Aldo-Keto Reductase 1 c3 (AKR1C3) enzyme such as castrate-resistant prostate cancer and hepatocellular carcinoma. AKR1C3 is also expressed in T-ALL, with the exclusion of *TLX1/3*-rearranged cases (129). *OBI-3424* is a pro-drug that releases a potent DNA-alkylating component upon intracellular reduction by AKR1C3. This agent has shown promising cytotoxic activity in T-ALL cell lines and patient-derived xenografts that express AKR1C3 (129). In September 2017, *OBI-3424* received FDA orphan drug designation for AKR1C3-expressing tumors including ALL, and it is currently investigated in a phase I/II clinical trial for solid tumors (NCT03592264).

Selinexor (KPT-330) is a selective inhibitor of Exportin-1 (XPO1) which has recently been approved in combination with dexamethasone for the treatment of refractory/relapsed multiple myeloma. XPO1 is the key player in nuclear export of receptors (e.g. NR3C1), tumor suppressor proteins (e.g. p53 and pRB) but also oncogenic mRNAs transcribed from *MDM2*, *BCL2* and *MYC*, which will be retained in the nucleus upon XPO1 inhibition. *Selinexor* treatment is currently investigated in a phase I clinical trial for relapsed pediatric acute leukemia (NCT02091245). Furthermore, the second generation XPO1 inhibitor, *eltanexor* (KPT-8602) can induce cytotoxicity and apoptosis in ALL models and can enhance the efficacy of dexamethasone treatment (130).

Histone deacetylases (HDAC) are key enzymes in chromatin remodeling and epigenetic gene regulation. HDACs are frequently overexpressed in cancer, including T-ALL. T-ALL patient samples demonstrate higher HDAC1 and HDAC4 but lower HDAC5 levels compared to B-ALL (131). The pan-HDAC inhibitor *panobinostat* has shown anti-leukemic activity in T-ALL preclinical models (132) and it is under clinical investigation for relapsed acute leukemia (**Table S1**). The same applies for *vorinostat*, which is already approved for the treatment of refractory/relapsed cutaneous T-cell lymphoma.

Additional epigenetic regulators that can be pharmacologically targeted are DNA methyltransferases. DNA methyltransferase inhibitors *decitabine* and *azacitidine* induce chromatin hypomethylation with a consequent alteration in gene transcription. They have been approved for the treatment of myelodysplastic syndromes and they are currently investigated in early phase clinical trials for pediatric ALL patients (**Table S1**). In 2016, Lu and colleagues showed that *decitabine* pre-treatment enhanced chemo-sensitivity of preclinical models of ETP-ALL (133). One year later, the successful treatment of a relapsed

adult ETP-ALL patient with decitabine was reported (134), therefore offering a promising opportunity for salvage therapy of ETP-ALL cases.

An alternative way to target oncogenic signaling pathways is by tackling protein stability or degradation. Cancer cells become addicted to the rapid elimination of tumor suppressor proteins or may require higher protein turnover to sustain their metabolism. Therefore, processes involved in protein degradation can provide leukemia-specific vulnerabilities that can be effectively targeted. *Bortezomib*, a *first-in-class* proteasome inhibitor, is approved for the treatment of refractory multiple myeloma. It inhibits the 26S subunit of the proteasome, impairing protein degradation that results in cell cycle arrest and eventually apoptosis. A recent report of the Children's Oncology Group highlights the safety of bortezomib during re-induction chemotherapy for pediatric relapsed ALL, and provided encouraging results for T-ALL, with an increase in patients achieving complete remission (135). Another way of altering protein stability and activity is through inhibition of the Nedd8-activating enzyme (NAE). NAE is an ubiquitin-like (UBL) protein that regulates the activity and the protein-protein interactions of NF- κ B and cullins, which are essential cell cycle regulators (136). Preclinical data showed that the NAE inhibitor *pevonedistat* (MLN4924) can induce cell cycle arrest and apoptosis in T-ALL models (136). Both bortezomib and pevonedistat are currently under clinical investigation for ALL patients (**Table S1**).

Aurora kinases (AURK) are mitotic regulators often overexpressed in cancer, including pediatric ALL (137). AURKA inhibitor alisertib (MLN8237) had shown promising results for both ALL and lymphoma cells *in vitro* (138). Unfortunately, a phase II clinical trial from the Children's Oncology Group reported objective response after alisertib single agent treatment in less than 5% of the pediatric patients with recurrent/refractory advanced solid tumor or acute leukemia (139). Recent evidence elucidates a role for AURKB in inhibiting proteasomal degradation of MYC, thus stabilizing this oncogenic protein (140). *In vitro* treatment of T-ALL cells with the AURKB inhibitor barasertib (AZD1152) leads to reduced MYC protein levels (140) and enhanced cell death (140,141). Furthermore, AZD1152 can act in synergy with vincristine (140).

CONCLUSIONS

The outcome for children diagnosed with T-ALL has dramatically improved in the last decades. Nevertheless, therapy resistance, disease relapse, treatment-related death, and long-term detrimental side effects for cancer survivors remain serious issues to be solved.

Additionally, the lack of predictive biomarkers at diagnosis remain an unmet need for T-ALL patients. In this review, we presented an overview of the current state of drug development and ongoing clinical trials that are of interest for the T-ALL field, integrating preclinical evidence and clinical data. Several molecular tumor profiling protocols have been initiated in Europe (*e.g.*, MOSCATO-01, iTHER, ESMART) (142) to identify actionable lesions for targeted treatment in specific subgroups of patients. This highlights the importance of bridging preclinical research with clinical practice to accelerate the use of promising novel drugs in effective new treatment combinations for T-ALL patients.

AUTHOR CONTRIBUTIONS

VC, JvdZ, KCB and JM wrote the manuscript. RP provided critical input and revised the manuscript.

AUTHORS' DISCLOSURES

No disclosures were reported.

ACKNOWLEDGEMENTS

This study was supported by grants of the Dutch Cancer Society (KWF Kankerbestrijding) grant number KWF2016_10355 (VC), Foundation 'Kinderen Kankervrij' (KiKa): KiKa-219 (JZ) and KiKa-295 (KCB)

REFERENCES

1. Patel AA, Thomas J, Rojek AE, Stock W. Biology and Treatment Paradigms in T Cell Acute Lymphoblastic Leukemia in Older Adolescents and Adults. *Curr Treat Options Oncol* **2020**;21(7):57 doi 10.1007/s11864-020-00757-5.
2. Pui CH, Evans WE. Treatment of acute lymphoblastic leukemia. *N Engl J Med* **2006**;354(2):166-78 doi 10.1056/NEJMra052603.
3. Pieters R, de Groot-Kruseman H, Van der Velden V, Fiocco M, van den Berg H, de Bont E, *et al.* Successful Therapy Reduction and Intensification for Childhood Acute Lymphoblastic Leukemia Based on Minimal Residual Disease Monitoring: Study ALL10 From the Dutch Childhood Oncology Group. *J Clin Oncol* **2016**;34(22):2591-601 doi 10.1200/JCO.2015.64.6364.
4. Pui CH, Pei D, Coustan-Smith E, Jeha S, Cheng C, Bowman WP, *et al.* Clinical utility of sequential minimal residual disease measurements in the context of risk-based therapy in childhood acute lymphoblastic leukaemia: a prospective study. *Lancet Oncol* **2015**;16(4):465-74 doi 10.1016/S1470-2045(15)70082-3.
5. Masson E, Relling MV, Synold TW, Liu Q, Schuetz JD, Sandlund JT, *et al.* Accumulation of methotrexate polyglutamates in lymphoblasts is a determinant of antileukemic effects in vivo. A rationale for high-dose methotrexate. *J Clin Invest* **1996**;97(1):73-80 doi 10.1172/JCI118409.
6. Jeha S, Pei D, Choi J, Cheng C, Sandlund JT, Coustan-Smith E, *et al.* Improved CNS Control of Childhood Acute Lymphoblastic Leukemia Without Cranial Irradiation: St Jude Total Therapy Study 16. *J Clin Oncol* **2019**;37(35):3377-91 doi 10.1200/JCO.19.01692.
7. van der Zwet JCG, Cordo V, Cante-Barrett K, Meijerink JPP. Multi-omic approaches to improve outcome for T-cell acute lymphoblastic leukemia patients. *Adv Biol Regul* **2019**;74:100647 doi 10.1016/j.jbior.2019.100647.
8. Waanders E, Gu Z, Dobson SM, Antic Z, Crawford JC, Ma X, *et al.* Mutational landscape and patterns of clonal evolution in relapsed pediatric acute lymphoblastic leukemia. *Blood Cancer Discov* **2020**;1(1):96-111 doi 10.1158/0008-5472.BCD-19-0041.
9. Dobson SM, Garcia-Prat L, Vanner RJ, Wintersinger J, Waanders E, Gu Z, *et al.* Relapse-Fated Latent Diagnosis Subclones in Acute B Lineage Leukemia Are Drug Tolerant and Possess Distinct Metabolic Programs. *Cancer Discov* **2020**;10(4):568-87 doi 10.1158/2159-8290.CD-19-1059.
10. Oshima K, Khiabani H, da Silva-Almeida AC, Tzoneva G, Abate F, Ambesi-Impiombato A, *et al.* Mutational landscape, clonal evolution patterns, and role of RAS mutations in relapsed acute lymphoblastic leukemia. *Proc Natl Acad Sci U S A* **2016**;113(40):11306-11 doi 10.1073/pnas.1608420113.
11. Li B, Brady SW, Ma X, Shen S, Zhang Y, Li Y, *et al.* Therapy-induced mutations drive the genomic landscape of relapsed acute lymphoblastic leukemia. *Blood* **2020**;135(1):41-55 doi 10.1182/blood.2019002220.
12. Wandler AM, Huang BJ, Craig JW, Hayes K, Yan H, Meyer LK, *et al.* Loss of glucocorticoid receptor expression mediates in vivo dexamethasone resistance in T-cell acute lymphoblastic leukemia. *Leukemia* **2020**;34(8):2025-37 doi 10.1038/s41375-020-0748-6.
13. Tzoneva G, Perez-Garcia A, Carpenter Z, Khiabani H, Tosello V, Allegretta M, *et al.* Activating mutations in the NT5C2 nucleotidase gene drive chemotherapy resistance in relapsed ALL. *Nat Med* **2013**;19(3):368-71 doi 10.1038/nm.3078.
14. Moreno L, Pearson ADJ, Paoletti X, Jimenez I, Geoerger B, Kearns PR, *et al.* Early phase clinical trials of anticancer agents in children and adolescents - an ITCC perspective. *Nat Rev Clin Oncol* **2017**;14(8):497-507 doi 10.1038/nrclinonc.2017.59.

15. Bene MC, Castoldi G, Knapp W, Ludwig WD, Matutes E, Orfao A, *et al.* Proposals for the immunological classification of acute leukemias. European Group for the Immunological Characterization of Leukemias (EGIL). *Leukemia* **1995**;9(10):1783-6.
16. Homminga I, Pieters R, Langerak AW, de Rooij JJ, Stubbs A, Verstegen M, *et al.* Integrated transcript and genome analyses reveal NKX2-1 and MEF2C as potential oncogenes in T cell acute lymphoblastic leukemia. *Cancer Cell* **2011**;19(4):484-97 doi 10.1016/j.ccr.2011.02.008.
17. Ferrando AA, Neuberg DS, Staunton J, Loh ML, Huard C, Raimondi SC, *et al.* Gene expression signatures define novel oncogenic pathways in T cell acute lymphoblastic leukemia. *Cancer Cell* **2002**;1(1):75-87 doi 10.1016/s1535-6108(02)00018-1.
18. Liu Y, Easton J, Shao Y, Maciaszek J, Wang Z, Wilkinson MR, *et al.* The genomic landscape of pediatric and young adult T-lineage acute lymphoblastic leukemia. *Nat Genet* **2017**;49(8):1211-8 doi 10.1038/ng.3909.
19. Seki M, Kimura S, Isobe T, Yoshida K, Ueno H, Nakajima-Takagi Y, *et al.* Recurrent SPI1 (PU.1) fusions in high-risk pediatric T cell acute lymphoblastic leukemia. *Nat Genet* **2017**;49(8):1274-81 doi 10.1038/ng.3900.
20. Coustan-Smith E, Mullighan CG, Onciu M, Behm FG, Raimondi SC, Pei D, *et al.* Early T-cell precursor leukaemia: a subtype of very high-risk acute lymphoblastic leukaemia. *Lancet Oncol* **2009**;10(2):147-56 doi 10.1016/S1470-2045(08)70314-0.
21. Li Y, Buijs-Gladdines JG, Cante-Barrett K, Stubbs AP, Vroegindeweij EM, Smits WK, *et al.* IL-7 Receptor Mutations and Steroid Resistance in Pediatric T cell Acute Lymphoblastic Leukemia: A Genome Sequencing Study. *PLoS Med* **2016**;13(12):e1002200 doi 10.1371/journal.pmed.1002200.
22. Zhang J, Ding L, Holmfeldt L, Wu G, Heatley SL, Payne-Turner D, *et al.* The genetic basis of early T-cell precursor acute lymphoblastic leukaemia. *Nature* **2012**;481(7380):157-63 doi 10.1038/nature10725.
23. La Starza R, Barba G, Demeyer S, Pierini V, Di Giacomo D, Gianfelici V, *et al.* Deletions of the long arm of chromosome 5 define subgroups of T-cell acute lymphoblastic leukemia. *Haematologica* **2016**;101(8):951-8 doi 10.3324/haematol.2016.143875.
24. Bond J, Marchand T, Touzart A, Cieslak A, Trinquand A, Sutton L, *et al.* An early thymic precursor phenotype predicts outcome exclusively in HOXA-overexpressing adult T-cell acute lymphoblastic leukemia: a Group for Research in Adult Acute Lymphoblastic Leukemia study. *Haematologica* **2016**;101(6):732-40 doi 10.3324/haematol.2015.141218.
25. Pui CH, Pei D, Cheng C, Tomchuck SL, Evans SN, Inaba H, *et al.* Treatment response and outcome of children with T-cell acute lymphoblastic leukemia expressing the gamma-delta T-cell receptor. *Oncoimmunology* **2019**;8(8):1599637 doi 10.1080/2162402X.2019.1599637.
26. Su XY, Della-Valle V, Andre-Schmutz I, Lemerrier C, Radford-Weiss I, Ballerini P, *et al.* HOX11L2/TLX3 is transcriptionally activated through T-cell regulatory elements downstream of BCL11B as a result of the t(5;14)(q35;q32). *Blood* **2006**;108(13):4198-201 doi 10.1182/blood-2006-07-032953.
27. Gutierrez A, Kentsis A, Sanda T, Holmfeldt L, Chen SC, Zhang J, *et al.* The BCL11B tumor suppressor is mutated across the major molecular subtypes of T-cell acute lymphoblastic leukemia. *Blood* **2011**;118(15):4169-73 doi 10.1182/blood-2010-11-318873.
28. Zuurbier L, Homminga I, Calvert V, te Winkel ML, Buijs-Gladdines JG, Kooi C, *et al.* NOTCH1 and/or FBXW7 mutations predict for initial good prednisone response but not for improved outcome in pediatric T-cell acute lymphoblastic leukemia patients treated on DCOG or COALL protocols. *Leukemia* **2010**;24(12):2014-22 doi 10.1038/leu.2010.204.

29. Paganin M, Grillo MF, Silvestri D, Scapinello G, Buldini B, Cazzaniga G, *et al.* The presence of mutated and deleted PTEN is associated with an increased risk of relapse in childhood T cell acute lymphoblastic leukaemia treated with AIEOP-BFM ALL protocols. *Br J Haematol* **2018**;182(5):705-11 doi 10.1111/bjh.15449.
30. Zuurbier L, Petricoin EF, 3rd, Vuerhard MJ, Calvert V, Kooi C, Buijs-Gladdines JG, *et al.* The significance of PTEN and AKT aberrations in pediatric T-cell acute lymphoblastic leukemia. *Haematologica* **2012**;97(9):1405-13 doi 10.3324/haematol.2011.059030.
31. Gutierrez A, Sanda T, Grebliunaite R, Carracedo A, Salmena L, Ahn Y, *et al.* High frequency of PTEN, PI3K, and AKT abnormalities in T-cell acute lymphoblastic leukemia. *Blood* **2009**;114(3):647-50 doi 10.1182/blood-2009-02-206722.
32. Roberts AW, Davids MS, Pagel JM, Kahl BS, Puvvada SD, Gerecitano JF, *et al.* Targeting BCL2 with Venetoclax in Relapsed Chronic Lymphocytic Leukemia. *N Engl J Med* **2016**;374(4):311-22 doi 10.1056/NEJMoa1513257.
33. Butterworth M, Pettitt A, Varadarajan S, Cohen GM. BH3 profiling and a toolkit of BH3-mimetic drugs predict anti-apoptotic dependence of cancer cells. *Br J Cancer* **2016**;114(6):638-41 doi 10.1038/bjc.2016.49.
34. Chonghaile TN, Roderick JE, Glenfield C, Ryan J, Sallan SE, Silverman LB, *et al.* Maturation stage of T-cell acute lymphoblastic leukemia determines BCL-2 versus BCL-XL dependence and sensitivity to ABT-199. *Cancer Discov* **2014**;4(9):1074-87 doi 10.1158/2159-8290.CD-14-0353.
35. Peirs S, Matthijssens F, Goossens S, Van de Walle I, Ruggero K, de Bock CE, *et al.* ABT-199 mediated inhibition of BCL-2 as a novel therapeutic strategy in T-cell acute lymphoblastic leukemia. *Blood* **2014**;124(25):3738-47 doi 10.1182/blood-2014-05-574566.
36. Suryani S, Carol H, Chonghaile TN, Frisimantas V, Sarmah C, High L, *et al.* Cell and molecular determinants of in vivo efficacy of the BH3 mimetic ABT-263 against pediatric acute lymphoblastic leukemia xenografts. *Clin Cancer Res* **2014**;20(17):4520-31 doi 10.1158/1078-0432.CCR-14-0259.
37. Lacayo NJ, Pullarkat VA, Stock W, Jabbour E, Bajel A, Rubnitz J, *et al.* Safety and Efficacy of Venetoclax in Combination with Navitoclax in Adult and Pediatric Relapsed/Refractory Acute Lymphoblastic Leukemia and Lymphoblastic Lymphoma. *Blood* **2019**;134(Supplement_1):285-doi 10.1182/blood-2019-126977.
38. La Starza R, Cambò B, Pierini A, Bornhauser B, Montanaro A, Bourquin JP, *et al.* Venetoclax and Bortezomib in Relapsed/Refractory Early T-Cell Precursor Acute Lymphoblastic Leukemia. *JCO Precision Oncology* **2019**(3):1-6 doi 10.1200/po.19.00172.
39. Li Z, He S, Look AT. The MCL1-specific inhibitor S63845 acts synergistically with venetoclax/ABT-199 to induce apoptosis in T-cell acute lymphoblastic leukemia cells. *Leukemia* **2019**;33(1):262-6 doi 10.1038/s41375-018-0201-2.
40. Choudhary GS, Al-Harbi S, Mazumder S, Hill BT, Smith MR, Bodo J, *et al.* MCL-1 and BCL-xL-dependent resistance to the BCL-2 inhibitor ABT-199 can be overcome by preventing PI3K/AKT/mTOR activation in lymphoid malignancies. *Cell Death Dis* **2015**;6:e1593 doi 10.1038/cddis.2014.525.
41. Chen X, Glytsou C, Zhou H, Narang S, Reyna DE, Lopez A, *et al.* Targeting Mitochondrial Structure Sensitizes Acute Myeloid Leukemia to Venetoclax Treatment. *Cancer Discov* **2019**;9(7):890-909 doi 10.1158/2159-8290.CD-19-0117.
42. Ni Chonghaile T, Sarosiek KA, Vo TT, Ryan JA, Tammareddi A, Moore Vdel G, *et al.* Pretreatment mitochondrial priming correlates with clinical response to cytotoxic chemotherapy. *Science* **2011**;334(6059):1129-33 doi 10.1126/science.1206727.

43. Takebe N, Nguyen D, Yang SX. Targeting notch signaling pathway in cancer: clinical development advances and challenges. *Pharmacol Ther* **2014**;141(2):140-9 doi 10.1016/j.pharmthera.2013.09.005.
44. Samon JB, Castillo-Martin M, Hadler M, Ambesi-Impioabato A, Paietta E, Racevskis J, *et al*. Preclinical analysis of the gamma-secretase inhibitor PF-03084014 in combination with glucocorticoids in T-cell acute lymphoblastic leukemia. *Mol Cancer Ther* **2012**;11(7):1565-75 doi 10.1158/1535-7163.MCT-11-0938.
45. Habets RA, de Bock CE, Serneels L, Lodewijckx I, Verbeke D, Nittner D, *et al*. Safe targeting of T cell acute lymphoblastic leukemia by pathology-specific NOTCH inhibition. *Sci Transl Med* **2019**;11(494) doi 10.1126/scitranslmed.aau6246.
46. Agnusdei V, Minuzzo S, Frasson C, Grassi A, Axelrod F, Satyal S, *et al*. Therapeutic antibody targeting of Notch1 in T-acute lymphoblastic leukemia xenografts. *Leukemia* **2014**;28(2):278-88 doi 10.1038/leu.2013.183.
47. Marchesini M, Gherli A, Montanaro A, Patrizi L, Sorrentino C, Pagliaro L, *et al*. Blockade of Oncogenic NOTCH1 with the SERCA Inhibitor CAD204520 in T Cell Acute Lymphoblastic Leukemia. *Cell Chem Biol* **2020** doi 10.1016/j.chembiol.2020.04.002.
48. Dastur A, Choi A, Costa C, Yin X, Williams A, McClanaghan J, *et al*. NOTCH1 Represses MCL-1 Levels in GSI-resistant T-ALL, Making them Susceptible to ABT-263. *Clin Cancer Res* **2019**;25(1):312-24 doi 10.1158/1078-0432.CCR-18-0867.
49. Tsaouli G, Ferretti E, Bellavia D, Vacca A, Felli MP. Notch/CXCR4 Partnership in Acute Lymphoblastic Leukemia Progression. *J Immunol Res* **2019**;2019:5601396 doi 10.1155/2019/5601396.
50. Filippakopoulos P, Qi J, Picaud S, Shen Y, Smith WB, Fedorov O, *et al*. Selective inhibition of BET bromodomains. *Nature* **2010**;468(7327):1067-73 doi 10.1038/nature09504.
51. Palomero T, Lim WK, Odom DT, Sulis ML, Real PJ, Margolin A, *et al*. NOTCH1 directly regulates c-MYC and activates a feed-forward-loop transcriptional network promoting leukemic cell growth. *Proc Natl Acad Sci U S A* **2006**;103(48):18261-6 doi 10.1073/pnas.0606108103.
52. Roderick JE, Tesell J, Shultz LD, Brehm MA, Greiner DL, Harris MH, *et al*. c-Myc inhibition prevents leukemia initiation in mice and impairs the growth of relapsed and induction failure pediatric T-ALL cells. *Blood* **2014**;123(7):1040-50 doi 10.1182/blood-2013-08-522698.
53. Loosveld M, Castellano R, Gon S, Goubard A, Crouzet T, Pouyet L, *et al*. Therapeutic targeting of c-Myc in T-cell acute lymphoblastic leukemia, T-ALL. *Oncotarget* **2014**;5(10):3168-72 doi 10.18632/oncotarget.1873.
54. Peirs S, Fris mantas V, Matthijssens F, Van Loocke W, Pieters T, Vandamme N, *et al*. Targeting BET proteins improves the therapeutic efficacy of BCL-2 inhibition in T-cell acute lymphoblastic leukemia. *Leukemia* **2017**;31(10):2037-47 doi 10.1038/leu.2017.10.
55. Knoechel B, Roderick JE, Williamson KE, Zhu J, Lohr JG, Cotton MJ, *et al*. An epigenetic mechanism of resistance to targeted therapy in T cell acute lymphoblastic leukemia. *Nat Genet* **2014**;46(4):364-70 doi 10.1038/ng.2913.
56. Ott CJ, Kopp N, Bird L, Paranal RM, Qi J, Bowman T, *et al*. BET bromodomain inhibition targets both c-Myc and IL7R in high-risk acute lymphoblastic leukemia. *Blood* **2012**;120(14):2843-52 doi 10.1182/blood-2012-02-413021.
57. McCarter AC, Gatta GD, Melnick A, Kim E, Sha C, Wang Q, *et al*. Combinatorial ETS1-dependent control of oncogenic NOTCH1 enhancers in T-cell leukemia. *Blood Cancer Discov* **2020**;1(2):178-97 doi 10.1158/2643-3230.bcd-20-0026.

58. Guo L, Li J, Zeng H, Guzman AG, Li T, Lee M, *et al.* A combination strategy targeting enhancer plasticity exerts synergistic lethality against BETi-resistant leukemia cells. *Nature communications* **2020**;11(1):740 doi 10.1038/s41467-020-14604-6.
59. Kloetgen A, Thandapani P, Ntziachristos P, Ghebrechristos Y, Nomikou S, Lazaris C, *et al.* Three-dimensional chromatin landscapes in T cell acute lymphoblastic leukemia. *Nat Genet* **2020**;52(4):388-400 doi 10.1038/s41588-020-0602-9.
60. Kwiatkowski N, Zhang T, Rahl PB, Abraham BJ, Reddy J, Ficarro SB, *et al.* Targeting transcription regulation in cancer with a covalent CDK7 inhibitor. *Nature* **2014**;511(7511):616-20 doi 10.1038/nature13393.
61. Cochran AG, Conery AR, Sims RJ, 3rd. Bromodomains: a new target class for drug development. *Nat Rev Drug Discov* **2019**;18(8):609-28 doi 10.1038/s41573-019-0030-7.
62. Astorgues-Xerri L, Vazquez R, Odore E, Rezai K, Kahatt C, Mackenzie S, *et al.* Insights into the cellular pharmacological properties of the BET-inhibitor OTX015/MK-8628 (birabresib), alone and in combination, in leukemia models. *Leuk Lymphoma* **2019**;60(12):3067-70 doi 10.1080/10428194.2019.1617860.
63. Graux C, Cools J, Melotte C, Quentmeier H, Ferrando A, Levine R, *et al.* Fusion of NUP214 to ABL1 on amplified episomes in T-cell acute lymphoblastic leukemia. *Nat Genet* **2004**;36(10):1084-9 doi 10.1038/ng1425.
64. Graux C, Stevens-Kroef M, Lafage M, Dastugue N, Harrison CJ, Mugneret F, *et al.* Heterogeneous patterns of amplification of the NUP214-ABL1 fusion gene in T-cell acute lymphoblastic leukemia. *Leukemia* **2009**;23(1):125-33 doi 10.1038/leu.2008.278.
65. Chen B, Jiang L, Zhong ML, Li JF, Li BS, Peng LJ, *et al.* Identification of fusion genes and characterization of transcriptome features in T-cell acute lymphoblastic leukemia. *Proc Natl Acad Sci U S A* **2018**;115(2):373-8 doi 10.1073/pnas.1717125115.
66. Fris mantas V, Dobay MP, Rinaldi A, Tchinda J, Dunn SH, Kunz J, *et al.* Ex vivo drug response profiling detects recurrent sensitivity patterns in drug-resistant acute lymphoblastic leukemia. *Blood* **2017**;129(11):e26-e37 doi 10.1182/blood-2016-09-738070.
67. Serafin V, Capuzzo G, Milani G, Minuzzo SA, Pinazza M, Bortolozzi R, *et al.* Glucocorticoid resistance is reverted by LCK inhibition in pediatric T-cell acute lymphoblastic leukemia. *Blood* **2017**;130(25):2750-61 doi 10.1182/blood-2017-05-784603.
68. Shi Y, Beckett MC, Blair HJ, Tirtakusuma R, Nakjang S, Enshaei A, *et al.* Phase II-like murine trial identifies synergy between dexamethasone and dasatinib in T-cell acute lymphoblastic leukemia. *Haematologica* **2020** doi 10.3324/haematol.2019.241026.
69. Maude SL, Dolai S, Delgado-Martin C, Vincent T, Robbins A, Selvanathan A, *et al.* Efficacy of JAK/STAT pathway inhibition in murine xenograft models of early T-cell precursor (ETP) acute lymphoblastic leukemia. *Blood* **2015**;125(11):1759-67 doi 10.1182/blood-2014-06-580480.
70. Delgado-Martin C, Meyer LK, Huang BJ, Shimano KA, Zinter MS, Nguyen JV, *et al.* JAK/STAT pathway inhibition overcomes IL7-induced glucocorticoid resistance in a subset of human T-cell acute lymphoblastic leukemias. *Leukemia* **2017**;31(12):2568-76 doi 10.1038/leu.2017.136.
71. de Bock CE, Demeyer S, Degryse S, Verbeke D, Sweron B, Gielen O, *et al.* HOXA9 Cooperates with Activated JAK/STAT Signaling to Drive Leukemia Development. *Cancer Discov* **2018**;8(5):616-31 doi 10.1158/2159-8290.CD-17-0583.
72. Verstovsek S, Kantarjian H, Mesa RA, Pardanani AD, Cortes-Franco J, Thomas DA, *et al.* Safety and efficacy of INCB018424, a JAK1 and JAK2 inhibitor, in myelofibrosis. *N Engl J Med* **2010**;363(12):1117-27 doi 10.1056/NEJMoa1002028.

73. Greenfield G, McPherson S, Mills K, McMullin MF. The ruxolitinib effect: understanding how molecular pathogenesis and epigenetic dysregulation impact therapeutic efficacy in myeloproliferative neoplasms. *J Transl Med* **2018**;16(1):360 doi 10.1186/s12967-018-1729-7.
74. Padi SKR, Luevano LA, An N, Pandey R, Singh N, Song JH, *et al*. Targeting the PIM protein kinases for the treatment of a T-cell acute lymphoblastic leukemia subset. *Oncotarget* **2017**;8(18):30199-216 doi 10.18632/oncotarget.16320.
75. Ribeiro D, Melao A, van Boxtel R, Santos CI, Silva A, Silva MC, *et al*. STAT5 is essential for IL-7-mediated viability, growth, and proliferation of T-cell acute lymphoblastic leukemia cells. *Blood Adv* **2018**;2(17):2199-213 doi 10.1182/bloodadvances.2018021063.
76. La Starza R, Messina M, Gianfelici V, Pierini V, Matteucci C, Pierini T, *et al*. High PIM1 expression is a biomarker of T-cell acute lymphoblastic leukemia with JAK/STAT activation or t(6;7)(p21;q34)/TRB@-PIM1 rearrangement. *Leukemia* **2018**;32(8):1807-10 doi 10.1038/s41375-018-0031-2.
77. De Smedt R, Peirs S, Morscio J, Matthijssens F, Roels J, Reunes L, *et al*. Pre-clinical evaluation of second generation PIM inhibitors for the treatment of T-cell acute lymphoblastic leukemia and lymphoma. *Haematologica* **2019**;104(1):e17-e20 doi 10.3324/haematol.2018.199257.
78. Cante-Barrett K, Spijkers-Hagelstein JA, Buijs-Gladdines JG, Uitdehaag JC, Smits WK, van der Zwet J, *et al*. MEK and PI3K-AKT inhibitors synergistically block activated IL7 receptor signaling in T-cell acute lymphoblastic leukemia. *Leukemia* **2016**;30(9):1832-43 doi 10.1038/leu.2016.83.
79. Lin YW, Beharry ZM, Hill EG, Song JH, Wang W, Xia Z, *et al*. A small molecule inhibitor of Pim protein kinases blocks the growth of precursor T-cell lymphoblastic leukemia/lymphoma. *Blood* **2010**;115(4):824-33 doi 10.1182/blood-2009-07-233445.
80. De Smedt R, Morscio J, Reunes L, Roels J, Bardelli V, Lintermans B, *et al*. Targeting cytokine- and therapy-induced PIM1 activation in preclinical models of T-cell acute lymphoblastic leukemia and lymphoma. *Blood* **2020**;135(19):1685-95 doi 10.1182/blood.2019003880.
81. Mendes RD, Sarmiento LM, Cante-Barrett K, Zuurbier L, Buijs-Gladdines JG, Povoia V, *et al*. PTEN microdeletions in T-cell acute lymphoblastic leukemia are caused by illegitimate RAG-mediated recombination events. *Blood* **2014**;124(4):567-78 doi 10.1182/blood-2014-03-562751.
82. Trinquand A, Tanguy-Schmidt A, Ben Abdelali R, Lambert J, Beldjord K, Lengline E, *et al*. Toward a NOTCH1/FBXW7/RAS/PTEN-based oncogenetic risk classification of adult T-cell acute lymphoblastic leukemia: a Group for Research in Adult Acute Lymphoblastic Leukemia study. *J Clin Oncol* **2013**;31(34):4333-42 doi 10.1200/JCO.2012.48.5292.
83. Lonetti A, Cappellini A, Sparta AM, Chiarini F, Buontempo F, Evangelisti C, *et al*. PI3K pan-inhibition impairs more efficiently proliferation and survival of T-cell acute lymphoblastic leukemia cell lines when compared to isoform-selective PI3K inhibitors. *Oncotarget* **2015**;6(12):10399-414 doi 10.18632/oncotarget.3295.
84. Lonetti A, Antunes IL, Chiarini F, Orsini E, Buontempo F, Ricci F, *et al*. Activity of the pan-class I phosphoinositide 3-kinase inhibitor NVP-BKM120 in T-cell acute lymphoblastic leukemia. *Leukemia* **2014**;28(6):1196-206 doi 10.1038/leu.2013.369.
85. Lonetti A, Cappellini A, Bertaina A, Locatelli F, Pession A, Buontempo F, *et al*. Improving nelarabine efficacy in T cell acute lymphoblastic leukemia by targeting aberrant PI3K/AKT/mTOR signaling pathway. *J Hematol Oncol* **2016**;9(1):114 doi 10.1186/s13045-016-0344-4.
86. Chiarini F, Fala F, Tazzari PL, Ricci F, Astolfi A, Pession A, *et al*. Dual inhibition of class IA phosphatidylinositol 3-kinase and mammalian target of rapamycin as a new therapeutic option for T-cell acute lymphoblastic leukemia. *Cancer Res* **2009**;69(8):3520-8 doi 10.1158/0008-5472.CAN-08-4884.

87. Hall CP, Reynolds CP, Kang MH. Modulation of Glucocorticoid Resistance in Pediatric T-cell Acute Lymphoblastic Leukemia by Increasing BIM Expression with the PI3K/mTOR Inhibitor BEZ235. *Clin Cancer Res* **2016**;22(3):621-32 doi 10.1158/1078-0432.CCR-15-0114.
88. Gazi M, Moharram SA, Marshall A, Kazi JU. The dual specificity PI3K/mTOR inhibitor PKI-587 displays efficacy against T-cell acute lymphoblastic leukemia (T-ALL). *Cancer Lett* **2017**;392:9-16 doi 10.1016/j.canlet.2017.01.035.
89. Batista A, Barata JT, Raderschall E, Sallan SE, Carlesso N, Nadler LM, *et al.* Targeting of active mTOR inhibits primary leukemia T cells and synergizes with cytotoxic drugs and signaling inhibitors. *Exp Hematol* **2011**;39(4):457-72 e3 doi 10.1016/j.exphem.2011.01.005.
90. Pikman Y, Alexe G, Roti G, Conway AS, Furman A, Lee ES, *et al.* Synergistic Drug Combinations with a CDK4/6 Inhibitor in T-cell Acute Lymphoblastic Leukemia. *Clin Cancer Res* **2017**;23(4):1012-24 doi 10.1158/1078-0432.CCR-15-2869.
91. Benjamin D, Colombi M, Moroni C, Hall MN. Rapamycin passes the torch: a new generation of mTOR inhibitors. *Nat Rev Drug Discov* **2011**;10(11):868-80 doi 10.1038/nrd3531.
92. Yun S, Vincelette ND, Knorr KL, Almada LL, Schneider PA, Peterson KL, *et al.* 4EBP1/c-MYC/PUMA and NF-kappaB/EGR1/BIM pathways underlie cytotoxicity of mTOR dual inhibitors in malignant lymphoid cells. *Blood* **2016**;127(22):2711-22 doi 10.1182/blood-2015-02-629485.
93. Martelli AM, Chiarini F, Evangelisti C, Cappellini A, Buontempo F, Bressanin D, *et al.* Two hits are better than one: targeting both phosphatidylinositol 3-kinase and mammalian target of rapamycin as a therapeutic strategy for acute leukemia treatment. *Oncotarget* **2012**;3(4):371-94 doi 10.18632/oncotarget.477.
94. Simioni C, Neri LM, Tabellini G, Ricci F, Bressanin D, Chiarini F, *et al.* Cytotoxic activity of the novel Akt inhibitor, MK-2206, in T-cell acute lymphoblastic leukemia. *Leukemia* **2012**;26(11):2336-42 doi 10.1038/leu.2012.136.
95. Lynch JT, McEwen R, Crafter C, McDermott U, Garnett MJ, Barry ST, *et al.* Identification of differential PI3K pathway target dependencies in T-cell acute lymphoblastic leukemia through a large cancer cell panel screen. *Oncotarget* **2016**;7(16):22128-39 doi 10.18632/oncotarget.8031.
96. Irving J, Matheson E, Minto L, Blair H, Case M, Halsey C, *et al.* Ras pathway mutations are prevalent in relapsed childhood acute lymphoblastic leukemia and confer sensitivity to MEK inhibition. *Blood* **2014**;124(23):3420-30 doi 10.1182/blood-2014-04-531871.
97. Jerchel IS, Hoogkamer AQ, Aries IM, Steeghs EMP, Boer JM, Besselink NJM, *et al.* RAS pathway mutations as a predictive biomarker for treatment adaptation in pediatric B-cell precursor acute lymphoblastic leukemia. *Leukemia* **2018**;32(4):931-40 doi 10.1038/leu.2017.303.
98. Driessen EM, van Roon EH, Spijkers-Hagelstein JA, Schneider P, de Lorenzo P, Valsecchi MG, *et al.* Frequencies and prognostic impact of RAS mutations in MLL-rearranged acute lymphoblastic leukemia in infants. *Haematologica* **2013**;98(6):937-44 doi 10.3324/haematol.2012.067983.
99. Richter-Pechanska P, Kunz JB, Hof J, Zimmermann M, Rausch T, Bandapalli OR, *et al.* Identification of a genetically defined ultra-high-risk group in relapsed pediatric T-lymphoblastic leukemia. *Blood Cancer J* **2017**;7(2):e523 doi 10.1038/bcj.2017.3.
100. Aries IM, van den Dungen RE, Koudijs MJ, Cuppen E, Voest E, Molenaar JJ, *et al.* Towards personalized therapy in pediatric acute lymphoblastic leukemia: RAS mutations and prednisolone resistance. *Haematologica* **2015**;100(4):e132-6 doi 10.3324/haematol.2014.112995.
101. Matheson EC, Thomas H, Case M, Blair H, Jackson RK, Masic D, *et al.* Glucocorticoids and selumetinib are highly synergistic in RAS pathway-mutated childhood acute lymphoblastic leukemia through upregulation of BIM. *Haematologica* **2019**;104(9):1804-11 doi 10.3324/haematol.2017.185975.

102. Kerstjens M, Driessen EM, Willekes M, Pinhancos SS, Schneider P, Pieters R, *et al.* MEK inhibition is a promising therapeutic strategy for MLL-rearranged infant acute lymphoblastic leukemia patients carrying RAS mutations. *Oncotarget* **2017**;8(9):14835-46 doi 10.18632/oncotarget.11730.
103. Jang W, Park J, Kwon A, Choi H, Kim J, Lee GD, *et al.* CDKN2B downregulation and other genetic characteristics in T-acute lymphoblastic leukemia. *Exp Mol Med* **2019**;51(1):4 doi 10.1038/s12276-018-0195-x.
104. Sawai CM, Freund J, Oh P, Ndiaye-Lobry D, Bretz JC, Strikoudis A, *et al.* Therapeutic targeting of the cyclin D3:CDK4/6 complex in T cell leukemia. *Cancer Cell* **2012**;22(4):452-65 doi 10.1016/j.ccr.2012.09.016.
105. Moharram SA, Shah K, Khanum F, Marshall A, Gazi M, Kazi JU. Efficacy of the CDK inhibitor dinaciclib in vitro and in vivo in T-cell acute lymphoblastic leukemia. *Cancer Lett* **2017**;405:73-8 doi 10.1016/j.canlet.2017.07.019.
106. Gojo I, Sadowska M, Walker A, Feldman EJ, Iyer SP, Baer MR, *et al.* Clinical and laboratory studies of the novel cyclin-dependent kinase inhibitor dinaciclib (SCH 727965) in acute leukemias. *Cancer Chemother Pharmacol* **2013**;72(4):897-908 doi 10.1007/s00280-013-2249-z.
107. Kurtzberg J, Ernst TJ, Keating MJ, Gandhi V, Hodge JP, Kisor DF, *et al.* Phase I study of 506U78 administered on a consecutive 5-day schedule in children and adults with refractory hematologic malignancies. *J Clin Oncol* **2005**;23(15):3396-403 doi 10.1200/JCO.2005.03.199.
108. Berg SL, Blaney SM, Devidas M, Lampkin TA, Murgu A, Bernstein M, *et al.* Phase II study of nelarabine (compound 506U78) in children and young adults with refractory T-cell malignancies: a report from the Children's Oncology Group. *J Clin Oncol* **2005**;23(15):3376-82 doi 10.1200/jco.2005.03.426.
109. Gokbuget N, Basara N, Baurmann H, Beck J, Bruggemann M, Diedrich H, *et al.* High single-drug activity of nelarabine in relapsed T-lymphoblastic leukemia/lymphoma offers curative option with subsequent stem cell transplantation. *Blood* **2011**;118(13):3504-11 doi 10.1182/blood-2011-01-329441.
110. Malone A, Smith OP. Nelarabine toxicity in children and adolescents with relapsed/refractory T-ALL/T-LBL: can we avoid throwing the baby out with the bathwater? *Br J Haematol* **2017**;179(2):179-81 doi 10.1111/bjh.14875.
111. Dunsmore KP, Winter SS, Devidas M, Wood BL, Esiashvili N, Chen Z, *et al.* Children's Oncology Group AALL0434: A Phase III Randomized Clinical Trial Testing Nelarabine in Newly Diagnosed T-Cell Acute Lymphoblastic Leukemia. *J Clin Oncol* **2020**;38(28):3282-93 doi 10.1200/JCO.20.00256.
112. Hoell JI, Ginzl S, Kuhlen M, Kloetgen A, Gombert M, Fischer U, *et al.* Pediatric ALL relapses after allo-SCT show high individuality, clonal dynamics, selective pressure, and druggable targets. *Blood Adv* **2019**;3(20):3143-56 doi 10.1182/bloodadvances.2019000051.
113. Bykov VJN, Eriksson SE, Bianchi J, Wiman KG. Targeting mutant p53 for efficient cancer therapy. *Nat Rev Cancer* **2018**;18(2):89-102 doi 10.1038/nrc.2017.109.
114. Ghione P, Moskowitz AJ, De Paola NEK, Horwitz SM, Ruella M. Novel Immunotherapies for T Cell Lymphoma and Leukemia. *Current hematologic malignancy reports* **2018**;13(6):494-506 doi 10.1007/s11899-018-0480-8.
115. Bride KL, Vincent TL, Im SY, Aplenc R, Barrett DM, Carroll WL, *et al.* Preclinical efficacy of daratumumab in T-cell acute lymphoblastic leukemia. *Blood* **2018**;131(9):995-9 doi 10.1182/blood-2017-07-794214.
116. Krejcik J, Casneuf T, Nijhof IS, Verbist B, Bald J, Plesner T, *et al.* Daratumumab depletes CD38+ immune regulatory cells, promotes T-cell expansion, and skews T-cell repertoire in multiple myeloma. *Blood* **2016**;128(3):384-94 doi 10.1182/blood-2015-12-687749.

117. Ofran Y, Ringelstein-Harlev S, Slouzkey I, Zuckerman T, Yehudai-Ofir D, Henig I, *et al.* Daratumumab for eradication of minimal residual disease in high-risk advanced relapse of T-cell/CD19/CD22-negative acute lymphoblastic leukemia. *Leukemia* **2020**;34(1):293-5 doi 10.1038/s41375-019-0548-z.
118. Trinquand A, Dos Santos NR, Tran Quang C, Rocchetti F, Zaniboni B, Belhocine M, *et al.* Triggering the TCR Developmental Checkpoint Activates a Therapeutically Targetable Tumor Suppressive Pathway in T-cell Leukemia. *Cancer Discov* **2016**;6(9):972-85 doi 10.1158/2159-8290.CD-15-0675.
119. Fleischer LC, Spencer HT, Raikar SS. Targeting T cell malignancies using CAR-based immunotherapy: challenges and potential solutions. *J Hematol Oncol* **2019**;12(1):141 doi 10.1186/s13045-019-0801-y.
120. Depil S, Duchateau P, Grupp SA, Mufti G, Poirot L. 'Off-the-shelf' allogeneic CAR T cells: development and challenges. *Nat Rev Drug Discov* **2020**;19(3):185-99 doi 10.1038/s41573-019-0051-2.
121. Mamonkin M, Rouce RH, Tashiro H, Brenner MK. A T-cell-directed chimeric antigen receptor for the selective treatment of T-cell malignancies. *Blood* **2015**;126(8):983-92 doi 10.1182/blood-2015-02-629527.
122. Gomes-Silva D, Srinivasan M, Sharma S, Lee CM, Wagner DL, Davis TH, *et al.* CD7-edited T cells expressing a CD7-specific CAR for the therapy of T-cell malignancies. *Blood* **2017**;130(3):285-96 doi 10.1182/blood-2017-01-761320.
123. Brandt LJB, Barnkob MB, Michaels YS, Heiselberg J, Barington T. Emerging Approaches for Regulation and Control of CAR T Cells: A Mini Review. *Front Immunol* **2020**;11:326 doi 10.3389/fimmu.2020.00326.
124. Cooper ML, Choi J, Staser K, Ritchey JK, Devenport JM, Eckardt K, *et al.* An "off-the-shelf" fratricide-resistant CAR-T for the treatment of T cell hematologic malignancies. *Leukemia* **2018**;32(9):1970-83 doi 10.1038/s41375-018-0065-5.
125. Wang X, Li S, Gao L, Yuan Z, Wu K, Liu L, *et al.* Abstract CT052: Clinical safety and efficacy study of TruUCAR™ GC027: The first-in-human, universal CAR-T therapy for adult relapsed/refractory T-cell acute lymphoblastic leukemia (r/r T-ALL). *Cancer Research* **2020**;80(16 Supplement):CT052-CT doi 10.1158/1538-7445.Am2020-ct052.
126. Sanchez-Martinez D, Baroni ML, Gutierrez-Aguera F, Roca-Ho H, Blanch-Lombarte O, Gonzalez-Garcia S, *et al.* Fratricide-resistant CD1a-specific CAR T cells for the treatment of cortical T-cell acute lymphoblastic leukemia. *Blood* **2019**;133(21):2291-304 doi 10.1182/blood-2018-10-882944.
127. Gao Z, Tong C, Wang Y, Chen D, Wu Z, Han W. Blocking CD38-driven fratricide among T cells enables effective antitumor activity by CD38-specific chimeric antigen receptor T cells. *J Genet Genomics* **2019**;46(8):367-77 doi 10.1016/j.jgg.2019.06.007.
128. Guo Y, Feng K, Tong C, Jia H, Liu Y, Wang Y, *et al.* Efficiency and side effects of anti-CD38 CAR T cells in an adult patient with relapsed B-ALL after failure of bi-specific CD19/CD22 CAR T cell treatment. *Cell Mol Immunol* **2020**;17(4):430-2 doi 10.1038/s41423-019-0355-5.
129. Evans K, Duan J, Pritchard T, Jones CD, McDermott L, Gu Z, *et al.* OBI-3424, a Novel AKR1C3-Activated Prodrug, Exhibits Potent Efficacy against Preclinical Models of T-ALL. *Clin Cancer Res* **2019**;25(14):4493-503 doi 10.1158/1078-0432.CCR-19-0551.
130. Verbeke D, Demeyer S, Prieto C, de Bock CE, De Bie J, Gielen O, *et al.* The XPO1 Inhibitor KPT-8602 Synergizes with Dexamethasone in Acute Lymphoblastic Leukemia. *Clin Cancer Res* **2020** doi 10.1158/1078-0432.CCR-20-1315.

131. Moreno DA, Scrideli CA, Cortez MA, de Paula Queiroz R, Valera ET, da Silva Silveira V, *et al.* Differential expression of HDAC3, HDAC7 and HDAC9 is associated with prognosis and survival in childhood acute lymphoblastic leukaemia. *Br J Haematol* **2010**;150(6):665-73 doi 10.1111/j.1365-2141.2010.08301.x.
132. Waibel M, Vervoort SJ, Kong IY, Heinzel S, Ramsbottom KM, Martin BP, *et al.* Epigenetic targeting of Notch1-driven transcription using the HDACi panobinostat is a potential therapy against T-cell acute lymphoblastic leukemia. *Leukemia* **2018**;32(1):237-41 doi 10.1038/leu.2017.282.
133. Lu BY, Thanawala SU, Zochowski KC, Burke MJ, Carroll WL, Bhatla T. Decitabine enhances chemosensitivity of early T-cell precursor-acute lymphoblastic leukemia cell lines and patient-derived samples. *Leuk Lymphoma* **2016**;57(8):1938-41 doi 10.3109/10428194.2015.1110747.
134. El Chaer F, Holtzman N, Binder E, Porter NC, Singh ZN, Koka M, *et al.* Durable remission with salvage decitabine and donor lymphocyte infusion (DLI) for relapsed early T-cell precursor ALL. *Bone Marrow Transplant* **2017**;52(11):1583-4 doi 10.1038/bmt.2017.191.
135. Horton TM, Whitlock JA, Lu X, O'Brien MM, Borowitz MJ, Devidas M, *et al.* Bortezomib reinduction chemotherapy in high-risk ALL in first relapse: a report from the Children's Oncology Group. *Br J Haematol* **2019**;186(2):274-85 doi 10.1111/bjh.15919.
136. Han K, Wang Q, Cao H, Qiu G, Cao J, Li X, *et al.* The NEDD8-activating enzyme inhibitor MLN4924 induces G2 arrest and apoptosis in T-cell acute lymphoblastic leukemia. *Oncotarget* **2016**;7(17):23812-24 doi 10.18632/oncotarget.8068.
137. Hartsink-Segers SA, Zwaan CM, Exalto C, Luijendijk MW, Calvert VS, Petricoin EF, *et al.* Aurora kinases in childhood acute leukemia: the promise of aurora B as therapeutic target. *Leukemia* **2013**;27(3):560-8 doi 10.1038/leu.2012.256.
138. Park SI, Lin CP, Ren N, Angus SP, Dittmer DP, Foote M, *et al.* Inhibition of Aurora A Kinase in Combination with Chemotherapy Induces Synthetic Lethality and Overcomes Chemoresistance in Myc-Overexpressing Lymphoma. *Targeted oncology* **2019**;14(5):563-75 doi 10.1007/s11523-019-00662-4.
139. Mosse YP, Fox E, Teachey DT, Reid JM, Safgren SL, Carol H, *et al.* A Phase II Study of Alisertib in Children with Recurrent/Refractory Solid Tumors or Leukemia: Children's Oncology Group Phase I and Pilot Consortium (ADVL0921). *Clin Cancer Res* **2019**;25(11):3229-38 doi 10.1158/1078-0432.CCR-18-2675.
140. Jiang J, Wang J, Yue M, Cai X, Wang T, Wu C, *et al.* Direct Phosphorylation and Stabilization of MYC by Aurora B Kinase Promote T-cell Leukemogenesis. *Cancer Cell* **2020**;37(2):200-15 e5 doi 10.1016/j.ccell.2020.01.001.
141. Goto H, Yoshino Y, Ito M, Nagai J, Kumamoto T, Inukai T, *et al.* Aurora B kinase as a therapeutic target in acute lymphoblastic leukemia. *Cancer Chemother Pharmacol* **2020**;85(4):773-83 doi 10.1007/s00280-020-04045-9.
142. Harttrampf AC, Lacroix L, Deloger M, Deschamps F, Puget S, Auger N, *et al.* Molecular Screening for Cancer Treatment Optimization (MOSCATO-01) in Pediatric Patients: A Single-Institutional Prospective Molecular Stratification Trial. *Clin Cancer Res* **2017**;23(20):6101-12 doi 10.1158/1078-0432.CCR-17-0381.

SUPPLEMENTARY DATA

Table S1. Relevant clinical trials investigating targeted therapies for T-ALL treatment

| Therapeutic agent | Target | Association with T-ALL subtype/ outcome | Trial identifier and year posted on clinicaltrials.gov | Tumor type | Phase/ status | Results | |
|-------------------------------|--------------------------------------|---|--|--|---------------|--------------------------------------|--|
| BH3 mimetics | Higher BCL2 expression | Higher in ETP-ALL | | | | | |
| Venetoclax (ABT-199) | | | NCT03236857 (p, ya); 2017 | R/R malignancies | I (R) | | |
| | | | NCT03808610 (a); 2019 | R/R ALL (with chemo) | I/II (R) | | |
| Navitoclax (ABT-263) | Higher BCL2 and BCLXL expression | | NCT00406809 (a); 2006 | R/R lymphoid malignancies | I/II (C) | Thrombocytopenia and neutropenia (1) | |
| | | | NCT03181126 (p, a); 2017 | R/R ALL or LBL (with chemo) | I (A) | | |
| AZD-5991 | Higher MCL1 expression | | NCT03218683 (a); 2017 | R/R hematologic malignancies (also with venetoclax) | I (A) | | |
| NOTCH1 inhibitors | NOTCH1 activating mutations | Favourable outcome | | | | | |
| Brontictuzumab (OMP-52M51) | | | NCT01703572 (a); 2012 | R/R lymphoid malignancies | I (C) | | |
| γ-secretase inhibitors | | | | | | | |
| LY3039478 | | | NCT02518113 (p, a); 2015 | T-ALL/T-LBL (with dexamethasone) | I/II (C) | | |
| BMS-906024 | | | NCT01363817 (a); 2011 | R/R T-ALL/LBL (alone or in combination with dexamethasone) | I (C) | | |
| PF-3084014 | | | NCT00878189 (ya, a); 2009 | R/R T-ALL/LBL and solid tumors | I (C) | Anti T-ALL activity (2) | |
| CXCR4 inhibitors | | | | | | | |
| Plerixafor (AMD3100) | | | NCT01319864 (p, a); 2011 | R/R ALL, AML, and MSD (with cytarabine and etoposide) | I (C) | No response in ALL patients (3) | |
| BL-8040 | | | NCT02763384 (a); 2016 | R/R T-ALL/LBL (with nelarabine) | II (R) | | |
| BET inhibitors | BRD4 activity; aberrant Myc activity | | | | | | |
| OTX015 (MK-8628) | | NCT01713582 (a); 2012 | R/R acute leukemia and MM | I (C) | | | |
| GSK525762 | | | NCT01943851 (a); 2013 | R/R hematologic malignancies | I/II (C) | | |
| ABL/SRC inhibitors | ABL1 fusions | | | | | | |
| Dasatinib | | NCT03117751 (p); 2017 | Dx ALL/LL (with chemo) | II/III (R) | | | |
| Imatinib | | NCT02551718 (p, a); 2015 | R/R acute leukemia | N/A (R) | | | |
| JAK1/2 inhibitor | IL7Rα, JAK1/3 and STAT5B mutations | Higher in ETP-ALL; associated with steroid resistance | | | | | |
| Ruxolitinib | | | NCT01251965 (ya, a); 2010 | R/R ALL/AML | I/II (T) | No clinical benefit * | |
| | | | NCT03613428 (p, a); 2018 | R/R ETP-ALL (with chemo) | I/II (NR) | | |
| | | | NCT03117751 (p); 2017 | Dx ALL/LL (with chemo) | II/III (R) | | |
| | | | NCT03515200 (p, ya); 2018 | R/R ALL (with chemo) | I (T) | | |

Table S1. Continued.

| Therapeutic agent | Target | Association with T-ALL subtype/ outcome | Trial identifier and year posted on clinicaltrials.gov | Tumor type | Phase/ status | Results | |
|----------------------------------|---|---|--|---|---------------|--|--|
| Pan-PI3K inhibitors | | | | | | | |
| Buparlisib (BMK120) | <i>PIK3R1</i> and <i>PIK3CA/D</i> mutations; <i>AKT</i> mutations; <i>PTEN</i> deletions; | Poor prognosis, therapy failure and relapse | NCT01396499 (a); 2011 | R/R acute leukemia | I (C) | | |
| Selective-PI3K inhibitors | | | NCT01833169 (a); 2013 | PIK3-activated solid and hematologic malignancies | II (C) | | |
| | | | NCT02711852 (a); 2016 | R/R hematologic malignancies | II (A) | | |
| | | | NCT03742323 (a); 2018 | R/R ALL | I/II (R) | | |
| mTOR inhibitors | | | | | | | |
| Everolimus (rapamycin, RAD001) | | | NCT00968253 (p, a); 2009 | R/R ALL (with chemo) | I/II (C) | The combination is tolerated with moderate activity in T-ALL (4) | |
| | | | NCT01523977 (p, ya); 2012 | R/R ALL (with chemo) | I (C) | The combination is feasible (5) | |
| | | | NCT00874562 (p, a); 2009 | R/R ALL (with steroids) | I (C) | | |
| | | | NCT03740334 (p,a); 2018 | R/R ALL (with dexamethasone and ribociclib) | I (R) | | |
| Temsilolimus (CCI-799) | | | NCT00084916 (a); 2004 | R/R leukemia | II (C) | | |
| | NCT01403415 (p, ya); 2011 | >2 relapses ALL/LBL (with re-induction chemo) | I (C) | Excessive toxicity (6) | | | |
| Dual PI3K/mTOR inhibitors | | | | | | | |
| Dactolisib (NVP-BE235) | | | NCT01756118 (a); 2012 | R/R acute leukemia | I (A) | | |
| AKT inhibitors | | | | | | | |
| MK-2206 (allosteric) | | | NCT01231919 (p, ya); 2010 | R/R solid tumors or leukemia | I (C) | | |
| MEK inhibitors | | | | | | | |
| Selumetinib | <i>NRAS/ KRAS</i> mutations | Higher in ETP-ALL; associated with steroid resistance | NCT03705507 (p, a); 2018 | R/R ALL (with dexamethasone) | I/II (R) | | |
| Trametinib | | | NCT00920140 (a); 2009 | R/R leukemias | I/II (C) | | |
| | | | NCT02551718 (p, a); 2015 | R/R acute leukemias | N/A (R) | | |
| Binimetinib (MEK162) | | | NCT01885195 (a); 2013 | RAS/RAF/MEK-activated malignancies | II (C) | | |

Table S1. Continued.

| Therapeutic agent | Target | Association with T-ALL subtype/ outcome | Trial identifier and year posted on clinicaltrials.gov | Tumor type | Phase/ status | Results |
|--------------------------|---|---|--|---|---------------|--|
| CDK4/6 inhibitors | | | | | | |
| Ribociclib (LEE011) | CDKN2A/B down-regulation; CDKN1B deletions; CCND3 up-regulation | Lower incidence in ETP-ALL | NCT02187783 (a); 2014 | CDK4/6-activated tumors | II (C) | |
| | | | NCT03740334 (p, a); 2018 | R/R ALL (with dexamethasone and everolimus) | I (R) | |
| | | | NCT02813135 (p); 2016 | R/R cancer | I/II (R) | |
| | | | NCT03792256 (p); 2019 | R/R ALL/LL (with re-induction chemo) | I (R) | |
| | | | NCT03132454 (ya, a); 2017 | R/R leukemia (with sorafenib, decitabine or dexamethasone) | I (R) | |
| | | | NCT03515200 (p, ya); 2018 | R/R ALL (with chemo) | I (T) | |
| Purine analog | Rapid DNA synthesis | | | | | |
| Nelarabine | | | NCT02551718 (p, a); 2015 | R/R acute leukemia | N/A (R) | |
| | | | NCT00866671 (p, ya); 2009 | R/R T-ALL/LBL with ≥2 prior treatments | IV (C) | The risk-benefit profile is positive (7) |
| | | | NCT00408005 (p, ya); 2006 | Dx T-ALL/LBL | III (A) | Increased disease-free survival rate (8) |
| MDM2 inhibitors | | | | | | |
| Idasanutlin | MDM2 over-expression | | NCT04029688 (p, ya); 2019 | R/R acute leukemia or solid tumors (with chemo or venetoclax) | I/II (R) | |
| HDM201 | | | NCT02143635 (a); 2014 | p53-WT advanced tumors, including ALL | I (C) | |
| ALRN-6924 | | | NCT03654716 (p, ya); 2018 | Pediatric cancer, including R/R ALL | I (R) | |
| Immunotherapy | | | | | | |
| Daratumumab | CD38 expression | | NCT00501826 (p, a); 2007 | T-ALL/T-LBL (with chemo) | II (R) | |
| | | | NCT03384654 (p); 2017 | R/R ALL/LBL (with chemo) | II (R) | |
| Isatuximab | | | NCT03860844 (p); 2019 | R/R ALL or AML (with chemo) | II (R) | |
| CAR T | | | | | | |
| Anti-CD5 CAR T | CD5 expression | | NCT03081910 (p, a); 2017 | R/R T-cell malignancies | I (R) | |
| Anti-CD7 CAR T | CD7 expression | | NCT03690011 (p, a); 2018 | R/R T-cell malignancies | I (NR) | |
| OTHER DRUGS | | | | | | |
| XPO1 inhibitor | Nuclear export of oncogenic proteins/ mRNA | | | | | |
| Selinexor (KPT-330) | | | NCT02212561 (p, ya); 2014 | R/R ALL, AML, or MSD | I (C) | Drug is safe with promising activity (9) |
| | | | NCT02091245 (p, ya); 2014 | R/R ALL and AML | I (A) | |

Table S1. Continued.

| Therapeutic agent | Target | Association with T-ALL subtype/ outcome | Trial identifier and year posted on clinicaltrials.gov | Tumor type | Phase/ status | Results |
|-------------------------------------|-----------------------------------|---|--|---|---------------|----------------------------------|
| HDAC inhibitors | High HDAC expression and activity | | | | | |
| Panobinostat | | | NCT00723203 (a); 2008 | R/R ALL or AML | II (T) | Lack of efficacy * |
| | | | NCT02518750 (p); 2015 | R/R T-ALL/LBL (with bortezomib and chemo) | II (T) | Slow accrual * |
| | | | NCT01321346 (p); 2011 | R/R acute leukemias (with cytarabine) and lymphomas | I (C) | |
| Vorinostat | | | NCT03117751 (p); 2017 | Dx ALL/LBL (with chemo) | II/III (R) | |
| | | | NCT01483690 (p, ya); 2011 | R/R ALL (with decitabine and chemo) | I/II (T) | Excessive toxicity * |
| | | NCT02553460 (p); 2015 | Dx ALL (with bortezomib and chemo) | II (R) | | |
| Methyltransferase inhibitors | DNA methyl-transferase activity | | | | | |
| 5-Azacitidine | | | NCT02551718 (p,a); 2015 | R/R acute leukemias | N/A (R) | |
| | | | NCT01861002 (p); 2013 | R/R ALL or AML (with chemo) | I (C) | |
| Decitabine | | | NCT02551718 (p, a); 2015 | R/R acute leukemias | N/A (R) | |
| | | | NCT01483690 (p, ya); 2011 | R/R ALL (with vorinostat and chemo) | I/II (T) | Excessive toxicity * |
| | | | NCT00349596 (p, a); 2006 | R/R ALL | I (C) | |
| | | | NCT03132454 (ya, a); 2017 | R/R ALL or AML (with palbociclib) | I (R) | |
| Proteasome inhibitors | | | | | | |
| Bortezomib | Rapid protein turnover | | NCT02518750 (p); 2015 | R/R T-ALL/LBL (with chemo) | II (T) | Slow accrual * |
| | | | NCT02553460 (p); 2015 | Dx ALL (with vorinostat and chemo) | I/II (R) | |
| | | | NCT02551718 (p, a); 2015 | R/R acute leukemias | N/A (R) | |
| | | | NCT00440726 (p); 2007 | R/R ALL (with chemo) | I/II (C) | |
| | | | NCT04224571 (p, ya); 2020 | R/R ALL (with chemo) | II (R) | |
| | | | NCT00873093 (p, a); 2009 | 1st relapse ALL/LBL (with chemo) | II (C) | Promising results for T-ALL (10) |
| | | | NCT02112916 (p, ya); 2014 | Dx T-ALL-LBL (with chemo) | III (A) | |
| | | | NCT03590171 (p); 2018 | R ALL (with chemo) | II (R) | |
| | | | NCT03117751 (p); 2017 | Dx ALL/LBL (with chemo) | II/III (R) | |
| | | | NCT03643276 (p); 2018 | Dx ALL (with chemo) | III (R) | |
| NAE inhibitor | | | | | | |
| Pevonedistat (MLN49243) | | | NCT03349281 (ya, a); 2017 | R/R ALL (with chemo) | I (R) | |

Table S1. Continued.

| Therapeutic agent | Target | Association with T-ALL subtype/ outcome | Trial identifier and year posted on clinicaltrials.gov | Tumor type | Phase/ status | Results |
|------------------------|----------------------|---|--|--------------------------------|---------------|------------------------|
| AURK inhibitors | AURK over expression | | | | | |
| Alisertib | | | NCT01154816 (p, ya); 2010 | R/R ALL, AML, and solid tumors | II (C) | Response rate <5% (11) |
| AT-9283 | | | NCT01431664 (p); 2011 | R/R acute leukemia | I (C) | No efficacy (12) |

List of clinical trials investigating the targeted agents described in this review. The clinical trials listed were chosen based on the following two selection criteria: the targeted drug investigated belongs to one of the categories of agents described in the text (modifiers of apoptosis, inhibitors of transcription regulation, signal transduction, cell cycle or immunotherapies) and the trial includes T-ALL patients.

* Source: <https://clinicaltrials.gov/>

Abbreviations: p= pediatric, ya= young adult, a= adults; ALL= acute lymphoblastic leukemia, LBL= lymphoblastic lymphoma, AML= acute myeloid leukemia, MDS= myelodysplastic syndrome, MM= multiple myeloma, Dx= newly diagnosed, R/R= refractory/relapsed; chemo= chemotherapy; dexa= dexamethasone; WT= wild-type; N/A= not applicable, R= recruiting, A= active, C= completed, T= terminated, NR= not yet recruiting.

SUPPLEMENTARY REFERENCES

1. Wilson WH, O'Connor OA, Czuczman MS, LaCasce AS, Gerecitano JF, Leonard JP, *et al.* Navitoclax, a targeted high-affinity inhibitor of BCL-2, in lymphoid malignancies: a phase 1 dose-escalation study of safety, pharmacokinetics, pharmacodynamics, and antitumour activity. *Lancet Oncol* **2010**;11(12):1149-59 doi 10.1016/S1470-2045(10)70261-8.
2. Papayannidis C, DeAngelo DJ, Stock W, Huang B, Shaik MN, Cesari R, *et al.* A Phase 1 study of the novel gamma-secretase inhibitor PF-03084014 in patients with T-cell acute lymphoblastic leukemia and T-cell lymphoblastic lymphoma. *Blood Cancer J* **2015**;5:e350 doi 10.1038/bcj.2015.80.
3. Cooper TM, Sison EAR, Baker SD, Li L, Ahmed A, Trippett T, *et al.* A phase 1 study of the CXCR4 antagonist plerixafor in combination with high-dose cytarabine and etoposide in children with relapsed or refractory acute leukemias or myelodysplastic syndrome: A Pediatric Oncology Experimental Therapeutics Investigators' Consortium study (POE 10-03). *Pediatr Blood Cancer* **2017**;64(8) doi 10.1002/pbc.26414.
4. Daver N, Bumber Y, Kantarjian H, Ravandi F, Cortes J, Rytting ME, *et al.* A Phase I/II Study of the mTOR Inhibitor Everolimus in Combination with HyperCVAD Chemotherapy in Patients with Relapsed/Refractory Acute Lymphoblastic Leukemia. *Clin Cancer Res* **2015**;21(12):2704-14 doi 10.1158/1078-0432.CCR-14-2888.
5. Place AE, Pikman Y, Stevenson KE, Harris MH, Pauly M, Sulis ML, *et al.* Phase I trial of the mTOR inhibitor everolimus in combination with multi-agent chemotherapy in relapsed childhood acute lymphoblastic leukemia. *Pediatr Blood Cancer* **2018**;65(7):e27062 doi 10.1002/pbc.27062.
6. Rheingold SR, Tasian SK, Whitlock JA, Teachey DT, Borowitz MJ, Liu X, *et al.* A phase 1 trial of temsirolimus and intensive re-induction chemotherapy for 2nd or greater relapse of acute lymphoblastic leukaemia: a Children's Oncology Group study (ADVL1114). *Br J Haematol* **2017**;177(3):467-74 doi 10.1111/bjh.14569.
7. Zwaan CM, Kowalczyk J, Schmitt C, Bielora B, Russo MW, Woessner M, *et al.* Safety and efficacy of nelarabine in children and young adults with relapsed or refractory T-lineage acute lymphoblastic leukaemia or T-lineage lymphoblastic lymphoma: results of a phase 4 study. *Br J Haematol* **2017**;179(2):284-93 doi 10.1111/bjh.14874.
8. Dunsmore KP, Winter SS, Devidas M, Wood BL, Esiashvili N, Chen Z, *et al.* Children's Oncology Group AALL0434: A Phase III Randomized Clinical Trial Testing Nelarabine in Newly Diagnosed T-Cell Acute Lymphoblastic Leukemia. *J Clin Oncol* **2020**;38(28):3282-93 doi 10.1200/JCO.20.00256.
9. Alexander TB, Lacayo NJ, Choi JK, Ribeiro RC, Pui CH, Rubnitz JE. Phase I Study of Selinexor, a Selective Inhibitor of Nuclear Export, in Combination With Fludarabine and Cytarabine, in Pediatric Relapsed or Refractory Acute Leukemia. *J Clin Oncol* **2016**;34(34):4094-101 doi 10.1200/JCO.2016.67.5066.
10. Horton TM, Whitlock JA, Lu X, O'Brien MM, Borowitz MJ, Devidas M, *et al.* Bortezomib reinduction chemotherapy in high-risk ALL in first relapse: a report from the Children's Oncology Group. *Br J Haematol* **2019**;186(2):274-85 doi 10.1111/bjh.15919.
11. Mosse YP, Fox E, Teachey DT, Reid JM, Safgren SL, Carol H, *et al.* A Phase II Study of Alisertib in Children with Recurrent/Refractory Solid Tumors or Leukemia: Children's Oncology Group Phase I and Pilot Consortium (ADVL0921). *Clin Cancer Res* **2019**;25(11):3229-38 doi 10.1158/1078-0432.CCR-18-2675.

12. Vormoor B, Veal GJ, Griffin MJ, Boddy AV, Irving J, Minto L, *et al.* A phase I/II trial of AT9283, a selective inhibitor of aurora kinase in children with relapsed or refractory acute leukemia: challenges to run early phase clinical trials for children with leukemia. *Pediatr Blood Cancer* **2017**;64(6) doi 10.1002/pbc.26351.

CHAPTER 5



Integrative phosphoproteomic analysis of T cell acute lymphoblastic leukemia xenografts reveals active signaling pathways and potential therapeutical targets

Valentina Cordo¹, Rico Hagelaar¹, Richard de Goeij-de Haas^{2,3}, Sander R. Piersma^{2,3}, Thang V. Pham^{2,3}, Koichi Oshima⁴, Adolfo A. Ferrando⁴, Frank N. van Leeuwen¹, Jean-Pierre Bourquin⁵, Jan Cools⁶, Rob Pieters¹, Connie R. Jimenez^{2,3,7}, and Jules P.P. Meijerink^{1,7,8}

¹ Princess Máxima Center for Pediatric Oncology, Utrecht, the Netherlands

² OncoProteomics Laboratory, Cancer Center Amsterdam, Amsterdam University Medical Centers, VU University, Amsterdam, the Netherlands

³ Department of Medical Oncology, Cancer Center Amsterdam, Amsterdam University Medical Centers, VU University, Amsterdam, the Netherlands

⁴ Institute for Cancer Genetics, Columbia University Medical Center, New York, NY, USA

⁵ Division of Oncology and Children's Research Center, University Children's Hospital Zurich, University of Zurich, Zurich, Switzerland

⁶ Center for Human Genetics, KU Leuven, Leuven, Belgium

⁷ These authors contributed equally

⁸ Present address: Acerta Pharma, Oss, The Netherlands

ABSTRACT

Tailored therapies are urgently needed for relapsed or refractory T-ALL patients that do not respond to conventional chemotherapy. Despite the extensive genetic knowledge of T-ALL, the paucity of targetable mutations and the lack of accurate response biomarkers have hampered the broad implementation of targeted drugs in the current treatment protocols. Here, we describe an *ex vivo* drug screening of 42 drugs, 10 conventional chemotherapeutic agents and 32 clinically relevant targeted agents, in a cohort of 47 T-ALL patient-derived xenografts (PDXs), including 11 matched diagnostic-relapse cases. Furthermore, we report targetable mutations identified by whole-exome sequencing and we present an unbiased, mass spectrometry-based, global phosphoproteomic profiling and microarray-based transcriptomic analysis of the 11 matched diagnostic-relapse PDX pairs. By integrating the results of the *ex vivo* drug screening with pathway enrichment analyses, inference of kinase activities, and analysis of differential phosphosites, we show that several signaling features are retained at relapse and we identify non-genomic leukemia vulnerabilities and determinants of sensitivity to kinase inhibitors.

INTRODUCTION

Acute lymphoblastic leukemia (ALL) is a hematological malignancy that results in aberrant proliferation of immature lymphocyte progenitors, and it is the most common form of cancer in children. The two major subtypes include B-cell precursor ALL (BCP-ALL) and T cell ALL (T-ALL), with the latter accounting for about only 15% of the total ALL cases. The overall survival (OS) for ALL has exceeded 90%. Nevertheless, both the 5-year and the 10-year OS for T-ALL patients are still notably lower [1] and have not improved in the last two decades [2], indicating the need for additional novel therapeutic interventions. The current standard treatment for T-ALL is a multi-agent, chemotherapeutic regimen. Patient are stratified based on minimal residual disease after the first two courses of conventional chemotherapy, with high-risk patient receiving the highest tolerated dosage and hematopoietic stem cell transplantation. Due to severe side effects that include organ toxicities and life-threatening or sometimes fatal infections [3], a further treatment intensification is impossible [3, 4]. Therefore, alternative, tailored approaches are urgently needed, especially for relapsed patients that frequently present a treatment-refractory disease [5].

Protein kinase inhibitors (PKI) are one of the most prominent targeted drugs in modern oncology. While Philadelphia chromosome-positive BCP-ALL patients can greatly benefit from the use of PKI like imatinib, dasatinib or ponatinib [1], currently no targeted drug or immunotherapy has been approved for the treatment of T-ALL patients yet [5].

Extensive gene expression analyses [6, 7] and genome sequencing studies [8, 9] have identified different T-ALL subtypes, uncovered developmental transcription factors as genetic drivers of disease, and highlighted the insurgence of secondary mutations that support leukemogenesis and survival (reviewed in [5, 10, 11]). *NOTCH1* mutations are the most frequent signaling mutations in T-ALL [8, 12]. Nevertheless, direct targeting of *NOTCH1* has shown disappointing results due to gastro-intestinal toxicities and insufficient efficacy (reviewed in [5, 13]). Other recurrent targetable mutations include the PI3K/AKT/mTOR axis [14], the RAS signaling pathway [15], and the IL7R-JAK-STAT signaling [16], with the latter being more frequent in the early T cell precursor (ETP)-ALL and TLX subtypes [8, 9, 17]. However, the actual prognostic value and the effective targetability of such mutations remain controversial [18]. T-ALL is a highly heterogeneous disease, with signaling mutations and rare targetable oncogenic fusions [19] like the *NUP214-ABL1* episomal amplification, mostly occurring in minor leukemic clones only [20]. Moreover, the selective pressure induced by the treatment can favor the acquisition of novel mutations that result in clones

selection and therapy resistance [21-23]. A comprehensive DNA and RNA sequencing study in a cohort of 309 pediatric cancer cases, including leukemia, identified actionable mutations in about 25% of the cases analyzed [24], indicating that genomics-guided therapy can benefit only a fraction of patients. Additional functional and molecular studies are needed to uncover early response biomarkers and relevant targets that would allow the enrolment of more patients into clinical trials. In the last years, functional molecular screenings that include *ex vivo* drug testing have highlighted that a few T-ALL cases are sensitive to small molecule-drugs, including the PKI dasatinib, in the absence of causative genomic abnormalities [25, 26]. Recently, we showcased the application of unbiased phosphoproteomic profiling for the identification of targetable kinases and for the design of combination therapies in T-ALL cell lines and *ex vivo* patient-derived xenografts (PDXs) [27].

Here, we describe an *ex vivo* drug screening of 42 drugs, comprising conventional chemotherapeutics and 32 clinically relevant targeted agents, in a cohort of 47 T-ALL PDXs, including 11 diagnostic-relapse paired samples, and we report targetable mutations identified by whole-exome sequencing (WES). Furthermore, we performed an unbiased, mass spectrometry-based, global phosphoproteomic profiling and microarray-based transcriptomic analysis in these 11 matched diagnostic-relapse T-ALL pairs to identify non-genomic vulnerabilities and determinants of sensitivity to small molecule-drugs. Our study shows that an integrative functional approach can complement genomic analyses, uncover active signaling pathways, and provides rational to extend the tailored therapeutic options for T-ALL.

MATERIALS AND METHODS

Generation of patient-derived xenografts

Leukemic blasts obtained from pediatric patients diagnosed with T-ALL were provided by the Children's Oncology Group (COG) or the Dutch Childhood Oncology Group (DCOG) upon signed informed consent and in accordance with the declaration of Helsinki. Animal experiments were approved by the Animal Welfare Committee of the Princess Máxima Center for pediatric oncology (Utrecht, the Netherlands) and were carried out at the animal facility of the Hubrecht Institute (Utrecht, the Netherlands) under specific pathogen-free conditions and in accordance with national regulations for animal welfare, FELASA (Federation of European Laboratory Animal Science Associations), ethical, and institutional guidelines. Mice were hosted in individually ventilated cages in groups of 2-3 mice per cage. Briefly, viably frozen human leukemic blasts were intravenously injected

into immunocompromised NOD/scid/Gamma (NSG) female mice of 8-10 weeks of age (Charles River, France). Mice were constantly monitored for leukemia development and disease burden was assessed by the percentage of detectable human CD45+ cells in the murine blood by tail vein cut and FACS analysis. Mice were sacrificed when presenting symptoms of leukemia (lack of grooming and activity, hunched back position, visible loss of weight) or when the circulating human CD45+ cells reached 50%. Human leukemic cells were isolated from the murine spleen using the Lymphoprep density gradient separation (STEMCELL technologies). Purified human cells were either immediately harvested for phosphoproteomic analyses or viably frozen until further usage.

Flow cytometry

Experiments were performed using the CytoFLEX LX (Beckman Coulter). For the identification of human leukemic blasts, single-cell suspensions obtained from the murine blood, spleen, bone marrow, and liver were stained with the anti-human CD45-Viogreen antibody (Miltenyi Biotec cat# 130-110-638) diluted 1:50 in autoMACS buffer (Miltenyi Biotec cat# 130-091-221) for 15 minutes on ice in the dark. Data analysis was performed using FlowJo v10.7.1 (FlowJo).

Phosphorylated peptide enrichment and mass spectrometry analysis

Human CD45+ leukemic blasts obtained from the murine spleen were immediately harvested after the Lymphoprep density gradient separation. Leukemic cells enrichment was analyzed via FACS and only samples with at least 90% human CD45+ cells were used for the phosphoproteomic profiling. Briefly, cells were spun down at 250 x g for 5 minutes, washed in cold PBS, spun down again, and harvested in 9 M urea/20 mM HEPES (pH 8) lysis buffer containing 1 mM sodium orthovanadate, 2.5 mM sodium pyrophosphate, and 1 mM β -glycerophosphate. Cell lysates were thoroughly vortexed at maximum speed for 30 seconds, snap-frozen in liquid nitrogen and stored at -80°C until further usage. Before the enrichment step, lysates were thawed, sonicated three times at 18-micron amplitude (30 seconds on/60 seconds off) using the MSE Soniprep 150 sonicator (MSE) on ice. Cleared lysates were diluted to a concentration of 2 mg/ml and 5 mg of protein input was used for each sample. Proteins were reduced with 2 mM DTT for 30 minutes at 55°C , alkylated using 5 mM iodoacetamide for 15 minutes at room temperature (RT) in the dark and eventually digested overnight with Sequencing Grade Modified Trypsin (Promega cat# V5111) at RT. Digested peptides were purified using OASIS HLB Cartridges (6 cc, 500 mg Sorbent, 60 μm particle size. Waters cat# 186000115) and lyophilized. Phospho-tyrosine peptides were enriched via immunoprecipitation (IP) using the PTMScan® Phospho-Tyrosine Rabbit

mAb (P-Tyr-1000) Kit (Cell Signaling Technology cat# 8803) according to the manufacturer protocol, using 4 μ l of bead slurry for each mg of protein input. Phospho-tyrosine peptides were eluted in 0.15% trifluoroacetic acid (TFA) and the unbound peptide fraction was used for complementary phospho-serine and phospho-threonine peptides capturing using custom-made TiO₂ C8-fitted tips. Eventually, eluted phosphorylated peptides were desalted using 20 μ l SDB-XC StageTips (prepared from Empore™ SPE Disks with SDB-XC, Sigma cat# 66884-U) prior to LC-MS analysis. For global protein expression analysis, 1 μ g of total lysate was subjected to liquid chromatography-mass spectrometry (LC-MS). LC-MS analyses were performed as previously described [27, 28]. Briefly, phosphopeptides were dried in a vacuum centrifuge and dissolved in 20 μ l 0.5% trifluoroacetic acid (TFA)/4% acetonitrile (ACN) prior to injection; 18 μ l was injected using partial loop injection. Peptides were separated by an Ultimate 3000 nanoLC-MS/MS system (Thermo Fisher) equipped with a 50 cm \times 75 μ m ID Acclaim Pepmap (C18, 1.9 μ m) column. After injection, peptides were trapped at 3 μ l/min on a 10 mm \times 75 μ m ID Acclaim Pepmap trap at 2% buffer B (buffer A: 0.1% formic acid (FA); buffer B: 80% ACN, 0.1% FA) and separated at 300 nl/min in a 10–40% buffer B gradient in 90 min (125 min inject-to-inject) at 35°C. Eluting peptides were ionized at a potential of +2 kVa into a Q Exactive HF mass spectrometer (Thermo Fisher). Intact masses were measured from m/z 350-1400 at resolution 120,000 (at m/z 200) in the Orbitrap using an AGC target value of 3E6 charges and a maxIT of 100 ms. The top 15 for peptide signals (charge-states 2+ and higher) were submitted to MS/MS in the HCD (higher-energy collision) cell (1.4 amu isolation width, 26% normalized collision energy). MS/MS spectra were acquired at resolution 15,000 (at m/z 200) in the Orbitrap using an AGC target value of 1E6 charges, a maxIT of 64 ms and an underfill ratio of 0.1%. This results in an intensity threshold for MS/MS of 1.3E5. Dynamic exclusion was applied with a repeat count of 1 and an exclusion time of 30 s. For peptide and protein identification, MS/MS spectra were searched against theoretical spectra from the UniProt complete human proteome FASTA file (release February 2019, 42,417 entries) using the MaxQuant 1.6.4.0 software [29] with the following settings: enzyme specificity= trypsin, missed cleavages allowed= 2, fixed modification= cysteine carboxyamidomethylation; variable modification= serine, threonine, and tyrosine phosphorylation, methionine oxidation, and N-terminal acetylation; MS tolerance= 4.5 ppm and MS/MS tolerance= 20 ppm. For both peptide and protein identifications, the false discovery rate was set at 1% for filtering using a decoy database strategy. The minimal peptide length was set at 7 amino acids, the minimum Andromeda score for modified peptides at 40, and the corresponding minimum delta score at 6. Moreover, the “match between runs” option was used to propagate the peptides identification across samples.

INKA analyses

Inference of highly active kinases from phosphoproteomic data was performed as previously described [27, 28]. Integrative iNferred Kinase Activity (INKA) scores are calculated based on 4 parameters: the sum of all phosphorylated peptides belonging to a kinase; the detection of the phosphorylated kinase activation domain (kinase-centric parameters), 3) the detection of known phosphorylated substrates and the presence of predicted phosphorylated substrates (substrate-centric parameters) [28, 30]. The latest version of the INKA pipeline is available online at <https://inkascore.org/>.

Whole exome sequencing

The 11 diagnostic-relapse paired patient samples had been sequenced in a previous study [31]. For the other diagnostic PDXs, human CD45+ leukemic blasts were purified from the murine spleen and enrichment for human cells was evaluated via FACS staining. Only samples containing more than 90% CD45+ cells were used for DNA extraction. In case of low enrichment, human CD45+ cells were positively selected using CD45 MicroBeads (Miltenyi cat# 130-045-801) according to the manufacturer's protocol, using 20 μ l of beads for 10×10^6 cells. DNA was extracted using the AllPrep DNA/RNA Micro Kit (QIAGEN, cat# 80284) or QIAamp DNA Mini Kit (QIAGEN, cat# 51304). Exome libraries were prepared using the KAPA HyperPrep kit (Roche) and the KAPA HyperExome kit (Roche). Paired-end sequencing was performed on an Illumina NovaSeq 6000 (Illumina) at 200x coverage. Reads were aligned to Hg38 using BWA [32] and duplicate reads were marked with Samtools 1.9 [33]. Variants were called using Mutect2 from GATK 4.2.0.0 [34]. Soft-clipped bases were skipped, whilst the rest of the settings were kept at default. Ensemble VEP 92 [35] was used to annotate the detected variants. Since no reference DNA was available for these samples, we performed a strict filtering to select causal variants and to reduce the number of false positives. The following filters were used: alternative read count (Alt.count) ≥ 75 , Variant Allele Frequency (VAF) ≥ 0.2 , predicted effect = high, biallelic genotype, and exclusion of variants present in the global SNPs collection from gnomAD 3.5 [36]. The list of recurrently mutated oncogenes in T-ALL was downloaded from Liu *et al.* [8] while the list of kinase-coding genes was downloaded from the KinBase database (<http://kinase.com/web/current/human/>). The oncoplots illustrating these mutations were generated using the R package Complexheatmap [37].

Microarray-based transcriptomics

Human CD45+ leukemic blasts were purified from the murine spleen and enrichment for human cells was evaluated via FACS staining. Human leukemic cells were positively

selected using CD45 MicroBeads (Miltenyi biotec cat# 130-045-801) according to the manufacturer's protocol, with a ratio of 20 μ l of beads for 10×10^6 cells. RNA was extracted using TRIzol Reagent (Thermo Fisher Scientific, cat #15596018), according to the manufacturer's protocol and as previously described [38]. Isolated RNA was purified using the EchoCLEAN RNA CleanUp Kit (BioEcho, cat# 020-002-050-050) following the manufacturer's protocol. Gene expression profiles were obtained using an Affymetrix HG-U133PLus2.0 array system as previously described [6]. Probe sets intensities were extracted from CEL files using the R package affy [39]. Probe sets intensities were normalized using the Robust Multichip Average (RMA) method [40].

Gene set enrichment analyses

Gene ontology enrichment analysis on differential protein expression at relapse (Supplementary Figure 3C) was performed with the online tool ShinyGO v0.75 (<http://bioinformatics.sdstate.edu/go/>) [41] using the entire proteomic expression dataset (N = 4176 proteins) as background, and with an FDR cutoff set at 0.05.

Gene Set Variation Analysis (GSVA) was performed as originally described by Hanzelmann and colleagues [42] using the R package GSVA (version 1.44.0). Normalized protein counts and RMA-normalized probe set values from the microarray dataset were used as input. GSVA analysis was performed using the *hallmarks of cancer* curated gene lists [43] (hallmark gene sets collection) or cell cycle-related pathways from the C2 collection obtained from the Molecular Signatures database (MsigDB, <https://www.gsea-msigdb.org/gsea/msigdb/>, version v7.5.1, updated January 2022).

Drug screenings

Cytotoxicity assays with single drugs were performed as previously described [16, 27]. Briefly, viably frozen human T-ALL blasts were cultured in RPMI1640+Glutamax medium supplemented with 20% fetal calf serum and antibiotics. Cells were treated with increasing concentrations of drugs (1nM–10 μ M range) in duplo and cell viability was assessed after 72 hours using the ATPLite assay (PerkinElmer). Cell survival was calculated in comparison to the vehicle only-treated control. The average cell doubling during the *ex vivo* screen was calculated comparing the intensity of the readout of untreated cells at the start of the assay (day 0) and after 72h in culture (day 3). Graphs were obtained using the GraphPad Prism 9.0.1 software (GraphPad Prism, nonlinear regression, inhibitor vs response; three parameters).

Statistical analyses

Statistical analyses were performed via either a paired or unpaired, two-sided Student's t-test using the GraphPad Prism 9.0.1 software (GraphPad Prism). The number of replicates and the exact p-values are indicated in the figure legends. For differential protein expression and phospho-site intensity, statistical analyses were performed using the R package limma [44].

RESULTS

Genomic mutations cannot fully explain drug sensitivity patterns in T-ALL

To study the applicability of small molecule inhibitors for the treatment of T-ALL, we performed an *ex vivo* drug screening on 36 diagnostic pediatric T-ALL patient-derived xenograft (PDX) samples. Additionally, for 11 diagnostic cases, a matched relapse PDX was obtained and included in the drug screening. A total of 42 drugs were tested on these 47 PDX samples, including standard chemotherapeutics, various kinase inhibitors, BH3-mimetics, proteasome inhibitors, and epigenetic drugs as listed in **Supplementary Table 1** and illustrated in **Figure 1A**. While the response to standard chemotherapeutics showed different degrees of sensitivity, the response to small molecule-inhibitors uncovered higher sensitivity for defined subsets of T-ALL samples, while most of the remaining cases remained insensitive. A subgroup of T-ALL xenografts showed sensitivity to the kinase inhibitor dasatinib (14/47 PDXs, ED50 < 100 nM). Interestingly, the sample PDX_8173 showed sensitivity (ED50 < 100 nM) to the MEK inhibitor selumetinib both in the diagnostic and relapse PDXs, while for another case (PDX_11451), only the relapse sample responded to selumetinib while its diagnostic counterpart (PDX_11451_D) was completely resistant to the MEK inhibitors (**Figure 1A**). These results indicate the possibility of a tailored approach for subsets of T-ALL cases. In general, all the T-ALL PDXs tested showed high sensitivity (ED50 < 100 nM) to the proteasomal inhibitor bortezomib. Moreover, 32 out of 47 T-ALL cases responded to the BET inhibitor BMS986158 (ED50 < 100 nM), the XPO1 inhibitor KPT-8600 (31/47 PDXs, ED50 < 100 nM), the CDK7 inhibitor AZD457 (35/47 PDXs, ED50 < 100 nM), and the BCL2/BCL-XL inhibitor navitoclax (38/47 PDXs, ED50 < 100 nM).

To identify possible biomarkers of response to these clinically relevant drugs, we analyzed the presence of somatic mutations that could explain the sensitivity to targeted inhibitors. In particular, to evaluate the potential applicability of protein kinase inhibitors (PKIs) for the treatment of T-ALL, we first analyzed the occurrence and the frequencies of genomic somatic mutations in kinase-coding genes (N = 538) in our PDX cohort as illustrated

in **Figure 1B**. Except for two PDXs (PDX-023 and PDX_8711_R), which carried several mutations in kinase-coding genes, most of the mutations occurred exclusively in only one sample. Mutations in genes coding for pharmacologically targetable kinases included *IGF1R* (2/46), but for both of these samples the *IGF1R* mutations did not confer increased sensitivity to the INSR/IGF-1R inhibitor BMS-754807 *ex vivo* (**Supplementary Figure 1A**). *JAK3*-mutations were observed in 3 PDX samples that includes both the diagnostic and matched relapse PDX for patient 8173 (PDX_8173_Dx and PDX_8173_Rel, as well as for sample PDX-016). These samples demonstrated high sensitivity to the JAK inhibitor ruxolitinib, the MEK inhibitors selumetinib and the BCL-2 inhibitor venetoclax (**Supplementary Figure 1B**). We then extended the analysis of mutations in kinase coding-genes using a previously published dataset that includes whole exome sequencing of 175 ALL patients (46 T-ALL, 129 B-ALL) [31]. Somatic mutations were described in 12 recurrently mutated kinase-coding genes (*ABL1*, *JAK1*, *JAK2*, *JAK3*, *SGK223*, *EPHA3*, *FLT3*, *MUSK*, *ERBB3*, *MAP3K7*, *BRAF*, and *FRK*) in the whole ALL dataset as illustrated in **Supplementary Figure 1C**. When looking at the T-ALL cases, only eight kinase-coding genes were affected by somatic mutations. The top three mutated genes were *JAK3* (8%), *JAK1* (7%), and the pseudo kinase *SGK223* (5%), with a higher incidence of mutations at relapse, as shown in **Supplementary Figure 1D**. Moreover, only one chimeric transcript involving a kinase (*NUP214--ABL1*) was detected in the T-ALL dataset analyzed [31]. This analysis indicates that the occurrence of (targetable) aberrations involving kinase coding-genes is notably low in T-ALL.

We then looked for mutations in known T-ALL oncogenes [8] in our PDX cohort as illustrated in the oncoplots in **Figure 1C**. Among the mutations found, the only lesions that can be potentially targeted by small molecule-inhibitors affected *NOTCH1* (16/47), *FBXW7* (4/47), *JAK3* (3/47), *JAK1* (3/47), *NRAS* (3/47), *PIK3CA* (2/47), *KIT* (1/47), *TP53* (1/47), and *ABL1* (1/47). Two out of three *NRAS*-mutant cases (PDX-026 and PDX-028) showed higher sensitivity to the MEK-inhibitors. However, other PDXs were sensitive to the MEK inhibitors in the absence of such mutations (PDX_8711_R, PDX_11451_R, PDX-005, PDX-015, PDX-019; ED50 < 300 nM; **Figure 1A**).

Therefore, the paucity of actionable mutations in both kinases and driving oncogenes indicates that sensitivity to targeted treatments cannot be solely explained by genomic aberrations. Thus, to extend the usage of PKIs and targeted inhibitors for the treatment of T-ALL, additional approaches which can complement the genomic information offered by genomic sequencing should be preferred.

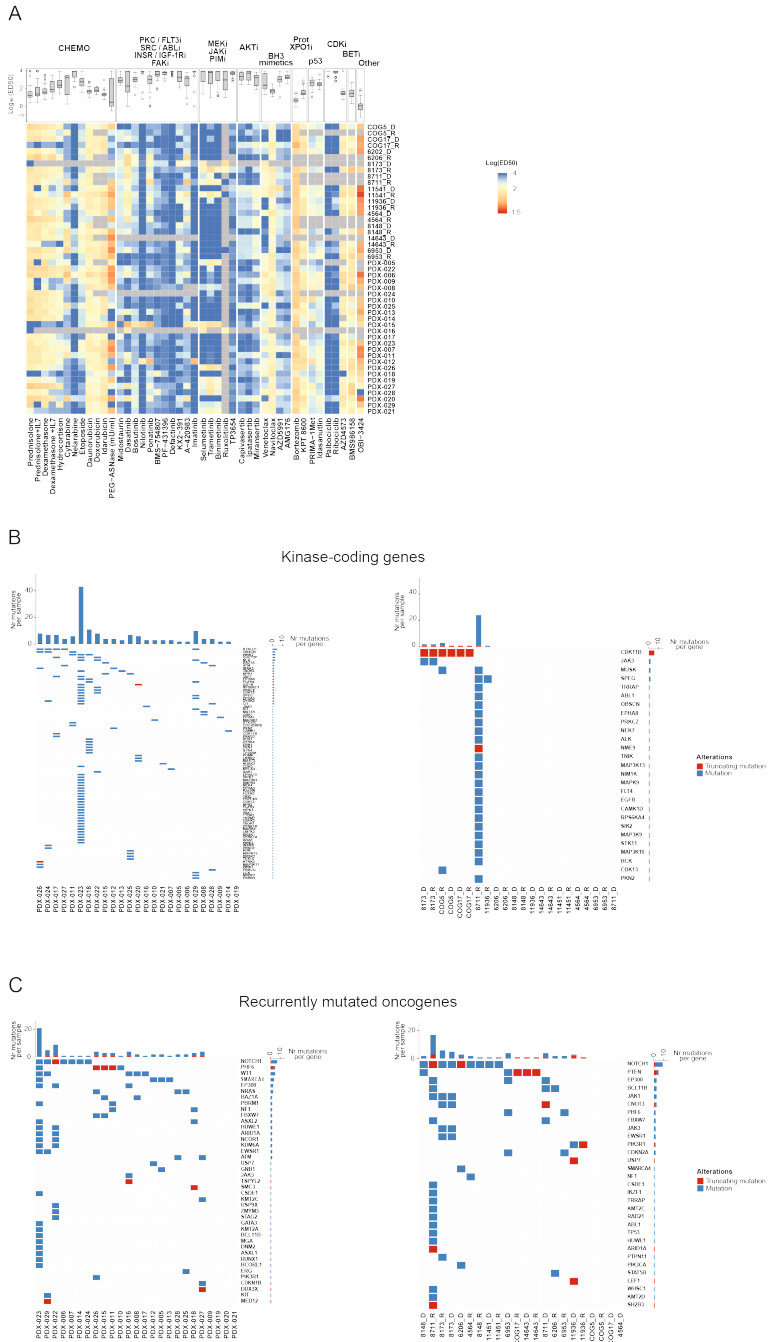


Figure 1. Ex vivo drug screening and mutational analysis of T-ALL xenografts. A) $\text{Log}_{10}(\text{ED}_{50})$ values of different drugs tested *ex vivo* for 72 hours. The boxplots represent the median $\text{Log}_{10}(\text{ED}_{50})$ for each drug in the PDX panel. B) Somatic mutations in kinase-coding genes. C) Somatic mutations in the most recurrently mutated oncogenes in T-ALL as described in Liu *et al.* [8]. Blue: mutation. Red: truncating mutation.



The overall proteome and transcriptome highlight inter-patient heterogeneity and maintenance of features at relapse

To explore the mechanisms of sensitivity to targeted inhibitors in T-ALL, we selected 11 matched diagnostic-relapse PDX samples, and we performed global, mass-spectrometry based proteomic and phosphoproteomic profiling to identify putative proteomic determinants of drug sensitivity or resistance to treatment. Additionally, we also performed microarray-based transcriptomic analysis to have a complete overview of gene and protein expression together with active signaling pathways, as illustrated in **Figure 2A**. A total of 4174 protein were detected in the entire proteomic dataset. Unsupervised clustering of all the identified proteins shows that the diagnostic-relapse paired samples from five patients clustered together, indicating that expression signatures are conserved from diagnosis to relapse in these cases, with a high inter-patient heterogeneity of the disease (**Supplementary Figure 2A**). Similarly, the unsupervised clustering of the whole microarray dataset which consists of more than 54,000 gene probes, also highlighted a close clustering of the diagnostic and the matched relapse sample for five out of 11 PDX couples, further indicating a conservation of gene expression patterns (**Supplementary Figure 2B**).

To evaluate common features that might be present at relapse, we searched for significantly different proteins between the diagnostic and relapse group. When comparing the total proteome of the diagnostic and the relapsed samples, we could identify 84 differentially expressed proteins ($p < 0.05$, $FC > 1.5$, **Supplementary Figure 3A**). In particular, the proteome of the relapsed PDXs highlighted an enrichment for proteins involved in mitochondrial activity with enhanced oxidative phosphorylation (**Supplementary Figure 3B and C**).

To have an overview of active pathways in T-ALL samples and to investigate whether selected gene expression and proteomic features might be retained at relapse, we performed Gene Set Variation Analysis (GSVA) [42] using the proteomic dataset. We evaluated the activation of the main cancer-related signaling pathways in each sample using as background curated gene lists that represent the hallmarks of cancer [43]. **Figure 2B** illustrates the enrichment scores for the main hallmarks investigated. Unsupervised clustering of the enrichment scores did not show a clear separation between the diagnostic and the relapse group, with two diagnostic-relapse pairs clustering together (11451 and 11936). NOTCH1 signaling has a pivotal role during T-cell development and *NOTCH1* mutations can be detected in more than 70% of pediatric T-ALL cases at diagnosis [8]. The median enrichment score for the NOTCH_SIGNALING hallmark was not significantly

different in the diagnostic group compared to the relapse cases (**Figure 2C**). *NOTCH1*-mutated PDXs have a higher median enrichment score for this hallmark, ($p < 0.05$, **Figure 2D**). Nevertheless, the sample PDX_COG17_D has one of the highest NOTCH signaling enrichment scores (0.61) but does not present any mutation in *NOTCH1* or its regulator *FBXW7* (**Supplementary Figure 4A**). These results suggest that the activation of the NOTCH pathway cannot solely be explained by the presence of mutations in *NOTCH1* or *FBXW7*. We performed GSVA also on the microarray dataset, and the obtained NOTCH signaling enrichment scores showed a similar pattern of pathway activation, but with much lower absolute values (**Supplementary Figure 4A**). In addition, the GSVA highlighted a positive enrichment for the HEDGEHOG signaling hallmark in seven out of 22 samples (**Figure 2B**). Notably, the samples with the highest enrichment for this pathway (HEDGEHOG signaling enrichment score > 0.4) belong to the relapse group (**Figure 2E**) and only one of these HEDGEHOG-high samples (PDX_14643_R) presented a mutation in the HEDGEHOG pathway that involves the *GLI2* gene (E735K). Therefore, single sample enrichment analysis can highlight multiple active pathways whose activation seems not be caused by direct mutations. Furthermore, four out of five samples with a high NOTCH signaling enrichment score present a zero or negative enrichment score for the HEDGEHOG signaling hallmark. Similarly, both HEDGEHOG-high samples (PDX_11936_R and PDX_14643_R) have a negative enrichment score for NOTCH signaling (**Figure 2F** and **Supplementary Figure 4B**). The same trend of reciprocal pathway activation was found via GSVA on the transcriptome level but with lower absolute scores (**Supplementary Figure 4C**). These results indicate that the NOTCH and HEDGEHOG pathways seem to be active in a mutually exclusive manner and that the effect of the pathway activation seems to be more evident on the proteomic level.

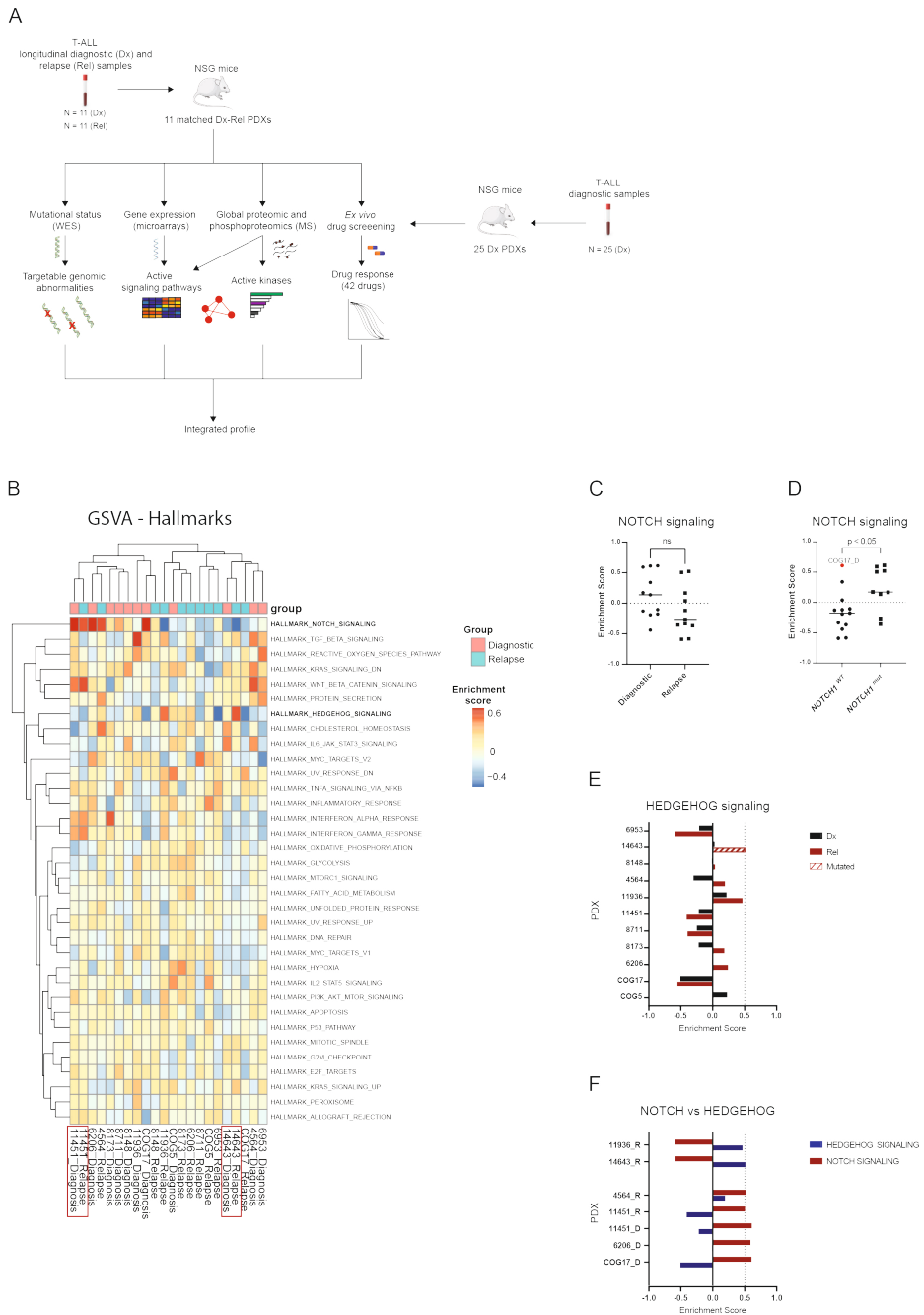


Figure 2. Proteomic analysis of active signaling pathways in T-ALL. A) Schematic overview of the workflow. For 11 matched diagnostic-relapse pairs, PDX models were derived and different downstream analyses were performed such as detection of somatic mutations via whole-exome sequencing [31], microarray-based transcriptomic analysis, proteome analysis, phosphoproteomic profiling for the prediction of active kinases and pathways, and ex vivo drug screenings. Moreover, an additional

PDX cohort of 25 diagnostic samples was used to extend the *ex vivo* drug screenings and the analysis of targetable mutations. B) Gene Set Variation Analysis (GSVA) performed using the proteomic expression data as described by Hanzelmann *et al.* [42], using as background curated lists of genes that represent the main hallmarks of cancer [43]. The heatmap represents the unsupervised clustering of the single-sample enrichment scores. Pink: diagnostic sample. Light Blue: relapse sample. C) Dot-plot of the enrichment scores for the NOTCH signaling hallmark in both diagnostic and relapse samples. ns: not significant (paired t-test, $p > 0.05$). The horizontal line indicates the median. D) Dot-plot of the enrichment scores for the NOTCH signaling hallmark in both *NOTCH1*-wild type (WT) and *NOTCH1*-mutated PDXs (unpaired t-test, $p < 0.05$). The horizontal line indicates the median. E) Bar plot illustrating the GSVA enrichment scores for the hallmark HEDGEHOG signaling. Black: diagnostic sample. Red: relapse sample. Striped pattern: mutation in the HEDGEHOG pathway. F) Bar plot illustrating the GSVA enrichment scores for the hallmarks NOTCH and HEDGEHOG signaling in selected PDXs. Blue: HEDGEHOG signaling score. Red: NOTCH signaling score.

Analysis of the phosphoproteome confirms the maintenance of signaling characteristics at relapse

To get further insights into the relevant signaling pathways and kinases that are activated in T-ALL, we performed an unbiased phosphoproteomic profiling of the 11 longitudinal PDX couples. In particular, we performed a phospho-tyrosine immunoprecipitation that yielded a total of about 1750 phosphopeptides and over 1300 phosphosites, and a complementary titanium dioxide (TiO₂) enrichment that allowed the identification of about 8000 phosphopeptides and 7600 phosphosites belonging to a total of 4174 proteins. Similar to the proteome and microarray data, unsupervised clustering of the two phosphoproteomic dataset shows that samples belonging to the same patient to cluster together for eight out 11 cases (**Supplementary Figure 5A-B**). These results indicate that inter-patient differences in the overall phosphorylation can be larger than the intra-patient (diagnostic and relapse samples from the same case) differences.

To have an overview of active kinases, we used the Integrative iNferred Kinase Activity (INKA) pipeline [27, 28] to infer kinase activity in each PDX sample. INKA analysis gives a numerical score to each detected kinase as proxy for its activity based both on the phosphorylation of the kinase itself and on the presence of phosphorylated substrates.

Supplementary Figure 6 illustrates the bar plots with the top20 kinases in each sample for the phospho-tyrosine dataset while the bar plots obtained from the TiO₂ datasets are illustrated in **Supplementary Figure 7**. **Figure 3A** and **3B** provide an overview of all the detected kinases in the diagnostic-relapse PDX panel. Overall, among the tyrosine-kinases, all the PDXs showed activation of several Src-family kinases (LCK, SRC, FYN, YES1, ABL1) but remarkably three out 22 samples (PDX_COG5_Dx, PDX_COG17_R, and PDX_8173_Rel) presented active LYN, a Src-family member usually expressed and activated in B lymphocytes and myeloid cells (**Figure 3A**). We then looked for tyrosine kinases that were activated only in specific samples to possibly find biomarkers of response

to targeted agents. High activation of JAK kinases (JAK1, JAK2, JAK3) was found only in the PDX_8173_Dx sample and was retained in the matched relapse case (PDX_8173_R) as depicted in **Figure 3A** and **3C**. The PDX_COG5 diagnostic-relapse sample pair also presented activation of JAK2 but with a much lower INKA score (**Supplementary Figure 6**). Interestingly, both PDX_8173_Dx and PDX_8173_R presented an activating mutation in *JAK3* (M511I, **Figure 1B-C**) and an additional *JAK1* mutation (A723D). Moreover, the presence of these mutations correlated not only with high JAK kinase activity but also sensitivity to the kinase inhibitor ruxolitinib (**Supplementary Figure 1B**).

Activation of the INSR/IGF-1R was detected in six out of 22 samples in the absence of any *INSR* or *IGF1R* mutations, with the highest scores in the matched samples of patient 11451 (**Figure 3D** and **3E**). Nevertheless, no samples within the matched diagnostic-relapse series showed sensitivity to the single treatment with the INSR/IGF-1R inhibitor BMS-754807 (**Figure 1A** and **Figure 3E**). AKT activation was detected in almost every PDX sample (**Figure 3B** and **3E**, and **Supplementary Figure 6**) in the absence of *AKT* mutations, while only five out of 22 samples carried a *PTEN* alteration (**Figure 3E**). Among the *PTEN*-mutated PDXs, only one PDX (PDX_COG17_R) showed high sensitivity to all three AKT inhibitors tested (capivasertib, ipatasertib, and miransertib; **Figure 3E**). We and other previously demonstrated that active INSR/IGF-1R signaling results in downstream AKT activity [27, 45]. Both the diagnostic and the relapse samples of patient 11451, which had the highest INKA scores for INSR/IGF-1R, showed active AKT (**Figure 3D**). Interestingly, the INSR-high samples PDX_11451_Dx and the matched relapse also showed high sensitivity to all the three AKT inhibitors in the absence of any signaling mutations (**Figure 3E**). Taken together, our results highlight that kinase activation patterns can be maintained at relapse and that sensitivity to AKT inhibitors can correlate with activation of INSR/IGF-1R in the absence of any other causing signaling mutation.

Integrative phosphoproteomic profiling of T-ALL xenografts

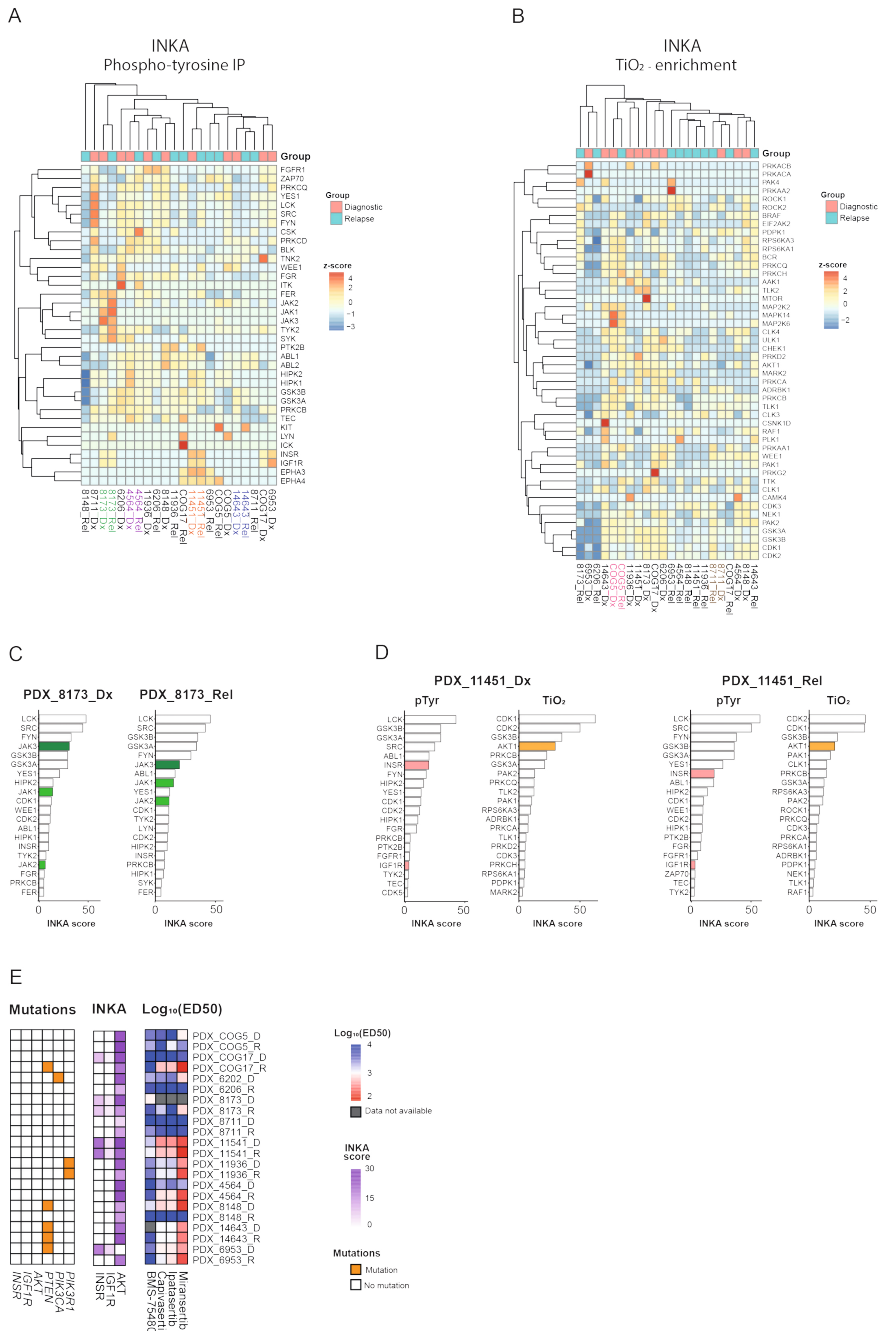


Figure 3. INKA-based overview of active kinases in T-ALL. A) Unsupervised clustering of the INKA scores obtained from the phospho-tyrosine IP dataset. Pink: diagnostic sample. Light Blue: relapse sample. B) Unsupervised clustering of the INKA scores obtained from the titanium dioxide (TiO₂) dataset. Pink: diagnostic sample. Light Blue: relapse sample. C) Bar plot illustrating the top20 active

kinases inferred from the phospho-tyrosine IP dataset in the matched sample PDX_8173 ranked on their INKA scores. Dark green: JAK3. Light green: JAK1 and JAK2. D) Bar plot illustrating the top20 active kinases inferred from both the phospho-tyrosine IP dataset and the TiO₂ dataset in the matched sample PDX_11451 ranked on their INKA scores. Pink: INSR and IGF1R. Orange: AKT. E) Presence of somatic mutations in PI3K/AKT and INSR-pathway genes, INKA scores for INSR, IGF1R, and AKT, and Log₁₀(ED50) values for INSR/IGF-1R inhibitor (BMS-754807) and AKT inhibitors (capivasertib, ipatasertib, miransertib). Grey: data not available. White: gene not mutated. Orange: gene with somatic mutation

Cell proliferation and cell cycle can correlate with sensitivity to dasatinib treatment

To identify additional signaling features that can explain the *ex vivo* drug sensitivity to kinase inhibitors, we looked for changes in sensitivity to kinase inhibitors in the matched diagnostic-relapse cohort. Most of the PDXs showed *ex vivo* sensitivity to the kinase inhibitor dasatinib (**Figure 1A**). However, for three diagnostic-relapse couples, the response to dasatinib drastically changed at relapse compared to diagnosis. In particular, while the diagnostic PDX_COG5_D showed a complete resistance to dasatinib (ED50 > 10 μ M), the matched relapse sample (PDX_COG5_R) showed some response to the treatment albeit at a high drug dosage (ED50 \sim 800 nM). Moreover, for two longitudinal couples, PDX_6953 and PDX_COG17, the diagnostic samples showed high sensitivity to dasatinib (ED50 \sim 100 nM) but the matched relapse cases became completely resistant to the drug (ED50 > 10 μ M) as illustrated in **Figure 4A**. Therefore, we searched for possible common determinants of sensitivity and resistance in these two matched cases. Given the lack of any common mutation acquired at relapse for PDX_6953 and PDX_COG17 that could explain the acquisition of resistance to dasatinib, we analyzed the proteome and phosphoproteome to highlight any differential feature. The single sample GSVA analysis on the proteome and on the transcriptome (**Supplementary Figure 8A**) highlighted a common higher enrichment for hallmarks related to cell cycle (MITOTIC_SPINDLE, G2M_CHECKPOINT, and E2F_TARGETS) and MYC targets in the two dasatinib-sensitive samples, while the resistant ones had higher enrichment for the hallmark OXIDATIVE_PHOSPHORYLATION, as depicted in **Figure 4B**. An additional GSVA analysis using curated gene list for cell cycle-related pathways also showed a similar trend, with the dasatinib-sensitive samples presenting higher enrichment scores (**Supplementary Figure 8B**). Next, we looked for differences in kinase activation that could explain the longitudinal change in drug sensitivity. When comparing the INKA scores for the paired samples, we could find higher INKA scores for the cell cycle-related kinases CDK1 and CDK2 in the sample PDX_COG17_D (dasatinib-sensitive) compared to the matched relapse case that showed a resistant phenotype (PDX_COG17_R) as highlighted in **Figure 4C**. A similar trend, albeit less pronounced, could be found the PDX_COG5 couple (**Supplementary Figure 8C**). Subsequently, we searched for differential phosphosites connected with the change in drug sensitivity. Fifty-nine differential

phosphosites (FDR < 0.1) could be found in the TiO₂ dataset (**Figure 4D**). In particular, among the phosphosites highly detected only in the dasatinib-sensitive samples, three belonged to proteins involved in the cell cycle progression such as the elongation factor EIF4G1 and the cell division – cycle associated protein CDCA3 (**Figure 4D**). Furthermore, we analyzed the pTyr-IP phospho-dataset and while no consistent difference could be found in activation of the kinases primarily targeted by dasatinib in T-ALL (LCK, SRC, ABL1, FYN, YES1), for two resistant samples (PDX_COG17_R and PDX_COG5_D), activation of the myeloid Src-family kinase LYN was found (**Figure 4E** and **Supplementary Figure 8D**), while their sensitive counterparts (PDX_COG17_D and PDX_COG5_R) did not present any activity predicted for this kinase. Similarly, the resistant samples PDX_COG17_R and PDX_6953_R presented an increase in TEC activity (**Figure 4E** and **Supplementary Figure 8E**). Lastly, we looked for differential tyrosine-phosphosites related to the longitudinal change in sensitivity and only 10 phosphosites could be found (**Figure 4F**, FDR < 0.1), with resistant samples presenting a higher phosphorylation of DOK1, a docking protein involved in the regulation of receptor tyrosine signaling kinases. Interestingly, the dasatinib-sensitive samples presented higher phosphorylation of the surface glycoprotein CD5 (**Figure 4F**), an important player in the regulation of the T-cell receptor (TCR) signaling and a known LCK and FYN target.

In conclusion, our results show that an integrative analysis of different *omic* layers can highlight differential biological features and uncover non-genetic determinants of sensitivity to targeted inhibitors.

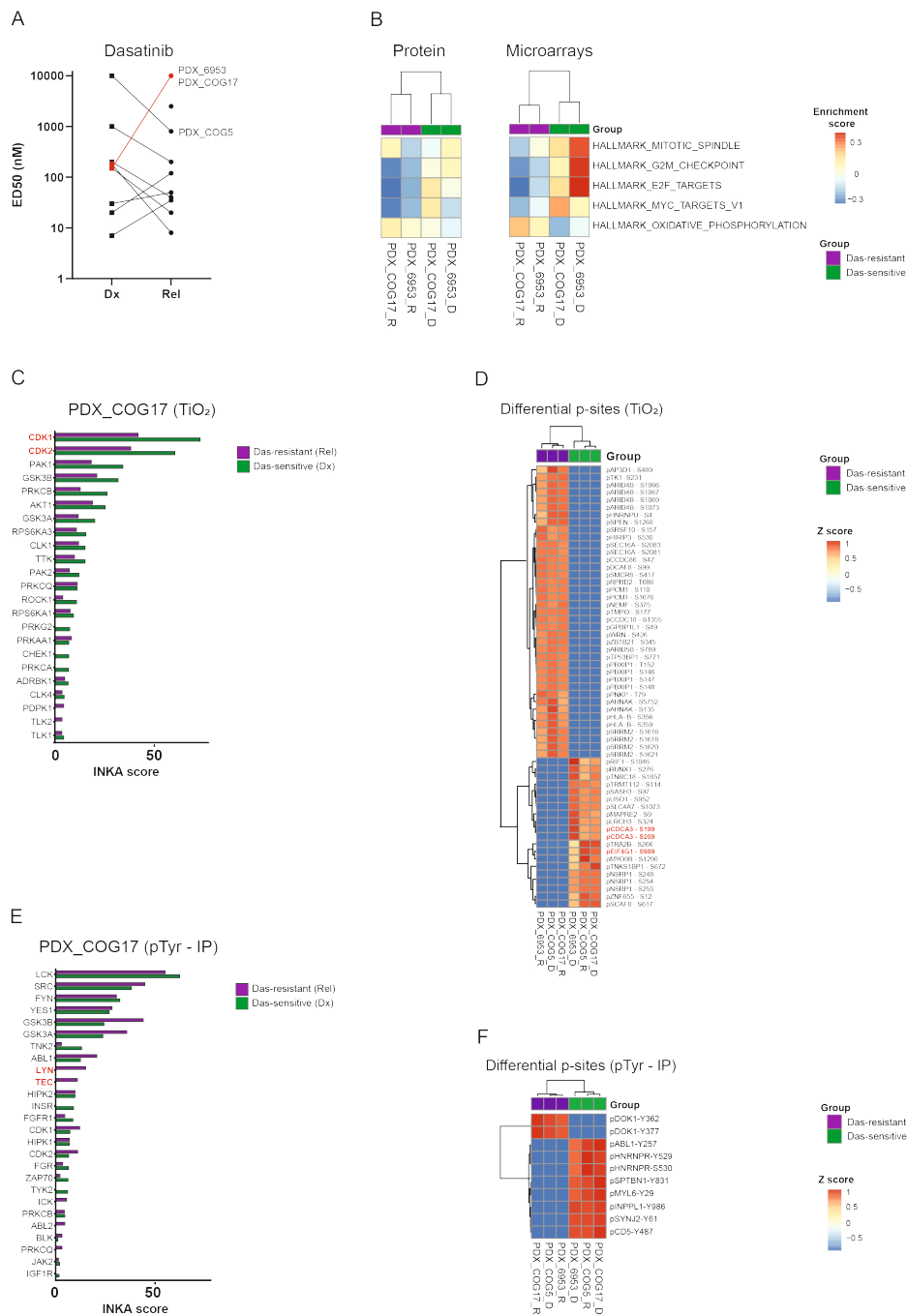


Figure 4. Cell cycle-related pathways can influence dasatinib sensitivity. A) ED50 values for dasatinib for 11 matched diagnostic (Dx) – relapse (Rel) samples after a 72h *ex vivo* drug screening. Red: PDX longitudinal samples with a change in dasatinib ED50 higher than two log-fold. B) Gene Set Variation Analysis (GSEA) performed using the proteomic expression data and the microarray-based

transcriptomic dataset as described by Hanzelmann *et al.* [42], using as background curated lists of genes that represent the main hallmarks of cancer [43]. The heatmap represents the unsupervised clustering of the single-sample enrichment scores for hallmarks that show a similar pattern in both datasets. Green: dasatinib-sensitive samples. Purple: dasatinib-resistant samples. C) Bar plot illustrating the top20 active kinases inferred from the TiO_2 dataset in the matched diagnostic-relapse sample PDX_COG17 ranked on their INKA scores. Green: dasatinib-sensitive sample (Dx). Purple: dasatinib-resistant sample (Rel). D) Differential phosphosites from the TiO_2 dataset (FDR < 0.1) in dasatinib-sensitive PDXs (green) and their matched dasatinib-resistant samples (purple). E) Bar plot illustrating the top20 active kinases inferred from the phospho-tyrosine IP (pTyr – IP) dataset in the matched diagnostic-relapse sample PDX_COG17 ranked on their INKA scores. Green: dasatinib-sensitive sample (Dx). Purple: dasatinib-resistant sample (Rel). F) Differential phosphosites from the phospho-tyrosine IP (pTyr – IP) dataset (FDR < 0.1) in dasatinib-sensitive PDXs (green) and their matched dasatinib-resistant samples (purple).

DISCUSSION

Tailored therapies are urgently needed for relapsed T-ALL patients that often suffer from a treatment-refractory disease. Despite the extensive knowledge on the genetics of T-ALL, the paucity of actionable mutations and the lack of accurate response biomarkers have hampered the use of targeted drugs for T-ALL patients. Recent clinical trials that include pediatric leukemia, highlight the need for a comprehensive tumor profiling to address the cancer complexity, identify targetable vulnerabilities and reliable biomarkers to guide the design of clinical trials [45, 46]. In particular, in the last few years, functional screenings including *ex vivo* drug testing, transcriptome analysis, and (phospho)proteomic profiling and have underscored the added value of an integrative approach for the identification of tumor vulnerabilities and therapeutical targets compared to a genomic only-driven approach [25, 46-49].

Phosphoproteomic profiling has had a pivotal role in the identification of targetable signaling networks in cancer, providing useful tools to uncover aberrant protein kinases that can be over expressed or aberrantly activated in the absence of any genomic defect in their coding genes [27, 50, 51]. Here, we presented an *ex vivo* drug screening of 42 drugs on a large panel of T-ALL xenografts and we integrated genomic mutations, protein expression, pathway enrichment analyses, and inference of kinase activity from phosphoproteomic data to uncover determinants of sensitivity to targeted agents. In particular, using 11 matched diagnostic – relapse PDXs, we highlight that several signaling features such as pathways activation and kinase activities are retained at relapse. PDXs are useful models since they allow the expansion of small human samples obtained via blood sampling or bone marrow biopsy. Woo and colleagues demonstrated that murine PDXs are evolutionary stable, highlighting that cancer cells engrafted in a murine host retained high fidelity to

the patient tumor of origin [52]. In particular, T-ALL xenografts present not only genomic stability but they also preserve the epigenetic [53] and the protein landscape [54] of their primary tumor.

Given the limited number of actionable DNA mutations in T-ALL patients in this and other studies [31], we focused our analysis on the proteome and phosphoproteome. Despite an elevated inter-patient heterogeneity, differential protein analysis highlighted a higher expression of protein involved in mitochondrial activity and oxidative phosphorylation at relapse compared to matched samples obtained at disease diagnosis. Interestingly, a recent study from Baran and colleagues demonstrated a fundamental role of oxidative phosphorylation for T-ALL cell survival and chemoresistance downstream of mutated *NOTCH1* [55], underscoring the role of metabolic reprogramming in favoring survival and drug resistance.

NOTCH1 activating mutations occur in nearly 70% of T-ALL patient at diagnosis and result in increased NOTCH1 activity. Gene set variation analysis performed at the proteome level uncovered an elevated NOTCH1 signaling even in the absence of activating *NOTCH1* mutations, indicating that aberrant signaling cannot be solely explained by genomic defects [56]. Moreover, activation of the NOTCH1 pathway and the HEDGEHOG signaling, another important pathway activated during T cell development and rarely mutated in T-ALL, seem to occur in a mutually exclusive way. Moreover, the pathway activation can change from diagnosis to relapse. This mutually exclusive pattern could be detected both at the proteome and at the transcriptomic level. The samples with the highest HEDGEHOG signaling enrichment belonged to the relapse group. Tosello and colleagues reported that under stress conditions like serum starvation, the HEDGEHOG pathway can be activated in T-ALL cells via stabilization of the transcription factor GLI1 [57]. Therefore, activation of the HEDGEHOG pathway at relapse may favor survival in unfavorable conditions such as limiting nutrients and oxygen that characterize the bone marrow microenvironment.

After analyzing the proteome, we provided an overview of the phosphoproteome of T-ALL. Moreover, we applied the INKA pipeline to infer kinase activity. While many kinases were active in the whole PDX panel (e.g., LCK, SRC, FYN, AKT, CDK1/2), selected kinases such as LYN, JAK3, and INSR were detected only in specific samples.

When integrating the presence of mutations in kinase-coding genes with elevated kinase activity, we could highlight that the presence of the activating *JAK3-M511I* mutation in the

PDX_8173_D sample resulted in elevated JAK3 activity and high sensitivity to the JAK inhibitor ruxolitinib. Notably, both the genetic mutation and the high JAK3 activity was retained in the matched relapse PDX.

We recently demonstrated that the INSR/IGF-1R axis can be activated in T-ALL in the absence of mutations in *INSR* or *IGF1R*, and that the signaling downstream the receptor converges on AKT [27]. Here, we confirmed the activation of INSR/IGF-1R signaling in a subset of T-ALL cases. In particular, the two matched diagnostic-relapse samples (PDX_11451) with the highest INSR score also showed sensitivity to three different AKT inhibitors, in the absence of mutations in *INSR*, *IGF1R*, *AKT*, *PIK3* or *PTEN*. These results underscore the added value of phosphoproteomic profiling and kinase activity inference for the identification of determinants of sensitivity to targeted treatments, particularly in the absence of actionable genomic lesions.

Lastly, we integrated the results of the *ex vivo* drug screening with pathway enrichment analysis, INKA scoring of active kinases, and analysis of differential phosphosites to identify determinants of change in sensitivity to the SRC-family kinase inhibitor dasatinib. In fact, for 3 longitudinal PDX couples, the cell sensitivity to dasatinib changed at relapse. Comparative analysis showed a higher enrichment for cell cycle-related pathways and higher CDK1/2 kinase activity in the dasatinib sensitive-samples compared to their matched resistant ones. Moreover, dasatinib sensitive PDXs presented high phosphorylation of the elongation factor EIF4G1 and the cell division-cycle associated protein CDCA3. Several studies reported an important role of the T cell receptor (TCR) signaling in LCK activation and dasatinib sensitivity [26, 58, 59] and in line with these results, we found an elevated phosphorylation of the surface protein CD5, a known target of LCK and FYN, and an important player in the activation of the TCR signaling, selectively in the dasatinib sensitive PDXs. Interestingly, ETP-ALL cases that do not respond to dasatinib [26], often show low or absent surface CD5 expression [60, 61].

In conclusion, our study provides a resource of *ex vivo* drug screens, a proteomic and a phosphoproteomic dataset of diagnostic and matched relapse T-ALL xenografts for the investigation of biological features underlining sensitivity and resistance to therapeutical agents. Furthermore, we highlight how the integration of transcriptomic, proteomic, and phosphoproteomic data can capture the leukemia complexity and uncover non-genetic determinants of drug sensitivity.

AUTHOR CONTRIBUTIONS

V.C. designed the study, designed and performed experiments, analyzed data, performed bioinformatic analyses, and wrote the manuscript. R.H. performed bioinformatic analyses. R.d.G.-d.H performed experiments. T.P. performed bioinformatic analyses. S.P. performed the mass spectrometry measurements and analyzed data. K.O, A.F., J-P.B., and J.C. provided samples. F.vL. and R.P. provided critical input and revised the manuscript. C.J. and J.M. supervised the study and wrote the manuscript.

ACKNOWLEDGEMENTS

The authors would like to thank the Children's Oncology Group (COG) for providing part of the pediatric T-ALL patient samples. This study was supported by the Dutch Cancer Society (KWF Kankerbestrijding, grant KWF2016_10355 to V.C.). Furthermore, Cancer Center Amsterdam and the Netherlands Organization for Scientific Research (NWO Middelgroot, grant #91116017) are acknowledged for the support of the mass spectrometry infrastructure.

REFERENCES

1. Teachey, D.T. and C.H. Pui, *Comparative features and outcomes between paediatric T-cell and B-cell acute lymphoblastic leukaemia*. *Lancet Oncol*, 2019. **20**(3): p. e142-e154.
2. Reedijk, A.M.J., et al., *Progress against childhood and adolescent acute lymphoblastic leukaemia in the Netherlands, 1990-2015*. *Leukemia*, 2021. **35**(4): p. 1001-1011.
3. van Binsbergen, A.L., et al., *Efficacy and toxicity of high-risk therapy of the Dutch Childhood Oncology Group in childhood acute lymphoblastic leukemia*. *Pediatr Blood Cancer*, 2022. **69**(2): p. e29387.
4. Inaba, H. and C.H. Pui, *Advances in the Diagnosis and Treatment of Pediatric Acute Lymphoblastic Leukemia*. *J Clin Med*, 2021. **10**(9).
5. Cordo, V., et al., *T-cell Acute Lymphoblastic Leukemia: A Roadmap to Targeted Therapies*. *Blood Cancer Discov*, 2021. **2**(1): p. 19-31.
6. Homminga, I., et al., *Integrated transcript and genome analyses reveal NKX2-1 and MEF2C as potential oncogenes in T cell acute lymphoblastic leukemia*. *Cancer Cell*, 2011. **19**(4): p. 484-97.
7. Ferrando, A.A., et al., *Gene expression signatures define novel oncogenic pathways in T cell acute lymphoblastic leukemia*. *Cancer Cell*, 2002. **1**(1): p. 75-87.
8. Liu, Y., et al., *The genomic landscape of pediatric and young adult T-lineage acute lymphoblastic leukemia*. *Nat Genet*, 2017. **49**(8): p. 1211-1218.
9. Zhang, J., et al., *The genetic basis of early T-cell precursor acute lymphoblastic leukaemia*. *Nature*, 2012. **481**(7380): p. 157-63.
10. Belver, L. and A. Ferrando, *The genetics and mechanisms of T cell acute lymphoblastic leukaemia*. *Nat Rev Cancer*, 2016. **16**(8): p. 494-507.
11. van der Zwet, J.C.G., et al., *Multi-omic approaches to improve outcome for T-cell acute lymphoblastic leukemia patients*. *Adv Biol Regul*, 2019. **74**: p. 100647.
12. Weng, A.P., et al., *Activating mutations of NOTCH1 in human T cell acute lymphoblastic leukemia*. *Science*, 2004. **306**(5694): p. 269-71.
13. Takebe, N., D. Nguyen, and S.X. Yang, *Targeting notch signaling pathway in cancer: clinical development advances and challenges*. *Pharmacol Ther*, 2014. **141**(2): p. 140-9.
14. Gutierrez, A., et al., *High frequency of PTEN, PI3K, and AKT abnormalities in T-cell acute lymphoblastic leukemia*. *Blood*, 2009. **114**(3): p. 647-50.
15. Irving, J., et al., *Ras pathway mutations are prevalent in relapsed childhood acute lymphoblastic leukemia and confer sensitivity to MEK inhibition*. *Blood*, 2014. **124**(23): p. 3420-30.
16. Li, Y., et al., *IL-7 Receptor Mutations and Steroid Resistance in Pediatric T cell Acute Lymphoblastic Leukemia: A Genome Sequencing Study*. *PLoS Med*, 2016. **13**(12): p. e1002200.
17. Cante-Barrett, K., et al., *MEK and PI3K-AKT inhibitors synergistically block activated IL7 receptor signaling in T-cell acute lymphoblastic leukemia*. *Leukemia*, 2016. **30**(9): p. 1832-43.
18. Burns, M.A., et al., *Identification of prognostic factors in childhood T-cell acute lymphoblastic leukemia: Results from DFCI ALL Consortium Protocols 05-001 and 11-001*. *Pediatr Blood Cancer*, 2021. **68**(1): p. e28719.
19. Steimle, T., et al., *Clinico-biological features of T-cell acute lymphoblastic leukemia with fusion proteins*. *Blood Cancer J*, 2022. **12**(1): p. 14.
20. Graux, C., et al., *Heterogeneous patterns of amplification of the NUP214-ABL1 fusion gene in T-cell acute lymphoblastic leukemia*. *Leukemia*, 2009. **23**(1): p. 125-33.

21. Tzoneva, G., et al., *Clonal evolution mechanisms in NT5C2 mutant-relapsed acute lymphoblastic leukaemia*. *Nature*, 2018. **553**(7689): p. 511-514.
22. Barz, M.J., et al., *Subclonal NT5C2 mutations are associated with poor outcomes after relapse of pediatric acute lymphoblastic leukemia*. *Blood*, 2020. **135**(12): p. 921-933.
23. Li, B., et al., *Therapy-induced mutations drive the genomic landscape of relapsed acute lymphoblastic leukemia*. *Blood*, 2020. **135**(1): p. 41-55.
24. Newman, S., et al., *Genomes for Kids: The Scope of Pathogenic Mutations in Pediatric Cancer Revealed by Comprehensive DNA and RNA Sequencing*. *Cancer Discov*, 2021.
25. Fris mantas, V., et al., *Ex vivo drug response profiling detects recurrent sensitivity patterns in drug-resistant acute lymphoblastic leukemia*. *Blood*, 2017. **129**(11): p. e26-e37.
26. Gocho, Y., et al., *Network-based systems pharmacology reveals heterogeneity in LCK and BCL2 signaling and therapeutic sensitivity of T-cell acute lymphoblastic leukemia*. *Nat Cancer*, 2021. **2**(3): p. 284-299.
27. Cordo', V., et al., *Phosphoproteomic profiling of T cell acute lymphoblastic leukemia reveals targetable kinases and combination treatment strategies*. *Nature Communications*, 2022. **13**(1): p. 1048.
28. Beekhof, R., et al., *INKA, an integrative data analysis pipeline for phosphoproteomic inference of active kinases*. *Mol Syst Biol*, 2019. **15**(4): p. e8250.
29. Tyanova, S., T. Temu, and J. Cox, *The MaxQuant computational platform for mass spectrometry-based shotgun proteomics*. *Nat Protoc*, 2016. **11**(12): p. 2301-2319.
30. van Alphen, C., et al., *Phosphotyrosine-based Phosphoproteomics for Target Identification and Drug Response Prediction in AML Cell Lines*. *Mol Cell Proteomics*, 2020. **19**(5): p. 884-899.
31. Oshima, K., et al., *Mutational and functional genetics mapping of chemotherapy resistance mechanisms in relapsed acute lymphoblastic leukemia*. *Nature Cancer*, 2020. **1**(11): p. 1113-1127.
32. Li, H. and R. Durbin, *Fast and accurate short read alignment with Burrows-Wheeler transform*. *Bioinformatics*, 2009. **25**(14): p. 1754-60.
33. Danecek, P., et al., *Twelve years of SAMtools and BCFtools*. *Gigascience*, 2021. **10**(2).
34. DePristo, M.A., et al., *A framework for variation discovery and genotyping using next-generation DNA sequencing data*. *Nat Genet*, 2011. **43**(5): p. 491-8.
35. McLaren, W., et al., *The Ensembl Variant Effect Predictor*. *Genome Biol*, 2016. **17**(1): p. 122.
36. Karczewski, K.J., et al., *The mutational constraint spectrum quantified from variation in 141,456 humans*. *Nature*, 2020. **581**(7809): p. 434-443.
37. Gu, Z., R. Eils, and M. Schlesner, *Complex heatmaps reveal patterns and correlations in multidimensional genomic data*. *Bioinformatics*, 2016. **32**(18): p. 2847-9.
38. Van Vlierberghe, P., et al., *The cryptic chromosomal deletion del(11)(p12p13) as a new activation mechanism of LMO2 in pediatric T-cell acute lymphoblastic leukemia*. *Blood*, 2006. **108**(10): p. 3520-9.
39. Gautier, L., et al., *affy--analysis of Affymetrix GeneChip data at the probe level*. *Bioinformatics*, 2004. **20**(3): p. 307-15.
40. Irizarry, R.A., et al., *Exploration, normalization, and summaries of high density oligonucleotide array probe level data*. *Biostatistics*, 2003. **4**(2): p. 249-64.
41. Ge, S.X., D. Jung, and R. Yao, *ShinyGO: a graphical gene-set enrichment tool for animals and plants*. *Bioinformatics*, 2020. **36**(8): p. 2628-2629.

42. Hanzelmann, S., R. Castelo, and J. Guinney, *GSVA: gene set variation analysis for microarray and RNA-seq data*. BMC Bioinformatics, 2013. **14**: p. 7.
43. Liberzon, A., et al., *The Molecular Signatures Database (MSigDB) hallmark gene set collection*. Cell Syst, 2015. **1**(6): p. 417-425.
44. Ritchie, M.E., et al., *limma powers differential expression analyses for RNA-sequencing and microarray studies*. Nucleic Acids Res, 2015. **43**(7): p. e47.
45. Langenberg, K.P.S., E.J. Looze, and J.J. Molenaar, *The Landscape of Pediatric Precision Oncology: Program Design, Actionable Alterations, and Clinical Trial Development*. Cancers (Basel), 2021. **13**(17).
46. Letai, A., P. Bhola, and A.L. Welm, *Functional precision oncology: Testing tumors with drugs to identify vulnerabilities and novel combinations*. Cancer Cell, 2022. **40**(1): p. 26-35.
47. Kornauth, C., et al., *Functional Precision Medicine Provides Clinical Benefit in Advanced Aggressive Hematologic Cancers and Identifies Exceptional Responders*. Cancer Discov, 2022. **12**(2): p. 372-387.
48. Malani, D., et al., *Implementing a Functional Precision Medicine Tumor Board for Acute Myeloid Leukemia*. Cancer Discov, 2022. **12**(2): p. 388-401.
49. Sengupta, S., et al., *Integrative omics analyses broaden treatment targets in human cancer*. Genome Med, 2018. **10**(1): p. 60.
50. Cutillas, P.R., *Role of phosphoproteomics in the development of personalized cancer therapies*. Proteomics Clin Appl, 2015. **9**(3-4): p. 383-95.
51. Doll, S., F. Gnad, and M. Mann, *The Case for Proteomics and Phospho-Proteomics in Personalized Cancer Medicine*. Proteomics Clin Appl, 2019. **13**(2): p. e1800113.
52. Woo, X.Y., et al., *Conservation of copy number profiles during engraftment and passaging of patient-derived cancer xenografts*. Nat Genet, 2021. **53**(1): p. 86-99.
53. Richter-Pechanska, P., et al., *PDX models recapitulate the genetic and epigenetic landscape of pediatric T-cell leukemia*. EMBO Mol Med, 2018. **10**(12).
54. Uzozie, A.C., et al., *PDX models reflect the proteome landscape of pediatric acute lymphoblastic leukemia but divert in select pathways*. J Exp Clin Cancer Res, 2021. **40**(1): p. 96.
55. Baran, N., et al., *Inhibition of mitochondrial complex I reverses NOTCH1-driven metabolic reprogramming in T-cell acute lymphoblastic leukemia*. Nat Commun, 2022. **13**(1): p. 2801.
56. Zuurbier, L., et al., *NOTCH1 and/or FBXW7 mutations predict for initial good prednisone response but not for improved outcome in pediatric T-cell acute lymphoblastic leukemia patients treated on DCOG or COALL protocols*. Leukemia, 2010. **24**(12): p. 2014-22.
57. Tosello, V., et al., *Responsiveness to Hedgehog Pathway Inhibitors in T-Cell Acute Lymphoblastic Leukemia Cells Is Highly Dependent on 5'AMP-Activated Kinase Inactivation*. Int J Mol Sci, 2021. **22**(12).
58. Shi, Y., et al., *Phase II-like murine trial identifies synergy between dexamethasone and dasatinib in T-cell acute lymphoblastic leukemia*. Haematologica, 2021. **106**(4): p. 1056-1066.
59. Laukkanen, S., et al., *Combination therapies to inhibit LCK tyrosine kinase and mTOR signaling in T-cell Acute Lymphoblastic Leukemia*. Blood, 2022.
60. Coustan-Smith, E., et al., *Early T-cell precursor leukaemia: a subtype of very high-risk acute lymphoblastic leukaemia*. Lancet Oncol, 2009. **10**(2): p. 147-56.
61. Arber, D.A., et al., *The 2016 revision to the World Health Organization classification of myeloid neoplasms and acute leukemia*. Blood, 2016. **127**(20): p. 2391-405.

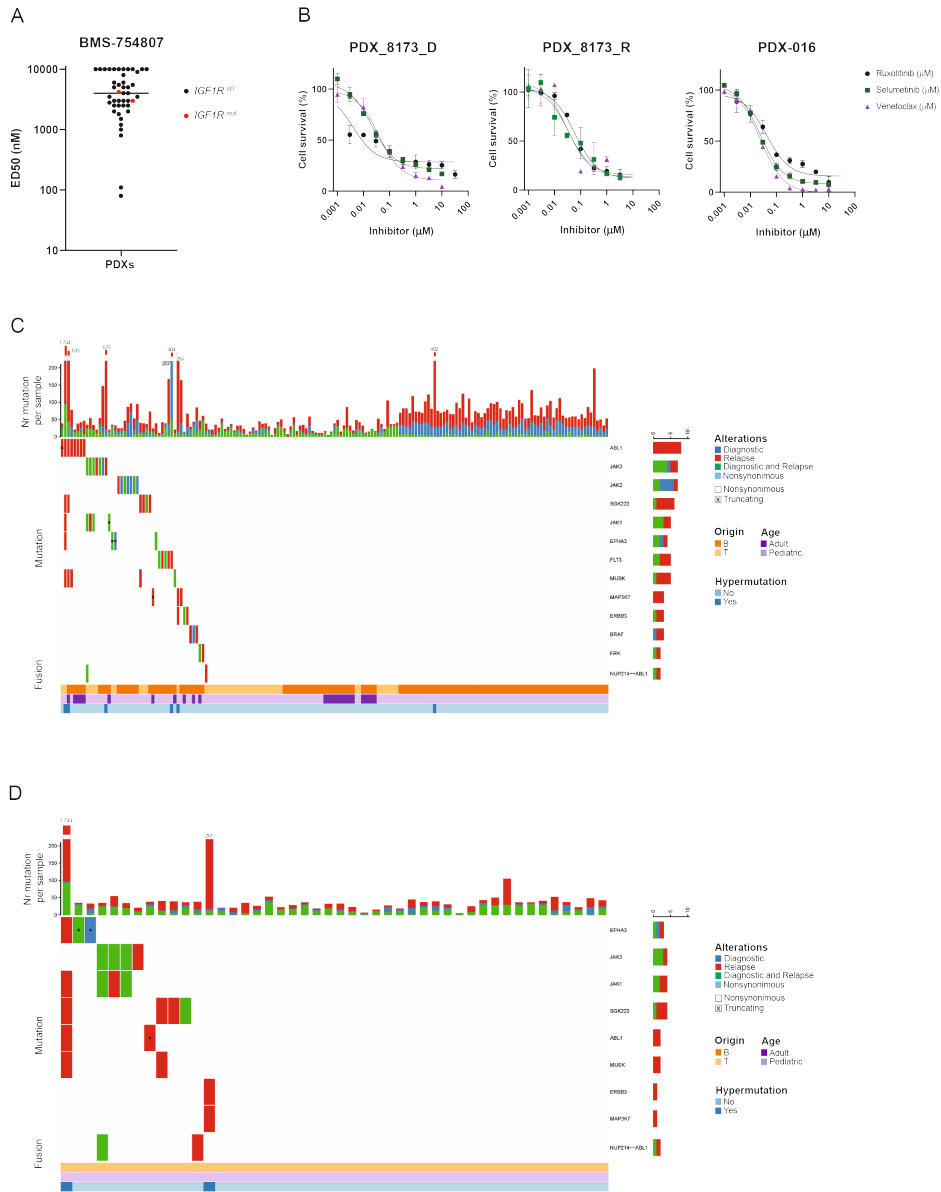
SUPPLEMENTARY DATA

Supplementary Table 1. Drugs used in this study.

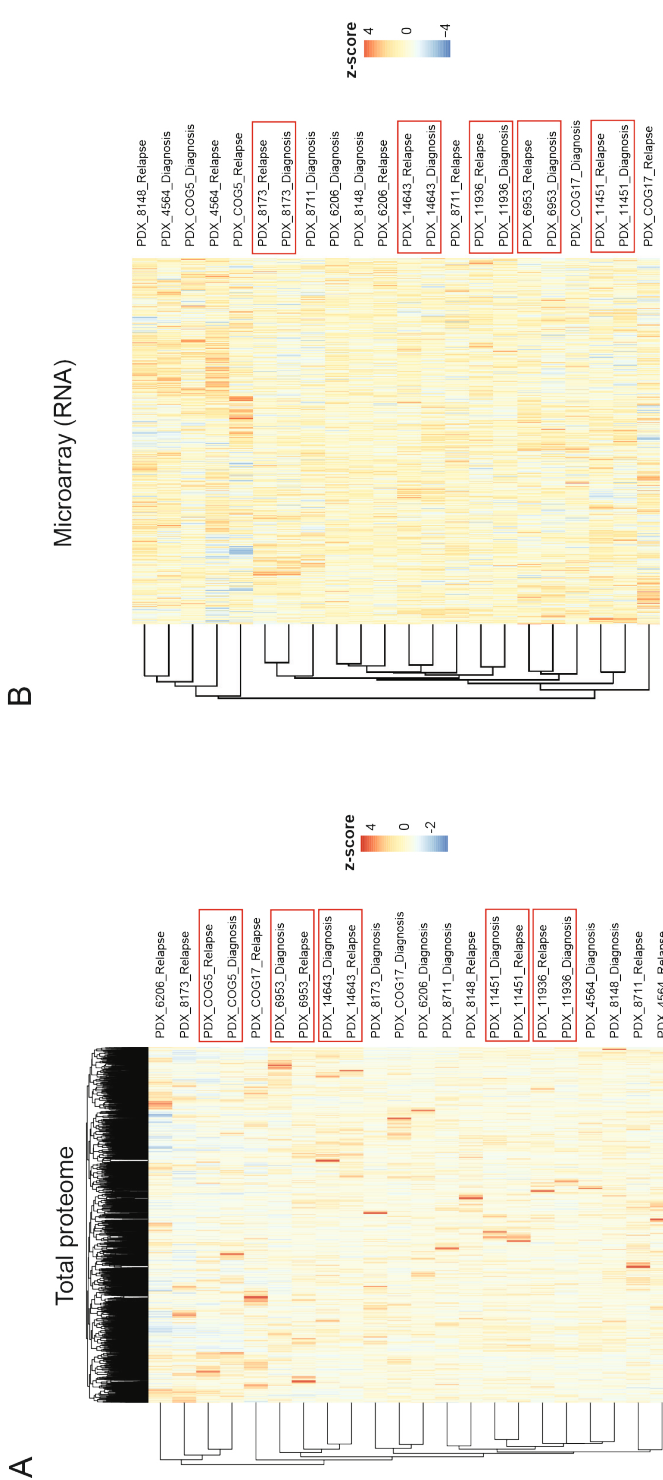
| Name | Category |
|-----------------------------|----------------------|
| Prednisolone | Chemotherapy |
| Dexamethasone | Chemotherapy |
| Hydrocortison | Chemotherapy |
| PEG-asparaginase (Oncaspar) | Chemotherapy |
| Cytarabine | Chemotherapy |
| Nelarabine | Chemotherapy |
| Etoposide | Chemotherapy |
| Daunorubicin | Chemotherapy |
| Doxorubicin | Chemotherapy |
| Idarubicin | Chemotherapy |
| Midostaurin | Kinase inhibitor |
| Dasatinib | Kinase inhibitor |
| Bosutinib | Kinase inhibitor |
| Nilotinib | Kinase inhibitor |
| Ponatinib | Kinase inhibitor |
| BMS-754807 | Kinase inhibitor |
| PF-431396 | Kinase inhibitor |
| Defactinib | Kinase inhibitor |
| KX2-391 | Kinase inhibitor |
| A-420983 | Kinase inhibitor |
| Imatinib | Kinase inhibitor |
| Selumetinib | Kinase inhibitor |
| Trametinib | Kinase inhibitor |
| Binimetinib | Kinase inhibitor |
| Capivasertib | Kinase inhibitor |
| Ipatasertib | Kinase inhibitor |
| Miransertib | Kinase inhibitor |
| Venetoclax | BH3-mimetic |
| Navitoclax | BH3-mimetic |
| AZD5991 | BH3-mimetic |
| AMG176 | BH3-mimetic |
| TP3654 | Kinase inhibitor |
| Bortezomib | Proteasome inhibitor |
| Ruxolitinib | Kinase inhibitor |
| BMS986158 | BET inhibitor |

Supplementary Table 1. Continued.

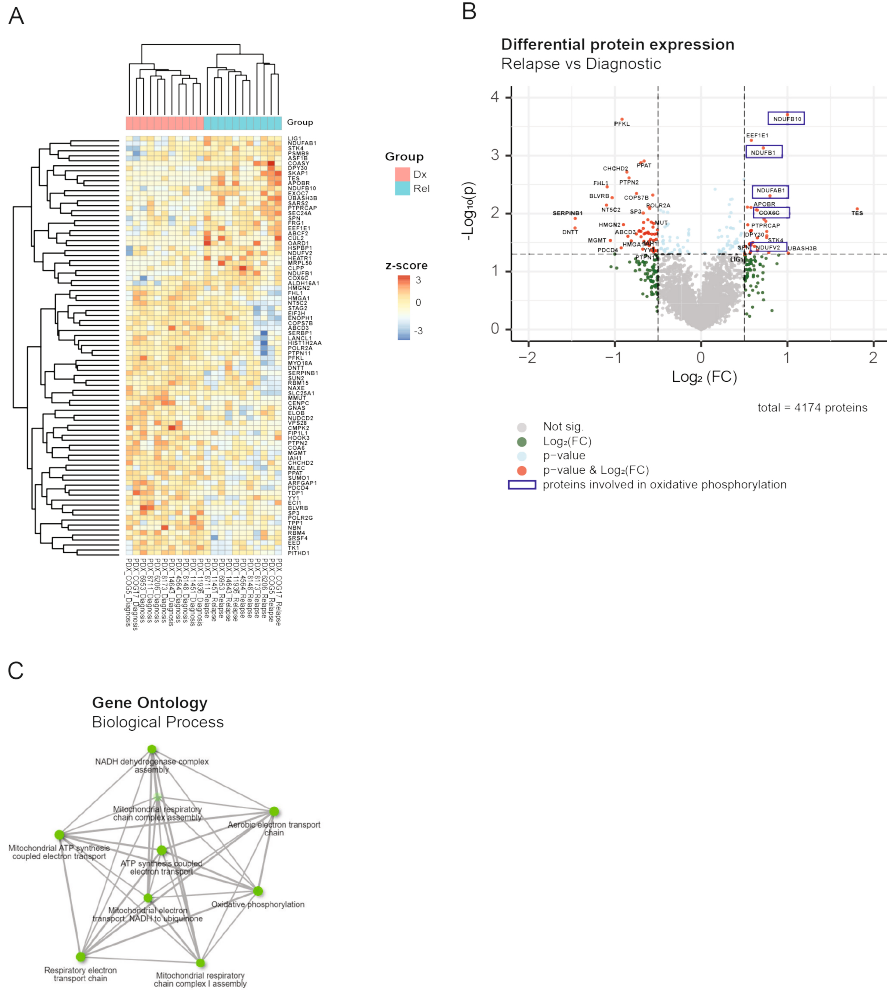
| Name | Category |
|-------------|--------------------------|
| PRIMA-1Met | p53 reactivator |
| Idasanutlin | MDM2 inhibitor |
| Palbociclib | Kinase inhibitor |
| Ribociclib | Kinase inhibitor |
| AZD4573 | Kinase inhibitor |
| KPT 8600 | XPO1 inhibitor |
| OBI-3424 | AKR1C3-activated prodrug |



Supplementary Figure 1. Ex vivo sensitivity to kinase inhibitors and somatic mutations in kinase-coding genes in T-ALL. A) Dot-plot of the ED50 values for the INSR/IGF-1R inhibitor BMS-754807. Red: *IGF1R*-mutant PDXs. B) Dose-response curves of the JAK inhibitor ruxolitinib (black), the MEK inhibitor selumetinib (green), and the BCL2 inhibitor venetoclax (purple) in three *JAK3*-mutated PDXs. C) The oncoplots illustrate the presence of gene fusions involving a kinase-coding gene (NUP214—ABL1) and somatic mutations detected in kinase-coding genes in 175 matched diagnostic-relapse ALL patient samples and D) 46 matched diagnostic-relapse T-ALL patient samples as reported in the dataset by Oshima and colleagues [1].

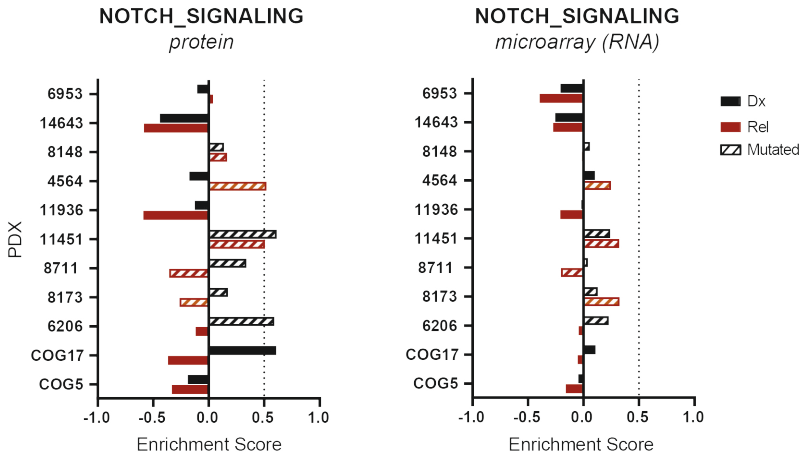


Supplementary Figure 2. Transcriptome and proteome overview of matched diagnostic-relapse T-ALL samples. A) unsupervised clustering of the whole proteomic dataset (4176 proteins). The red boxes highlight the close clustering of the matched diagnostic-relapse samples. B) unsupervised clustering of the whole microarray-based transcriptomic dataset (54,675 probes). The red boxes highlight the close clustering of the matched diagnostic-relapse samples.

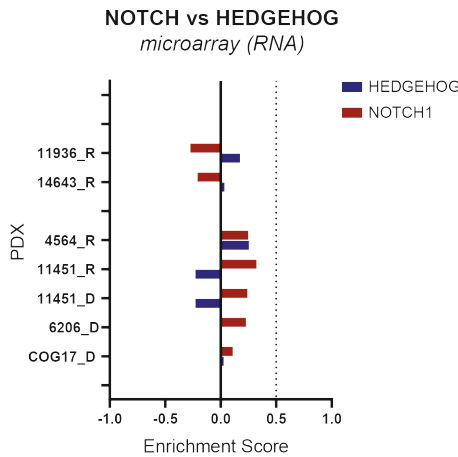


Supplementary Figure 3. Differential protein expression and signaling features. A) Supervised clustering of differentially expressed proteins ($p < 0.05$, $\log_2FC < 0.5$ or $\log_2FC > 0.5$) between the diagnostic and the relapse group. Pink: diagnostic sample. Light blue: relapse sample. B) Volcano plot of the supervised differentially expressed proteins ($p < 0.05$, $\log_2FC < 0.5$ or $\log_2FC > 0.5$) between the diagnostic and the relapse group. Blue box: proteins involved in oxidative phosphorylation. C) Gene ontology enrichment of biological processes of differentially expressed proteins with a higher expression at relapse ($p < 0.05$, $\log_2FC > 0.5$).

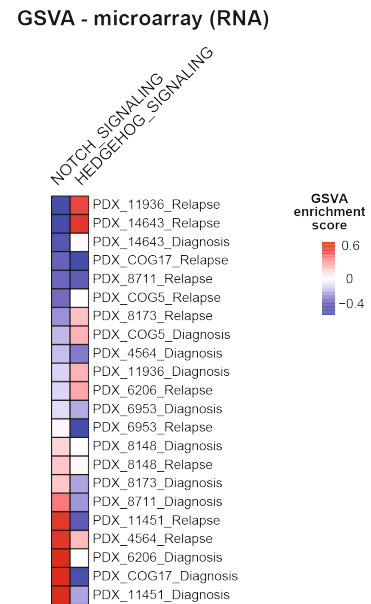
A



B

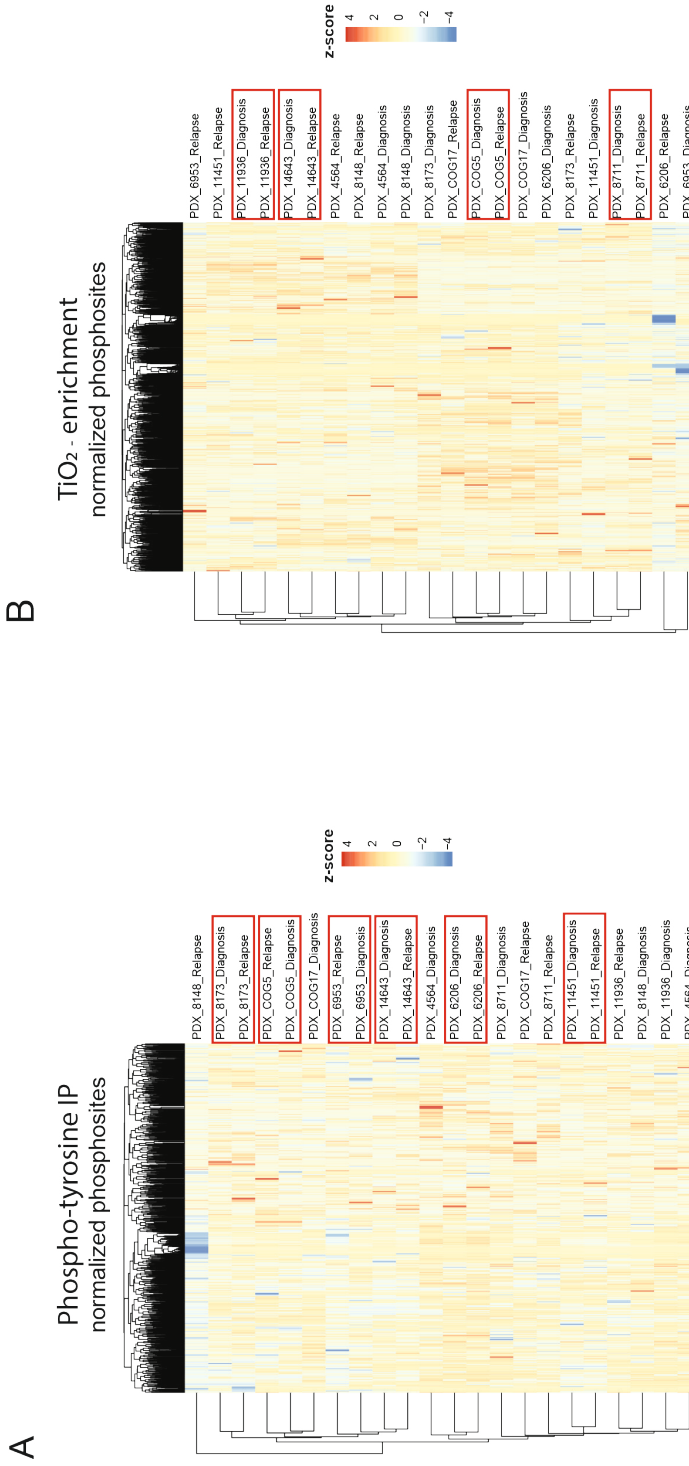


C



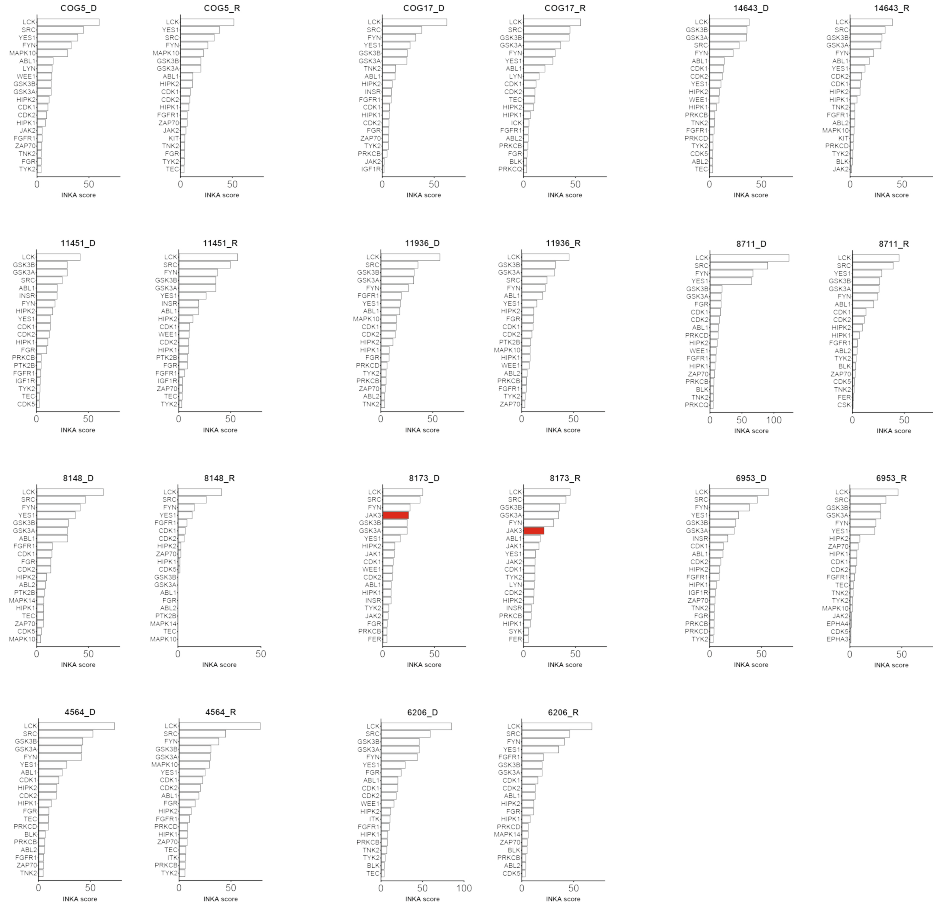
Supplementary Figure 4. GSVAs scores of NOTCH and HEDGEHOG pathways. A) Bar plot illustrating the GSVAs enrichment scores for the hallmark NOTCH signaling in both the proteomic and microarray datasets. Black: diagnostic sample. Red: relapse sample. Striped pattern: mutation in the NOTCH pathway (*NOTCH1*, *FBXW7*). B) GSVAs enrichment scores for the hallmarks NOTCH and HEDGEHOG signaling in 11 matched diagnostic-relapse PDX samples. C) Bar plot illustrating the GSVAs enrichment scores for the hallmarks NOTCH and HEDGEHOG signaling in selected PDXs using the microarray dataset. Blue: HEDGEHOG signaling score. Red: NOTCH signaling score.





Supplementary Figure 5. Unsupervised clustering of the phosphoproteomic datasets. A) Normalized intensities of phosphosites identified from the phospho-tyrosine immunoprecipitation (IP) and B) from TiO₂-enrichment. The red boxes highlight the close clustering of the matched diagnostic-relapse samples.

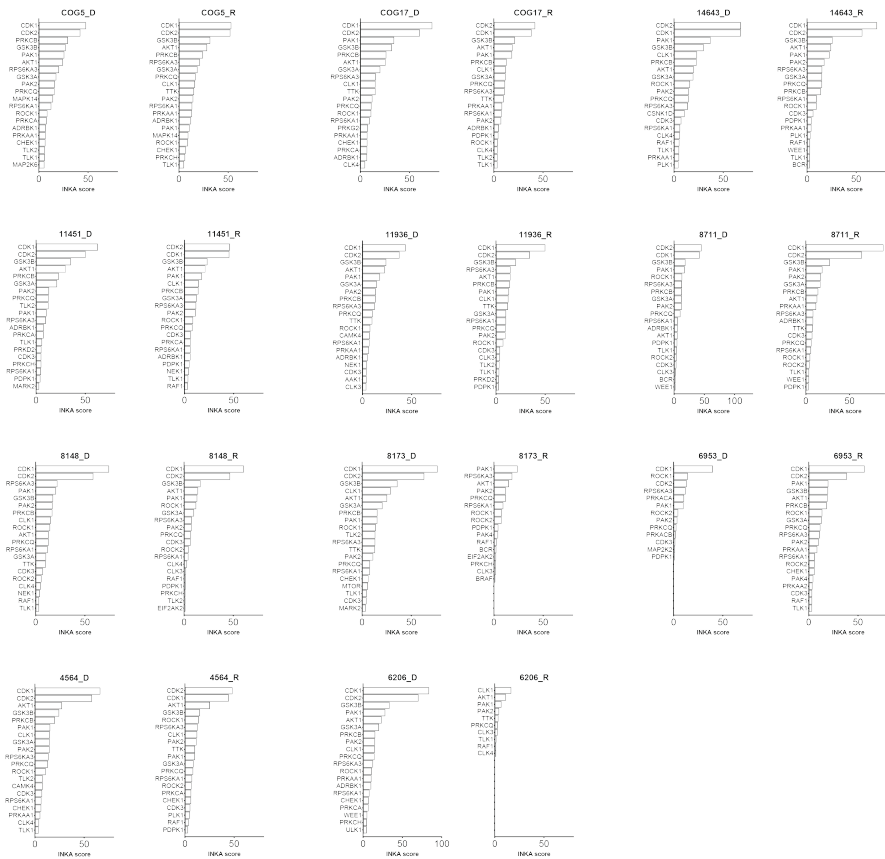
Top20 active kinases (phospho-tyrosine dataset)



Supplementary Figure 6. Single-sample INKA scores (phospho-tyrosine). Bar plot illustrating the top20 active kinases inferred from the phospho-tyrosine IP dataset in 11 matched diagnostic-relapse PDX samples, ranked on their INKA score. Red: JAK3



Top20 active kinases (TiO₂ dataset)



Supplementary Figure 7. Single-sample INKA scores (TiO₂). Bar plot illustrating the top20 active kinases inferred from the TiO₂ dataset in 11 matched diagnostic-relapse PDX samples, ranked on their INKA score.



Supplementary Figure 8. Cell cycle-related pathways can influence dasatinib sensitivity. A) Gene Set Variation Analysis (GSVA) performed using the proteomic expression data and the microarray-based transcriptomic dataset as described by Hanzelmann *et al.* [2], using as background curated lists of genes that represent the main hallmarks of cancer [3]. The heatmap represents the



Chapter 5

unsupervised clustering of the single-sample enrichment scores. Green: dasatinib-sensitive samples. Purple: dasatinib-resistant samples. B) GSVA single-sample enrichment scores of cell cycle-related pathways obtained using as background curated lists of genes from BIOCARTA, WikiPathways, KEGG, REACTOME, PID, and Sigma Aldrich (SA) downloaded from MsigDB. C) Bar plot illustrating the top20 active kinases inferred from the TiO_2 dataset in the matched diagnostic-relapse sample PDX_COG5 ranked on their INKA score. Green: dasatinib-sensitive sample (Rel). Purple: dasatinib-resistant sample (Dx). D) Bar plot illustrating the top20 active kinases inferred from the phospho-tyrosine IP (pTyr – IP) dataset in the matched diagnostic-relapse sample PDX_COG5 ranked on their INKA score. Green: dasatinib-sensitive sample (Rel). Purple: dasatinib-resistant sample (Dx). E) Bar plot illustrating the top20 active kinases inferred from the phospho-tyrosine IP (pTyr – IP) dataset in the matched diagnostic-relapse sample PDX_6953 ranked on their INKA score. Green: dasatinib-sensitive sample (Dx). Purple: dasatinib-resistant sample (Rel). Red: TEC.

SUPPLEMENTARY REFERENCES

1. Oshima, K., et al., *Mutational and functional genetics mapping of chemotherapy resistance mechanisms in relapsed acute lymphoblastic leukemia*. *Nature Cancer*, 2020. **1**(11): p. 1113-1127.
2. Hanzelmann, S., R. Castelo, and J. Guinney, *GSVA: gene set variation analysis for microarray and RNA-seq data*. *BMC Bioinformatics*, 2013. **14**: p. 7.
3. Liberzon, A., et al., *The Molecular Signatures Database (MSigDB) hallmark gene set collection*. *Cell Syst*, 2015. **1**(6): p. 417-425.

CHAPTER 6



A novel human cell line to investigate the pathophysiological IL7 signaling in T cell acute lymphoblastic leukemia

Valentina Cordo¹, Vera M. Poort¹, Rico Hagelaar¹, Jessica G.C.A.M. Buijs-Gladdines¹, Richard R. de Goeij-de Haas^{2,3}, Sander R. Piersma^{2,3}, Alex A. Henneman^{2,3}, Thang V. Pham^{2,3}, Koichi Oshima⁴, Adolfo A. Ferrando⁴, Frank N. van Leeuwen¹, Rob Pieters¹, Connie R. Jimenez^{2,3,5}, and Jules P.P. Meijerink^{1,5,6}

¹ Princess Máxima Center for Pediatric Oncology, Utrecht, the Netherlands

² OncoProteomics Laboratory, Cancer Center Amsterdam, Amsterdam University Medical Centers, VU University, Amsterdam, the Netherlands

³ Department of Medical Oncology, Cancer Center Amsterdam, Amsterdam University Medical Centers, VU University, Amsterdam, the Netherlands

⁴ Institute for Cancer Genetics, Columbia University Medical Center, New York, NY, USA

⁵ These authors jointly supervised this work

⁶ Present address: Acerta Pharma, Oss, The Netherlands

ABSTRACT

Cell lines are fundamental models in preclinical cancer research. Nevertheless, many established cell lines have deviated from their original phenotype due to the acquisition of mutations during prolonged culture *in vitro*. Thus, it is questionable whether commercially available cell lines are still fully representative of their tumors of origin.

T cell acute lymphoblastic leukemia (T-ALL) is a rare cancer and given the lack of approved targeted therapies for the treatment of relapsed/refractory T-ALL, the investigation of mechanisms of therapy resistance is fundamental. In addition to genome sequencing, functional screenings can uncover leukemia vulnerabilities. The use of patients' leukemic blasts from blood or bone marrow biopsies should be preferred for these analyses, but the need of a substantial number of cells and the lack of proliferation of T-ALL cells *ex vivo* are critical limiting factors.

Interleukin-7 (IL7) can support the survival and proliferation of healthy T cell precursors but also T-ALL blasts. Here, we describe the establishment of a new IL7-dependent T-ALL cell line obtained by expanding human leukemic cells first in murine xenografts and subsequently *ex vivo*. Moreover, using phosphoproteomics and integrative inferred kinase activity (INKA) analysis, we characterize the role of IL7 in sustaining continuous cell proliferation as well as the effect of the cytokine on the sensitivity of this cell line to prednisolone treatment. From this IL7-dependent line, we derived a second line that can grow in the absence of IL7. Together, these paired cell lines constitute novel tools for studying IL7 signaling and drug sensitivity in T-ALL.

INTRODUCTION

Cell lines have been essential tools in preclinical cancer research. In the last decade, several large-scale studies using panels of cell lines across different tumor types allowed the identification of genomic drivers of cancer [1], tumor vulnerabilities, and mechanism of resistance to therapy [2-5]. Nevertheless, many established cell lines obtained via spontaneous immortalization of tumor biopsies, have lost their original phenotype due to prolonged culture *in vitro* (reviewed in ref [6]) that can favor the insurgence of additional mutations and the positive selection of sub-clones. Thus, it is questionable whether commercially available cell lines are still fully representative of their tumors of origin [6-8]. As an alternative, recently, many researchers prefer the use of patient biopsies as direct experimental tools. However, this approach is still strictly dependent on several factors such as signed informed consent from the patients, correct handling and storage of tumor biopsies to preserve all the original features [9], the presence of residual healthy tissue or stromal/immune cells within the biopsies which could influence the experimental results, and the need of standardized protocols to obtain reproducible and comparable experimental results within collaborating research centers. Therefore, there is still an unmet need for reliable and representative *in vitro/ex vivo* cancer models. While for solid cancers, tumor organoids grown from patient biopsies have become the predominant and most widely used tools [10, 11], for leukemia, most of the preclinical studies still rely on commercial cell lines and patient-derived xenografts (PDXs) as disease models.

T cell acute lymphoblastic leukemia (T-ALL) is a rare cancer, accounting for only 12-15% of the total pediatric ALL cases [12]. While the overall survival has reached 80% thanks to risk-adapted chemotherapeutic regimens [12, 13], patients who are refractory to the treatment or experience a disease relapse, still have a poor prognosis due to the insurgence of therapy resistance. Moreover, long-term survivors suffer from detrimental side effects of the treatment. Given the lack of approved targeted therapies for the treatment of relapsed/refractory T-ALL [14], the investigation of mechanisms of therapy resistance and the selection of biomarkers for an improved patient stratification remain of utmost importance. In addition to genome sequencing, functional screenings such as genome-wide knock-out or knock-down screens, drug testing, (phospho)proteome and transcriptome profiling, and BH3-profiling are valuable tools to uncover leukemia vulnerabilities [15-19]. Thus, the direct use of T-ALL blasts obtained from blood or bone marrow aspirates of patients would be the ideal strategy for personalized and precision medicine. However, the need of a substantial

amount of primary material, the possible contamination with healthy blood cells, and the inability of T-ALL cells to proliferate *ex vivo*, are important limiting factors.

The cytokine interleukin-7 (IL7) plays a pivotal role in normal T cell development in the thymus [20] and regulates the proliferation, differentiation, and activity of mature lymphocytes. Similarly, IL7 can also favor the proliferation of T-ALL blasts [21, 22]. Moreover, IL7-induced signaling has emerged as one of the major players in the insurgence of resistance to glucocorticoids in T-ALL [23]. In addition to the effect of exogenous IL7 produced within the leukemic microenvironment, activating mutations in the IL7 signaling pathway (*IL7Ra*, *JAK1*, *JAK3*, *PTPN2*, *STAT5B*) are frequently described at T-ALL diagnosis [24, 25] and these mutations are also associated with resistance to synthetic steroids [24, 26].

Here, we describe the establishment of a new IL7-dependent T-ALL cell line from a pediatric T-ALL patient. Human leukemic cells were first expanded in murine xenografts and subsequently, purified T-ALL cells were cultured *ex vivo*, with the addition of human IL7 to the culture medium. After several passages *in vitro*, we named the cell line PDX-COG17-IL7. We characterized the role of IL7 in sustaining a continuous proliferation of these cells. Moreover, we investigated the IL7-induced signaling in PDX-COG17-IL7 cells by unbiased phosphoproteomic profiling and we analyzed the cellular response to glucocorticoids, the cornerstone of T-ALL therapy. In addition, we also report a second T-ALL cell line, derived from the PDX-COG17-IL7 line, that can grow in the absence of IL7 (PDX-COG17-IND) after a prolonged *in vitro* culture without the exogenous cytokine. Taken together, these two models constitute novel important tools for the investigation of the IL7 signaling pathway and the mechanisms of drug resistance in T-ALL.

MATERIALS AND METHODS

T-ALL patient derived xenograft

The first patient-derived xenograft was generated from cryopreserved human leukemic blasts (pediatric T-ALL patient at disease diagnosis) at the Irving Cancer Research Center of Columbia University Medical Center as previously reported [19]. The second generation of xenografts was obtained at the Hubrecht Institute (Utrecht, the Netherlands). Animal experiments were approved by the Animal Welfare Committee of the Princess Máxima Center for pediatric oncology (Utrecht, the Netherlands) and were carried out at the animal facility of the Hubrecht Institute (Utrecht, the Netherlands) under specific pathogen-free conditions and in accordance with animal welfare, FELASA (Federation of European Laboratory Animal Science Associations), ethical, and institutional guidelines. Mice were housed in individually ventilated cages in groups of 2-3 mice per cage. Briefly, 1.5-5 million viably frozen human leukemic blasts obtained from the first xenograft were intravenously injected into immunocompromised NOD/scid/Gamma (NSG) female mice of 8-10 weeks of age (Charles River, France). Mice were constantly monitored for leukemia development and disease burden was assessed by detection of human CD45+ cells in the murine blood by tail vein cut and FACS analysis. Mice were sacrificed when presenting symptoms of leukemia (lack of grooming and activity, hunched back position, visible loss of weight) or when the circulating human CD45+ cells reached 50%. Human leukemic cells were isolated from the murine spleen using the Lymphoprep density gradient separation (STEMCELL technologies) or from the bone marrow by flushing the femur bones with PBS. Purified cells were either immediately used for cell culture attempts or viably frozen until further usage.

Cell line establishment and culture

T-ALL blasts obtained from the second generation of xenografts were isolated from the bone marrow, washed in PBS, and seeded in a 24 multi-well plate in RPMI1640 + GlutaMax® (Gibco) medium supplemented with 20% Fetal Bovine Serum (Gibco) and antibiotics in the presence or absence of recombinant human IL7 (10 ng/ml, R&D systems). The culture medium was refreshed periodically, and cells were split when the concentration exceeded 2×10^6 cells/ml. Cells were kept at a density between 0.5 and 2×10^6 cells/ml. Cell viability was assessed using Trypan Blue and an automatic cell counter (BioRad, USA). Cells were grown *in vitro* for more than nine months and could be viably frozen and successfully thawed to restart the culture. Cells were periodically tested for the absence of mycoplasma contamination using the MycoAlert™ Mycoplasma Detection Kit (Lonza). For the IL7 depletion experiments, cells were counted, washed twice in PBS, and seeded in 20%FCS-RPMI1640

+ GlutaMax® medium without IL7. For the IL7-pulse experiment, cells previously deprived of IL7 overnight were treated with IL7 (25 ng/ml) for 30 minutes and subsequently cells were harvested for phosphoproteomic profiling or western blotting.

Ba/F3 cells were purchased from DSMZ (Germany). Ba/F3 cells were cultured in 10% FCS-RPMI1640 + GlutaMax® supplemented with murine IL3 (10 ng/ml). For the IL3-pulse experiment, cells previously deprived of IL3 overnight were treated with IL3 (10 ng/ml) for 30 minutes and subsequently cells were harvested for phosphoproteomic profiling or western blotting.

Phosphorylated peptides enrichment and mass spectrometry analysis

Cultured cells were spun down at 250 x g for 5 minutes, washed in cold PBS, spun down again, and harvested in 9M urea/20 mM HEPES (pH 8) lysis buffer containing 1 mM sodium orthovanadate, 2.5 mM sodium pyrophosphate, and 1 mM β -glycerophosphate. Cell lysates were thoroughly vortexed at maximum speed for 30 seconds, snap-frozen in liquid nitrogen and stored at -80°C until further usage. Before the enrichment step, lysates were thawed, sonicated three times at 18-micron amplitude (30 seconds on/60 seconds off) using the MSE Soniprep 150 sonicator (MSE) on ice. Cleared lysates were diluted to a concentration of 2 mg/ml and 5 mg of protein input was used for each sample. Proteins were reduced with 2 mM DTT for 30 minutes at 55°C, alkylated using 5 mM iodoacetamide for 15 minutes at room temperature (RT) in the dark and eventually digested overnight with Sequencing Grade Modified Trypsin (Promega, cat# V5111) at RT. Digested peptides were purified using OASIS HLB Cartridges (6 cc, 500 mg Sorbent, 60 μ m particle size. Waters, cat# 186000115) and lyophilized. Phospho-tyrosine peptides were enriched via immunoprecipitation (IP) using the PTMScan® Phospho-Tyrosine Rabbit mAb (P-Tyr-1000) Kit (Cell Signaling Technology, cat# 8803) according to the manufacturer protocol, using 4 μ l of bead slurry for each mg of protein input. Phospho-tyrosine peptides were eventually eluted in 0.15% trifluoroacetic acid (TFA). In parallel, a global phosphorylated peptide enrichment was performed using the AssayMap Bravo automated platform (Agilent Technologies) as previously described [27]. Desalted peptides corresponding to 200 μ g of protein were used as input for an automated Fe(III)-IMAC enrichment. Phosphorylated peptides were enriched using the AssayMAP Fe(III)-NTA cartridges (Agilent Technologies, cat# G5496-60085) and eluted in 5% ammonium hydroxide/30% acetonitrile in Milli-Q water. Eventually, eluted phosphorylated peptides were desalted using 20 μ l SDB-XC StageTips (prepared from Empore™ SPE Disks with SDB-XC, Sigma, cat# 66884-U) prior to LC-MS analysis. For global protein expression analysis, 1 μ g of total lysate was subjected

to liquid chromatography-mass spectrometry (LC-MS). LC-MS analyses were performed as previously described [16, 28]. Briefly, phosphopeptides were dried in a vacuum centrifuge and dissolved in 20 μ l 0.5% TFA/4% acetonitrile (ACN) prior to injection; 18 μ l was injected using partial loop injection. Peptides were separated by an Ultimate 3000 nanoLC-MS/MS system (Thermo Fisher) equipped with a 50 cm \times 75 μ m ID Acclaim Pepmap (C18, 1.9 μ m) column. After injection, peptides were trapped at 3 μ l/min on a 10 mm \times 75 μ m ID Acclaim Pepmap trap at 2% buffer B (buffer A: 0.1% formic acid (FA); buffer B: 80% ACN, 0.1% FA) and separated at 300 nl/min in a 10–40% buffer B gradient in 90 min (125 min inject-to-inject) at 35°C. Eluting peptides were ionized at a potential of +2 kV into a Q Exactive HF mass spectrometer (Thermo Fisher). Intact masses were measured from m/z 350–1400 at resolution 120,000 (at m/z 200) in the Orbitrap using an AGC target value of 3E6 charges and a maxIT of 100 ms. The top 15 for peptide signals (charge-states 2+ and higher) were submitted to MS/MS in the HCD (higher-energy collision) cell (1.4 amu isolation width, 26% normalized collision energy). MS/MS spectra were acquired at resolution 15,000 (at m/z 200) in the Orbitrap using an AGC target value of 1E6 charges, a maxIT of 64 ms and an underfill ratio of 0.1%. This results in an intensity threshold for MS/MS of 1.3E5. Dynamic exclusion was applied with a repeat count of 1 and an exclusion time of 30 s. For peptide and protein identification, MS/MS spectra were searched against theoretical spectra from the UniProt complete human proteome FASTA file (release January 2021, 42,383 entries) or the murine (*Mus musculus*) proteome FASTA file (25,131 entries) using the MaxQuant 1.6.10.43 software [29] with the following settings: enzyme specificity= trypsin, missed cleavages allowed= 2, fixed modification= cysteine carboxyamidomethylation; variable modification= serine, threonine, and tyrosine phosphorylation, methionine oxidation, and N-terminal acetylation; MS tolerance= 4.5 ppm and MS/MS tolerance= 20 ppm. For both peptide and protein identifications, the false discovery rate was set at 1% for filtering using a decoy database strategy. The minimal peptide length was set at 7 amino acids, the minimum Andromeda score for modified peptides at 40, and the corresponding minimum delta score at 6. Moreover, the “match between runs” option was used to propagate the peptides identification across samples.

Cell line authentication and whole-exome sequencing

Short tandem Repeat (STR) profiling was performed to exclude any possible contamination with any other commercially available cell line (Cell line Authentication Service, Eurofins Genomics).

The first xenograft and the matching patient sample were sequenced via whole-exome sequencing in a previous study [19], the corresponding somatic mutations and their variant allele frequencies (VAF) are listed in Table 1. To analyze the somatic mutations in the newly generated PDX-COG17-lines, DNA was extracted using the AllPrep DNA/RNA Micro Kit (QIAGEN, cat# 80284). Exome libraries were prepared using the KAPA HyperPrep kit (Roche) and the KAPA HyperExome kit (Roche). Paired-end sequencing was performed on an Illumina NovaSeq 6000 (Illumina) at 200x coverage. Reads were aligned to Hg38 using BWA [30] and duplicates reads were marked with Samtools 1.9 [31]. Variants were called using Mutect2 from GATK 4.2.0.0 [32]. Soft-clipped bases were skipped, while the rest of the settings were kept at default. Ensemble VEP 92 [33] has been used to annotate the detected variants. Since no reference DNA was available for these samples, we performed a strict filtering to select causal variants and to reduce the number of false positives. The following filters were used: alternative read count (Alt.count) ≥ 75 , Variant Allele Frequency (VAF) ≥ 0.2 , predicted effect = high, biallelic genotype, and exclusion of variants present in the global SNPs collection from gnomAD 3.5 [34].

INKA analyses

Inference of highly active kinases from phosphoproteomic data was performed as previously described [16, 28]. Integrative iNferred Kinase Activity (INKA) scores are calculated based on 4 parameters: the sum of all phosphorylated peptides belonging to a kinase; the detection of the phosphorylated kinase activation domain (kinase-centric parameters), 3) the detection of known phosphorylated substrates and the presence of predicted phosphorylated substrates (substrate-centric parameters) [28, 35]. The latest version of the INKA pipeline is available online at <https://inkascore.org/>.

***In vitro* drug screening**

Cells were dispensed into a 384 multi well plate (Corning) using the semi-automated Multidrop dispenser (Thermo Fisher) in duplicates. Drugs were diluted in DMSO (ruxolitinib) or 0.3% Tween-20/PBS (prednisolone) at a concentration of either 100 nM or 10 nM and dispensed using a TECAN D300e digital dispenser in a range of 0.1 nM – 32 μ M (ruxolitinib) or 0.2 μ M – 514 μ M (prednisolone). Cell viability was evaluated at the time of seeding ($t = 0$) and after a 96 hour-incubation using the CellTiter-Glo[®] 2.0 Cell Viability Assay (Promega, cat# G9242) according to the manufacturer protocol. Cell viability was calculated in relation to vehicle-only treated cells. Graphs were obtained using the GraphPad Prism 9.0.1 software.

Western Blotting

Membranes were incubated with the following primary antibodies (CST, 1:1000 dilution, if not stated otherwise): anti-phospho Src Family (Tyr416) #2110, anti-Src L4A1 #2110, anti-Lck #2752, anti-AKT #9272, anti-phospho AKT (S473) #9271, anti-p44-42 MAPK (ERK1/2) (137F5) #4695, anti-phospho p44-42 MAPK (T202/Y204) (D13.14.4E) #4370, anti-STAT5 (D2O6Y) rabbit Ab #94205, anti-phospho STAT5 (Y694) #9351, and anti- β actin (1:10,000; Abcam, #ab6276).

Flow cytometry

Experiments were performed using the BioRad ZE5 (BioRAD, USA). For surface markers detection, live cells were washed in AutoMACS buffer (Miltenyi biotec, cat# 130-091-221) and incubated with the following antibodies for 30 minutes on ice in the dark: anti-CD127-PE (Miltenyi biotec, cat# 130-098-094, 1:100), anti-CD3-BUV496 (BD Biosciences, cat# 564810, 1:500), anti-CD7-BV786 (BD Biosciences, cat# 740964, 1:500), anti-CD44-BV510 (Biolegend, cat# 103044, 1:1000), anti-CD4-PE Cy7 (BD Biosciences, cat# 560644, 1:500), anti-CD8-BV711 (Biolegend, cat# 301043, 1:500), and anti-CD1a-PE (Biolegend, cat# 300105, 1:1000). For cell cycle analysis, 200,000 cells for each condition were stained with Hoechst (7.5 μ g/ml) for 1 hour at 37°C and then incubated for 15 minutes on ice before FACS analysis. For Annexin V/propidium iodide (PI) staining of apoptotic cells, 200,000 cells were stained with Annexin V-APC antibody (Biolegend, cat# 640920) diluted 1:20 in Annexin V-binding buffer (Invitrogen, cat# V13246) for 15 minutes at RT in the dark. PI (Miltenyi biotec, cat# 130-093-233) was added at a final concentration of 0.5 μ g/ml just before FACS measurement. Data analysis was performed using FlowJo v10.7.1 and bar graphs were obtained using the GraphPad Prism 9.0.1 software.

Quantitative real-time PCR

RNA was isolated using the RNeasy Plus Mini Kit (QIAGEN, cat# 74134). Amplification of cDNA was obtained using the following primers: *GAPDH* Fw primer 5'-GTCGGAGTCAACGGATT-3' and Rev primer 5'-AAGCTTCCCGTTCTCAG-3'. *BIM* Fw primer 5'-GCGCCAGAGATATGGAT-3' and Rev primer 5'-CGCAAAGAACCTGTCAAT-3'. *IL7R* Fw primer 5'-AGTAAATGCAAAGCACCTGAG-3' and Rev primer 5'-TAAATGGGGCTTAAGCTCTGAC-3'. *MCL1* Fw primer 5'-CGCCAAGGACACAAAG-3' and Rev primer 5'-AAGGCACAAAAGAAATG-3'. *NR3C1* Fw primer 5'-TGTTTTGCTCCTGATCTGA-3' and Rev primer 5'-TCGGGGAATTCAATACTCA-3'. *FKBP5* Fw primer 5'-GAATGGTGAGGAAACGC-3' and Rev primer 5'-TGCCTCCATCTTCAAATAA-3'. *GILZ* Fw

primer 5'TGGCCATAGACAACAAGAT-3' and Rev primer 5'-TTGCCAGGGTCTTCAA-3'. *SGK1* Fw primer 5'-GGAGCCTGAGCTTATGAAT-3' and Rev primer 5'-TTCCGCTCCGACATAATA-3'.

The fold changes in gene expression were calculated applying the delta-delta Ct method (ddCt) using as control the normal culturing condition of each cell line in the absence of prednisolone (“+IL7” for the PDX-COG17-IL7 line and “no IL7” for the PDX-COG17-IND line, respectively).

RESULTS

Establishment of a novel human IL7-dependent T-ALL cell line

To create new tools and models for investigating the biology of T-ALL, we attempted the *in vitro* culture of leukemic blasts expanded via xenotransplantation and purified from different tissues of NSG mice in the absence of any feeder layer. Given the fundamental role of IL7 in sustaining survival, proliferation, and therapy resistance in T-ALL, we tested whether the addition of IL7 in the culture medium could facilitate the survival and expansion of T-ALL blasts *ex vivo*. Briefly, human leukemic blasts collected at diagnosis of a pediatric T-ALL patient were expanded in NSG mice (PDX-COG17-Dx) for two consecutive rounds of xenotransplantation. After the second round of xenotransplantation, CD45+ leukemic cells purified from the murine bone marrow were cultured in suspension in the presence or absence of IL7 (10 ng/ml) and kept at a high cellular density, as illustrated in **Figure 1A**. In the absence of IL7, cells did not proliferate *in vitro*, and after one week in culture, their viability rapidly decreased (**Figure 1B** and **Supplementary Figure 1A**). On the contrary, cells cultured with IL7 kept high viability and rapidly started to proliferate with a doubling time of 48-72 hours (**Figure 1B**). After passaging cells for over a month, we tested whether cultured PDX-COG17-Dx cells were still dependent on IL7 for their survival and proliferation. Therefore, cells were thoroughly washed and deprived of IL7 for two weeks. In the absence of IL7, cells did not die but they stopped proliferating (**Figure 1C**) indicating that IL7 is necessary for the active proliferation of the PDX-COG17-Dx cells *in vitro*. These cells could be cultured continuously for more than six months (reaching over 30 passages *in vitro*) and could be successfully viably frozen and re-thawed several times. Therefore, we named this newly established T-ALL cell line *PDX-COG17-IL7* line. Since cells deprived of IL7 had remained viable in culture, despite the lack of active proliferation, we attempted to prolong the culture for over a month to see if a putative minor clone would emerge, or if an acquired mutation would give a selective growth advantage, or if any other adaptation would occur, allowing the proliferation of cells in the absence of IL7 (**Figure 1A**). After four

weeks of culture in IL7-deprived medium, cells slowly started to proliferate (**Supplementary Figure 1B**) and once they could be periodically split and expanded in the absence of any cytokine, we named the derived IL7-independent line *PDX-COG17-IND*. To further characterize these two new T-ALL cell lines, we compared the surface markers expression of the PDX of origin and the cultured cells (after eight passages *in vitro* for the PDX-COG17-IL7 line, and 18 passages for the PDX-COG17-IND line). Human CD45⁺ leukemic cells purified from the murine bone marrow and spleen showed some heterogeneity in the expression of CD1a, CD44, CD8, and CD4 while both cell lines showed a clonal immunophenotype sCD3⁻; CD7⁺; CD1a⁺; CD44⁻; CD4⁻; CD8⁻ (**Figure 1D**), indicating that a minor subclone of the original leukemic blast population purified from the murine bone marrow was selected and expanded during the *ex vivo* culturing. Overall, the immunophenotype of the two cell lines resembles the one of double negative, cortical T-cell progenitors.

Subsequently, we investigated whether the acquisition of somatic mutations in culture might have had a role in promoting the survival of cells *ex vivo*. Thus, we compared the somatic mutations present in the first xenograft and the newly established cell lines, as listed in **Table 1**. Interestingly, the two cell lines did not acquire any mutation in *TP53* or any inactivation of a tumor suppressor gene that could promote an aberrant proliferation and survival *ex vivo*. In addition, no mutation was found in the *IL7R* gene or in any *IL7R*-signaling pathway genes in the derived IL7-independent line.

Next, we investigated the role of the IL7 signaling in promoting survival and proliferation of these cells. Therefore, IL7-dependent cells were deprived of IL7 for 10 days and cells arrested their proliferation (**Figure 1E**). Cell cycle analysis revealed an increase in the sub-G1 phase, indicating a possible induction of apoptosis or exit from the cell cycle (**Figure 1F**). Annexin V – propidium iodide (PI) staining highlighted a slight increase in the apoptotic fraction as well as a minor increase in the necrotic cell population upon IL7 removal, suggesting that IL7-induced signaling can promote cell survival. On the other hand, for the IL7-independent line, the addition of IL7 in the culture medium did not provoke any evident alteration in cell proliferation, the cell cycle, or the induction of apoptosis (**Figure 1F**).



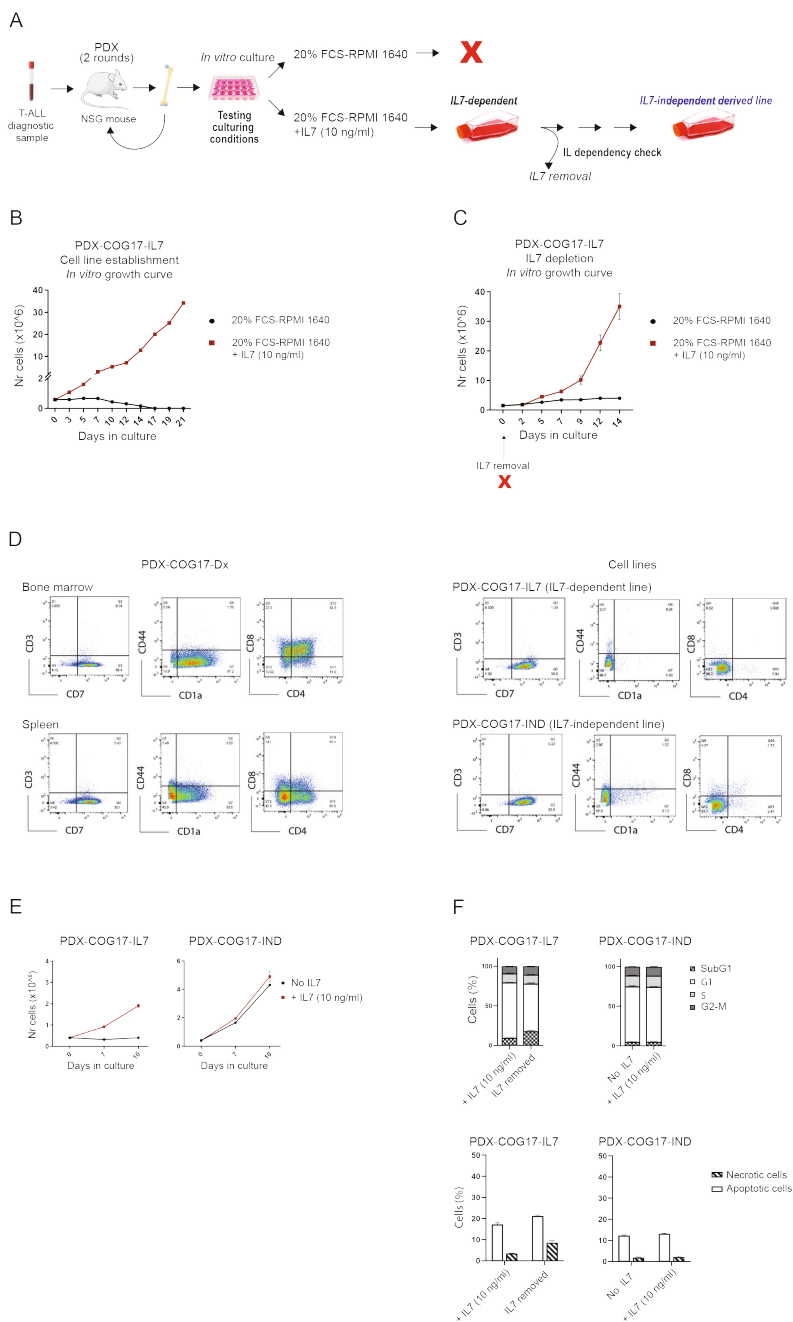


Figure 1. Establishment of a novel, IL7-dependent T-ALL cell line. A) Experimental overview. Patient leukemic blasts were expanded in NSG mice for two consecutive rounds of xenotransplantation (PDX) and purified from the murine bone marrow. Subsequently, cells were put in culture in the presence or absence of human IL7 (10 ng/ml). T-ALL cells rapidly died without IL7 while they started to proliferate in the presence of the cytokine. Cell counts were monitored using a trypan blue staining and automatic

cell counting (B, day 0 = leukemic blasts purification from the murine bone marrow). After several passages in culture, IL7 was removed from the medium to check whether cells still needed the cytokine to actively proliferate. Cells did not proliferate without IL7 for two weeks (C). After prolonged culture in the absence of any cytokine, cells started to proliferate and an additional, IL7-independent cell line was derived. D) FACS analysis of surface markers expression of the leukemic blast population purified from the murine xenograft (PDX-COG17-Dx, bone marrow and spleen) and the two derived cell lines (PDX-COG17-IL7, IL7-dependent, after eight passages in culture, and PDX-COG17-IND, IL7-independent, after 18 passages in vitro). E) Growth curves of the cell lines in the absence or presence of human IL7 (10 ng/ml) for ten days. Cells were incubated with or without cytokine for ten days and the cell counts were monitored using a trypan blue staining automatic cell counting. The graphs show the average and the standard deviation of triplicates. F) Cell cycle analysis and staining of apoptotic cells of the PDX-COG17-IL7 (IL7-dependent) and PDX-COG17-IND (IL-independent) cell lines after ten days in culture with or without human IL7 (10 ng/ml). Cells were deprived or incubated with human IL7 (10 ng/ml) for ten days. Apoptotic cells were defined as the sum of AnnexinV+/PI- (pre-apoptotic) and AnnexinV+/PI+ (fully apoptotic) cells, while AnnexinV-/PI+ cells were considered necrotic. Cell cycle analysis was performed via HOECHST-DNA staining and FACS analysis of DNA content. The bar plots show the average and standard deviation of triplicates.



Table 1. Somatic mutations in PDX-COG17-Dx and in the derived PDX-COG17-lines.

| Chromosome | Chr position | Ref Seq | Variant | Gene | Protein | Predicted protein product | PDX VAF (%) | IL7 - line VAF (%) | IND - line VAF (%) |
|------------|--------------|---------|---------|----------|--------------|---------------------------|-------------|--------------------|--------------------|
| 4 | 86035 | C | T | ZNF595 | ZNF595 | T2131 | 100 | - | - |
| 7 | 148106477 | C | G | CNTNAP2 | CNTNAP2 | - | 59 | - | - |
| 2 | 69093012 | G | A | BMP10 | BMP-10 | I342 | 51 | 51 | 51 |
| 11 | 114121228 | C | T | ZBTB16 | ZBTB16 | P658L | 50 | 52 | 51 |
| 11 | 130278529 | A | G | ADAMTS8 | ADAM-TS8 | I643 | 50 | 47 | 53 |
| 16 | 88599699 | CCTCTGG | C | ZFPM1 | ZFPM1, FOG-1 | PLA445P | 50 | 100 | 100 |
| 2 | 1653280 | C | T | PXDN | PXDN | A758T | 48 | 51 | 48 |
| 11 | 62549750 | A | G | TAF6L | TAF6L | N258D | 48 | 44 | 47 |
| 6 | 7571628 | C | T | DSP | TS-DSP1 | R572W | 45 | 49 | 48 |
| 5 | 73207378 | C | T | ARHGEF28 | p190-RhoGEF | S1642 | 44 | 49 | 46 |
| 9 | 43816630 | C | CT | CNTNAP3B | CNTNAP3B | - | 25 | - | - |
| 11 | 47640398 | T | C | MTCH2 | MTCH2 | K300R | 25 | - | - |
| 7 | 142460388 | C | T | PRSS1 | PRSS1 | G187 | 24 | - | - |
| 1 | 248637367 | A | G | OR2T3 | OR2T3 | H239R | 23 | - | - |
| 6 | 32714164 | T | C | HLA-DQA2 | HLA-DQA1 | L254P | 18 | - | - |
| 2 | 131414975 | A | T | POTEJ | POTEJ | Y881F | 17 | - | - |
| 2 | 131415008 | T | C | POTEJ | POTEJ | M892T | 14 | - | - |
| 1 | 176145089 | G | A | RFD2 | hCOP1 | N174 | 10 | - | - |
| 6 | 88221109 | C | T | SLC35A1 | CMP-SA-Tr | - | 9 | - | - |
| 11 | 76872028 | G | A | MYO7A | MYO7A | G404R | 9 | - | - |
| 11 | 47644289 | C | A | MTCH2 | MTCH2 | T263 | 8 | - | - |
| 11 | 120343759 | C | T | ARHGEF12 | ARHGEF12 | R986C | 4 | - | - |
| 1 | 5875102 | T | A | NPHP4 | NPHP4 | - | - | 100 | 100 |
| 1 | 171208951 | C | T | FMO2 | FMO 2 | Q472* | - | 100 | 100 |
| 14 | 31483548 | G | A | GPR33 | GPR33 | R140* | - | 100 | 98 |
| 16 | 81141373 | G | A | PKD1L2 | PKD1L2 | Q1096* | - | 100 | 100 |
| 18 | 63712604 | G | T | SERPINB1 | SERPINB1 | E90* | - | 100 | 100 |

Table 1. Continued.

| Chromosome | Chr position | Ref Seq | Variant | Gene | Protein | Predicted protein product | PDX VAF (%) | IL7 - line VAF (%) | IND- line VAF (%) |
|------------|--------------|---------|---------|----------|---------------|---------------------------|-------------|--------------------|-------------------|
| 19 | 42935542 | G | A | PSG7 | PSBG-9 | R98* | - | 100 | 100 |
| X | 134413910 | C | T | PHF6 | PHF6 | R225* | - | 100 | 100 |
| X | 152728157 | G | C | CSAG1 | CSAG1, CT24.1 | Y28* | - | 100 | 100 |
| 8 | 141494938 | C | T | MROH5 | MROH5 | - | - | 55 | 53 |
| 17 | 82058417 | C | G | DUSIL | DUSIL | - | - | 52 | 47 |
| 7 | 142400325 | G | T | TRBV10-1 | TRBV10-1 | E98* | - | 51 | 50 |
| 11 | 124250452 | C | G | OR8G1 | OR8G1 | Y259* | - | - | 44 |
| 10 | 88668560 | C | T | LIPF | LIPF | Q76* | - | 51 | 45 |
| 11 | 50033053 | G | T | OR4C45 | OR4C45 | *60Y | - | 50 | 47 |
| 11 | 66560624 | C | T | ACTN3 | ACTN3 | R577* | - | 50 | 48 |
| 7 | 149833805 | A | G | SSPO | SSPO | - | - | 49 | 46 |
| 9 | 34372875 | G | C | MYORG | MYORG | Y23* | - | 48 | 48 |
| 13 | 98213393 | C | T | FARP1 | FARP1 | Q51* | - | 48 | 50 |
| 1 | 155172894 | T | C | KRTCAP2 | KCP-2 | - | - | 44 | 49 |
| 7 | 128938247 | T | G | IRF5 | IRF-5 | - | - | 44 | 47 |
| 21 | 10569701 | C | T | TPTE | TPTE, CT44 | R229* | - | 31 | 30 |
| 19 | 41586462 | A | T | CEACAM21 | CEACAM21 | - | - | - | 50 |
| 9 | 41040359 | C | T | PGM5P2 | - | - | - | - | 48 |

Abbreviations: chr: chromosomal; ref seq: reference sequence; VAF: variant allele frequency; PDX: PDX-COG17-Dx; IL7-line: PDX-COG17-IL7; IND-line: PDX-COG17-IND.



IL7-induced signaling causes JAK-STAT activation

To characterize the responsiveness to IL7 of these newly established cell lines, we first investigated the surface expression of the IL7 receptor (IL7R) in the cell lines. FACS analysis revealed the expression of the IL7R α (CD127) in both lines, even in the IL7-independent cell line as shown in **Figure 2A**. Moreover, the IL7R expression could be modulated by the presence of exogenous IL7. In fact, after adding IL7 to the culture medium for 72 hours, the CD127 expression decreased, possibly due to internalization of the receptor-ligand complex [36] in both lines (**Figure 2A**).

To study the intracellular signaling induced by IL7 in PDX-COG17-IL cells, we deprived the cells of IL7 overnight and subsequently added IL7 for a short incubation (30 minutes) to activate the IL7R signaling cascade (*IL7 pulse*). We performed global, unbiased phosphoproteomic profiling on PDX-COG17-IL7 cells before and after the *IL7 pulse* to identify active mediators of IL7 signaling. By using a phospho-tyrosine immunoprecipitation and a complementary global, IMAC-based enrichment coupled to mass spectrometry analysis, we aimed to obtain a comprehensive view of both tyrosine and serine/threonine phosphorylation. To study the change of signaling after the cytokine pulse, we inferred kinase activity from the phosphoproteomic data using the INKA pipeline [16, 28] to give a numerical score to each kinase, calculated using both the phospho-kinase and the phospho-substrate data, as a proxy for their activation. As shown in the bar plots depicted in **Figure 2B**, the IL7 pulse causes activation of the kinase JAK3 (ranking 5/20) while cells deprived of the cytokine do not have any JAK3 activity. On the other hand, no relevant signaling change was detected in MAP kinases or any other serine/threonine kinases. A similar result was obtained using the IL3-dependent murine pro-B cell line Ba/F3 (**Figure 2C**). In fact, Ba/F3 cells deprived overnight of IL3 and subsequently subjected to an IL3 pulse, show activation of JAK2 (ranking 2/20) among the tyrosine kinases. Additionally, Ba/F3 cells also show activation of the MAPK axis (MAPK1/ERK2 ranking 4/20, MAPK3/ERK1 ranking 10/20, and MAP2K1 ranking 17/20, respectively in the IMAC-INKA dataset upon IL3 pulse), as illustrated in **Figure 2C**. Further analysis of the phosphoproteomic data confirmed an increase in phosphorylation of JAKs upon cytokine pulse (**Figure 2D**). These results indicate that IL7-induced signaling, similarly to the IL3-induced signaling in murine Ba/F3 cells, converges on increased JAK activation in our PDX-COG17-IL line.

To investigate the downstream signaling cascade, we performed western blotting in PDX-COG17 cells before and after the administration of the IL7 pulse. Exogenous IL7 induced an evident STAT5 phosphorylation in the PDX-COG17-IL7 line and even in IL7-independent

PDX-COG17-IND cells (**Figure 2E**). A similar increase in STAT5 phosphorylation on residue Y694 could be seen also in the phosphoproteomic profiling (**Figure 2F**). Again, no increase in ERK phosphorylation was seen in the PDX-COG17-lines, while the IL7-responsive T-ALL cell line CCRF-CEM showed increased ERK1/2 (T202/Y204) and AKT (S473) phosphorylation upon IL7-induced signaling (**Supplementary Figure 1C**). Similarly, Ba/F3 cells presented an increase in phospho-ERK (T202/Y204) upon exogenous IL3 pulse in addition to STAT5 phosphorylation, as illustrated in **Supplementary Figure 1D**.

These results indicate that the IL7-induced signaling in PDX-COG17 cells mainly converges on the activation of the JAK3-STAT5 axis.



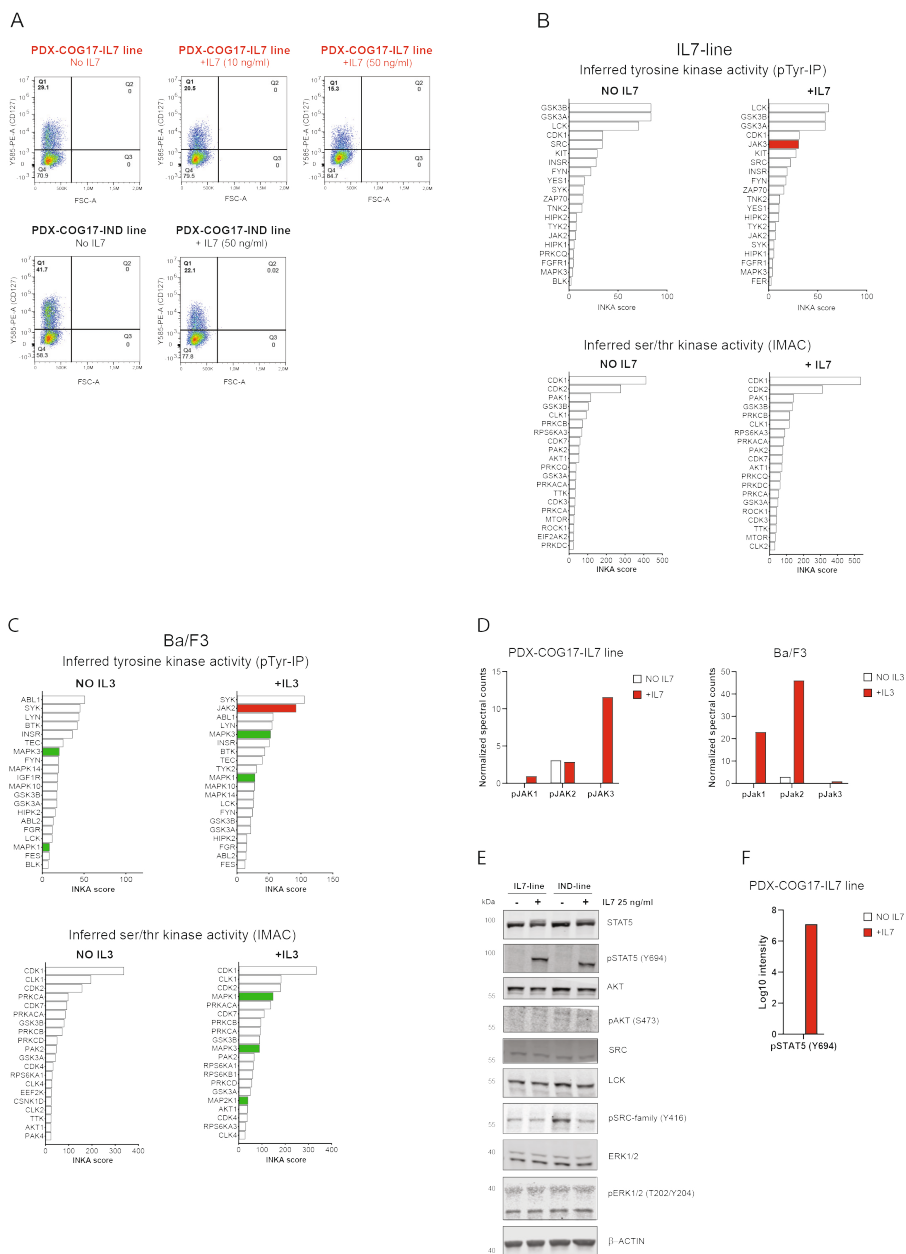


Figure 2. IL7-induced signaling converges on JAK3. A) Surface expression of the IL7Rα (CD127). Both cell lines (PDX-COG17-IL7 and PDX-COG17-IND) were incubated in the presence or absence of human IL7 (10 or 50 ng/ml) for 72h and cells were stained with anti-CD127 antibody before FACS analysis. B) INKA bar plots illustrating the top 20 active kinases in PDX-COG17-IL7 cells inferred from the phospho-tyrosine immunoprecipitation (pTyr-IP) and the IMAC dataset. NO IL7: cells were deprived overnight of the cytokine. +IL7: after an overnight culture without IL7, cells were incubated for 30 minutes with the cytokine (25 ng/ml). Red: JAK3. C) INKA bar plots illustrating the top 20 active kinases in Ba/F3 cells inferred from the phospho-tyrosine immunoprecipitation (pTyr-IP) and the IMAC dataset.

NO IL3: cells were deprived overnight of the cytokine. +IL3: after an overnight culture without IL3, cells were incubated for 30 minutes with the cytokine (10 ng/ml). Red: JAK3. Green: MAPK. D) Bar plots illustrating the sum of the normalized spectral counts of phosphopeptides belonging to JAK1 (pJAK1), JAK2 (pJAK2) and JAK3 (pJAK3) in PDX-COG17-IL7 and Ba/F3 cells before (NO IL7/IL3) and after the cytokine pulse (+IL7/IL3). E) Western blotting of PDX-COG17-IL7 and PDX-COG17-IND cells before (NO IL7) and after the cytokine pulse (+IL7 25 ng/ml). Cells were cultured overnight in the absence of IL7, subsequently incubated with the cytokine (25 ng/ml) for 30 minutes and harvested for protein extraction. F) Bar plots illustrating the normalized log₁₀ intensity of the phosphorylation of the tyrosine residue 694 on STAT5 (pSTAT5-Y694) in PDX-COG17-IL7 (NO IL7) and after the cytokine pulse (+IL7).

PDX-COG17-lines are resistant to prednisolone

STAT5 activation and its transcriptional activity have been proven pivotal for the survival of T-ALL cells [21]. Moreover, increased JAK/STAT activity induced by either exogenous IL7 or due to mutations in genes involved in the IL7R signaling pathway, play a fundamental role in sustaining resistance to glucocorticoids in T-ALL [23, 24, 26, 37]. Therefore, we tested the sensitivity of the two PDX-COG17 lines to prednisolone, in the presence or absence of exogenous IL7. As illustrated in **Figure 3A**, PDX-COG17-IL7 cells are resistant to prednisolone *in vitro* in the presence of exogenous IL7. When cells are deprived of IL7 for 3 days and subsequently treated with prednisolone, they seem only slightly more sensitive to the treatment. Similarly, PDX-COG17-IND cells are resistant to prednisolone and the resistance is slightly increased in the presence of exogenous IL7 (**Figure 3B**).

To evaluate the response to glucocorticoid treatment and the possible role of IL7 in influencing the steroid response, we performed qPCR for several *NR3C1*-target genes in both cell lines after a 4-day prednisolone treatment, in the presence or absence of exogenous IL7. As shown in **Figure 3C**, PDX-COG17-IL7 cells show upregulation of the glucocorticoid receptor (*NR3C1*) and of its target genes, including the pro-apoptotic *BIM*. For PDX-COG17-IND cells, both in the presence or absence of IL7, a similar upregulation of *NR3C1*-target genes could be seen (**Figure 3D**). Taken together, these data showed that both cell lines, despite being resistant to glucocorticoids *in vitro*, retain a *NR3C1*-mediated steroid response at the transcriptional level.

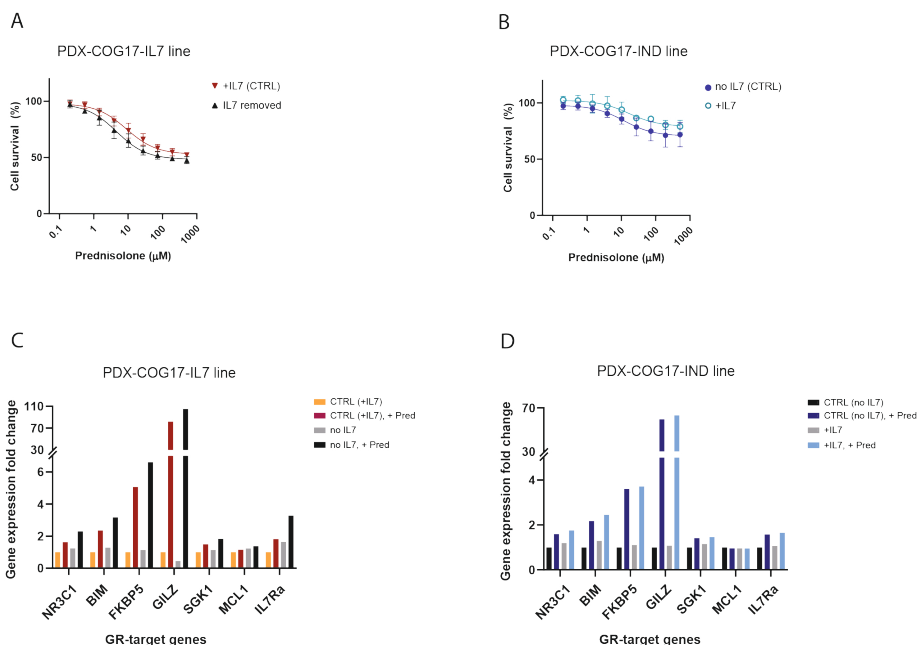


Figure 3: PDX-COG17 cells are resistant to prednisolone. A) Dose-response curves of prednisolone treatment in PDX-COG17-IL7 cells. Cells were incubated with increasing concentrations of prednisolone (0 – 514 μM) for 96 hours in the presence or absence of IL7 (10 ng/ml). IL7 removed: cells were deprived of IL7 for 72 hours (day -3) before the addition of the drug (day 0) and kept without cytokine during the assay. Relative survival was calculated in comparison with cells treated with vehicle only. The graph shows the average and the standard deviation of two independent experiments performed in duplicate. B) Dose-response curves of prednisolone treatment in PDX-COG17-IND cells. Cells were incubated with increasing concentrations of prednisolone (0 – 514 μM) for 96 hours in the presence or absence of IL7 (10 ng/ml). +IL7: cells were incubated with IL7 for 72 hours (day -3) prior to the addition of the drug (day 0) and cultured in presence of the cytokine during the assay. Relative survival was calculated in comparison with cells treated with vehicle only. The graph shows the average and the standard deviation of two independent experiments performed in duplicate. C) Gene expression of glucocorticoid receptor (GR)-target genes in PDX-COG17-IL7 cells following prednisolone treatment for 96 hours, in the presence or absence of exogenous IL7 (10 ng/ml). The fold change was calculated compared to the normal culturing condition of PDX-COG17-IL7 cells (in the presence of IL7, indicated as CTRL (+IL7) in orange). D) Gene expression of GR-target genes in PDX-COG17-IND cells following prednisolone treatment for 96 hours, in the presence or absence of exogenous IL7 (10 ng/ml). The fold change was calculated compared to the normal culturing condition of PDX-COG17-IND cells (no IL7, indicated as CTRL in black).

The JAK inhibitor ruxolitinib synergizes with prednisolone in PDX-COG17-IL7 cells

Since PDX-COG17 cells showed resistance to prednisolone and since the presence of IL7 could even slightly increase the resistance to glucocorticoid *in vitro* (**Figure 3A-B**), we questioned whether the targeting of JAK3 activity upon IL7 signaling could be an effective strategy to sensitize cells to prednisolone. PDX-COG17-IL7 cells did not show sensitivity to ruxolitinib as single treatment, with an IC₅₀ of 10 μM in the presence of IL7 and even higher in the absence of the cytokine (**Figure 4A**). When combining ruxolitinib and prednisolone in the absence of IL7, synergy could be found only at very high concentration of both drugs (NO IL7; prednisolone > 27.2 μM and ruxolitinib > 10 μM) as illustrated in **Figure 4B**. Interestingly, when the drug combination is tested in the constant presence of IL7, synergy can be found using a much lower ruxolitinib concentration (0.32 μM , **Figure 4B-C**). Furthermore, when PDX-COG17-IL7 cells are first deprived of IL7 and then incubated with the cytokine (IL7 pulse) together with the drugs, the synergistic effect of the drug combination can be seen already when using 0.1 μM ruxolitinib (**Figure 4B**). For PDX-COG17-IND cells, the addition of IL7 also induced a higher synergy of the combined ruxolitinib and prednisolone treatment but only in the higher drug concentration range (**Supplementary Figure 2A-B**, ruxolitinib > 1 μM). These results indicate that the increased JAK3 activity induced by active IL7 signaling in PDX-COG17-IL7 cells is targetable and can sensitize leukemic cells to prednisolone treatment. Moreover, our results indicate that the PDX-COG17-IL7 line can be used as model for studying the reversal of steroid resistance in T-ALL.

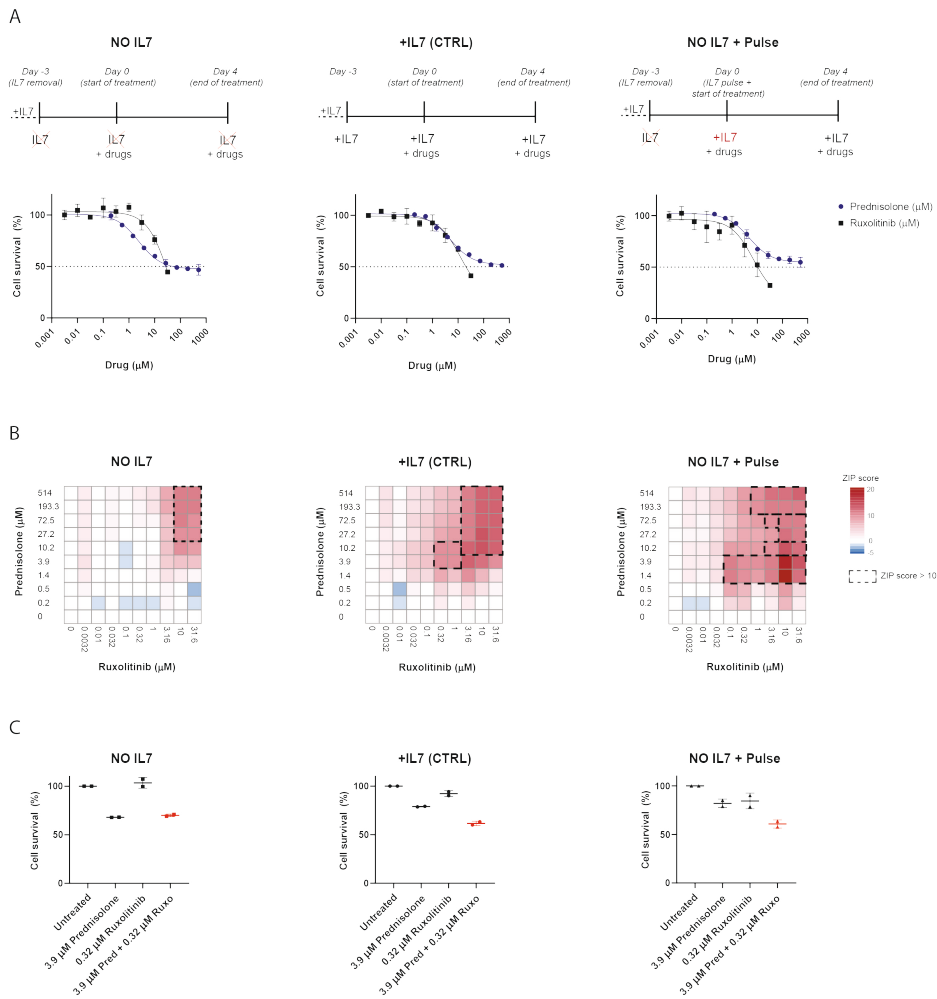


Figure 4: ruxolitinib and prednisolone have synergistic effect in PDX-COG17-IL7 cells. A) Dose-response curves of prednisolone and ruxolitinib single treatments in PDX-COG17-IL7 cells. Cells were incubated with increasing concentrations of prednisolone (0 – 514 μM) or ruxolitinib (0 – 32 μM) for 96 hours in the presence or absence of IL7 (10 ng/ml). NO IL7: cells were deprived of IL7 for 72 hours (day -3) prior to the addition of drugs (day 0) and kept without cytokine during the assay. +IL7: cells were cultured in the presence of IL7 as normally done for this cell line. NO IL7 + PULSE: cells were deprived of IL7 for 72 hours (day -3) prior to the addition of drugs (day 0). Subsequently, IL7 (10 ng/ml) was added when seeding cells with the drugs at day 0. Relative survival was calculated in comparison with cells treated with vehicle only. The graph shows the average and the standard deviation of duplicates. B) Zero-Interaction Potency (ZIP) synergy scores for the combination of ruxolitinib (0 – 32 μM) and prednisolone (0 – 514 μM). Cells were treated with either one of the single drugs or a drug combination for 96 hours in duplicate. Cell survival was calculated in comparison to vehicle-only treated cells. ZIP values lower than 0 indicate an antagonistic effect of the drug combination (blue), values between 0 and 10 indicate an additive effect (white to light red) while values above 10 (corresponding to a deviation from the reference model above 10%) indicate synergy (dark red and outside black dashed line). Each drug screening was performed in duplicate. C) Cell survival of PDX-COG17-IL7 cells upon single prednisolone/ruxolitinib or combination treatment. Each dot represents the relative survival (compared to vehicle-only treated cells) after 96 hours treatment with 3.9 μM prednisolone, 0.32 μM ruxolitinib or combination of both drugs. The error bars represent the standard deviation of the duplicate.

DISCUSSION

The use of patient biopsies is becoming the preferred choice for studying cancer biology and mechanisms of therapy resistance. Functional screenings such as *ex vivo* drug testing and unbiased analysis like phosphoproteomic profiling are becoming fundamental tools to identify druggable targets and to design personalized therapies. Nevertheless, for T-ALL, many preclinical studies still rely on commercial cell lines or patient-derived murine xenografts used as disease model, given the lack of cell proliferation and poor survival of T-ALL blasts *ex vivo*. In the last few years, to increment both cell survival and proliferation of primary cells, different co-culture platforms have been set up where T-ALL blasts are cultured on a stromal layer, typically mesenchymal stem cells, and successfully used for drug screenings combined with FACS analysis or imaging readouts [38, 39]. Furthermore, novel patient-derived T-ALL cell lines have been established in the last two decades, such as the IL7-dependent TAIL7 cell line [40], the NOTCH1-dependent cell line CUTTL1 [41], the *MYC*-translocated cell line UP-ALL13 [42], and two T-ALL cell lines from the Children's Oncology Group that can grow at both atmospheric (20%) and bone marrow-like (5%) oxygen concentrations [43]. Here, we presented a new, IL7-dependent T-ALL cell line obtained from the leukemic blasts of a pediatric T-ALL patient (PDX-COG17-IL7). Moreover, we also described the sub-derivatization of an IL7-independent cell line (PDX-COG17-IND) from the original one. Interestingly, the two cell lines do not present any inactivating mutation in tumor suppressor genes such as *TP53* that could favor the proliferation of cells *ex vivo*. Therefore, differently from most of the commercially available cell lines, these new lines possibly retain an intact DNA-damage response. In addition, the IL7-independent PDX-COG17-IND cells did not acquire any mutation in the *IL7R* (or any other gene involved in the IL7 signaling cascade) that could explain the IL7-independence *in vitro*. This evidence indicates that possible metabolic rewiring, alternative signaling loops, and adaptation to different culturing conditions can occur and favor the survival of leukemic cells *ex vivo* even the absence of IL7.

Phosphoproteomic profiling and INKA prediction of active kinases highlighted the activation of JAK3 upon cytokine stimulation in PDX-COG17-IL7 cells. Similarly, in the IL3-dependent pro-B murine Ba/F3 cells, upon exogenous administration of murine IL3, high JAK2 activity was induced. However, while Ba/F3 cells also present an increase in ERK activity upon IL3 administration, PDX-COG17-IL7 cells do not show any downstream ERK or AKT activation after IL7-induced signaling. In our cell line, the IL7-induced signaling converges on the activation of JAK3 and the transcription factor STAT5. Since activation of the IL7R-JAK-STAT

pathway has been described as one of the major cause of resistance to glucocorticoids [23, 24], the cornerstone of T-ALL therapy, we tested the sensitivity of our PDX-COG17-lines to prednisolone and both cell lines showed a resistant phenotype, regardless of IL7-induced signaling. Interestingly, for the IL7-dependent line, in the absence of exogenous IL7, there was only a minor sensitization to prednisolone. Furthermore, we also showed the both the IL7-dependent and the IL7-independent lines retain a glucocorticoid transcriptional response, with the upregulation of various *NR3C1*-target genes, including the pro-apoptotic BIM. Recently, Meyer and colleagues demonstrated that glucocorticoids can paradoxically induce steroid resistance in T-ALL by directly upregulating the expression of *IL7Ra* [44]. In our two cell lines, this paradoxical upregulation of the *IL7Ra* upon prednisolone seemed to be more pronounced in the PDX-COG17-IL7 line.

Since the phosphoproteomic profiling underscored a predominant role of JAK3 in IL7-induced signaling, we evaluated the response of PDX-COG17-IL7 cells to the JAK inhibitor ruxolitinib. While single ruxolitinib treatment did not show an effect in PDX-COG17-IL7 cells even in the presence of IL7, the combined JAK inhibition by ruxolitinib and prednisolone showed a high synergy in the presence of IL7. In the last few years, several studies have highlighted the role of active JAK3, either due to mutational *gain-of-function* or exogenous IL7-induced signaling, in conferring resistance to steroid treatment in T-ALL [17, 23, 24, 26]. In particular, Delgado-Martin and colleagues demonstrated that exogenous IL7 can induce steroid resistance and that the treatment with the JAK inhibitor ruxolitinib can sensitize a subset of T-ALL blasts to glucocorticoid *ex vivo* [23]. Similarly, we could model the synergistic effect of ruxolitinib and prednisolone when JAK3 is activated by exogenous IL7 in our cell lines. Therefore, PDX-COG17-IL7 cells and the derived PDX-COG17-IND line can be used as tools not only for investigating the JAK3-STAT5 signaling downstream of IL7, but they can also be used to model the resistance to glucocorticoids of T-ALL cells.

IL3-dependent Ba/F3 cells are usually the preferred model to study the oncogenic potential and the transforming capacity of gene overexpression or gene mutation [45]. However, the Ba/F3 line is a murine pro-B cell line. Therefore, our IL7-dependent cell line could be used in future studies as valid alternative to Ba/F3 cells to have a direct model of human leukemia oncogenic dependency. Lastly, our two cell lines allow the investigation of drug sensitivity to agents that require an active proliferation to exert their effect, such as nucleotide analogues and cyclin-dependent kinase inhibitors, or other small-molecule inhibitors that may need a prolonged treatment to affect the cellular phenotype like epigenetic drugs.

AUTHOR CONTRIBUTIONS

V.C. designed the study, designed and performed experiments, analyzed data, performed bioinformatic analyses, and wrote the manuscript. V.P., J.B-G, and R.d.G.-d.H performed experiments. R.H., A.H., and T.P. performed bioinformatic analyses. S.P. performed the mass spectrometry measurements and analyzed data. K.O. and A.F. provided samples. F.vL. and R.P. provided critical input and revised the manuscript. C.J. and J.M. supervised the study and revised the manuscript.

ACKNOWLEDGEMENTS

The authors would like to thank the Children's Oncology Group (COG) for providing the pediatric T-ALL patient samples. This study was supported by the Dutch Cancer Society (KWF Kankerbestrijding, grant KWF2016_10355 to V.C.) and the foundation "Kinderen Kankervrij" (grant KiKa-335 to V.P.). Furthermore, Cancer Center Amsterdam and the Netherlands Organization for Scientific Research (NWO Middelgroot, grant #91116017) are acknowledged for the support of the mass spectrometry infrastructure.



REFERENCES

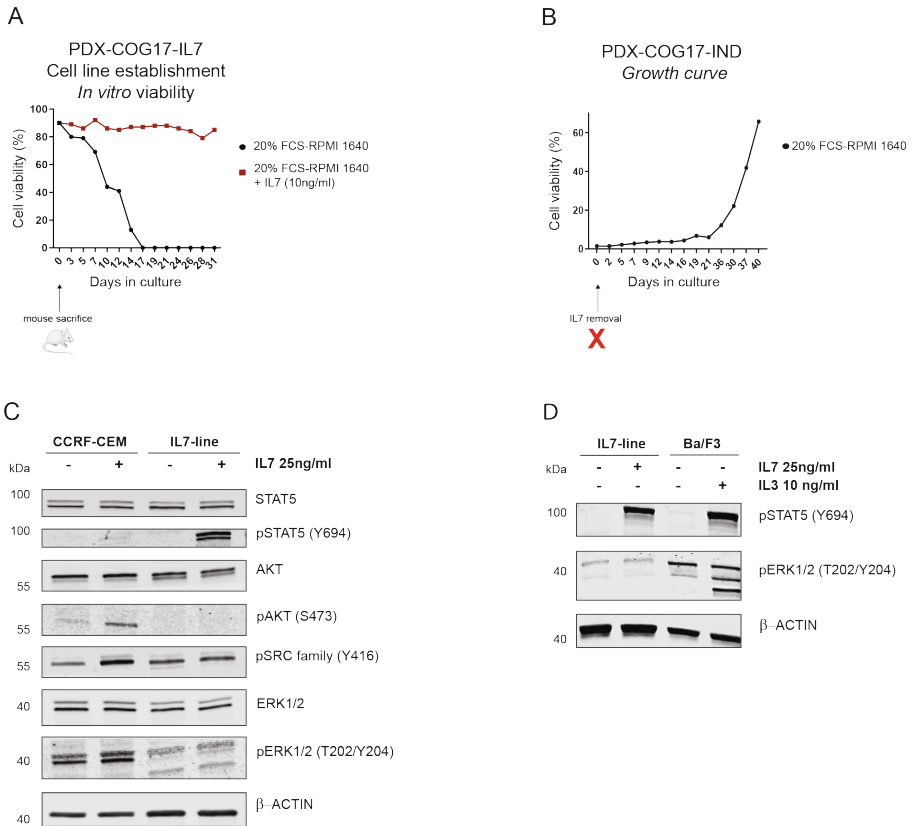
1. Ghandi, M., et al., *Next-generation characterization of the Cancer Cell Line Encyclopedia*. Nature, 2019. **569**(7757): p. 503-508.
2. McDonald, E.R., 3rd, et al., *Project DRIVE: A Compendium of Cancer Dependencies and Synthetic Lethal Relationships Uncovered by Large-Scale, Deep RNAi Screening*. Cell, 2017. **170**(3): p. 577-592 e10.
3. Li, H., et al., *The landscape of cancer cell line metabolism*. Nat Med, 2019. **25**(5): p. 850-860.
4. Dwane, L., et al., *Project Score database: a resource for investigating cancer cell dependencies and prioritizing therapeutic targets*. Nucleic Acids Res, 2021. **49**(D1): p. D1365-D1372.
5. Jaaks, P., et al., *Effective drug combinations in breast, colon and pancreatic cancer cells*. Nature, 2022. **603**(7899): p. 166-173.
6. Hughes, P., et al., *The costs of using unauthenticated, over-passaged cell lines: how much more data do we need?* BioTechniques, 2007. **43**(5): p. 575-586.
7. Ben-David, U., et al., *Genetic and transcriptional evolution alters cancer cell line drug response*. Nature, 2018. **560**(7718): p. 325-330.
8. Warren, A., et al., *Global computational alignment of tumor and cell line transcriptional profiles*. Nat Commun, 2021. **12**(1): p. 22.
9. van Alphen, C., et al., *The influence of delay in mononuclear cell isolation on acute myeloid leukemia phosphorylation profiles*. J Proteomics, 2021. **238**: p. 104134.
10. Bleijs, M., et al., *Xenograft and organoid model systems in cancer research*. EMBO J, 2019. **38**(15): p. e101654.
11. Calandrini, C. and J. Drost, *Normal and tumor-derived organoids as a drug screening platform for tumor-specific drug vulnerabilities*. STAR Protoc, 2022. **3**(1): p. 101079.
12. Winter, S.S., et al., *Improved Survival for Children and Young Adults With T-Lineage Acute Lymphoblastic Leukemia: Results From the Children's Oncology Group AALL0434 Methotrexate Randomization*. J Clin Oncol, 2018. **36**(29): p. 2926-2934.
13. Reedijk, A.M.J., et al., *Progress against childhood and adolescent acute lymphoblastic leukaemia in the Netherlands, 1990-2015*. Leukemia, 2021. **35**(4): p. 1001-1011.
14. Cordo, V., et al., *T-cell Acute Lymphoblastic Leukemia: A Roadmap to Targeted Therapies*. Blood Cancer Discov, 2021. **2**(1): p. 19-31.
15. van der Zwet, J.C.G., et al., *Multi-omic approaches to improve outcome for T-cell acute lymphoblastic leukemia patients*. Adv Biol Regul, 2019. **74**: p. 100647.
16. Cordo, V., et al., *Phosphoproteomic profiling of T cell acute lymphoblastic leukemia reveals targetable kinases and combination treatment strategies*. Nature Communications, 2022. **13**(1): p. 1048.
17. Bodaar, K., et al., *JAK3 mutations and mitochondrial apoptosis resistance in T-cell acute lymphoblastic leukemia*. Leukemia, 2022.
18. Butler, M., et al., *BTK inhibition sensitizes acute lymphoblastic leukemia to asparaginase by suppressing the amino acid response pathway*. Blood, 2021. **138**(23): p. 2383-2395.
19. Oshima, K., et al., *Mutational and functional genetics mapping of chemotherapy resistance mechanisms in relapsed acute lymphoblastic leukemia*. Nature Cancer, 2020. **1**(11): p. 1113-1127.

20. Hong, C., M.A. Luckey, and J.H. Park, *Intrathymic IL-7: the where, when, and why of IL-7 signaling during T cell development*. *Semin Immunol*, 2012. **24**(3): p. 151-8.
21. Ribeiro, D., et al., *STAT5 is essential for IL-7-mediated viability, growth, and proliferation of T-cell acute lymphoblastic leukemia cells*. *Blood Adv*, 2018. **2**(17): p. 2199-2213.
22. Silva, A., et al., *IL-7 contributes to the progression of human T-cell acute lymphoblastic leukemias*. *Cancer Res*, 2011. **71**(14): p. 4780-9.
23. Delgado-Martin, C., et al., *JAK/STAT pathway inhibition overcomes IL7-induced glucocorticoid resistance in a subset of human T-cell acute lymphoblastic leukemias*. *Leukemia*, 2017. **31**(12): p. 2568-2576.
24. Li, Y., et al., *IL-7 Receptor Mutations and Steroid Resistance in Pediatric T cell Acute Lymphoblastic Leukemia: A Genome Sequencing Study*. *PLoS Med*, 2016. **13**(12): p. e1002200.
25. Liu, Y., et al., *The genomic landscape of pediatric and young adult T-lineage acute lymphoblastic leukemia*. *Nat Genet*, 2017. **49**(8): p. 1211-1218.
26. van der Zwet, J.C.G., et al., *MAPK-ERK is a central pathway in T-cell acute lymphoblastic leukemia that drives steroid resistance*. *Leukemia*, 2021. **35**(12): p. 3394-3405.
27. Murillo, J.R., et al., *Automated phosphopeptide enrichment from minute quantities of frozen malignant melanoma tissue*. *PLoS One*, 2018. **13**(12): p. e0208562.
28. Beekhof, R., et al., *INKA, an integrative data analysis pipeline for phosphoproteomic inference of active kinases*. *Mol Syst Biol*, 2019. **15**(4): p. e8250.
29. Tyanova, S., T. Temu, and J. Cox, *The MaxQuant computational platform for mass spectrometry-based shotgun proteomics*. *Nat Protoc*, 2016. **11**(12): p. 2301-2319.
30. Li, H. and R. Durbin, *Fast and accurate short read alignment with Burrows-Wheeler transform*. *Bioinformatics*, 2009. **25**(14): p. 1754-60.
31. Danecek, P., et al., *Twelve years of SAMtools and BCFtools*. *Gigascience*, 2021. **10**(2).
32. DePristo, M.A., et al., *A framework for variation discovery and genotyping using next-generation DNA sequencing data*. *Nat Genet*, 2011. **43**(5): p. 491-8.
33. McLaren, W., et al., *The Ensembl Variant Effect Predictor*. *Genome Biol*, 2016. **17**(1): p. 122.
34. Karczewski, K.J., et al., *The mutational constraint spectrum quantified from variation in 141,456 humans*. *Nature*, 2020. **581**(7809): p. 434-443.
35. van Alphen, C., et al., *Phosphotyrosine-based Phosphoproteomics for Target Identification and Drug Response Prediction in AML Cell Lines*. *Mol Cell Proteomics*, 2020. **19**(5): p. 884-899.
36. Mazzucchelli, R. and S.K. Durum, *Interleukin-7 receptor expression: intelligent design*. *Nat Rev Immunol*, 2007. **7**(2): p. 144-54.
37. Oliveira, M.L., et al., *IL-7R-mediated signaling in T-cell acute lymphoblastic leukemia: An update*. *Adv Biol Regul*, 2019. **71**: p. 88-96.
38. Fris mantas, V., et al., *Ex vivo drug response profiling detects recurrent sensitivity patterns in drug-resistant acute lymphoblastic leukemia*. *Blood*, 2017. **129**(11): p. e26-e37.
39. Gocho, Y., et al., *Network-based systems pharmacology reveals heterogeneity in LCK and BCL2 signaling and therapeutic sensitivity of T-cell acute lymphoblastic leukemia*. *Nat Cancer*, 2021. **2**(3): p. 284-299.
40. Barata, J.T., et al., *IL-7-dependent human leukemia T-cell line as a valuable tool for drug discovery in T-ALL*. *Blood*, 2004. **103**(5): p. 1891-900.

Chapter 6

41. Palomero, T., et al., *CUTLL1, a novel human T-cell lymphoma cell line with t(7;9) rearrangement, aberrant NOTCH1 activation and high sensitivity to gamma-secretase inhibitors*. *Leukemia*, 2006. **20**(7): p. 1279-87.
42. Tosello, V., et al., *A Novel t(8;14)(q24;q11) Rearranged Human Cell Line as a Model for Mechanistic and Drug Discovery Studies of NOTCH1-Independent Human T-Cell Leukemia*. *Cells*, 2018. **7**(10).
43. Sheard, M.A., et al., *Preservation of high glycolytic phenotype by establishing new acute lymphoblastic leukemia cell lines at physiologic oxygen concentration*. *Exp Cell Res*, 2015. **334**(1): p. 78-89.
44. Meyer, L.K., et al., *Glucocorticoids paradoxically facilitate steroid resistance in T cell acute lymphoblastic leukemias and thymocytes*. *J Clin Invest*, 2020. **130**(2): p. 863-876.
45. Warmuth, M., et al., *Ba/F3 cells and their use in kinase drug discovery*. *Curr Opin Oncol*, 2007. **19**(1): p. 55-60.

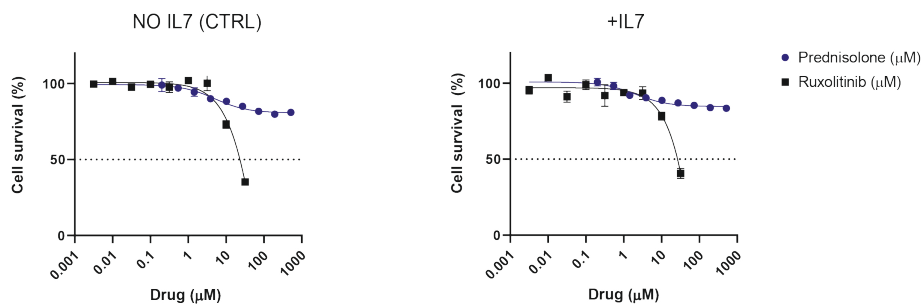
SUPPLEMENTARY FIGURES



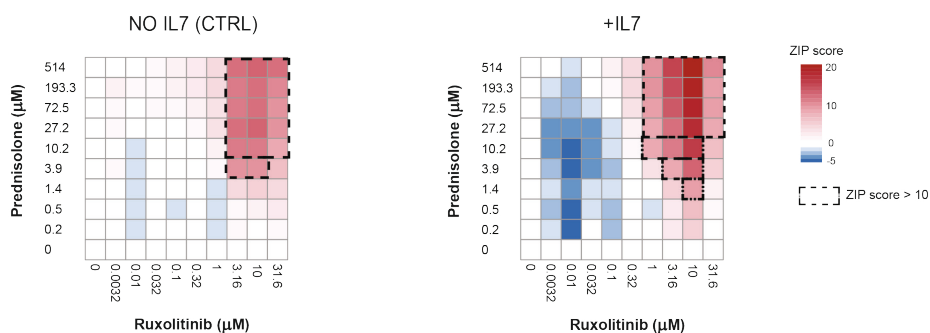
Supplementary Figure 1. A) Cell viability of PDX-COG17-IL7 cells cultured *in vitro*. T-ALL blast purified from the murine bone marrow were cultured in the presence or absence of human IL7 (10 ng/ml). Cell viability was assessed via trypan blue staining and automatic cell counting. B) Growth curve of PDX-COG17-IND cells. Cells were kept in culture in the absence of IL7 for more than a month and cell counts were assessed via trypan blue staining and automatic cell counting. C) Western blotting of PDX-COG17-IL7 and CCRF-CEM cells before (NO IL7) and after the cytokine pulse (+IL7 25 ng/ml). Cells were cultured overnight in the absence of IL7, subsequently incubated with the cytokine (25 ng/ml) for 30 minutes and harvested for protein extraction. D) Western blotting of PDX-COG17-IL7 and Ba/F3 cells before (NO IL7/IL3) and after the cytokine pulse (+IL7 25 ng/ml, +IL3 10 ng/ml). Cells were cultured overnight in the absence of IL7/IL3, subsequently incubated with the cytokines for 30 minutes and harvested for protein extraction.



A



B



Supplementary Figure 2. Ruxolitinib and prednisolone have a synergistic effect in PDX-COG17-IND cells. A) Dose-response curves of prednisolone and ruxolitinib in PDX-COG17-IND cells. Cells were incubated with increasing concentrations of prednisolone (0 – 514 μM) or ruxolitinib (0 – 32 μM) for 96 hours in the presence or absence of IL7 (10 ng/ml). NO IL7: cells were cultured without IL7 and kept without cytokine during the assay. +IL7: IL7 (10 ng/ml) was added when cells were seeded with the drugs. Relative survival was calculated in comparison with cells treated with vehicle only. The graph shows the average and the standard deviation of duplicates. B) Zero-Interaction Potency (ZIP) synergy scores for the combination of ruxolitinib (0 – 32 μM) and prednisolone (0 – 514 μM). Cells were treated with either one of the single drugs or a drug combination for 96 hours in duplicate. Cell survival was calculated in comparison to vehicle-treated cells. ZIP values lower than 0 indicate an antagonistic effect of the drug combination (blue), values between 0 and 10 indicate an additive effect (white to light red) while values above 10 (corresponding to a deviation from the reference model above 10%) indicate synergy (dark red and outside black dashed line). Each drug screening was performed in duplicate.



CHAPTER 7



Summary, general discussion, and future perspectives

ON THE ROAD TOWARDS TARGETED TREATMENTS FOR T-ALL

T cell acute lymphoblastic leukemia (T-ALL) originates when genetic lesions accumulate in the DNA of immature T cell precursors. These genomic aberrations allow the expression and activation of developmental transcription factors, normally not active in mature T cells, which induce a differentiation arrest and promote an uncontrolled proliferation of immature progenitors.

Despite ALL being the most common form of cancer in children, T-ALL accounts for only 10-15% of the pediatric ALL cases [1], with an overall survival (OS) of 80% that has been achieved using a risk-based stratification of intensive, multi-agent chemotherapeutic protocols [2, 3]. The current therapeutic regimen includes a combination of chemotherapeutic agents such as steroids, microtubules-destabilizing agents, alkylating agents, anthracyclines, anti-metabolites, nucleoside analogues, L-asparaginase and, in selected patients, an additional stem cell transplantation. Some agents present a lymphoid lineage-specific effect, such as synthetic steroids that induce apoptosis in lymphocytes [4]. Also the amino acid-depleting enzyme L-asparaginase has a lineage-specific effect since ALL cells present a low or absent asparagine synthetase activity, making them vulnerable to the exogenous asparagine depletion [5]. Another example is the antifolate methotrexate (MTX) that inhibits *de novo* purine synthesis and, consequently DNA and RNA synthesis. Since ALL blasts present a higher intracellular retention of the drug and of its polyglutamate metabolites, its effect is more elevated in ALL cells [6], albeit recent evidence highlights that T-lymphoblasts retain less MTX metabolites compared to B-ALL cells [7]. Nevertheless, the remaining drugs are conventional chemotherapeutics that target highly proliferating cells, including healthy tissues. Therefore, the intense treatment of pediatric patients with cytotoxic agents will not only impact their quality of life during therapy, but it will cause long-term, chronic sequelae in survivors together with an increased risk for the development of a secondary malignancy [8].

Patients are assigned to standard, medium, or high-risk group based on minimal residual disease (MRD) after the first two courses of chemotherapy [3, 9]. A recent study from the Dutch Childhood Oncology Group highlighted that the limit of treatment intensification for high-risk patients has been achieved, since the number of pediatric patients who die because of a leukemia relapse equals the number of patients dying from treatment-related toxicities [10]. Therefore, alternative, more targeted therapeutic options are warranted to reduce the toxic effects of chemotherapy and increase the cure rate.

In the last twenty years, the only additional drug approved for the treatment of T-ALL was the deoxyguanosine analogue nelarabine which received FDA-approval in 2005 for the treatment of relapsed patients with T-ALL or lymphoblastic lymphoma. T-lymphoblasts are more sensitive to nelarabine treatment compared to other hematopoietic cells [11] due to the higher accumulation of the active nelarabine metabolite ara-G, a purine nucleoside analogue that induces an arrest of DNA synthesis and consequent induction of apoptosis. In 2020, a phase III clinical trial demonstrated high efficacy and tolerability of nelarabine treatment in newly diagnosed pediatric T-ALL patients [12], indicating a possibility for integrating nelarabine already in the first-line treatment. In fact, the current ALLtogether1 study includes nelarabine treatment for high-risk pediatric and young adult T-ALL cases that are refractory to the first two courses of chemotherapy after diagnosis [NCT04307576].

Protein kinase inhibitors are one of the most used targeted treatments in modern oncology. Nevertheless, no kinase inhibitor or any other small molecule-drug has been approved yet for the treatment of T-ALL patients, mostly because of the lack of accurate predictive biomarkers for the stratification of patients [13]. Several clinical trials are currently investigating the use of kinases inhibitors based on the detection of recurrent genomic lesions in oncogenes, such as the JAK inhibitor ruxolitinib for T-ALL cases that present JAK-STAT signaling activating mutations (NCT03117751), the MEK inhibitor selumetinib in case of detection of mutations in the RAS pathway (NCT03705507), and the ABL inhibitors imatinib or dasatinib for *ABL1*-fusion positive T-ALL cases (NCT03117751, NCT02551718).

This thesis

Extensive genomic studies performed via whole-exome and whole-genome sequencing have uncovered the genetic drivers of T-ALL [14-16] which are developmental transcription factors ectopically expressed due to genomic rearrangements (*type A* aberrations) [17, 18]. The expression and activation of such transcription factors promote a differentiation arrest and induce an aberrant proliferation of immature progenitors. While direct targeting of aberrant transcription factors is trivial, identification of secondary mutations that act in concert with genetic drivers to promote leukemogenesis and favor proliferation and survival, can provide important opportunities for genomic-driven precision medicine. These secondary mutations (*type B* aberrations) usually occur in surface receptors like the *IL7R* and *NOTCH1*, kinases (e.g., *JAK1/3*, *AKT*, *PIK3*) and their regulators (e.g., *PTEN*, *RAS*, *PTPN11*) [14, 16, 19]. Nevertheless, many clinical trials showed disappointing results on the use of targeted agents based on a genomic only-driven informed treatment in T-ALL and also for other types of cancer [13, 20-22]. Therefore, we aimed to go beyond the genomics of T-ALL

and to perform an unbiased analysis of the proteome and phosphoproteome to uncover relevant signaling pathways and active kinases and leverage such hyper-active proteins as putative targets for therapy.

In **chapter 2**, we extensively reviewed the most frequent genetic aberrations in T-ALL and we analyzed the main characteristics of the four main T-ALL subtypes [17]. Each of the four T-ALL subtypes, namely the most immature subgroup, the early T cell precursor – ALL (ETP-ALL), the TLX, the TLX1/NKX2.1 (also known as *proliferative* subgroup), and the most mature subtype, the TAL/LMO subgroup, have defined genomic abnormalities, gene expression profiles, and surface markers. In particular, the ETP-ALL subtype presents the highest mutational burden compared to the other subtypes. Despite this detailed knowledge on the most common genomic aberrations occurring in T-ALL, only a few genetic lesions could be associated with prognosis, such as the presence of NOTCH1 pathway activating mutations that are associated with a good outcome [23-25] while aberrations in the PI3K axis and in the RAS signaling pathway are related to a poor prognosis [25-27]. Nevertheless, none of them is currently used for the risk-stratification of patients [28]. Therefore, we proposed a more comprehensive analysis of the biology T-ALL. In addition to genome sequencing, RNA, proteome, and phosphoproteome profiling should be integrated to fully capture the complexity of the disease and uncover non-genomic leukemia dependencies. In fact, a sequencing study from the Children's Oncology Group reported that, except for *JAK* and *FLT3* mutations, no other somatic mutation could be found in tyrosine-kinase coding genes or their mediators, in a group of high-risk pediatric acute lymphoblastic leukemia patients, despite their gene expression profile suggested an elevated kinase signaling [29]. Thus, selected patient could benefit from the use of kinase inhibitors even in the absence of genetic mutations. The analysis of active signaling pathways via transcriptome, proteome, and phosphoproteome profiling can complement the detection of genetic aberrations. This *multi-omic* and integrative tumor profiling can enlarge not only our knowledge on the biology of the disease, but also extend the list of actionable targets for precision oncology [17, 30].

In the search for actionable targets, proteins are of great interest since they are ultimate mediators of the cellular phenotype and their analysis can directly reveal how DNA mutations, external stimuli, signaling, and metabolic rewiring are eventually translated at the functional level. Active signaling pathways and aberrant kinase activities can provide useful information for drug prioritization and the design of effective combination treatments in the context of personalized medicine, in particular when no actionable target is found via

a genomic-driven approach. Phosphoproteomics has had a pivotal role in the identification of aberrant signaling networks that could be exploited as molecular targets for therapy [31-33]. For T-ALL, only limited phosphoproteomics studies have been reported. Kinome array and reverse-phase protein array (RPPA) studies identified differential signaling features between B- and T-ALL [34] and activation of the LCK/calcineurin axis in ETP-ALL [35, 36]. While kinome arrays and the RPPA approach provide information about a selected panels of kinases and their targets, mass spectrometry (MS)-based phosphoproteomics allows the simultaneous investigation of multiple proteins and signaling routes without the need for any *a priori* target selection. Degryse and colleagues used MS-based phosphoproteomic profiling to study the signaling downstream of mutant JAK3 [37]. Recently, Franciosa and colleagues applied phosphoproteomic analyses to identify possible mediators of resistance to γ -secretase inhibitors, the most common NOTCH1 inhibitors, in T-ALL models [38].

In **chapter 3** we presented an exploratory, global, unbiased profiling of tyrosine, serine, and threonine phosphorylation in T-ALL. Furthermore, we leveraged the phosphoproteomic profiling to infer kinase activities at baseline in each sample using the integrative inferred kinase activity (INKA) pipeline [39, 40]. Based on the kinase activation profiles, we designed effective treatment combinations that we validated *ex vivo* in patient-derived murine xenografts [40]. Previous studies had demonstrated that a subset of T-ALL cells is sensitive to the SRC-family kinase inhibitor dasatinib [41-43]. We showed high activation of LCK, SRC, ABL1, and other Src-family members even in the absence of genomic rearrangements involving *LCK* or *ABL1*. While single dasatinib treatment might not be effective in all T-ALL cases, INKA-guided design of combination treatments uncovered a synergistic effect of the simultaneous inhibition of the INSR/IGF-1R axis and LCK/SRC signaling by dasatinib. Importantly, none of the cell lines and patient samples analyzed presented aberrations in the *LCK*, *SRC*, *INSR*, and *IGF1R* genes, underscoring the added value of unbiased phosphoproteomic profiling in the identification of non-genomic vulnerabilities which can be exploited as therapeutical targets.

Previous studies uncovered the involvement of the IGF-1R signaling in supporting survival and growth of T-ALL blasts both *in vitro* [44] and *in vivo* [45, 46]. We showed that the activation of the INSR/IGF-1R can cause resistance to SRC/LCK inhibition by dasatinib and this connection opens important questions about the possible protective role of the microenvironment. In fact, the involvement of the INSR/IGF-1R signaling in inducing resistance to different tyrosine kinase inhibitors, including EGFR inhibitors, has been shown in the context of solid tumors [39, 47, 48]. Therefore, future studies should address the

complicated relationship between leukemic blasts and their bone marrow niche also in relation to therapy sensitivity, in order to further elucidate the mechanisms behind the insurgence of drug resistance.

Differently from many other types of cancer, no targeted treatment has been approved for the treatment of T-ALL yet. Nevertheless, several targeted agents are currently under clinical investigation to increase the cure rate of T-ALL and to improve the quality of life of patients by limiting the chemotherapy-induced toxicities and long-term side effects. In **Chapter 4**, we reviewed the main actionable targets in T-ALL and we provided an extensive overview of the most promising novel agents investigated in clinical trials, such as modifiers of apoptosis (BH3-mimetics), signal transduction inhibitors (including kinase inhibitors), cell cycle inhibitors, transcriptional regulator inhibitors, epigenetic drugs, and immunotherapies. While a single treatment might not be sufficient to eradicate the whole leukemia population, the possibility of combining a targeted agent with a less intense chemotherapy regimen holds promising possibilities to effectively target the malignant cells and, at the same time, reduce the insurgence of toxicities. Furthermore, the combined use of targeted inhibitors and chemotherapeutics can overcome the drug resistant phenotype that often characterizes T-ALL at relapse. Preclinical studies already showed the successful combination of dasatinib and dexamethasone in LCK-overexpressing T-ALL cells [36, 42], AKT inhibitors and glucocorticoids in *PTEN*-mutated leukemic blasts [49], ruxolitinib and glucocorticoids in JAK-activated T-ALLs [50, 51], and the successful combination of MEK inhibitors and synthetic steroids [16, 52-54] that is currently investigated in the phase I/II international SeluDex trial (NCT03705507).

Eventually, we also highlighted novel agents that showed promising results in preclinical research models and that might soon enter upcoming clinical trials. It is of utmost importance to bridge preclinical research with clinical settings to promote and accelerate the translation of innovative therapies from *bench-to bedside*.

In the last 15 years, there has been a huge international effort to characterize the genome of several cancer types to identify targetable lesions. The American National Institute of Health created The Cancer Genome Atlas (TCGA) project to promote a systematic analysis of cancer genomes. With the increasing developments in the field of proteomics, a similar initiative was launched to create a Clinical Proteomic Tumor Analysis Consortium (CPTAC) in 2011 to promote the proteomic characterization of cancer and the integration of genomic and proteomic data in a *proteogenomic* profile. Unfortunately, T-ALL has not been included

in TCGA or in CPTAC, indicating a lack of a systematic investigation of the disease at the proteome and at the proteogenomic level. In **chapter 5** we performed a transcriptomic, proteomic, and phosphoproteomic profiling using a panel of 11 matched diagnostic-relapse patient-derived xenografts (PDXs) to obtain an overview of active signaling pathways and kinases in T-ALL. We integrated these data with the detection of somatic mutations via whole-exome sequencing, and with the *ex vivo* cellular response to 42 drugs to identify possible determinants of sensitivity. We extended our drug screening to an additional cohort of 25 PDXs and we showed that subsets of T-ALL cases are sensitive to small molecule-agents such as the kinase inhibitors dasatinib, selumetinib, and trametinib, in the absence of known genetic lesions. These results underscore the importance of going beyond genomics to increase the possibilities of precision medicine. In fact, functional screenings such as *ex vivo* drug tests can provide important and rapid indications on the cancer phenotypes, and they have been already proven successful in guiding clinical treatment decisions in selected T-ALL patients who showed an exceptional response to a targeted agent [41, 55], and in two prospective clinical trials for acute myeloid leukemia [56] and aggressive hematological malignancies [57].

To gain insights into possible differences between diagnostic and relapse T-ALLs, we compared the proteome of diagnostic and relapse PDXs, and we found an enrichment for proteins involved in mitochondrial activity and oxidative phosphorylation in the relapse group. A deregulation of the cellular metabolism has been recognized as an hallmark of cancer [58] since it gives a selective advantage to malignant cells. Therefore, the detection of an increased mitochondrial metabolism in the relapse T-ALLs could be related to cellular adaptation to the microenvironment but also to treatment and could be therefore possibly involved in therapy resistance.

Furthermore, we performed pathway enrichment analyses, differential protein expression analysis, and inference of kinase activities, and we highlighted that both proteomic and phosphoproteomic features that are present at diagnosis can be retained at relapse, such as the activation of the JAKs and the INSR/IGF-1R kinases, and they correlate to cellular sensitivity to the JAK inhibitor ruxolitinib and to three different AKT inhibitors, respectively. Therefore, selected patients could benefit already at initial diagnosis from a targeted agent.

Lastly, we found an enrichment for cell cycle and proliferation pathways in dasatinib-sensitive PDXs at the transcriptome, proteome, and phosphoproteome level. Interestingly, these proliferation-signature was abrogated in their matched relapse samples that acquired

resistance to the kinase inhibitor. Thus, cellular quiescence could be involved in the insurgence of drug resistance. In fact, previous studies correlated dasatinib responsiveness to LCK activation downstream of active T cell receptor (TCR) signaling [42, 43]. Similarly, we uncover an elevated phosphorylation of CD5, a known LCK target and an essential player in the activation of the TCR signaling, exclusively in three dasatinib sensitive samples and the lack of such phosphosite in their matched resistant counterparts.

Therefore, our study provides an important multi-omic resource to uncover non-genetic determinants of sensitivity to targeted therapies and allows the investigation of the complexity of the biology of T-ALL at the signaling level.

PDXs have become widely used in preclinical research since they allow the expansion of patient samples, they provide an *in vivo* model of a human disease, and they maintain the main characteristics of their tumor of origin [59-61]. The generation of several murine xenografts allowed us to perform multiple analysis such as *ex vivo* drug screenings, sequencing, transcriptomic and (phospho)proteomic profiling on the same sample, starting from only a few million leukemic blasts obtained from patient's biopsies. Moreover, in **chapter 6**, we reported the establishment of two novel T-ALL cell lines from a patient-derived xenograft. In particular, the first cell line presented a dependency on the presence of human IL7 for growth and expansion *in vitro*, while the second cell line that was sub-derived from the IL7-dependent one, did not need any cytokine to proliferate. IL7-induced signaling correlated with active JAK3 signaling as highlighted by the INKA ranking of active kinases upon cytokine stimulus. Moreover, we demonstrated a synergistic effect of the JAK3 inhibitor ruxolitinib and prednisolone in the presence of IL7 in our IL7-dependent cell line, as previously demonstrated for T-ALL blasts treated *ex vivo* [50]. Therefore, our novel IL7-dependent cell line could be used to investigate possible mechanisms of re-sensitization to glucocorticoids but also, given the continuous proliferation of these cells *in vitro*, to study the mechanisms of action and the cellular sensitivity to all those agents that require an active cell cycle to be effective (e.g., CDK inhibitors, nucleoside analogs...) or a longer exposure to the treatment (e.g., epigenetic drugs). Furthermore, our novel cell lines do not present any *TP53* mutations. Therefore, differently from many commercial T-ALL cell lines that have acquired an inactivation of the tumor suppressor p53, our cell lines recapitulate the lack of *TP53* mutations at T-ALL diagnosis [14] and allow the study of the effects induced by DNA damage. Lastly, the dependency on IL7 for an active proliferation could be leveraged to study the oncogenic potential of gene mutations, deletions or over-expression as commonly done using the murine, IL3-dependent, pro-B, Ba/F3 cells. In fact,

our cell line can possibly allow the investigation of such oncogenic mechanisms directly in a human model of cancer.

T-ALL and precision medicine: a look ahead

The outcome for children diagnosed with T-ALL has dramatically improved over the last decades thanks to risk-directed chemotherapeutic protocols [10, 62, 63]. Nevertheless, the insurgence of relapse, often accompanied by refractory disease, together with severe side-effect induced by chemotherapy, remain unmet needs. Recent clinical trials have proven that the limit for treatment intensification has been reached [10, 63]. Thus, further improvement in cure rate and quality of life heavily relies on tailored treatments such as targeted agents and immunotherapies, including chimeric antigen receptor T (CAR T) cells and monoclonal antibodies. Several monoclonal antibodies are approved for the treatment of both hematological and solid cancers. Daratumumab and isatuximab (NCT03860844), two CD38-directed antibodies, are also currently investigated for the treatment of pediatric T-ALL patients, since T-ALL blasts also express CD38 on the cell surface [64]. Promising results from the phase II DELPHINUS study (NCT03384654) recently presented at the American Society of Clinical Oncology meeting demonstrated safety and efficacy of the addition of daratumumab to the chemotherapy backbone in pediatric and young adult T-ALL or lymphoblastic lymphoma (LL) patients who had a relapse or present a refractory disease [65].

CAR T cells have revolutionized the treatment of pediatric B-ALL but their application for the treatment of T-ALL has been limited because of the many similarities between T-ALL cells and their healthy counterparts, T cells. Therefore, for the design of effective CAR T for the treatment of T cell malignancies, several factors must be considered such as the expression of common targets in both leukemic blasts and T cells that would cause the so-called “fratricide effect”, the need for selectively isolating healthy T cells from the donor without any lymphoblast contamination, and a sustained expansion of CAR T cells *in vivo* [66]. Thanks to the development of more sophisticated genome editing techniques, it has been possible to design fratricide-resistant CAR T cells from both patients and heterologous sources and those innovative therapies have shown impressive results in early clinical trials [67-70], indicating a future for immunotherapy for the tailored treatment of T-ALL.

Several international molecular tumor profiling protocols have been initiated to extend the access of tailored treatments also to pediatric patients [71-73]. DNA and RNA sequencing are becoming routinely used for the identification of actionable targets even though the

clinical benefit of this genomic-driven approach seems to be limited [74, 75]. Therefore, future T-ALL research should promote the integration of functional studies, such as *ex vivo* drug (combination) screenings and functional profiling via phosphoproteomics for treatment selection in the absence of a targetable DNA aberration. In fact, based on a recently published study that demonstrate the sensitivity of a subset of T-ALL cases to LCK inhibition *ex vivo* in the absence of *ABL1*-fusions, in particular in non-ETP-ALL cases [43], a new clinical trial will investigate the addition of the Src-family inhibitor ponatinib to chemotherapy in relapsed/refractory T-ALL patients (NCT05268003). Moreover, phosphoproteomic analyses have shown promising results in identifying targetable proteins and guide the design of combination treatments [39, 40]. We presented an exploratory phosphoproteomic profiling of T-ALL cell lines and PDXs to predict drug sensitivity. However, given the lack of a systematic proteomic and proteogenomic analysis of T-ALL, future studies should address the proteomic and phosphoproteomic landscape of the different T-ALL subtypes, also in relation to the most common genomic aberrations and copy number variations, to provide a proteogenomic map of this rare malignancy. In addition, the systematic study of the T-ALL surface proteome could uncover novel potential targets for the development of immunotherapies. While the application of proteomics and phosphoproteomics in the clinical setting is still limited to RPPA and kinome arrays, recent advances showcased an increased sensitivity, reduced analysis time, and the need for a lower amount of input material, and the possibility to perform analyses at the single cell level [76] to identify heterogeneity also for MS-based proteomics. Thus, there are promising expectations for a future translation of (phospho)proteomics measurements as predictive response biomarkers [32, 77] and for a broader application in the context of precision medicine.

REFERENCES

1. Patel, A.A., et al., *Biology and Treatment Paradigms in T Cell Acute Lymphoblastic Leukemia in Older Adolescents and Adults*. *Curr Treat Options Oncol*, 2020. **21**(7): p. 57.
2. Pui, C.H. and W.E. Evans, *Treatment of acute lymphoblastic leukemia*. *N Engl J Med*, 2006. **354**(2): p. 166-78.
3. Pieters, R., et al., *Successful Therapy Reduction and Intensification for Childhood Acute Lymphoblastic Leukemia Based on Minimal Residual Disease Monitoring: Study ALL10 From the Dutch Childhood Oncology Group*. *J Clin Oncol*, 2016. **34**(22): p. 2591-601.
4. Schmidt, S., et al., *Glucocorticoid-induced apoptosis and glucocorticoid resistance: molecular mechanisms and clinical relevance*. *Cell Death Differ*, 2004. **11 Suppl 1**: p. S45-55.
5. Butler, M., L.T. van der Meer, and F.N. van Leeuwen, *Amino Acid Depletion Therapies: Starving Cancer Cells to Death*. *Trends Endocrinol Metab*, 2021. **32**(6): p. 367-381.
6. Masson, E., et al., *Accumulation of methotrexate polyglutamates in lymphoblasts is a determinant of antileukemic effects in vivo. A rationale for high-dose methotrexate*. *J Clin Invest*, 1996. **97**(1): p. 73-80.
7. Lopez-Lopez, E., et al., *Pharmacogenomics of intracellular methotrexate polyglutamates in patients' leukemia cells in vivo*. *J Clin Invest*, 2020. **130**(12): p. 6600-6615.
8. Mulrooney, D.A., et al., *The changing burden of long-term health outcomes in survivors of childhood acute lymphoblastic leukaemia: a retrospective analysis of the St Jude Lifetime Cohort Study*. *Lancet Haematol*, 2019. **6**(6): p. e306-e316.
9. Pui, C.H., et al., *Clinical utility of sequential minimal residual disease measurements in the context of risk-based therapy in childhood acute lymphoblastic leukaemia: a prospective study*. *Lancet Oncol*, 2015. **16**(4): p. 465-74.
10. van Binsbergen, A.L., et al., *Efficacy and toxicity of high-risk therapy of the Dutch Childhood Oncology Group in childhood acute lymphoblastic leukemia*. *Pediatr Blood Cancer*, 2022. **69**(2): p. e29387.
11. Kurtzberg, J., et al., *Phase I study of 506U78 administered on a consecutive 5-day schedule in children and adults with refractory hematologic malignancies*. *J Clin Oncol*, 2005. **23**(15): p. 3396-403.
12. Dunsmore, K.P., et al., *Children's Oncology Group AALL0434: A Phase III Randomized Clinical Trial Testing Nelarabine in Newly Diagnosed T-Cell Acute Lymphoblastic Leukemia*. *J Clin Oncol*, 2020. **38**(28): p. 3282-3293.
13. Cordo, V., et al., *T-cell Acute Lymphoblastic Leukemia: A Roadmap to Targeted Therapies*. *Blood Cancer Discov*, 2021. **2**(1): p. 19-31.
14. Liu, Y., et al., *The genomic landscape of pediatric and young adult T-lineage acute lymphoblastic leukemia*. *Nat Genet*, 2017. **49**(8): p. 1211-1218.
15. Zhang, J., et al., *The genetic basis of early T-cell precursor acute lymphoblastic leukaemia*. *Nature*, 2012. **481**(7380): p. 157-63.
16. Li, Y., et al., *IL-7 Receptor Mutations and Steroid Resistance in Pediatric T cell Acute Lymphoblastic Leukemia: A Genome Sequencing Study*. *PLoS Med*, 2016. **13**(12): p. e1002200.
17. van der Zwet, J.C.G., et al., *Multi-omic approaches to improve outcome for T-cell acute lymphoblastic leukemia patients*. *Adv Biol Regul*, 2019. **74**: p. 100647.

18. Gianni, F., L. Belver, and A. Ferrando, *The Genetics and Mechanisms of T-Cell Acute Lymphoblastic Leukemia*. Cold Spring Harb Perspect Med, 2020. **10**(3).
19. Vicente, C., et al., *Targeted sequencing identifies associations between IL7R-JAK mutations and epigenetic modulators in T-cell acute lymphoblastic leukemia*. Haematologica, 2015. **100**(10): p. 1301-10.
20. Takebe, N., D. Nguyen, and S.X. Yang, *Targeting notch signaling pathway in cancer: clinical development advances and challenges*. Pharmacol Ther, 2014. **141**(2): p. 140-9.
21. Massard, C., et al., *High-Throughput Genomics and Clinical Outcome in Hard-to-Treat Advanced Cancers: Results of the MOSCATO 01 Trial*. Cancer Discov, 2017. **7**(6): p. 586-595.
22. Marquart, J., E.Y. Chen, and V. Prasad, *Estimation of the Percentage of US Patients With Cancer Who Benefit From Genome-Driven Oncology*. JAMA Oncol, 2018. **4**(8): p. 1093-1098.
23. Asnafi, V., et al., *NOTCH1/FBXW7 mutation identifies a large subgroup with favorable outcome in adult T-cell acute lymphoblastic leukemia (T-ALL): a Group for Research on Adult Acute Lymphoblastic Leukemia (GRAALL) study*. Blood, 2009. **113**(17): p. 3918-24.
24. Fogelstrand, L., et al., *Prognostic implications of mutations in NOTCH1 and FBXW7 in childhood T-ALL treated according to the NOPHO ALL-1992 and ALL-2000 protocols*. Pediatr Blood Cancer, 2014. **61**(3): p. 424-30.
25. Bandapalli, O.R., et al., *NOTCH1 activation clinically antagonizes the unfavorable effect of PTEN inactivation in BFM-treated children with precursor T-cell acute lymphoblastic leukemia*. Haematologica, 2013. **98**(6): p. 928-36.
26. Zuurbier, L., et al., *The significance of PTEN and AKT aberrations in pediatric T-cell acute lymphoblastic leukemia*. Haematologica, 2012. **97**(9): p. 1405-13.
27. Paganin, M., et al., *The presence of mutated and deleted PTEN is associated with an increased risk of relapse in childhood T cell acute lymphoblastic leukaemia treated with AIEOP-BFM ALL protocols*. Br J Haematol, 2018. **182**(5): p. 705-711.
28. Burns, M.A., et al., *Identification of prognostic factors in childhood T-cell acute lymphoblastic leukemia: Results from DFCL ALL Consortium Protocols 05-001 and 11-001*. Pediatr Blood Cancer, 2021. **68**(1): p. e28719.
29. Loh, M.L., et al., *Tyrosine kinome sequencing of pediatric acute lymphoblastic leukemia: a report from the Children's Oncology Group TARGET Project*. Blood, 2013. **121**(3): p. 485-8.
30. Sengupta, S., et al., *Integrative omics analyses broaden treatment targets in human cancer*. Genome Med, 2018. **10**(1): p. 60.
31. Jimenez, C.R. and H.M. Verheul, *Mass spectrometry-based proteomics: from cancer biology to protein biomarkers, drug targets, and clinical applications*. Am Soc Clin Oncol Educ Book, 2014: p. e504-10.
32. Doll, S., F. Gnad, and M. Mann, *The Case for Proteomics and Phospho-Proteomics in Personalized Cancer Medicine*. Proteomics Clin Appl, 2019. **13**(2): p. e1800113.
33. Casado, P., et al., *Impact of phosphoproteomics in the translation of kinase-targeted therapies*. Proteomics, 2017. **17**(6).
34. van der Sligte, N.E., et al., *Kinase activity profiling reveals active signal transduction pathways in pediatric acute lymphoblastic leukemia: a new approach for target discovery*. Proteomics, 2015. **15**(7): p. 1245-54.
35. Serafin, V., et al., *Phosphoproteomic analysis reveals hyperactivation of mTOR/STAT3 and LCK/Calcineurin axes in pediatric early T-cell precursor ALL*. Leukemia, 2017. **31**(4): p. 1007-1011.

36. Serafin, V., et al., *Glucocorticoid resistance is reverted by LCK inhibition in pediatric T-cell acute lymphoblastic leukemia*. *Blood*, 2017. **130**(25): p. 2750-2761.
37. Degryse, S., et al., *Mutant JAK3 phosphoproteomic profiling predicts synergism between JAK3 inhibitors and MEK/BCL2 inhibitors for the treatment of T-cell acute lymphoblastic leukemia*. *Leukemia*, 2018. **32**(3): p. 788-800.
38. Franciosa, G., et al., *Proteomics of resistance to Notch1 inhibition in acute lymphoblastic leukemia reveals targetable kinase signatures*. *Nat Commun*, 2021. **12**(1): p. 2507.
39. Beekhof, R., et al., *INKA, an integrative data analysis pipeline for phosphoproteomic inference of active kinases*. *Mol Syst Biol*, 2019. **15**(4): p. e8250.
40. Cordo', V., et al., *Phosphoproteomic profiling of T cell acute lymphoblastic leukemia reveals targetable kinases and combination treatment strategies*. *Nature Communications*, 2022. **13**(1): p. 1048.
41. Frisimantas, V., et al., *Ex vivo drug response profiling detects recurrent sensitivity patterns in drug-resistant acute lymphoblastic leukemia*. *Blood*, 2017. **129**(11): p. e26-e37.
42. Shi, Y., et al., *Phase II-like murine trial identifies synergy between dexamethasone and dasatinib in T-cell acute lymphoblastic leukemia*. *Haematologica*, 2021. **106**(4): p. 1056-1066.
43. Gocho, Y., et al., *Network-based systems pharmacology reveals heterogeneity in LCK and BCL2 signaling and therapeutic sensitivity of T-cell acute lymphoblastic leukemia*. *Nat Cancer*, 2021. **2**(3): p. 284-299.
44. Gusscott, S., et al., *IGF1R Derived PI3K/AKT Signaling Maintains Growth in a Subset of Human T-Cell Acute Lymphoblastic Leukemias*. *PLoS One*, 2016. **11**(8): p. e0161158.
45. Lyu, A., et al., *Tumor-associated myeloid cells provide critical support for T-ALL*. *Blood*, 2020. **136**(16): p. 1837-1850.
46. Triplett, T.A., et al., *Endogenous dendritic cells from the tumor microenvironment support T-ALL growth via IGF1R activation*. *Proc Natl Acad Sci U S A*, 2016. **113**(8): p. E1016-25.
47. Wan, X., et al., *IGF-1R Inhibition Activates a YES/SFK Bypass Resistance Pathway: Rational Basis for Co-Targeting IGF-1R and Yes/SFK Kinase in Rhabdomyosarcoma*. *Neoplasia*, 2015. **17**(4): p. 358-66.
48. Zanella, E.R., et al., *IGF2 is an actionable target that identifies a distinct subpopulation of colorectal cancer patients with marginal response to anti-EGFR therapies*. *Sci Transl Med*, 2015. **7**(272): p. 272ra12.
49. Piovan, E., et al., *Direct reversal of glucocorticoid resistance by AKT inhibition in acute lymphoblastic leukemia*. *Cancer Cell*, 2013. **24**(6): p. 766-76.
50. Delgado-Martin, C., et al., *JAK/STAT pathway inhibition overcomes IL7-induced glucocorticoid resistance in a subset of human T-cell acute lymphoblastic leukemias*. *Leukemia*, 2017. **31**(12): p. 2568-2576.
51. Verbeke, D., et al., *Ruxolitinib Synergizes With Dexamethasone for the Treatment of T-cell Acute Lymphoblastic Leukemia*. *Hemasphere*, 2019. **3**(6): p. e310.
52. van der Zwet, J.C.G., et al., *MAPK-ERK is a central pathway in T-cell acute lymphoblastic leukemia that drives steroid resistance*. *Leukemia*, 2021. **35**(12): p. 3394-3405.
53. Irving, J., et al., *Ras pathway mutations are prevalent in relapsed childhood acute lymphoblastic leukemia and confer sensitivity to MEK inhibition*. *Blood*, 2014. **124**(23): p. 3420-30.
54. Matheson, E.C., et al., *Glucocorticoids and selumetinib are highly synergistic in RAS pathway-mutated childhood acute lymphoblastic leukemia through upregulation of BIM*. *Haematologica*, 2019. **104**(9): p. 1804-1811.



55. He, Y., et al., *Dasatinib-therapy induced sustained remission in a child with refractory TCF7-SP11 T-cell acute lymphoblastic leukemia*. *Pediatr Blood Cancer*, 2022: p. e29724.
56. Malani, D., et al., *Implementing a Functional Precision Medicine Tumor Board for Acute Myeloid Leukemia*. *Cancer Discov*, 2022. **12**(2): p. 388-401.
57. Kornauth, C., et al., *Functional Precision Medicine Provides Clinical Benefit in Advanced Aggressive Hematologic Cancers and Identifies Exceptional Responders*. *Cancer Discov*, 2022. **12**(2): p. 372-387.
58. Hanahan, D., *Hallmarks of Cancer: New Dimensions*. *Cancer Discov*, 2022. **12**(1): p. 31-46.
59. Richter-Pechanska, P., et al., *PDX models recapitulate the genetic and epigenetic landscape of pediatric T-cell leukemia*. *EMBO Mol Med*, 2018. **10**(12).
60. Uzozie, A.C., et al., *PDX models reflect the proteome landscape of pediatric acute lymphoblastic leukemia but divert in select pathways*. *J Exp Clin Cancer Res*, 2021. **40**(1): p. 96.
61. Sun, H., et al., *Comprehensive characterization of 536 patient-derived xenograft models prioritizes candidates for targeted treatment*. *Nat Commun*, 2021. **12**(1): p. 5086.
62. Pui, C.H., et al., *Treating childhood acute lymphoblastic leukemia without cranial irradiation*. *N Engl J Med*, 2009. **360**(26): p. 2730-41.
63. Jeha, S., et al., *Improved CNS Control of Childhood Acute Lymphoblastic Leukemia Without Cranial Irradiation: St Jude Total Therapy Study 16*. *J Clin Oncol*, 2019. **37**(35): p. 3377-3391.
64. Bride, K.L., et al., *Preclinical efficacy of daratumumab in T-cell acute lymphoblastic leukemia*. *Blood*, 2018. **131**(9): p. 995-999.
65. Hogan, L.E., et al., *Efficacy and safety of daratumumab (DARA) in pediatric and young adult patients (pts) with relapsed/refractory T-cell acute lymphoblastic leukemia (ALL) or lymphoblastic lymphoma (LL): Results from the phase 2 DELPHINUS study*. *Journal of Clinical Oncology*, 2022. **40**(16_suppl): p. 10001-10001.
66. Fleischer, L.C., H.T. Spencer, and S.S. Raikar, *Targeting T cell malignancies using CAR-based immunotherapy: challenges and potential solutions*. *J Hematol Oncol*, 2019. **12**(1): p. 141.
67. Wang, X., et al., *Safety and efficacy results of GC027: The first-in-human, universal CAR-T cell therapy for adult relapsed/refractory T-cell acute lymphoblastic leukemia (r/r T-ALL)*. *Journal of Clinical Oncology*, 2020. **38**(15_suppl): p. 3013-3013.
68. Ghobadi, A., et al., *A Phase 1/2 Dose-Escalation and Dose-Expansion Study of the Safety and Efficacy of Anti-CD7 Allogeneic CAR-T Cells (WU-CART-007) in Patients with Relapsed or Refractory T-Cell Acute Lymphoblastic Leukemia (T-ALL)/Lymphoblastic Lymphoma (LBL)*. *Blood*, 2021. **138**(Supplement 1): p. 4829-4829.
69. Yang, J., et al., *A Novel and Successful Patient or Donor-Derived CD7-Targeted CAR T-Cell Therapy for Relapsed or Refractory T-Cell Lymphoblastic Lymphoma (R/R T-LBL)*. *Blood*, 2021. **138**(Supplement 1): p. 652-652.
70. Pan, J., et al., *Donor-Derived CD7 Chimeric Antigen Receptor T Cells for T-Cell Acute Lymphoblastic Leukemia: First-in-Human, Phase I Trial*. *Journal of Clinical Oncology*, 2021. **39**(30): p. 3340-3351.
71. van Tilburg, C.M., et al., *The Pediatric Precision Oncology INFORM Registry: Clinical Outcome and Benefit for Patients with Very High-Evidence Targets*. *Cancer Discov*, 2021. **11**(11): p. 2764-2779.
72. Harttrampf, A.C., et al., *Molecular Screening for Cancer Treatment Optimization (MOSCATO-01) in Pediatric Patients: A Single-Institutional Prospective Molecular Stratification Trial*. *Clin Cancer Res*, 2017. **23**(20): p. 6101-6112.

73. Berlanga, P., et al., *The European MAPPYACTS Trial: Precision Medicine Program in Pediatric and Adolescent Patients with Recurrent Malignancies*. *Cancer Discov*, 2022. **12**(5): p. 1266-1281.
74. Langenberg, K.P.S., E.J. Looze, and J.J. Molenaar, *The Landscape of Pediatric Precision Oncology: Program Design, Actionable Alterations, and Clinical Trial Development*. *Cancers (Basel)*, 2021. **13**(17).
75. Letai, A., P. Bholra, and A.L. Welm, *Functional precision oncology: Testing tumors with drugs to identify vulnerabilities and novel combinations*. *Cancer Cell*, 2022. **40**(1): p. 26-35.
76. Lun, X.K. and B. Bodenmiller, *Profiling Cell Signaling Networks at Single-cell Resolution*. *Mol Cell Proteomics*, 2020. **19**(5): p. 744-756.
77. Casado, P., et al., *Implementation of Clinical Phosphoproteomics and Proteomics for Personalized Medicine*. *Methods Mol Biol*, 2022. **2420**: p. 87-106.

APPENDICES



Nederlandse samenvatting

Riassunto in italiano

List of publications

Curriculum Vitae

Acknowledgements

NEDERLANDSE SAMENVATTING

T cel acute lymfatische leukemie (T-ALL) is een zeldzame hematologische maligniteit, verantwoordelijk voor ongeveer 15% van alle gevallen van ALL op kinderleeftijd. Het ontstaat wanneer genetische afwijkingen opstapelen in het DNA van de voorloper T cellen. De behandeling is gebaseerd op intensieve chemotherapie en dit heeft ervoor gezorgd dat de overleving van T-ALL patiënten boven de 80% is. De 5 en 10 jaar overleving zijn echter niet meer verbeterd de afgelopen twee decennia. Ondanks de goede overleving overleeft één op de vijf T-ALL patiënten de ziekte niet. Dit komt doordat de ziekte bij hen terugkeert en dan meestal resistent is tegen therapie. Daarnaast veroorzaakt de intensieve behandeling toxiciteit bij T-ALL patiënten en overlevenden, wat insinueert dat het niet mogelijk is om de behandeling met chemotherapie te intensiveren voor hoog-risico patiënten en patiënten met een recidief. Dit geeft het uiterste belang aan van therapie op maat, om zo de overleving van patiënten te verbeteren en ernstige bijwerkingen van de therapie te verminderen.

De mogelijkheden om differentiatie te vermijden en om te dedifferentiëren zijn recent erkend als *'hallmarks of cancer'*, specifieke eigenschappen van tumorcellen. De afwijkende expressie van transcriptiefactoren, vaak enkel tijdens de vroege stadia van differentiatie, zorgen ervoor dat leukemische cellen in een voorloperstadium blijven. Dit zorgt voor een halt van differentiatie en komt een afwijkende celdeling ten goede. Uitgebreide transcriptomische en genomische sequencing studies hebben aangetoond dat de belangrijkste afwijkingen die T-ALL veroorzaken ontwikkelingstranscriptiefactoren zijn met ectopische expressie door genherschikkingen.

Gebaseerd op genexpressie profielen en de aanwezigheid van herhaaldelijke genomische afwijkingen, zijn vier subtypen van T-ALL ontdekt. Dit zijn vroege T-cel voorloper – ALL (ETP-ALL), TLX, TLX1/NKX2.1 (wordt ook wel *proliferatief* genoemd), en TAL/LMO. ETP-ALL is het meest immature subtype, en wordt gekarakteriseerd door verhoogde expressie van genen die betrokken zijn bij zelf-hernieuwing van de cel (*LMO2*, *LYL1*, *HHEX*, en het anti-apoptotische eiwit *BCL2*). Daarnaast hebben de ETP-ALL cellen een genexpressie profiel dat vergelijkbaar is met hematopoëtische stamcellen. De TLX-groep heeft óf geen functionele T cel receptor (TCR), óf een γ/δ TCR in combinatie met herschikkingen in de transcriptiefactor *TLX3*. De TLX1/NKX2.1 subgroep wordt onder andere gekenmerkt door verhoogde expressie van genen die de progressie van de celcyclus reguleren (als gevolg hiervan wordt dit subtype ook wel *proliferatief* genoemd), en genherschikkingen in *TLX1*

en NKX2.1. Ten slotte is er de TAL/LMO subgroep, die uit ongeveer 50% van alle T-ALL patiënten bestaat en wordt gekenmerkt door ectopische expressie van *TAL1/2*, *LYL1* en *LMO1/2/3*.

Hoewel het direct bestrijden van deze afwijkende transcriptiefactoren onvoldoende is, kan het identificeren van secundaire mutaties, die samen met de belangrijkste genetische afwijkingen de T-ALL veroorzaken, mogelijkheden bieden voor therapie op maat. In het bijzonder eiwitkinases, die de belangrijkste effectors van signaaltransductie zijn en elk aspect van het cellulaire fenotype reguleren. Afwijkingen in kinases zijn niet de belangrijkste aanstouwers voor de ziekte, maar secundaire mutaties in receptoren (*NOTCH1* en *IL7R*), genen die voor kinases coderen (*JAK1*, *JAK3*, *FLT3*, *AKT* en *PI3K*), en hun regulatoren (*PTEN* en *NRAS*) kunnen het ontstaan van leukemie ondersteunen en ten gunste komen van celdeling en overleving. Het ETP-ALL subtype wordt gekenmerkt door het hoogste aantal mutaties per eiwitcoderend gebied, in vergelijking tot andere subtypen, terwijl afwijkingen in *PTEN* met name voorkomen in het TAL/LMO subtype. Deze afwijkingen zijn geassocieerd met een slechte uitkomst. Genfusies in genen die coderen voor kinases zijn zeldzaam in T-ALL en worden vaak alleen gezien in kleine subklonen. Dit limiteert de mogelijkheid voor genomisch gedreven therapie op maat.

Informatie over actieve signaalroutes en afwijkende kinase activiteit kan nuttig zijn voor het prioriteren van medicatie en het ontwikkelen van effectieve combinatietherapie in de context van therapie op maat, met name wanneer een genomisch-gedreven benadering niet mogelijk is. Massaspectrometrie (MS) gebaseerd op fosfoproteomics heeft een belangrijke rol gespeeld in het identificeren van afwijkende signaalroutes die gebruikt zouden kunnen worden als moleculaire doelwitten voor therapie. Sterker nog, fosfoproteomics gebaseerd op MS heeft ervoor gezorgd dat het mogelijk is om simultaan meerdere eiwitten en signaalroutes te onderzoeken, zonder dat er *a priori* doelwit selectie nodig is.

Er is nog geen therapie op maat goedgekeurd voor de behandeling van T-ALL patiënten, en het gebrek aan accurate voorspellende biomarkers houdt de juiste toepassing van therapie op maat tegen. Het doel van dit proefschrift is daarom ook om verder te gaan dan genomica in T-ALL en om te zoeken naar niet-genomische afhankelijkheden die gezien kunnen worden als kwetsbaarheid van de leukemiecellen. We hebben hierom onder andere een onbevooroordeelde analyse van het proteoom en fosfoproteoom uitgevoerd

met het doel om relevante signaalroutes and actieve kinases aan het licht te brengen en om deze hyperactieve eiwitten te gebruiken als doelwitten voor therapie op maat.

In **hoofdstuk 2** geven we een overzicht van de meest voorkomende genetische afwijkingen in T-ALL en hebben we de meest belangrijke karakteristieken van de vier subtypes in T-ALL geanalyseerd. Daarnaast hebben we uitgelicht hoe functionele studies die signaalroutes onderzoeken op RNA en eiwitniveau waardevolle inzichten kunnen bieden om mechanismen van therapieresistentie te achterhalen en nieuwe therapeutische doelwitten te kunnen ontdekken. We stellen een integratieve, multi-omische benadering voor om elk aspect van T-ALL te bestuderen, om op deze manier de complexiteit van leukemie vast te leggen, en op deze manier de *Achilleshiel* van T-ALL te vinden.

In **hoofdstuk 3** presenteren we een verkennende, globale, onbevooroordeelde profilering van tyrosine, serine en threonine fosforylering in T-ALL. Daarnaast demonstreren we de toepasbaarheid van globale fosfoproteomische profilering en kinase activiteit inferentie om kinases te identificeren die als doelwit gebruikt kunnen worden in T-ALL voor het ontwerpen van therapie op maat. Door het gebruik van 11 T-ALL cellijnen en vier muismodellen afgeleid van patiëntmateriaal (PDX modellen), verstrekken we een overzicht van kinase activiteit in T-ALL en ontdekken we een rol voor INSR/IGF-1R signalering in het handhaven van resistentie tegen de Src-familie kinase remmer dasatinib.

Op dit moment worden er meerdere medicijnen op maat onderzocht voor T-ALL in een klinische studie. In **hoofdstuk 4** hebben we uitgebreid literatuuronderzoek uitgevoerd op genomische doelwitten en relevante signaalroutes in T-ALL. Daarnaast laten we een volledig overzicht zien van alle therapieën op maat die op dit moment onderzocht worden in klinische studies en relevante stoffen die veelbelovende resultaten lieten zien in preklinische T-ALL modellen. Dit betrof verscheiden klassen van kleine-molecuul inhibitoren en immuuntherapieën.

Ondanks de ontdekking van terugkomende signaalroutes in T-ALL is het gebruik van deze afwijkingen voor de prognose van de patiënt of als biomarker voor de ziekte nog steeds minimaal. In **hoofdstuk 5** beschrijven we een *ex vivo* screen voor medicatie op een panel van 47 T-ALL PDX modellen. Daarnaast rapporteren we mutaties die als doelwit voor therapie kunnen fungeren en hebben we genomische informatie geïntegreerd met microarray-gebaseerde transcriptomische, proteomische en fosfoproteomische analyses om relevante signaalroutes en determinanten van gevoeligheid voor medicijnen aan het

licht te brengen. Door het gebruik van 11 gematchte diagnose en recidief PDX-modellen laten we zien dat bepaalde signaleringspatronen (eiwitexpressie, interacties tussen signaalroutes en kinase activiteit) behouden blijven tijdens een recidief.

PDX modellen zijn fundamenteel geworden in preklinisch onderzoek. In **hoofdstuk 6** rapporteren we de implementatie van een nieuwe T-ALL cellijn gebaseerd op PDX cellen, die *in vitro* gekweekt kan worden in de aanwezigheid van humaan IL7. Gezien de overheersende rol van exogeen IL7 in het behoud van celdeling en ten gunste van resistentie tegen therapie met glucocorticoiden, de basis van de behandeling voor T-ALL, hebben we deze cellijn ingezet om IL7-geïnduceerde kinase signalering te bestuderen en om mogelijke effectieve combinatietherapieën te identificeren.

In **hoofdstuk 7** geven we een opsomming van de belangrijkste bevindingen en argumenten in dit proefschrift, met een bredere blik richting de toekomst van preklinisch en translationeel T-ALL onderzoek.

RIASSUNTO IN ITALIANO

La leucemia linfoblastica acuta a cellule T (T-ALL) è una rara forma di tumore che rappresenta solamente il 15% dei casi totali di leucemia linfoblastica acuta in ambito pediatrico. Insorge a seguito di un accumulo di anomalie nel DNA a livello dei progenitori di linfociti T ed è caratterizzata da una proliferazione incontrollata di cellule immature. Grazie ad intensi regimi chemioterapici, adattati in base alle fasce di rischio, il tasso di sopravvivenza per i pazienti pediatrici affetti da T-ALL ha raggiunto l'80%, ma, purtroppo, negli ultimi vent'anni non si è registrato nessun miglioramento per quanto riguarda i tassi di sopravvivenza a cinque e a dieci anni dalla diagnosi. Un paziente su cinque sarà affetto da una ricaduta, spesso accompagnata da resistenza alla chemioterapia e da una prognosi cattiva. Inoltre, i pazienti sono affetti da severi effetti collaterali come infezioni e malattie croniche causati dalla chemioterapia. Dunque, un'ulteriore intensificazione del regime chemioterapico attuale, in particolare per i pazienti ad alto rischio, risulta impossibile. Quindi, l'utilizzo di terapie mirate è fondamentale per aumentare la sopravvivenza dei pazienti, ma anche per limitare i dannosi effetti collaterali causati dalla chemioterapia.

La capacità di evadere il processo di differenziazione cellulare è stata di recente descritta come uno dei tratti principali (*hallmark*) del cancro. Le cellule leucemiche, grazie all'espressione ed attivazione di fattori di trascrizione, tipici dei primi stadi del differenziamento cellulare, mantengono uno stato di cellule progenitrici che causa un blocco del differenziamento cellulare ed una continua proliferazione. Infatti, studi di trascrittomici e di sequenziamento del genoma hanno dimostrato che i *driver* genetici della T-ALL sono fattori di trascrizione evolutivi, i quali vengono espressi in seguito a riarrangiamenti genici. Si possono distinguere quattro diversi sottotipi di T-ALL, in base al profilo di espressione genica e alla presenza di anomalie genomiche ricorrenti. I principali sottotipi sono: ETP-ALL (*Early T cell Precursor*), TLX, TLX1/NKX2.1 (anche noto come *proliferative*) e TAL/LMO.

Il sottotipo ETP-ALL raggruppa i casi più immaturi di T-ALL che presentano un profilo di espressione genica molto simile alle cellule staminali ematopoietiche. Inoltre, i casi ETP-ALL sono caratterizzati da un'elevata espressione di geni che garantiscono il continuo auto-rinnovo cellulare come *LMO2*, *LYL1*, *HHEX* e la proteina anti-apoptotica *BCL2*.

I casi del sottogruppo TLX sono caratterizzati dall'assenza totale di un recettore T funzionale o presentano un recettore T del tipo γ/δ , in aggiunta a riarrangiamenti che coinvolgono il fattore di trascrizione *TLX3*. Invece, il sottogruppo TLX1/NKX2.1 presenta

un'elevata espressione di geni coinvolti nella regolazione e progressione del ciclo cellulare (da cui deriva l'annotazione *proliferative*) e riarrangiamenti genici che coinvolgono i fattori di trascrizione *TLX1* ed *NKX2.1*. Infine, il sottogruppo TAL/LMO include circa la metà dei casi totali di T-ALL e si caratterizza per l'espressione di *TAL1/2*, *LYL1* e *LMO1/2/3*. L'utilizzo di fattori di trascrizione come bersagli molecolari è ancora limitato, ma l'identificazione di mutazioni secondarie che agiscono insieme ai *driver* genetici, può fornire importanti informazioni per la medicina di precisione.

Le protein-chinasi sono i principali componenti della trasduzione del segnale e regolano ogni processo che influenza il fenotipo cellulare. Mutazioni secondarie in geni che codificano per recettori cellulari come *NOTCH1* e *IL7R*; chinasi come *JAK1*, *JAK3*, *FLT3*, *AKT* e *PIK3*; regolatori di chinasi come *PTEN* e *NRAS*, supportano la trasformazione tumorale e favoriscono la sopravvivenza e la proliferazione di cellule maligne. In particolare, i casi ETP-ALL presentano il più alto tasso di mutazioni, mentre aberrazioni che coinvolgono *PTEN* di solito occorrono frequentemente nel sottotipo TAL/LMO e si associano ad una prognosi cattiva. Inoltre, fusioni geniche che coinvolgono chinasi sono rare nei casi di T-ALL e spesso sono identificate solamente in sottopopolazioni cellulari. Quindi, raramente, tali fusioni geniche possono essere utilizzate come biomarcatore predittivo per l'utilizzo di terapie mirate come, ad esempio, gli inibitori di chinasi.

L'attivazione selettiva di *pathway* e la rilevazione di elevate attività chinasiche possono fornire importanti informazioni per la scelta dei trattamenti più adeguati e per la formulazione di terapie combinate nell'ambito della medicina personalizzata, soprattutto quando nessun bersaglio terapeutico può essere identificato in base al solo profilo genetico del paziente.

Le analisi del proteoma (la totalità delle proteine in una cellula) e del fosfoproteoma (l'insieme delle proteine fosforilate da chinasi) attraverso la spettrometria di massa hanno avuto un ruolo fondamentale nell'identificazione di circuiti e *pathway* attivati in maniera anomala che possono essere sfruttati come bersagli molecolari. Infatti, la fosfoproteomica combinata alla spettrometria di massa permette l'analisi simultanea di tutte le proteine cellulari e di tutti i *pathway* di trasduzione del segnale, senza la necessità di fare una selezione a priori delle proteine d'interesse.

Purtroppo, ancora nessuna terapia mirata è stata ufficialmente approvata per il trattamento della T-ALL e la mancanza di biomarcatori predittivi accurati limita le possibilità di assegnazione dei pazienti al miglior trattamento mirato. Lo scopo del nostro progetto di

ricerca è stato di andare oltre la genetica della T-ALL per poter identificare nuovi bersagli terapeutici. In particolare, abbiamo effettuato una analisi globale del proteoma e del fosfoproteoma per rilevare i *pathway* di trasduzione del segnale e le protein-chinasi più attive, con lo scopo finale di sfruttare tali proteine come nuovi bersagli terapeutici.

Il **capitolo 2** descrive le aberrazioni genetiche più frequenti nei casi di T-ALL e le principali caratteristiche dei quattro sottotipi della malattia. Inoltre, abbiamo evidenziato come gli studi funzionali che analizzano i *pathway* di trasduzione del segnale a livello di RNA e proteine possano fornire importanti dettagli per capire i meccanismi di resistenza alle terapie attuali e per scegliere i migliori bersagli terapeutici. Proponiamo un approccio integrativo e *multi-omico* (che combina genomica, trascrittomica e proteomica) per studiare la T-ALL sotto ogni aspetto, così da essere in grado di valutare la complessità del tumore e di poter trovare il suo tallone d'Achille.

Nel **capitolo 3**, abbiamo presentato un'analisi globale della fosforilazione del proteoma nella T-ALL. Inoltre, abbiamo dimostrato come l'utilizzo della fosfoproteomica e dell'inferenza di attività chinasiche possano aiutare l'identificazione di chinasi iperattive. Tali chinasi possono essere sfruttate come bersaglio terapeutico. Utilizzando undici diverse linee cellulari di T-ALL e quattro modelli murini derivati da cellule di pazienti (*patient-derived xenografts*, PDXs), abbiamo fornito una panoramica delle chinasi più attive nelle cellule di T-ALL. Abbiamo poi scoperto che l'attivazione del recettore per l'insulina (INSR) e per l'IGF1 (IGF-1R) possono contribuire alla resistenza al trattamento con dasatinib, un inibitore delle chinasi della famiglia Src, le principali tirosin-chinasi attive nelle cellule di T-ALL analizzate.

Diverse terapie mirate sono al momento incluse in studi clinici per i pazienti affetti da T-ALL. Nel **capitolo 4**, abbiamo fatto una ricerca in letteratura riguardo alle principali aberrazioni genetiche della T-ALL che possono essere sfruttate come bersagli molecolari. Inoltre, abbiamo fatto una panoramica di tutte le terapie mirate che hanno raggiunto la sperimentazione clinica e dei nuovi farmaci che hanno dimostrato dei risultati molto promettenti in modelli preclinici di T-ALL. Questi farmaci includono vari classi di inibitori e immunoterapie.

Nonostante l'identificazione di mutazioni ricorrenti nei casi di T-ALL, l'utilizzo di tali anomalie genetiche come biomarcatori di prognosi o di risposta alla terapia è ancora limitato. Nel **capitolo 5**, abbiamo descritto uno screening di agenti terapeutici *ex vivo* usando 47 modelli murini derivati da pazienti di T-ALL. Inoltre, abbiamo riportato le principali mutazioni

genetiche e abbiamo integrato le informazioni genetiche con analisi di trascrittomica, proteomica e fosfoproteomica per identificare i principali *pathway* di trasduzione del segnale attivi e possibili fattori che determinano la risposta ai diversi farmaci. Utilizzando undici casi longitudinali (prima diagnosi di T-ALL e recidiva ottenuti dallo stesso paziente), abbiamo dimostrato che alcune caratteristiche (espressione di proteine, attivazione di *pathway* e attivazione di chinasi) sono presenti alla prima diagnosi e vengono mantenute nella recidiva.

I modelli murini derivati da campioni di pazienti sono diventati strumenti fondamentali nella ricerca preclinica. Nel **capitolo 6**, abbiamo riportato la creazione di una nuova linea cellulare di T-ALL a partire da uno di questi modelli. In particolare, questa linea cellulare può essere coltivata *in vitro* con l'aggiunta dell'interleuchina 7 (IL7) umana. Dato che IL7 ha un ruolo importante nel sostenere la proliferazione di cellule leucemiche nel microambiente del midollo osseo e può favorire l'insorgenza di resistenza ai glucocorticoidi, uno dei principali componenti del regime terapeutico per la T-ALL, abbiamo sfruttato questa linea cellulare per studiare l'attivazione di chinasi indotta da IL7 e per identificare possibili combinazioni di farmaci efficaci.

Infine, il **capitolo 7** fornisce un riassunto dei principali risultati descritti in questa tesi, visti anche in prospettiva dei futuri studi preclinici e clinici della T-ALL.

LIST OF PUBLICATIONS

1. **Cordo' V**, Meijer M.T., Hagelaar R., de Goeij-de Haas R., Poort V.M., Henneman A.A., Piersma S.R., Pham T., Oshima K., Ferrando A.A., Zaman G.J.R., Jimenez C.R., and Meijerink J.P.P. (2022). "Phosphoproteomic profiling of T cell acute lymphoblastic leukemia reveals targetable kinases and combination treatment strategies." Nat Commun **13**(1): 1048.
2. van der Zwet J.C.G, **Cordo' V**, Buijs-Gladdines J.G.C.A.M., Hagelaar R., Smits W., Vroegindewij E., Graus L., Poort V.M., Pieters R., and Meijerink J.P.P. (2022). "STAT5 does not drive steroid resistance in T-cell acute lymphoblastic leukemia despite its activation of BCL2 and BCLXL following glucocorticoid treatment." (Haematologica, online ahead of print).
3. Cante-Barrett K., Meijer M.T., **Cordo' V**, Hagelaar R., Yang W., Yu J., Smits W.K., Nulle M.E., Jansen J.P., Pieters R, Yang J.J., Haigh J., Goossens S., and Meijerink J.P.P. (2022). "The MEF2C oncogene opposes NOTCH1 in T versus B lineage decision and drives leukemia in the thymus context." JCI Insight **7**(13):e150363.
4. Smits W.K., Mohammed Y., de Ru A.H., **Cordo' V**, Friggen A.H., van Veelen P.A., and Hensbergen P.J. (2022). "*Clostridioides difficile* phosphoproteomics shows an expansion of phosphorylated proteins in stationary growth phase." mSphere **7**(1): e00911-21.
5. **Cordo' V**, van der Zwet J.C.G., Canté-Barrett K., Pieters R., and Meijerink J.P.P. (2021). "T-cell acute lymphoblastic leukemia: a roadmap to targeted therapies." Blood Cancer Discovery **2**(1): 19-31.
6. van der Zwet J.C.G., Buijs-Gladdines J.G.C.A.M., **Cordo' V**, Debets D.O., Smits W.K., Chen Z., Dylus J., Zaman G.J.R., Altelaar M., Oshima K., Bornhauser B., Bourquin J.-P., Cools J., Ferrando A.A., Vormoor J., Pieters R., Vormoor B., and Meijerink J.P.P. (2021). "MAPK-ERK is a central pathway in T-cell acute lymphoblastic leukemia that drives steroid resistance." Leukemia **35**: 3394-3405.
7. Apfel, V., Begue D., **Cordo' V**, Holzer L., Martinuzzi L., Buhles A., Kerr G., Barbosa I., Naumann U., Piquet M., Ruddy D., Weiss A., Ferretti S., Almeida R., Bonenfant D., Tordella L., and Galli G.G. (2021). "Therapeutic assessment of targeting ASNS Combined with

I-asparaginase treatment in solid tumors and investigation of resistance mechanisms.” ACS Pharmacol Transl Sci **4**(1): 327-337.

8. Cante-Barrett K., Holtzer L., van Ooijen H., Hagelaar R., **Cordo' V.**, Verhaegh W., van de Stolpe A., and Meijerink J.P.P. (2020). “A molecular test for quantifying functional Notch signaling pathway activity in human cancer.” Cancers (Basel) **12**(11).
9. van der Zwet J.C.G., **Cordo' V.**, Cante-Barrett K., and Meijerink J.P.P. (2019). “Multi-omic approaches to improve outcome for T-cell acute lymphoblastic leukemia patients.” Adv Biol Regul **74**: 100647.
10. Bleu M., Gaulis S., Lopes R., Sprouffske K., Apfel V., Holwerda S., Pregnotato M., Yildiz U., **Cordo' V.**, Dost A.F.M., Knehr J., Carbone W., Lohmann F., Lin C.Y., Bradner J.E., Kauffmann A., Tordella L., Roma G., and Galli G.G. (2019). “PAX8 activates metabolic genes via enhancer elements in renal cell carcinoma.” Nat Commun **10**(1): 3739.
11. Belver L., Yang A.Y., Albero R., Herranz D., Brundu F.G., Quinn S.A., Perez-Duran P., Alvarez S., Gianni F., Rashkovan M., Gurung D., Rocha P.P., Raviram R., Reglero C., Cortes J.R., Cooke A.J., Wendorff A.A., **Cordo' V.**, Meijerink J.P., Rabadan R., and Ferrando A.A. (2019). “GATA3-controlled nucleosome eviction drives MYC enhancer activity in T-cell development and leukemia.” Cancer Discov **9**(12): 1774-1791.
12. Corver, J., **Cordo' V.**, van Leeuwen H.C., Klychnikov O.I., and Hensbergen P.J. (2017). “Covalent attachment and Pro-Pro endopeptidase (PPEP-1)-mediated release of *Clostridium difficile* cell surface proteins involved in adhesion.” Mol Microbiol **105**(5): 663-673.

CURRICULUM VITAE

Valentina Cordo' was born on April 23rd, 1992, in Rho, in the province of Milan, Italy. She obtained her high school diploma *cum laude* from the “Falcone e Borsellino” scientific lyceum in 2011. In the autumn of the same year, she started her bachelor's in medical biotechnology at the faculty of medicine of the University of Milan. In 2014, she won an Erasmus scholarship that allowed Valentina to perform an internship at the Leiden University Medical Center (LUMC), in the Netherlands. In October 2014, she obtained her bachelor's degree *cum laude* and started working as research assistant at the national institute of molecular genetics (INGM) in Milan until February 2015, when she moved to the Netherlands to start her master's in biomedical sciences at Leiden University. In February 2017, Valentina obtained her master's degree after performing her final internship at the Center for Proteomics and Metabolomics of the LUMC, under the supervision of dr. Paul J. Hensbergen. In March 2017, she moved to Switzerland to work at the oncology division of the Novartis Institutes for Biomedical Research in Basel, under the supervision of dr. Giorgio G. Galli. In the autumn of 2017, Valentina returned to the Netherlands to start her PhD at the Princess Máxima Center for Pediatric Oncology in Utrecht in a collaborative project with the OncoProteomics laboratory of the Amsterdam University Medical Center, under the supervision of dr. Jules P.P. Meijerink and prof. Connie R. Jiménez. During her PhD, Valentina won an abstract achievement award from the American Society of Hematology for the best abstract presented by a junior researcher (2020) and presented her scientific results at several national and international congresses. The major findings of Valentina's PhD are described in this thesis. In addition to her scientific role, she was one of the founders of the *PriMá PhD group*, a representative organ for PhD students at the Princess Máxima Center and organized several scientific and social events within the institute.



In September 2022, Valentina joined the European Medicines Agency (EMA) in Amsterdam where she currently works as scientific specialist in the Regulatory Science and Innovation Task Force.

ACKNOWLEDGEMENTS / RINGRAZIAMENTI

When I started this journey back in 2017, young and naive Vale had no idea what a rollercoaster it would be (and most of you know that I am terrified by height and rollercoasters!). Despite many challenges, unexpected changes, failed experiments, and a global pandemic who put us on hold for almost two years, when I look back at the past five years, I cannot be prouder. People told me that a PhD is not only a career advance, but it is also a long journey for personal development. Yes, they were absolutely right. I am not only grateful for the possibility of getting the *Dr* title, for several publications, and a new job. I am grateful for the scientist and woman I have become, and this would have not been possible without many amazing and inspiring people who walked this route with me or simply crossed my path along the way. I would need another book to mention all the great stories and memories. I will try to do my best here to tell you my most sincere *grazie*.

I must start with the people who guided me on this project. **Jules**, your passion and enthusiasm for research are your thriving force. You believed in me since the very first time we briefly spoke on the phone. Thank you for your unconditional trust in my capabilities and for pushing me to the limits to reach “*what you deserve*”. I know that it must have been challenging to handle this little Italian volcano who refused to speak Dutch (despite understanding almost every single word of your language) and did not let anyone stand in her way. Sometimes we had different opinions, but we managed to find a compromise and you have always valued my contribution. You assigned me a very demanding project and you gave me the space and freedom to choose my own path. You never had a single doubt that I would succeed. I could not see it back then, but yes, you were right.

Connie, I still remember the day of my interview at the CCA with your whole group and somehow it feels like yesterday. Thank you for making me feel part of the OPL group since the very first day. It has not been easy to work between two institutes, especially at the beginning, but I never felt an outsider in Amsterdam. Thank you for challenging me with this difficult project and believing in me. You once told me “*Do not worry about what will happen in 10 years. With your experience, your motivation, and your personality, you have a bright future in front of you*”. I will keep repeating these words to myself.

Rob, thanks for the support and for the precious advice. When I started, the building of the Princess Maxima Center did not even exist. Now, it is a thriving center to be really proud of.

I have good memories of the dinner in Orlando during the ASH congress of 2019 when you came to us PhD students to ask about our projects in an informal way, told us good stories, and gave some tips on how to be successful. A special *thank you* goes also to **Jacqueline** who has always been ready to assist and help.

Frank, thanks for welcoming me in your group during the last year. Your calm and pragmatic attitude was definitely what I needed to complete this journey. I always enjoyed our scientific discussions but also your jokes and funny stories with a good cup of coffee.

My immense gratitude goes to my paranynphs Rico and Gabriele who always had my back. I feel so lucky to have you by my side during the defense.

Rico, we both started our new job at the Princess Maxima Center in October 2017, and we immediately got along well. Your positive attitude, your sense of humor, your deep love for coffee (and coffee breaks) and your bioinformatic skills make you the perfect colleague. Thanks for helping me not only with R and colorful heatmaps but especially in the hardest moments when everything seemed to go wrong. You were always there to support me and to help me seeing the positive side of things in a rational and balanced way. Our weekly coffee-meetings (and gossip sessions) have been one of the most valuable things in this long last year. Last, but not least, thanks for becoming a good friend too.

Gabriele, where do I start? Before coming to the Netherlands, I had only seen you a couple of times outside the university or at the library in Milan. Who would have thought that we could become such good friends after we both moved to Leiden for our studies? We have grown up together and you have become family to me. I just cannot list all the good (and less good) experiences we shared but I know that many more adventures will come. Of one thing I am really sure, I will always have a place in Leiden that I can call home.

I cannot thank enough all the members of the Meijerink group at the Princess Maxima Center. You have been the greatest colleagues. Even though I was the only foreigner of the group for most of the time, I never felt like one. The happy atmosphere inside and outside the lab, the jokes (mainly about me being Italian and obsessed with food or too short to survive in this country of giants, or both), the funny pictures, the lab meetings that sometimes lasted for too long, our group retreats, and the borrels are just a few of the awesome memories I will bring with me.

Vera and Emma, I am so glad you joined the group and that we could share our PhD journey. We have always supported each other inside and outside the lab and I am sure that you will be both successful women. You are smart, enthusiastic, active, and very determined to reach your goals. Never change this great attitude! And yes, we love gossip and chatting. Everybody knows by now that we can be very efficient at sharing important information as soon as possible under the motto “sharing is caring”. Together with Jordy, we had the best PhD team I could hope for, standing united in the moment we needed it the most.

Jordy, the medical doctor who wanted to teach me how to separate proteins on a gel during my first week in the lab. Someone might say that I am competitive but actually, we both are. Better said, we are ambitious. Luckily, we never competed against each other, instead we helped each other. Your positive attitude and your team spirit made the long days in the lab fly by (with the help of a cool playlist in the cell culture, I am sure that even our cell lines enjoyed the sound) up to a point when Jules asked “Guys, are you also working or just having fun here?”. Definitely both! We did not even need to talk to communicate, we could just look into each other’s face (and most of the times you were winking back, we still need to work on that!) and immediately understand. Thanks for all the “complaining sessions” but also the funny jokes and great laughs together, and hopefully many more to come.

Jessica, this last year brought us closer, and I am glad I shared with you my last few months in the lab. Your calm and perseverant attitude makes every PhD student feel reassured. You are a precious colleague.

Wilco, our early morning talks in the cell culture and in the office while nobody was around yet, were the best way to start the day! I loved your jokes, but I also appreciated all your comments and suggestions after every presentation.

Kirsten, thanks for the wise advice you were always willing to share.

Eric, thanks for sharing not only your knowledge but also your great sense of humor (and many candies!)

Mariska, you joined the lab at the beginning of my last year, and I am so glad we met. Thanks for always keeping an eye on me (yes, I know you still do it) and for reminding me to stop and just breathe. Our talks in the mouse facility while we were disconnected from

the outside world helped us both to move forward. I am so happy we have become good friends and I am excited to see what the future will bring.

Marloes, thanks for sharing those long mornings in the mouse facility with me. **Laura**, thanks for joining the project as a student and for your constant interest in the developments. **Chris**, the best mood booster the in the Meijerink group. You were a talented student who brought a happy atmosphere in the lab, even after spending hours in the cell culture. I am really happy that you can continue your career at the Princess Maxima Center.

I was lucky to have colleagues at the Amsterdam Medical Center that supported me throughout this phosphoproteomic journey. *Grazie* to **Richard** for the support with the phospho-enrichment and funny chats and coffee breaks during the incubations steps. **Sander, Alex, Thang**, and **Jaco** for handling all the data and always adding a personal note with a few words in Italian to every email sent to me. **Irene, Ayse, Tim, Andrea, Frank, Franziska, Giulia, Iris, Robin**, and **Madalena** for always making me feel welcome in the lab and in the office. **Mariette**, thanks for the scientific conversations and the advice and feedbacks you gave me after every presentation. And thanks to all the members of the OPL for the (sometimes very long) experiments and scientific discussions on Friday afternoons but also for the great social events.

I am very grateful to all the members of the van Leeuwen group who welcomed me last year. **Trisha**, as we know, being a foreigner in the Netherlands can be challenging sometimes. I feel lucky that we could support each other inside and outside the lab. **Britt**, you always bring good energy and a smile, and I loved our *end-of-the-day* conversations in front of the western blot reader. Hopefully we can continue the good habit of having great dinners and parties with Jordy, Vera, Emma, **Willem, Gawin** and **Miriam**. Looking forward to the next one! Thank you, **Laurens** and **Dorette** for the good scientific (non) discussions.

Evelyn, Winnie, Lindy, Keylee, Michelle, Janna, Loes, Eline, Leah, and all the other PhD students that joined the PriMa PhD group. I feel so lucky to have had the chance of starting this great initiative that brought us together and leaves a legacy at the Maxima.

Karlijn and **Naomi**, I enjoyed so much our experience at ASH in 2019 with our little Florida de-tour with Jordy. **Maria**, our chats in the corridor while running from one lab to the other were a blessing! **Flavia**, grazie per tutti gli sfoghi e le lamentele ma anche per le tue battute che riescono a strappare una risata anche nei momenti più difficili.

A special *thanks* to all the members of the Drost group that “adopted” me in their side of the office garden for a couple of years. **Camilla**, quante ne abbiamo passate da quel 2 ottobre 2017. Due italiane con i capelli ricci iniziano il dottorato nello stesso giorno. Che avventura! È stato meraviglioso poter sempre contare su di per una chiacchierata, uno sfogo, le lamentele sul pullman, ma anche per tante risate, soddisfazioni e i biscotti della Mulino Bianco durante la pausa caffè.

Francisco, even though you loved throwing stuff at me from your side of the office wall (and kidnapped my Giant Microbes collection), I enjoyed a lot our talks, your deep knowledge on almost everything, your sense of humor, and the precious advice you gave me to successfully finish my PhD. ¡Espero verte pronto!

Ari, gli ultimi tre anni sono stati davvero intensi per entrambe e per fortuna ci siamo trovate! Grazie per i saggi consigli, gli sfoghi e per aver portato un po' di accento milanese in ufficio. Vivere la pandemia da lontano è stato difficile, tra gli esperimenti da portare avanti e i titoli di Repubblica letti durante la pausa pranzo, ma almeno eravamo insieme. Non si molla mai!

Tito, ogni tanto una bella pausa caffè di due ore è quello che serve. Menomale che c'è stato il tuo umorismo a salvarmi dalle lunghissime giornate in laboratorio!

Maroussia, it was so much fun sharing with you the struggles of being a short woman in a lab designed for tall Dutch people. You will do great, go girl!

Juliane, thanks for always having a good word and a reassuring smile at the end of the day.

Irene, always active and enthusiastic, it was great having you around!

Femke, the queen of the ML1. Having you sitting in the hood 2 was reassuring and I enjoyed a lot our late afternoon talks while nobody else was around. Thanks for the good advice and the lovely talks about Switzerland. Your motivation, commitment, and determination are unvaluable.

Additionally, I want to thank my former supervisors who met me as a student and shared with me not only their knowledge and skills but also fundamental tools to succeed during my PhD. **Paul**, thanks for introducing me to the proteomics field. You are a great teacher

and supervisor, plus your Italian-speaking skills are pretty good too. Hopefully, we will keep meeting each other randomly while biking through Leiden.

Giorgio, the six months I spent in your lab in Switzerland were a blessing! Thanks for the trust you put in me and for sharing your experience and advice. Like you always say: “Avanti!”.

A warm *thank you* goes to all my new colleagues at the EMA that welcomed me into the team and showed great interest in my research and background. Now you can finally read it all!

In addition to the support of colleagues at work, I could have not reached this milestone without the care and love of friends and family.

Nora and **Xavi**, mi queridos amigos que considero mi familia en Leiden. We met as young students, grow up together, and hopefully we will share many more memorable moments. I am so happy that you both decided to come back to Leiden. And for the delicious comida you are always ready to share. ¡Os quiero muchísimo!

Tino, ci conosciamo ormai da più di dieci anni ed è sempre bello ricordare tutti i momenti passati insieme. Sei una persoda di poche parole ma il tuo supporto è sempre presente. We have shared (and we will continue) all the excitement and struggles of *PhD life*, especially with **Mouraya**. Girl, thanks for the hugs, the late-night dinners after spending 12 hours in the lab, the good glasses of wine, some tears but also plenty of laughs and gossip. You are the next doctor on the way!

George, Maria, Paraschos and **Katerina**. The best Greeks in Leiden who are always ready to have fun, dance and share good homemade food!

Sonia, grazie per aver ascoltato tutte le mie lamentele e per avere sempre un consiglio pronto per la piccola Vale che corre come super Mario per riuscire a prendere il treno in orario. E soprattutto per le lunghe passeggiate di riflessione con **Giulia** a cui tocca ascoltare tutti i nostri discorsi.

Lida, always ready to help and to plan the next trip around the world. Thanks for being supportive, understanding, and for trying to find the positive side in everything. I hope that

the future will bring you some sparkles because you deserve it. I will be there cheering for you as you have done for me during these years! Σε αγαπώ.

Cesar, your charismatic and positive attitude to life is priceless (junto a los chismes de comadres mientras compartimos chilaquiles). The evenings with Lida, **Iba** and our beloved **Fotis** are always memorable moments.

Bas, the very first person that I met when moving to the Netherlands in 2015. Many years have passed and luckily, we keep sharing good moments. Thanks for the numerous dinners and the funny competitions on who can cook best. And for always being available for a good espresso.

Nathal, thanks for sharing the ups and downs of a PhD. I loved our “complaining break” but also the dinners and the Swiss chocolate you always brought me.

Renier, thanks for always having a good word for me. As you can see, the bachelor student you met in the lab a few years ago has grown up. **Jasmine**, thanks for being always so inspirational and honest with me.

I feel lucky for the support I have here in the Netherlands and even luckier to have my dearest Italian friends and family cheering for me despite being more than a thousand kilometers away.

Ila, un libro intero non basterebbe per dirti quanto ci tengo a te. Ne abbiamo passate tante dai tempi del liceo e sono grata di poter ancora contare su di te. Grazie per le lunghe chiamate la sera tardi e le corse tra Leiden, Milano e Torino per poter passare anche solo una giornata insieme. Ti voglio bene, *my friend*. **Silvia**, la nostra party animal del gruppo. Grazie per le gite e le serate organizzate all'ultimo minuto. Tutti dovrebbero avere un'amica come te che porta tanta energia e leggerezza. Abbiamo condiviso le gioie e dolori della vita da dottorande e spero di poter contare su di te per tante nuove avventure.

Benedetta, anche se purtroppo non abitiamo più a cinque minuti di distanza, ogni volta che ci vediamo sembra che il tempo non sia mai passato. Sei sempre stata interessata al mio lavoro e ora puoi finalmente vederlo finito.

Dalma, grazie per essere sempre pronta ad organizzare una vacanza per interrompere la routine lavorativa. E per le tantissime risate che aiutano a sdrammatizzare le situazioni più difficili.

Non può mancare un grazie di cuore ai miei storici compagni di università **Anna, Santra, Paolo, Fede, Marco e Fra**. Anche se le nostre strade si sono separate ormai qualche anno fa, siamo riusciti a tenerci in contatto e le nostre reunion sono semplicemente fantastiche.

Teresa e Angelica, mi mancate da quando non lavorate più in Olanda. Grazie per i saggi consigli e per le belle giornate estive passate insieme (con la collaborazione speciale di **Stani**).

Chiara, abbiamo condiviso tanti momenti della vita, dal liceo e la pallavolo fino a condividere parte del dottorato in Olanda. Grazie per essere sempre stata onesta e per i preziosi consigli. E soprattutto per le cene con **Ale**. Quelle mancano davvero tanto!

Sam and Keti, my dearest cousins with whom I share the expat life. When I moved to the Netherlands, you moved to Scotland, and it was such a big change for our family. Grazie per credere sempre in me e per la vostra curiosità sul mio lavoro (specialmente sui topolini). Le nostre gite con **Mattia** sono diventate ormai obbligatorie ogni volta che torniamo tutti in Italia. Non vedo l'ora del nostro prossimo viaggio!

Cari **mamma e papà**, dopo aver ringraziato tutti devo assolutamente rivolgere il mio più grande *grazie* e *ti voglio bene* a voi. Non sarei mai potuta arrivare fino a qui da sola e vi sarò eternamente grata per tutte le possibilità che avete dato a me e a **Fra**. *My little brother* (che ormai così piccolo non lo è più), nonostante tu sia uno di poche parole, so che sei il mio fan numero uno. Sai benissimo che ci sarò sempre per te. Solo ora capisco quanto sia stato difficile per voi vedermi andare via di casa otto anni fa alla ricerca di un futuro tutto mio. Nonostante la distanza, il vostro amore incondizionato e la vostra fiducia cieca in me si sentono ogni giorno fino a qui.

